Det Kongelige Danske Videnskabernes Selskab
Biologiske Meddelelser, bind **21**, nr. 7

Dan. Biol. Medd. **21**, no. 7 (1951)

THE RHEOLOGY OF THE CROSS STRIATED MUSCLE FIBRE

WITH PARTICULAR REFERENCE TO ISOTONIC CONDITIONS

BY

FRITZ BUCHTHAL AND E. KAISER

in Collaboration with
POUL ROSENFALCK

København
i kommission hos Ejnar Munksgaard
1951

Printed in Denmark.
Bianco Lunos Bogtrykkeri.

CONTENTS

Preface.

Rheology is a relatively new term introduced into physics about twenty years ago and its application to physiology has been rather scarce, so that a few words of definition might be useful. It denotes that branch of physics which deals with the *deformation and flow of matter.* While the physics of the last century and the beginning of the present mainly dealt with simple rheological systems, such as the Hookean body and the Newtonian fluid, in modern rheology "the ideal elastic body and the perfect fluid are almost as systematically disregarded as they are overemphasized in classical mechanics of continua" (REINER 1949a, b). Biological structures hardly display any example of the simple type of rheological behaviour and the recent progress in the description and understanding of the complex elastic and flow properties of rubber-like substances and of plastics, i. e. substances with high particle size or molecular weight provides a basis for an application of these conceptions to biological systems as well.

The mechanical properties of skeletal muscle for many years have been a problem of special interest to physiologists and ever since WEBER and BLIX in the middle and at the end of the last century they have been considered a central problem in the understanding of the minute structural changes underlying the mechanism of contraction. In more recent times important contributions from studies on *whole muscle* have come chiefly from HILL and his collaborators. The present paper deals with properties of the *isolated* fibre at rest and during shortening (isotonic). It represents a continuation of a study previously published in this series (1942) which mainly treated the mechanical behaviour of the isolated muscle fibre recorded at constant length (isometric). We have attempted to apply some of the concepts developed in modern rheology for a description of the experimental results

and the minute structural interpretation. In the last section a molecular model is analyzed and on its basis a theory of contraction is suggested as far as possible in quantitative terms. In view of the extent of the present report the authors feel it necessary to emphasize that it does not pretend to represent a review or a monograph with a complete survey of the literature on the mechanical behaviour and structure of muscle. The reader interested in the older literature is referred to A. FICK's book (1882) and to more recent reviews as for example HILL (1931), LINDHARD 1931, BUCHTHAL and LINDHARD 1939, FENN 1945, BARER 1948, the Biological Symposium on Muscle (1940), the New York Academy of Science symposium on Muscular Contraction (1947), and the articles in the Annual Reviews of Physiology of 1939 to 1951.

The authors feel that an apology is necessary for the large volume of the present paper. It is a consequence of the fact that some of the experimental material was acquired during the years of the last war wherein conditions arose which were unsuitable, indeed, at times impossible for the adequate treatment or the publication of the data. With the return of the status quo ante other aspects of the problem had meanwhile been followed up which stressed the need for further elaboration both theoretically and experimentally.

In the mathematical treatment of the results, especially those dealing with the theory (Part IV) and the description of the transient experiments (Part II), the authors wish to acknowledge the most valuable collaboration of Mr. POUL ROSENFALCK, M. Sc.

In the first development of the theory Mr. BENT FUGLEDE, M. Sc. has rendered valuable assistance. Mr. ALEXANDER MAURO, Ph. D., kindly read the manuscript and gave us valuable suggestions for which the authors are very grateful. Finally we wish to express our thanks to Mr. VAGN ANDERSEN for his technical assistance in constructing the myograph used in the isotonic recording of the single fibre contractions which represented a very delicate mechanical problem.

The work has been supported by grants from the CARLSBERG FOUNDATION, the MICHAELSEN FOUNDATION, and the ROCKEFELLER FOUNDATION.

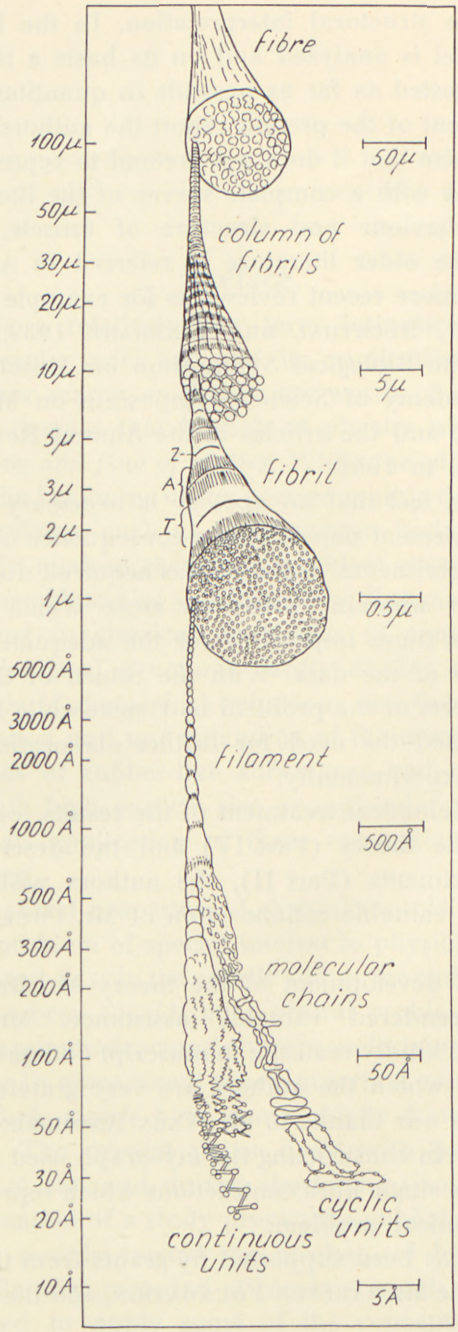

Fig. 1. Diagram of microscopical and submicroscopical fibre structure. Ordinate in μ and ångström (Å).

Introduction.

In dealing with the cross striated muscle fibre, knowledge of the minute structure and its relationship to physiological properties are the basis for understanding the process of contraction. The direct methods for the investigation of fine structure, electron microscopy and X-ray diffraction, have so far given important information. For example, electron microscopy has shown that the submicroscopic filaments apparently continue uninterrupted through the isotropic and anisotropic substance and retain their straight course both in the resting and contracted fibril (HALL *et al.* 1946). However, the contractile process does not proceed in dimensions which lie within the resolving power of the electron microscope and therefore the site of the deformations must be sought within molecular dimensions.

Decisive information was expected from X-ray diffraction analysis; but although these investigations have yielded important knowledge about the structure, especially with regard to the similarity between myosin and muscle substance and between myosin and other fibrillar proteins (keratin and fibrinogen, ASTBURY 1938, 1947), it has not been possible to determine the site of the mechanical deformation. X-ray diagrams of normal living, contracted, and resting muscle fibres show no significant difference in the molecular patterns, and diagrams from stretched and unstretched muscle differ only as regards the degree of orientation. It is furthermore significant that even considerable degrees of shortening, such as are obtained in irreversible contractions, are not accompanied by conspicuous disorientation.

While mechanical properties such as rubber-like elasticity and contractility can be demonstrated both on macroscopic and microscopic levels, unfortunately the direct methods mentioned above for a submicroscopic analysis with respect to the site of

the deformations only tell us where they in any case do *not* occur. The negative results of X-ray diffraction, which are especially disappointing in this respect, are interpreted as being caused by a relatively strongly refractive, well orientated crystalline substance, which gives a comparatively regular diffraction pattern and which on account of its considerable rigidity takes part only to a small extent in the mechanical deformations (Astbury 1947). The mechanical deformations are assumed to be localized in structural elements which are in series with this inert material. The contractility must, therefore, be assumed to lie in structural elements of molecular dimensions, which have so far escaped direct analysis.

Among the various *indirect methods for the investigation of fine structure*, the mechanical methods have special advantages, since detailed information on the functional state and the concomitant properties of the minute structure can be obtained during the normal function of the muscle.

In previous investigations, carried out under *isometric* conditions, the tension was found to be the dominant factor in determining the elastic properties of muscle fibres. Hill's investigations have further shown the influence of *load* on the velocity of shortening in whole muscles. Under *isotonic* conditions, the error which occurs when one part of the muscle stretches another, is practically eliminated, and similarly the distortion of the time course of the mechanical events caused by liberation of stored elastic energy is reduced. It is thus obvious that it is advantageous to keep the load at a chosen constant level, i. e. to work under isotonic conditions (Fenn 1936). Correction is thereby avoided for the influence of the variable tension on the mechanical constants. The difficulties in setting up this method of recording, which are considerably greater than in isometric recording, have so far prevented satisfactory investigations on the dynamic properties of the *single fibre* under isotonic conditions. The necessity of working on isolated fibres or small bundles of muscle fibres is illustrated by comparative investigations on large bundles or whole muscles, where the shunting connective tissue often conceals the structural changes which characterize the process of contraction. Using isolated fibres gives furthermore the advantage that transmission of temperature changes and dif-

fusion occur with essentially higher velocity than in whole muscles.

The present paper is divided into four sections: *Part I* comprises a description of the experimental technique for the determination of static and dynamic properties in the single muscle fibres.—*Part II* gives an analysis of the length-tension diagram of the muscle fibre with respect to elastic and viscous forces and plastic deformation and with respect to the components arising from the different structural elements of the fibre as for example the sarcolemma. The elastic properties are investigated by studying the effect of sudden changes in length or tension (transient experiments), and by introducing periodic changes in load on the fibre (vibration experiments). An attempt will be made to localize the different mechanical properties of the muscle fibre to its minute structural elements and to the textural pattern in which these elements are organized. *Part III* contains an analysis of the dynamic mechanical properties during contraction using as an indicator the velocity of shortening and its changes under different external and internal conditions. In the last section of the paper, *Part IV*, an attempt is made to interpret the experimental findings by a simple *quantitative* picture of the minute structure.

Part I.

Method.

The isotonic myograph

The recording of the shortening, the shortening velocity, and the elastic properties in the single fibre required a recording system in which the forces of inertia are small as compared with the forces which the fibre itself can produce. We have tried to obtain this by an arrangement (fig. 2) in which the forces of the fibre were transferred by means of a lever (a) to a moving coil (c) suspended by a knife-edge (d), as used in an analytical balance. The excursions of lever (a) are limited by the adjustable stop screw (n) for the recording of afterload contractions. The coil was placed in a magnetic field and consisted of 15 turns of wire with a diameter of 0.12 mm and had a resistance of 4.7 ohms. At a distance of 25 mm from the axis of rotation on the lever

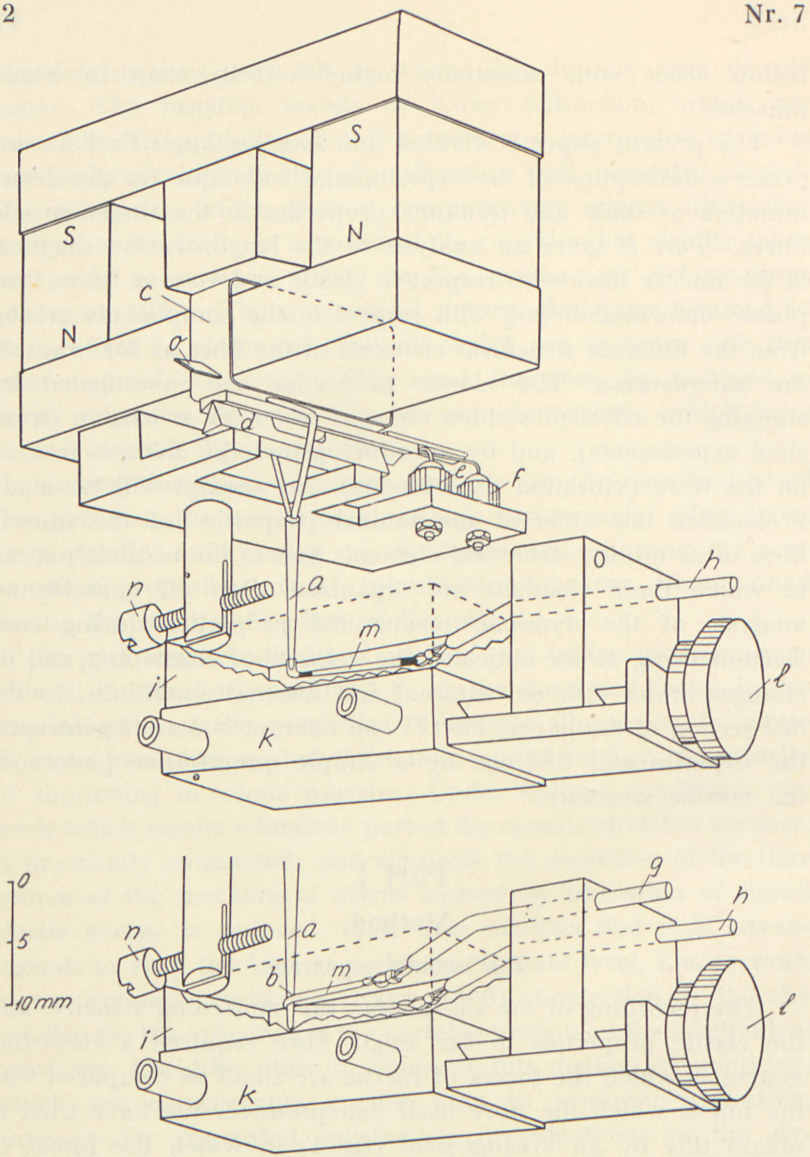

Fig. 2. *Isotonic myograph.*

a = lever in rigid connection with moving coil (c).
b = point of pull of fibre on (a).
d = knife-edge suspension for (a) and (c).
e and *f* = mercury cups leading current to (c).
g and *h* = pairs of micro-tweezers to hold the tendon ends of the fibre.
i = ringer bath.
k = chamber for cooling or heating.
l = micrometer screw for adjustment of fibre length.
m = muscle fibre, on the lower graph as a loop around (a), on the upper graph one tendon end attached to (a).
n = stop-screw for the adjustment of afterload.
o = mirror for recording of coil movements.
S–N = permanent magnet producing the magnetic field around (c).

(a) a force of 5 dynes per mA was produced by passing current through the coil. Thus, any desired load could be imposed upon the fibre by setting the current at a given level. In order to pass both direct current and alternating current independently through the coil, it was necessary that the direct current circuit and the alternating current circuit have as large a resistance as possible as

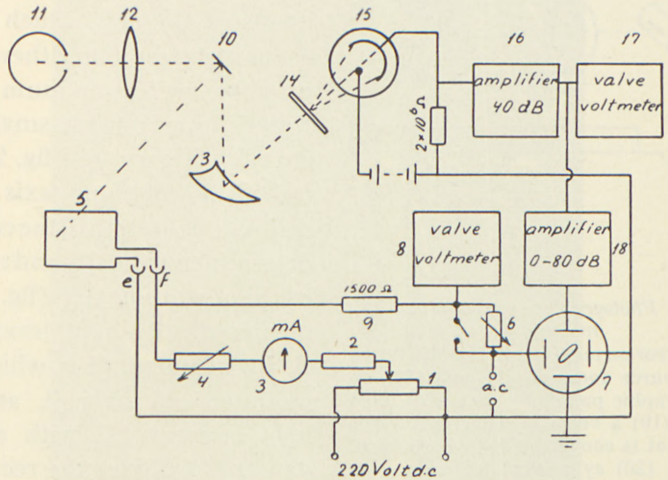

Fig. 3. *Electrical and optical circuits for the determination of elastic and viscous stiffness. Constant load* on the muscle fibre introduced as d.c. current in coil (5), varied by potentiometer (1), transmitted through resistor (2) and measured by milliamperemeter (3) led through variable resistor (4) to the terminals of coil (5). *Alternating load* derived from alternating current (a. c.) of variable frequency transmitted through resistors (6) and (9) to the coil and to the X-plates of the cathode ray oscilloscope (7) and measured by valve-voltmeter (8).
The movements of the coil are recorded photo-electrically. Mirror (1) is attached to the coil (5), reflects the image of linear light source (11) upon triangular concave mirror (13). Variations in angle of (10) change the amount of light falling on (13). Mirror (13) focusses a picture of (10) on ground glass (14) diffusing light on photo-cathode (15). The photo-current is amplified in (16) and (18), measured by valve-voltmeter (17) and connected to the Y-plates of (7).

compared with that of the coil. In this way a certain change in resistance in one of the circuits gave only a slight variation in impedance between the terminals of the coil. It has, therefore, been necessary to work with relatively high voltages in order to be able to use a resistance of 300—550 Ohms. The variation in impedance did not exceed 1 per cent at the frequencies of alternating current used. The alternating current circuit (fig. 3) consisted of a variable resistance of 150 ohms, 600 watts, which

was inserted over 220 volts main voltage and was used as a potentiometer (1). The current from the arm of the potentiometer flowed via a constant resistance of 300 ohms, 100 watts (2) to the galvanometer (3) and then further through a variable resistance of 200 ohms, 50 watts (4) to the coil (5).

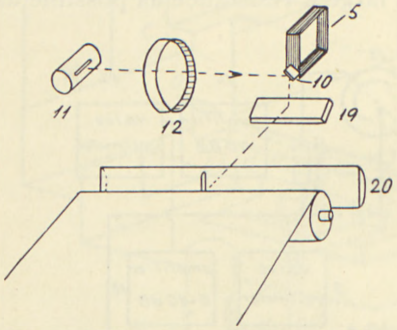

Fig. 4. *Photographic recording of coil movements.*
(10) mirror on moving coil (5). (11) linear light source focussed through (12) on photographic paper. By means of fixed mirror (19) a vertical deflection of the light spot is converted to a horizontal. (20) cylindrical lense.

In order to reduce frictional resistance against the movements of the coil, which might occur at its terminals, these were provided with platinum wire, which dipped into two small mercury containers (e, f fig. 2) placed in the rotational axis of the coil. The deflection of the coil was determined optically and recorded photographically (fig. 4) by means of the light lever consisting of mirror (10), which was mounted on the coil, and the light source (11) with a condenser (12). Since the recording system moved on a horizontal axis and hence the light spot moved vertically, it was necessary to let the light rays be reflected by the mirror (19) in order to be able to use the available recording cameras, in which the film runs in a vertical direction and where a horizontal movement of the light spot is required (fig. 4).

Dynamic elastic properties as they are revealed in vibration experiments.

Fundamental definitions.

The dynamic elastic properties of the muscle fibre were investigated by superimposing small periodic variations in load on the fibre. In previous experiments we have studied the mechanical reaction of the fibre to periodic changes in length (Buchthal 1942, Buchthal *et al.* 1944 a). In the present experiments the length alterations produced by the periodic changes in load amounted to 0.05 to 2.0 per cent of the equilibrium length (de-

flection measured from the mean position). When the periodic changes in load and length as they occurred during a vibration were transformed to electrical quantities and led to the X and Y plates of a cathode ray oscilloscope a Lissajous figure was ob-

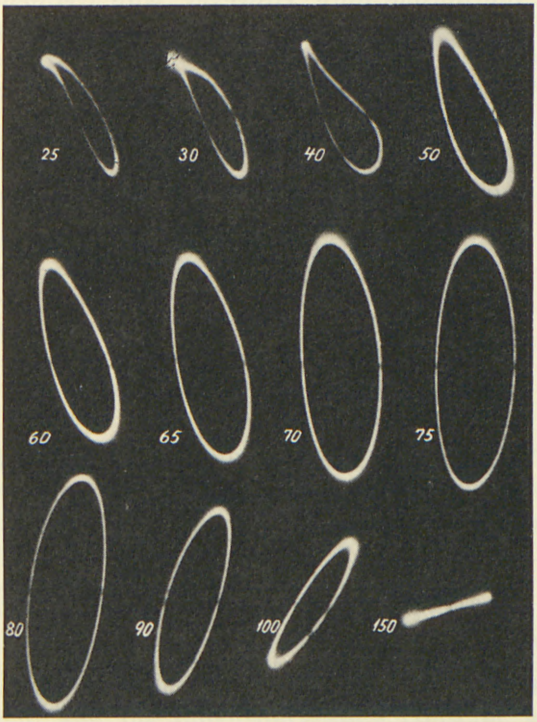

Fig. 5. Lissajous figures representing alternating amplitude (ordinates) versus force (abscissae) at different vibrational frequencies, given by the figures on the curves in c.p.s.
Constant force amplitude, approximately 80 dynes peak to peak. 0° C.

tained as shown in the examples of fig. 5. The fact that this figure was not an oblique line but resembled an ellipse indicated that the changes in length did not follow the changes in external load, i. e. there is a phase difference which corresponds to the presence of a damping in the system. Hence, the Lissajous figure illustrates the mutual relation between the enforced changes in load and the resulting changes in length. At resonance frequency special conditions occur which are dealt with below.

In a series of experiments Lissajous figures were recorded with an approximately constant amplitude of the periodic changes

in load at different frequencies of vibrations (fig. 5). The figures at frequencies < 50 c.p.s. in this case are asymmetrical and, if at all, markedly distorted ellipses. The distortion is an expression of the non-linear hysteresis which characterizes the length-tension diagram of the muscle fibre. However, with frequencies around resonance (in fig. 5. 75 c.p.s.) the Lissajous figures with good

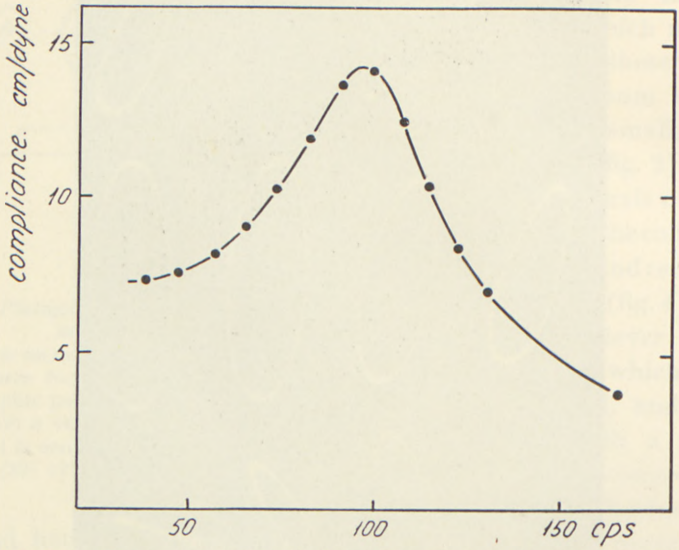

Fig. 6. *Mechanical impedance* of oscillating system + muscle fibre as a function of frequency of vibration. 0° C. Resonance defined by peak impedance = 95 c.p.s., resonance defined by 90° displacement between force and length amplitude = 100 c.p.s.
ordinate: compliance in cm $\times 10^{-5}$ per dyne
abscissa: vibrational frequency in c.p.s.

approximation are ellipses. Hence the simplest assumption is to consider the total oscillating system consisting of muscle fibre plus measuring device as a system which comprises an inertia coupled to a Voigt-element, i.e. a linear damping in parallel with a linear elastic element, moving under the influence of an external alternating force. A further illustration of the applicability of this very simple assumption is given in the experiment represented by fig. 6, which is of the same type as that represented by the ellipses of fig. 5. It shows the ratio between length amplitude and force amplitude as a function of vibrating frequency. The variation of this ratio with frequency is comparable to that which can be expected for

the equivalent system mentioned above. However, the displacement in phase did not correspond to that present in the simple equivalent system (cf. p. 107).

In view of the similarities mentioned, it was appropriate to characterize the dynamic mechanical properties of the muscle fibre around resonance by means of the elastic constants of the simple equivalent system which is composed of a Voigt-element plus an inertia, i. e. the *elastic stiffness* G_{elast} and the damping (η, viscosity) or a quantity derived from η as for example the *viscous stiffness* G_{visc}.

The equivalent system moves under the influence of the periodic force

$$\sigma(t) = \sigma_0 \cos \omega t \tag{1}$$

according to the equation of motion:

$$m\ddot{\gamma} + \eta\dot{\gamma} + G\gamma = \sigma_0 \cos \omega t, \tag{2}$$

where $\gamma(t)$ denotes the deformation, $\dot{\gamma}$ the velocity, $\ddot{\gamma}$ the acceleration of the movement, m the inertia in the system, G_{elast} the elastic stiffness, and η the damping (viscosity). The stationary solution of (2) is of the type:

$$\gamma(t) = \gamma_0 \cos (\omega t - \psi), \tag{3}$$

where the integration constant γ_0 denotes the maximal amplitude of movement, and the other integration constant ψ the phase displacement between the external alternating force and the periodic movement produced by this force. By insertion of (3) and the corresponding velocity and acceleration in (2) two relations are obtained between the integration constants γ_0 and ψ and the constants m, G_{elast}, η, σ_0, and the cyclic frequency ω, which characterize the oscillating system and the alternating force:

$$(G_{\text{elast}} - m\omega^2)\,\gamma_0 = \sigma_0 \cos \psi \tag{4}$$

$$\eta\omega\gamma_0 = \sigma_0 \sin \psi \tag{5}$$

From (4) and (5) we get the following expressions for the maximal amplitude (γ_0) and the phase displacement (ψ):

$$\gamma_0 = \frac{\sigma_0}{\sqrt{(G_{\text{elast}} - m\omega^2)^2 + (\eta\omega)^2}} \tag{6}$$

$$\psi = \tan^{-1}\left(\frac{\eta\omega}{G_{\text{elast}} - m\omega^2}\right) \qquad (o \leq \psi \leq \pi) \tag{7}$$

At *resonance*, defined as the frequency ω_0 at which the external force and the corresponding deformation show a mutual displacement in phase of $\frac{\pi}{2}$, the expression for elastic and viscous stiffness are according to (4) and (5)

$$G_{\text{elast}} = m\omega_0^2 \tag{8}$$

and

$$\eta\omega_0 = \frac{\sigma_0}{\gamma_0} \tag{9}$$

The quantity $\eta\omega_0$ has the dimension of a stiffness and in the following is denoted as G_{visc}, viscous stiffness.

$$G_{\text{visc}} = \omega_0\eta = \frac{\sigma_0}{\gamma_0}. \tag{10}$$

At resonance frequency, the elastic and viscous stiffness which characterize the mechanical properties of the muscle fibre in vibration experiments, can be determined from (8) and (9). By adjusting the frequency of the oscillating system to resonance we obtain G_{elast} (8) and by measuring the corresponding maximal amplitude of movement we obtain G_{visc} (9).

As mentioned above, at resonance the Lissajous figures obtained with good approximation were ellipses. However, a systematic study of these figures gave a small but significant deviation from the shape of a pure ellipse also for these frequencies. It is seen from fig. 5 that one half of the ellipse is more flat than the other. This deviation must be considered an expression of non-linear properties and indicates that the linearly damped equivalent system can be applied only with approximation. This is also obvious from the observation that the dynamic stiffness varies with the amplitude of the alternating force, a phenomenon which will not occur in an equivalent

system of the type applied and which will be dealt with in detail in a later section.

In vibration experiments in which the amplitude of the alternating force produced deformations in the muscle fibre which exceeded 2 per cent of the equilibrium length, the Lissajous figures were always so distorted that they were unsuited for a determination of dynamic stiffness.

From the elastic and viscous stiffness two other quantities can be defined which also characterize the visco-elastic properties of the muscle fibre:

1) The total stiffness of the fibre, G_{tot}:

$$G_{tot} = \sqrt{G_{elast}^2 + G_{visc}^2} \tag{11}$$

a quantity which also was determined in the former vibration experiments performed at a constant mean length of the fibre, and

2) The ratio of viscous and elastic stiffness denoted as sr:

$$sr = \frac{G_{visc}}{G_{elast}}. \tag{12}$$

sr denotes the tangent to the phase displacement between the alternating force acting within the fibre and the length amplitude produced by it.

Arrangement for the determination of the vibrational stiffness.

The external periodic loads were obtained by passing an alternating current via resistance (9) (1500 ohms) through the coil (fig. 3, 5). A low frequency a. c. generator was used as a source for the alternating current (0—330 cycles per sec., output impedance 2400 ohms, power output 3 watts). Since a direct photographic recording of the movements of the coil was not suited for stiffness measurements, the vibration amplitude of the fibre produced by the alternating current was transformed to electrical values.[1] For this purpose a single filament lamp (11)

[1] In recent experiments the photoelectric transmission has been replaced by a transmission which uses variations in electrical capacity, with the coil (*c* fig. 2) as movable condenser plate (BUCHTHAL 1942).

was focussed by the lens (12) upon the mirror (10), which reflected the picture upon a triangular concave mirror (13). The image of the filament of the lamp formed a line of light, which stood parallel to the shortest side of the triangular section of the concave mirror. This line moved across the triangle, the amount of light reflected from the mirror being largest, when the light hit the neighbourhood of the base line of the triangle. The concave mirror reflected an image of the mirror on the photocell (15) and the light spot then illuminated the same area of the cathode of the vacuum photocell (15) independent of the deflection of the mirror (10). A ground glass disc (14) was placed immediately in front of the photocell. This diffused the light and compensated for inaccuracies which might have arisen from small movements of a sharp and brilliant image on the cathode of the photocell, on account of differences in sensitivity in the light sensitive layer. The alternating component of the photoelectric current was amplified approximately 100 times (16) and was led to a sensitive valve voltmeter (17) for measurement and over an amplifier to the Y-plates of the cathode ray oscilloscope (18). The deflection of the electron beam produced by the signal on the Y-plates, thus corresponded *to the instantaneous value of the amplitude of vibration* (γ). The signal for the X-axis was derived from the alternating current generator either directly or over the resistance (6) (5000—2000 ohms) dependent upon the force amplitude necessary to obtain a suitably broad Lissajous figure. This current was a measure of the *instantaneous value of the alternating force* (σ), the mean value of which was read on the valve voltmeter (8). At the resonance frequency for the oscillating system plus muscle fibre the amplitude is at its maximum when the alternating force passes its zero value and vice versa, i. e. when the phase displacement between the force and amplitude is $\frac{\pi}{2}$. This is the case when the axes of the ellipse coincide with the X- and Y-axes of the oscilloscope screen. The elastic stiffness (G_{elast}) can thus be determined from the resonance frequency:

$$G_{\text{elast}} = \omega_0^2 \cdot m = 4\,\pi^2 \cdot m \cdot \nu_0^2, \qquad (13)$$

where ν_0 denotes the resonance frequency in c.p.s. $= \omega_0/2\,\pi$

and m the equivalent mass of the recording system (see equation (2) p. 17).

Fig. 7 shows the position of the ellipse at 3 different frequencies near resonance. The resonance frequency for the fibre investigated was about 74 c.p.s. The frequency range investigated lay between 20 and 200 c.p.s. corresponding to elastic

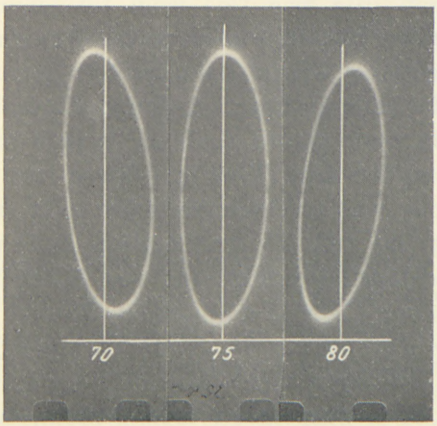

Fig. 7. Lissajous figures giving the correlation between alternating force and alternating length during the oscillation period (alternating length amplitude 2 per cent of L_0 peak to peak). The ellipse marked 75 is close to resonance (74 c.p.s.); displacement of the longitudinal axis to the right corresponds to a frequency of 6 c.p.s. *above* and displacement to the left to a frequency of 4 c.p.s. *below* resonance frequency.

stiffnesses of between 700 and 70000 dynes $\times$ cm^{-1}. The width of the ellipse was a measure of the alternating force introduced, the exact value of which was read on the valve voltmeter (8). Its height was a measure of the amplitude of movement, which was read on the valve voltmeter (17). By this the resistance component, "the viscous stiffness", was determined at resonance frequency ($\eta \cdot \omega_0$). The narrower the ellipse in proportion to its height, the less force was required for the maintenance of the oscillations, and the less the damping, i. e. the viscous stiffness.

Mounting of the muscle fibre.

The muscle fibre or small bundles of 2–10 fibres were fastened by the ends of the tendons to two small pieces of aluminium tubes or to two pairs of silver forceps (g, h, fig. 2) and kept in

a chamber (i) with double walls between which solutions of different temperatures were passed. Thereby the Ringer's solution and the muscle in the silver chamber could quickly be brought to any temperature between — 3° and 30° C. The silver chamber and the forceps were mounted on a plate, which could easily be removed and placed under a binocular microscope for mounting the fibre.

When using the aluminium tubes the fibre was connected to the lever (a, fig. 2) by slipping the thin walled tube which was squeezed on the tendon over the lever. In some experiments the tendon ends were placed each in its pair of forceps (fig. 2 lower graph) and the fibre hung in a loose loop in the Ringer's solution. The loop was placed around the lever (a), which could stretch the fibre (m) with the load desired. Both pairs of forceps could be moved together backwards and forwards by means of a micrometer screw (1) and adjusted at different distances from each other. By transferring the load directly by the lever arm (a) to the fibre, it was possible to avoid the extra mass, introduced by the weight of a suspension arrangement, which could be removed. This type of suspension furthermore had the advantage that the force in the fibre was doubled and the length halved, hence the forces of inertia for a given relative change in length were halved. Comparison of the latter type of suspension with the former, where the fibre was straight, showed that the mechanical and physiological properties of the fibre were not significantly different.

Determination of the constants of the recording system.

(1) *The force in dynes* which acted on the lever (a) by the flow of a given current through the coil (c, fig. 2) could be determined statically by means of a torsion balance or dynamically by a determination of the equivalent mass of the system m,

$$m = \frac{I}{l^2}, \tag{14}$$

where I is the moment of inertia and l the length of the lever; both procedures have been used and gave, in good agreement,

values of 5.0 dynes per mA. The static determination was the more accurate. In this case the error was due to small variations in the length of the lever arm and was about 2 per cent, corresponding to a displacement of the point of action of the force of 0.5 mm. In a range of length variations of 1 cm the variations of the force-strength constant did not exceed 5 per cent.

(2) *The equivalent mass* (m) was also determined in two ways. When a known alternating force, $\sigma_0 \cos \omega t$ with a known angular frequency (ω) was introduced into the oscillating system, m was found from the maximal amplitude measured (γ_0):

$$m = \frac{\sigma_0}{\gamma_0 \cdot \omega^2}. \tag{15}$$

The equivalent mass was further determined by loading the oscillating system with a known additional mass m'. When σ_0 and ω were kept constant and the amplitude of oscillation was measured *with* (γ_0') and *without* (γ_0) additional mass, we obtain:

$$m + m' = \frac{\sigma_0}{\gamma_0' \cdot \omega^2}. \tag{16}$$

From this we find

$$m = \frac{m' \cdot \gamma_0'}{\gamma_0 - \gamma_0'} \quad \text{and} \quad \sigma_0 = \frac{\omega^2 \cdot m' \cdot \gamma_0 \cdot \gamma_0'}{\gamma_0 - \gamma_0'}. \tag{17}$$

With both procedures the equivalent mass was found to be 0.045 g. This figure refers to the oscillating system in air. In liquids the acceleration of the liquid masses which surround the lever (a), introduced an extra mass, which was equal to about 0.010 g. The increase in equivalent mass produced by the fibre or fibre bundle did not exceed 5 per cent of the total equivalent mass. In the later experiments an improved oscillating system was used in which the equivalent mass could be reduced to 0.023 g.

(3) *Damping of the system.* In model experiments, in which the muscle fibre was replaced by a very thin spiral spring, at resonance a vertical line was obtained on the screen of the oscilloscope instead of an ellipse, which appears with the muscle. This indicated that the damping of the system itself in air was without significance for the measuring results. Using a metal

spiral spring which together with the recording system had resonance at a frequency of 100 c.p.s., the damping resistance in air was 0.1 dynes cm^{-1} sec., i. e. the viscous stiffness was 1/300 of the elastic stiffness. When the lever of the oscillating system was immersed in Ringer's solution, a damping arose, which, however, was less than 10 per cent of that found for the muscle fibre.

The inertia of the system is of decisive importance in evaluating the velocity and amplitude of variations in length. This is illustrated by a typical example of an isotonic contraction at low load and high temperature (25° C.). Low load and high temperature were chosen in order to obtain large forces of inertia in proportion to the forces developed by the fibre. This was obtained, not only because the fibre tension was small, but also because the velocity of shortening and hence the acceleration was large. In the example examined the equilibrium length of the fibre was 0.5 cm (in the recording system 0.25 cm) and the load 150 dynes, corresponding to 0.20 P_0. With this load and at 25° C., the maximum shortening was reached within 60 msec. The shortening amounted to 0.1 cm (in the system 0.05 cm), corresponding to 20 per cent of the equilibrium length. In the first 5 msec., the fibre had reached its "maximal shortening velocity", which amounted to 5.5 cm per sec. (corresponding to 2.75 cm per sec. in the system). The relative shortening velocity was about 11 L_0 per sec. (L_0 = equilibrium length). In the present recording system, which had an equivalent mass of 0.055 g. (reduced to the point of action of the fibre), the acceleration from velocity 0 to a velocity in the recording system of 2.75 cm per sec. within the interval 5 msec. required a force of inertia of about 30 dynes in addition to the constant force of 150 dynes.

In the next 40 msec. the velocity decreased continuously from 2.75 cm per sec. to 0. This gives a force of inertia of 4 dynes. At the load used, the stiffness of the fibre was twice the resting stiffness, i. e. 8000 dynes $\times$ cm^{-1} and the force of inertia will, therefore, give a shortening of 5 μ in addition to the purely isotonic one. This corresponded to an increased shortening caused by the forces of inertia, of the fibre of 2.5 per cent of the shortening in a system without mass. This artifact decreased with increasing load, since the stiffness increases and the acceleration is reduced, because of decreasing velocity of change in length.

The ratio between the force developed by the fibre (P_0) and the force of acceleration caused by the mass of the recording system, P_s, gives a possibility to compare the recording system used here with a good system used for whole muscles. In the present example, with a fibre length of 0.5 cm, a P_0 of 750 dynes, a maximal shortening velocity of 5.5 cm per sec. (corresponding to a velocity in the recording system of 2.75 cm/sec.), and an acceleration in the system of 69 cm $\times$ sec.$^{-2}$, the relative shortening velocity was 11 L_0 per sec., and the relative acceleration 274 $L_0 \times$ sec.$^{-2}$. The force of acceleration was 4 dynes. This gives a P_s which is 0.5 per cent of P_0.

When a pair of sartorius muscles with an equilibrium length of 3 cm, a P_0 of 10^5 dynes, and a corresponding relative acceleration is considered, which in the isolated fibre was 274 $L_0 \times$ cm^{-2}, the true acceleration is 822 cm $\times$ sec.$^{-2}$. With an equivalent mass of 3 g the force of acceleration becomes 2466 dynes and P_s = 2.5 per cent of P_0. Recently ABBOTT and RITCHIE (1951, b) have used a recording system for whole muscle with an equivalent mass of 75 mg. With a P_0 = 40 g this gives a P_s = 0.16 per cent of P_0.

Sensitivity of the recording system to variations in length and load.

In the direct photographic recording a light lever was used which gave a magnification of 10 times. Assuming 0.1 mm on the recorded curve to be the limit of accurate reading, this corresponded to a change in length of the fibre of 0.01 mm. The stiffness of the recording system was measured to 8—10 dynes $\times$ cm^{-1}, i. e. a load of 0.01 dyne could still be detected on the muscle fibre.

In the experiments the length was recorded photographically as a function of time. The velocity of the change in length corresponded to the gradient of the recorded curve employing the magnification 1:10 between the change of length of the fibre and the light spot on the film (recording velocity 25—100 mm per sec.). By this method we have measured the velocity of shortening and relaxation during and after contraction and the velocities of

the changes in length produced by sudden variations in load at rest and during contraction.

By using a photoelectric transmission, the sensitivity was increased considerably. A change in length of only 0.5 μ could be detected; this corresponded to measurements of changes in the fibre length of 0.01 per cent of L_0. By using the photoelectric transmission the linear recording range corresponded to a movement of 1 mm of the lever, measured at the point of action of the fibre. The linearity was controlled by reading the deflection in millivolts caused by the alternating amplitude, when the oscillating light spot covered different areas of the concave mirror (13, fig. 3) corresponding to different mean positions of the lever (a, fig. 2).

The sensitivity to periodic variations in load depended upon their frequency and on the frequency characteristic of the oscillating system plus the fibre, varying with the elastic and viscous stiffness of the fibre (fig. 6). The maximal frequency at which measurements still could be taken amounted to 300 oscillations per second.

Before and after each experiment the absolute sensitivity for changes in length was determined by introducing a known length amplitude and measuring the amplified alternating current component of the photoelectric current by the valve voltmeter (17). The accuracy of this calibration depended on the accuracy with which the deflection of the light spot could be determined and its error did not exceed 5 per cent. A maximal amplitude of deflection (peak to peak) of 0.5 cm, which after amplification gives 100—150 mV, usually was used for calibration (denoted mV_5). At a magnification of 1:10, the amplitude of deflection of 0.5 cm corresponded to a movement of the fibre of 0.05 cm, i. e. the maximal deflection from the equilibrium position was 0.025 cm.

By means of the valve voltmeter (17, fig. 3) the length amplitude γ_0 was determined in cm:

$$\gamma_0 = \frac{0.025}{mV_5} \times mV_x, \tag{18}$$

where mV_x denotes the length amplitude in millivolt produced by the alternating force applied.

The maximal value of the alternating force σ_0 is expressed in dynes:

$$\sigma_0 = \mathrm{mA_{eff}} \cdot \sqrt{2} \cdot 5, \tag{19}$$

where 5 gives the conversion factor from mA to dynes, and $\sqrt{2}$ the ratio between the maximal and the effective value of the current. The alternating voltage was measured by means of the valve voltmeter (8). By introducing a resistance of 1500 ohms (9, fig. 3) the current in mA was obtained by multiplying the voltage read on the valve voltmeter with $\frac{1000}{1500} = 0.667$; σ_0 then becomes:

$$\begin{aligned} \sigma_0 &= \mathrm{Volt_{eff}} \cdot 0.667 \cdot \sqrt{2} \cdot 5 \\ &= \mathrm{Volt_{eff}} \cdot 4.7 . \end{aligned} \tag{20}$$

The ratio between viscous and elastic stiffness (sr) is obtained by substituting the values measured for σ_0, γ_0, and ν_0 and the equivalent mass m in equations (8), (10) and (12) p. 18:

$$sr = \frac{\mathrm{Volt_{eff}}}{\mathrm{mV}_x} \times \frac{\mathrm{mV}_5 \cdot 85.5}{\nu_0^2}, \tag{21}$$

where ν_0 denotes the frequency of the periodic variations in load, measured at resonance in c.p.s.

Sources of error in mounting the fibre in the measuring device.

The fastening of the fibre in the forceps (g, h, fig. 2) introduced a slight increase in stiffness in the immediate vicinity of the point of attachment, since the possibilities for deformation here were limited. This error must be considered to be proportional to the stiffness itself; it was only of significance in the estimation of absolute values of stiffness and moduli of elasticity. This error was reduced by the choice of thin and long preparations.

When the fibre was placed in the V-shape, an error in the determination of stiffness was introduced by stretching the fibre

with the lever (a, fig. 2). The deformations of the fibre were limited in the region where it touched the glass rod. Further inspection of this region showed, however, that the fibre was pressed tightly against the glass rod, so tightly that even with much larger movements than those which were used in the present experiments, it was impossible to detect any slip in the area of contact. In order to ensure that as small parts of the fibre as possible were blocked, it was desirable to use a glass rod as thin as possible without, however, damaging the fibre or blocking the propagation of the contraction. Comparisons with experiments in which the fibre was placed in a straight line by fastening it directly to the lever, showed that the V-shaped mounting did not measurably influence the viability or contractility of the fibre (see p. 22).

With regard to the free mobility of the lever it was important, especially for short fibres, that the distance between the forceps was less than 2 mm. The two halves of the fibre did not lie completely parallel, which implied that the resulting force was less than the arithmetic sum of the forces in the two halves. This could cause a difference of a few per cent between the measured and the actual stiffness. Since in these experiments fibres or fibre bundles were used which were as long as possible (large Hungarian frogs), this deviation lay below the accuracy of measurement.

The determination of the absolute value of the *elastic stiffness* was affected, as previously mentioned (p. 23), by changes in the equivalent mass of the system, which arose on account of the acceleration of liquid masses round the lever and of the mass of the fibre itself, when it was placed in the Ringer solution. Hence a slight decrease in resonance frequency should have been expected as compared with the frequency which was found when the fibre was examined in a moist chamber in air. However, an increased resonance frequency was found when the fibre was transferred from air to Ringer's solution, but only as long as the fibre was subjected to a small load. The difference amounted to up to 20 per cent in resonance frequency. The reduced stiffness which was found for the fibre in air, presumably was caused by the surface tension of the Ringer solution which adhered to the fibre and took over part of the force which the

lever transferred to the fibre. Since stiffness is a function of tension, the stiffness arising from the internal tension of the fibre will be reduced. The length-tension diagram, obtained by placing a fibre bundle of 1 mm diameter alternatively in air and in Ringer's solution, showed that the surface tension at a low degree of stretch gave an additional force of about 30 dynes when the bundle was in air. This error was of no significance when the fibre was investigated in Ringer's solution. The Ringer's solution in the chamber was filled up to the same height in relation to the position of the fibre and the lever, hence the small error, which was due to the damping caused by the solution, was kept constant. By comparing the *viscous resistance* of the muscle fibre, with and without Ringer's solution, it was found that the damping introduced by the Ringer's solution was less than 10 per cent of the viscous stiffness measured.

The accuracy of measurement in the determination of elastic and viscous stiffness.

The errors, which arose from uncertainty in the determination of the constants of the oscillating system or in the absolute calibration, were constant errors for a series of measurements. The measurements in the experiments were encumbered with the following uncertainties:

1. The accuracy in the visual phase determination on the screen of the cathode ray oscilloscope was 1 degree.

2. The accuracy of the frequency standard which entered into the determination of the resonance frequency was 0.5 per cent.

3. The accuracy of determining the ratio between the amplitude of the force applied and the alternating amplitude arising from it $\left(\frac{\sigma_0}{\gamma_0}\right)$ corresponded to the errors introduced by the two valve voltmeters amounting to 2 per cent plus the uncertainty, arising from noise in the amplifier which for the smallest amplitudes applied (0.05 per cent of L_0) was 2 per cent. This gave a total uncertainty of at most 3.5 per cent.

The uncertainties (1) and (2) gave a resulting accuracy for

the determination of the elastic stiffness of about 2.2 per cent when $sr = 1$, and 1 per cent when $sr = 0.5$. In addition to this there were the previously mentioned constant errors. The uncertainty in the determination of sr amounted to 3.5 per cent, excluding the error on the calibration for m, σ, γ.

Procedures used in transient experiments.

1. Introduction of a sudden change in load (isotonic transient).

An increase or decrease in load was effected by a change in the current in the coil (a) of the isotonic myograph (fig. 2). The resulting change in length of the fibre was recorded either by a direct optical method or via the photoelectric transmission described. In the latter case a relay system was used for adjusting the time intervals between release of a single sweep on the cathode ray oscilloscope and the time for the change in load. The effect of the forces of inertia on the size and time course of the change in length are discussed in the section which deals with the initial process (see p. 45).

2. Introduction of a sudden change of length (isometric transient).

The electromagnetic arrangement, which was previously used for measurements of elasticity under isometric conditions, and which produced changes in length, was employed for this purpose (Buchthal *et al.* 1944a, fig. 1). A sudden change in current in the coil of the electromagnet was introduced instead of periodic changes in length. This produced a sudden movement of the forceps, which was limited by two adjustable stops. The time necessary for the system to adjust itself to the new length depended partly upon its equivalent mass (0.4 g.) and partly upon the velocity with which the moving force in the system increased when the current passed through the coil. Within the short intervals during which the variation in length took place, it must be considered that the moving force on account of inductance in the recording system, increased linearly with time and consequently that the length varied with the third power of time (p. 57).

Recording of isometric release contractions. Release from the isometric maximum with different constant release velocities.

The elements of the experimental device are shown by the block diagram in fig. 8. The muscle fibre was placed in a chamber at 0° C. and fastened with two pairs of forceps at the tendon ends (1) and (2). The mechanical tension was transferred via the forceps (1) to the condenser myograph (BUCHTHAL *et al.* 1944a).

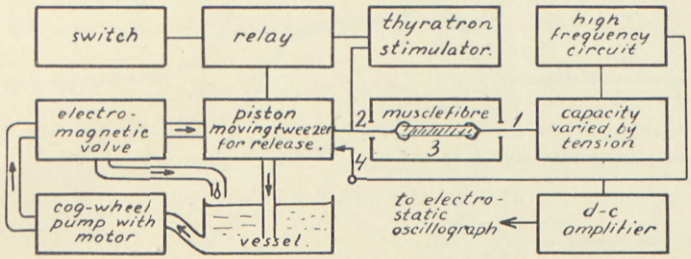

Fig. 8. Block diagram of the arrangement for recording work diagrams during release contraction. (1) and (2) pairs of micro-tweezers to hold tendon ends of fibre. (3) muscle fibre. (4) contact recording 5 mm movement of piston and tweezer (2).

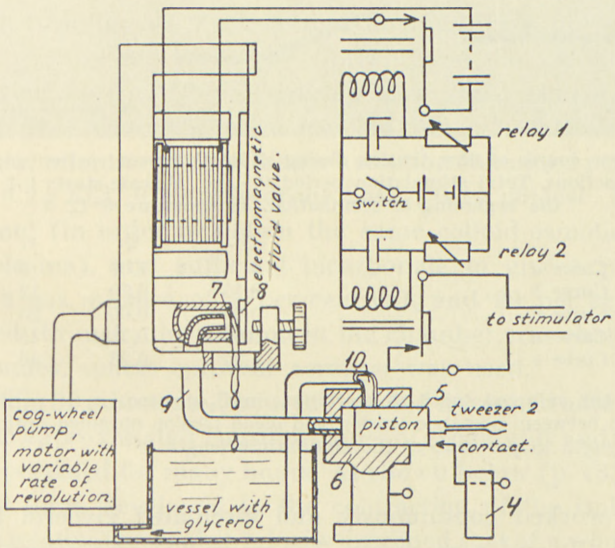

Fig. 9. *Device for operating release.*
Electromagnetic fluid valve (7) governing movement of piston (5). relays operating release (1) and stimulator (2). (4) contact marking a movement of 5 mm. (6) cylinder in which (5) moves. (8) disc to close valve (7). (9) tube connection to (5). (10) tube connection to vessel with glycerol, to prevent excessive pressure.

The variation in length was introduced via the forceps (2) through an electrically operated hydraulic transmission. The forceps (2) was connected with the piston (5) which moved in the cylinder (6). A cog-wheel pump with variable rate of re-

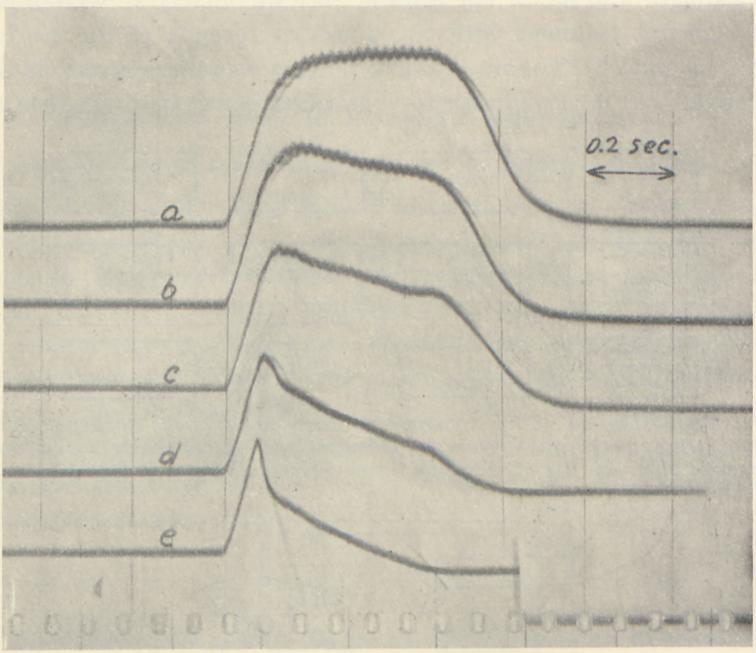

Fig. 10. Time course of fibre tension during a) isometric contraction and b–e) release contractions. Total stimulation period 0.5 sec. Release starts 0.1 sec. after the beginning of stimulation. Temperature 0° C.

	V.	Q.	x.
Curve a	0	1.00	0
Curve b	0.15	0.79	12
Curve c	0.30	0.60	23
Curve d	0.93	0.31	45
Curve e	1.27	0.23	46

V denotes the enforced speed of shortening in L_0 per sec.
Q the ratio between isometric tension and mean tension obtained during release.
x release-length in per cent of the equilibrium length.

volution worked continuously and circulated glycerol between the valve (7) and a reservoir. The valve (7) was operated electromagnetically. To close the valve (fig. 9) the relay operated a disc (8) and the liquid was pumped through the pipe (9) to the piston (5). This caused the forceps (2) to move with con-

stant velocity. When the piston (5) had moved the forceps (2) about 1 cm, the liquid left the cylinder (6) through the tube (10). By means of a switch (see fig. 9) the current was led to relay (2). The time of contact of these relays could be independently delayed. By this means the muscle fibre could be stimulated and allowed to contract isometrically (relay 2) before the change in length was released by means of relay (1). The stimulation was continued during the whole change in length, or in other experiments for 5 seconds. For controlling the velocity, the switch (4) indicated the time, when the piston had moved 5 mm.

The work produced was calculated as the product of the mean value of the tension during the release experiment and the change in length introduced. The effect of the velocity of release on the tension produced in contraction is seen in fig. 10.

Preparation of the muscle fibre.

The experiments were carried out on single fibres or small bundles consisting of 3—20 fibres, from the semitendinosus muscle of the frog (*Rana esculenta* and *Rana temporaria*). The muscle fibre was isolated in ice-cold Ringer's solution under a binocular microscope. The Ringer's solution contained per liter 6.7 g NaCl, 0.2 g KCl, 0.2 g anhydrous $CaCl_2$, 0.2 g glucose, 3 per cent dextrane[1] (in order to obtain the same colloid-osmotic pressure as in plasma), and sufficient bicarbonate to give a pH of 7.3, when a gas mixture of 1 per cent CO_2 and 99 per cent O_2 was bubbled through; the solution in the chamber was changed every 15 minutes, unless constant aeration was used.

Within 30 minutes to 1 hour the isolated fibres had adjusted themselves to approximately constant values of excitability and shortening which persisted for many hours. As shown below (p. 133, 149) the specific force developed in the contraction of the isolated fibre and its relative shortening velocity exceeded that of a whole muscle, and it will hardly be justified to interpret possible differences as being due to "weak spots" or "invisible injuries". An injury,

[1] Dextrane kindly was supplied by A. B. Pharmacia, Stockholm.

however small, caused an essential decrease in contractility and excitability in the course of 10 minutes and these fibres obviously had to be excluded from further measurements. Also small injuries could be detected optically as an increase in opacity of the fibre.

Temperature: In the majority of the experiments the standard temperature in the Ringer's solution surrounding the muscle fibre was 0° C. To obtain constant temperature salt water of suitable temperature adjusted by means of a thermostat was passed by a circulation pump through the side walls and the bottom of the muscle chamber (k, fig. 2). In the circulation system a stop cock was inserted, whereby it was possible to shift quickly from circulating fluid of 0° C. to a desired higher temperature. By a thermocouple placed in immediate neighbourhood of the muscle fibre, the temperature of the Ringer's solution was checked continuously.

Electrical stimulation.

The fibre was stimulated by rectangular pulses, the strength, duration, and frequency of which could be varied. The duration and frequency were adjusted to give maximal reaction at the temperature in question. The strength was at least 3—5 times the threshold value and was measured by a valve voltmeter in the stimulation circuit. In experiments at 0° C. an impulse with the duration of 10 msec. usually was applied, and, in tetanic contraction, the stimulation frequency was 15—20 c.p.s.

For stimulation an electric field was produced along the length of the fibre (Ramsey and Street 1941) by leading the stimulus to two silver plates coated with silver chloride, which were placed, at right angles to the axis of the fibre, at the forceps and at the lever arm, respectively. Between these plates a homogeneous field was produced. By adjusting the stimulation to be sufficiently above the threshold value, it was possible to excite the fibre so as to get simultaneous activation of the major part of it. Even if a propagation of the impulse over the whole length of the fibre had to be taken into account, this would only take 10 msec.[1]

[1] Assuming a propagation time of 1.6 m. per sec. (20° C., Katz 1948) and a temperature coefficient $Q_{10} = 2$.

and would not be of decisive importance either for the shortening velocity or the position of the initial maximum of stiffness. In order to produce a homogeneous field along the longitudinal axis, the walls of the muscle chamber were covered with an electrically insulating paint. When the stimulation was transferred exclusively by way of the forceps, and the fibre was placed in V-shape, the conditions for obtaining maximal reaction were less well defined. Part of the experiments were performed on fibres from completely curarized muscles (d-tubocurarine chloride[1] 50—250 μg per g frog).

Determination of equilibrium length and measurement of changes in length.

The equilibrium length (L_0) of the fibre or the fibre bundle was defined in the present experiments as the length with a load of 5 dynes (appr. 0.005 P_0), and was determined directly with a microscope. The forceps were adjusted with the micrometer screw (1, fig. 2) until the recording system came into equilibrium. The position of the light spot on the recording camera (20, fig. 4) or on the triangular concave mirror (13, fig. 3) was used as an indicator and the value was read on the micrometer screw. Every change in the length of the fibre was shown by a movement of the light spot and was measured by moving the micrometer screw until the spot regained its original position. The difference between the readings of the micrometer screw at equilibrium length and the new length gave the variation in length in mm.

In order to be able to compare the experimental results from fibres or fibre bundles of different diameters in the final treatment of the material, the relative length was used instead of the length measured in cm, the equilibrium length (L_0) being used as a reference length (see p. 40). The velocity of movement was also expressed relatively, the absolute velocity measured in cm per sec. being divided by the equilibrium length of the fibre measured in cm.

[1] Tubarine, Borroughs-Wellcome Co.

Experimental procedure:

1. Determination of fibre length at rest and during contraction as a function of load and time.

At rest the length of the fibre was determined at a given load by the compensation method, i. e. through a movement of the micrometer screw (1, fig. 2) with the light spot as an indicator. During isotonic contraction the length was recorded photographically for direct analysis of the length-time dependence as shown in fig. 4.

Measurements of the force in isometric contractions were performed by supporting the fibre (n, fig. 2) at a definite length at rest. A force P_0 was transmitted by way of the lever (P_0 denoted the maximal force in isometric tetanic contraction). The supported and loaded fibre was stimulated to tetanus, and after 1—2 sec. of stimulation, when the maximum tension of contraction could be expected to have been reached, the external force was decreased until a movement of the light spot was just observed. The deviation from purely isometric conditions was less than 0.5 per cent of the equilibrium length.

2. Recording of release contractions with different loads at rest.

The experiments started by the application of the desired load at rest and measurement of the corresponding length by compensation with the micrometer screw. The fibre was then supported at this length and a load was introduced which exceeded P_0. The latter was measured by a slow reduction of the load as in isometric contraction; and the load was then reduced *during the tetanus* until the resting load was reached. The new length in contraction could be measured by compensation with the micrometer screw.

3. Determination of dynamic elastic and viscous stiffness at rest and in tetanic contraction.

Measurement of the resonance frequency (ω_0) at rest with different amplitudes of the periodically varying load was performed by varying the frequency of the alternating current

generator until the axes of the Lissajous figure ("ellipse") coincided with the axes of the oscilloscope screen. The amplitude of oscillation was varied from the lowest value which permitted phase discrimination, stepwise upwards, until the periodic variations in load caused changes in length of the fibre of about 2 per cent of L_0 (peak to peak). The measurements at low amplitude were then repeated. Values for the force and length amplitude were read on the valve voltmeters (8) and (17) (fig. 3). Unless otherwise stated in the following the values of amplitude denote the deflection from the mean position. The absolute value of the smallest *amplitude of oscillation* used amounted to 1 μ which was measured with an accuracy of about 0.1 μ; the largest amplitudes used were 50 μ. The length amplitudes (γ_0) were expressed in per cent of L_0. Their absolute values were calculated by means of equation (18). Hence the length amplitude in per cent of the equilibrium length becomes:

$$\gamma_0 = \frac{2.5\ \mathrm{mV}_x}{L_0\ \mathrm{mV}_5}, \qquad (22)$$

where L_0 denotes the equilibrium length measured in cm, mV_x the deflection in millivolts measured on the valve voltmeter (17, fig. 3), corresponding to a definite force amplitude, and mV_5 the deflection read in millivolts on the valve voltmeter, which corresponded to a length amplitude of the recording system of 0.05 cm (peak to peak). The relative length amplitude in the experiments varied between 0.02 and 1 per cent. At an amplitude of movement of about 3 per cent, the oscillations of the force amplitude were of the same order of magnitude as the mean tension.

The amplitudes of the oscillating force producing the length amplitudes varied between 15 and 80 dynes. In the majority of experiments the force did not exceed 50 dynes. The force acting on the fibre can be obtained by subtracting the inertial force from the external force (p. 80). In order to minimize errors in the measurement of the resonance frequency in isotonic tetanic contraction the displacement of the light spot was compensated for by moving the entire contracted fibre and the attached lever back to the initial position. This ensured that the same area of the light sensitive layer of the photo-electric cell was illuminated

as at rest. ω_0 was then adjusted in the same way as described above for the resting fibre. During isometric contraction the resonance frequency was determined when P_0 was reached and the load just permitted the fibre no longer to touch the support n (fig. 2). Also during isotonic and isometric contraction the measurements were performed at different amplitudes of oscillation.

When measuring stiffness during tetanic contraction, the small fluctuations of length, which at high temperature (20°—24° C.) even at maximal tetanic contraction could not be avoided, caused the Lissajous figure to "jitter" and a satisfactory determination of the resonance frequency became extremely difficult. Therefore, it was necessary in these experiments to use a phase-corrected high-pass filter. In the frequency range 25—150 cycles per sec. the phase displacement of the filter introduced an error in the resonance frequency measurements of less than 1 cycle per sec. In the experiments in question the resonance frequency was measured at rest and during tetanic contraction using the same filter.

In order to investigate elastic and viscous stiffness under the same conditions, but with *different* ω_0, an additional mass (equivalent mass = 0.7 g) was placed on the lever, so that the equilibrium between the force of inertia and the elastic force was obtained at about a quarter of the resonance frequency without extra mass. In order to check on time effects during a given experiment the resonance frequencies with additional mass were determined before and after the basic measurements, i. e. determinations without additional mass.

Part II.

1) The rheology of the resting fibre.

Length-tension diagram of the resting fibre.

A length-tension diagram of the resting muscle fibre showed in agreement with previous investigations carried out under isometric conditions (Buchthal 1942), an approximately exponential increase in tension with increasing length (fig. 11). Length 100 denotes the equilibrium length (L_0), and the tension (P) is expressed in relative units (P/P_0), where P_0 corresponds to the

isotonic load which causes the shortening velocity zero, i. e. the tension found at the indifference point of the length-tension diagram, the point at which the curve for the isometric maxima and the curve for the resting fibre coincide. This tension corresponds very closely to the maximal tension, developed in an

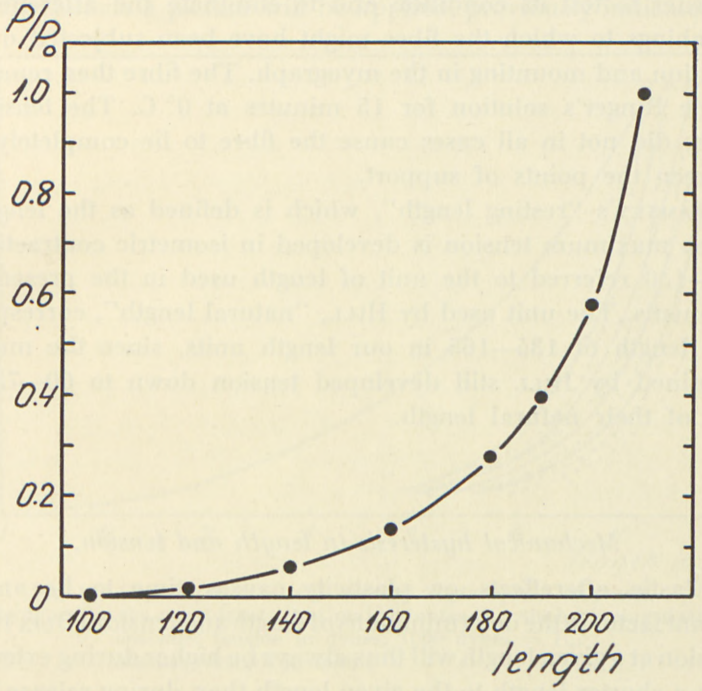

Fig. 11. Static length-tension diagram of the isolated fibre at rest. Mean curve of many experiments performed with increasing and decreasing length. 0° C.
ordinate: tension in units of P_0.
abscissa: length in per cent of L_0, definition of L_0 see text p. 35.

isometric tetanic contraction (Hill 1938). The curve given in fig. 11 represents a mean value of many experiments at 0° C., each of which is a mean curve for rising and falling tension. Also in the present material *static stiffness*, i. e. the gradients of the length-tension diagram, increased proportionally to the load corresponding to the exponential increase in tension with elongation of the fibre (cf. Buchthal 1942).

Since different investigators have used different criteria for a reference length, it is necessary to define the length unit used in the present experiments and to relate it to "resting length" (Ram-

SEY and STREET 1940) and "natural length", "length in the body" (HILL 1949, e).[1] By equilibrium length (length 100) is understood the length at which the fibre develops a tension of 5 dynes corresponding to approximately 0.005 P_0. Before the equilibrium length was determined, the fibre was stimulated to 1—3 twitches in order to test its condition and to eliminate the aftereffect of stretchings to which the fibre might have been subjected during isolation and mounting in the myograph. The fibre then remained in the Ringer's solution for 15 minutes at 0° C. The tension 5 dynes did not in all cases cause the fibre to lie completely taut between the points of support.

RAMSEY'S "resting length", which is defined as the length at which maximum tension is developed in isometric contraction is 120—130 referred to the unit of length used in the present experiments. The unit used by HILL, "natural length", corresponds to a length of 135—165 in our length units, since the muscles examined by HILL still developed tension down to 60—75 per cent of their natural length.

Mechanical hysteresis in length and tension,

Elastic aftereffects or plasticity causes time to be an important factor in the determinations of length and tension (BLIX 1892). Tension at a given length will thus always be higher during extension from a shorter length to the given length than during release from a longer length. Moreover, the tension will be lower the *longer the time interval* in which the muscle fibre had previously been subjected to stretching, and the higher the degree of stretching to which it had been subjected. Due to these different factors, a length-tension diagram will show *hysteresis*, the amount of which depends upon the way in which the length-tension diagram is obtained. As indicated by a number of different findings (e. g. transient experiments cf. p. 45 ff.), this hysteresis is not caused by Newtonian viscosity, i. e. a resistance arising from internal friction which increases linearly with the velocity of deformation but is explained as a "*structural viscosity*".

[1] ABBOTT (1951) uses "maximum length in the body, (resting length)" as reference.

In the following it will be shown in detail, how the muscle fibre adjusts itself with considerable retardation to changes in its state, e. g. in length, tension, or temperature. Neither a linearly acting damping, nor fluid displacements can explain this delay adequately. Therefore, in the interpretation of the following experiments a picture will be applied, previously indicated by

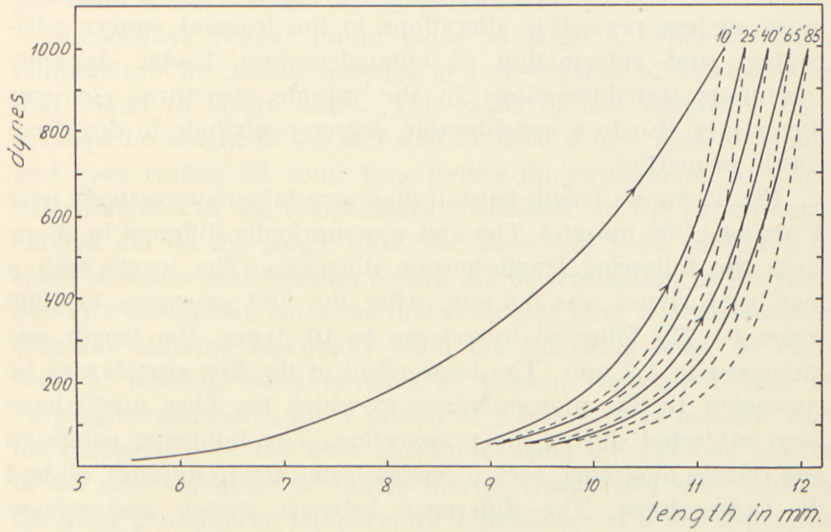

Fig. 12. *Series of successively recorded length-tension diagrams.* 0° C. The figures on the curve denote the time in minutes after the beginning of stretch.
ordinate: tension in dynes, 1000 dynes = P_0.
abscissa: length in mm.

Hill (1931) for the active fibre which corresponds with certain modifications to the conception of minute structure arrived at in rubber-like substances and in high polymers.

The fibre is assumed to consist of chains of contractile material which are entangled at random, but hold a certain degree of longitudinal orientation. The disrupture and the reformation of the entanglements will determine the delayed reaction of the fibre to external or internal mechanical alterations. This interpretation of the minute structure is supported by the fact that torsional rigidity of the isolated fibre exceeds 20—5 times that of a system of parallel chains without entanglements (Sten-Knudsen 1950). This finding demonstrates the important rôle of cross-linkages for the minute structural pattern. A change in load will imply

an alteration in the minute structural pattern of the fibre. The velocity with which this proceeds depends upon the frequency for the transitions in the structure which cause these alterations; its final size depends upon the minute structural elements and the texture in which these are organized. A difference in length at the same tension obtained by extension or release under static and semidynamic conditions must essentially be interpreted as more or less reversible alterations in the textural pattern (disrupture and reformation of entanglements). Under dynamic conditions transformations in the minute structural elements themselves also to a considerable degree contribute to the viscoelastic properties.

Fig. 12 shows length-tension diagrams taken successively over a period of 90 minutes. The first was markedly different in shape from the following length-tension diagrams. The length with a load of 5 dynes was 6.5 mm. After the first extension to 1000 dynes ($= P_0$) followed by release to 10 dynes, the length was increased to 8.7 mm. The large effect of the first stretch may be concealed by the manipulations to which the fibre might have been subjected during the preparation. The following extension and release diagrams, each of which lasted for 15 minutes, all had the same shape. The difference between stretch and release amounted maximally to 0.35 mm and the elongation after a cycle was about 0.2 mm.

The difference between the first curve and the following length-tension diagrams must be due to a large alteration in the minute structural pattern of the fibre, which required about 1 hour for restitution. This alteration in structure was also reflected in the change in the elastic properties. The stiffness of the fibre *varied* more strongly with the tension after the first extension, the stiffness then being higher at maximal loads and—considerably lower at small loads.

Effect of temperature.

The *temperature* only very slightly affects the length-tension diagram of the resting fibre. The variation in tension with temperature is maximal at length 120 and the increase in tension

at the same length amounted to 0.15 per cent per degree of increase in temperature (BUCHTHAL et *al.* 1944a). The percentage variation in tension thus was less than half of the corresponding variation in absolute temperature, in contrast to rubber, for example, for which a proportionality to the absolute temperature is found. The temperature coefficient found for the resting tension of the muscle fibre corresponded to a decrease in *length* of 1 per cent at an increase in temperature of 25° C.

JOSENHANS (1949) found twice as large a dependence on temperature for whole muscles at low degrees of extension as that found in single fibres. The cause of this difference may perhaps be sought in the fact that he used a new muscle, which had been resting for some time before the experiment, for each determination of the temperature coefficient. In the experiments carried out on the single fibre, the fibre had been subjected to some stretches and releases before the determination of the temperature coefficient, since the first stretching gave a length-tension diagram differing essentially from the following ones. At each level of tension, measurements of tension were performed at varying temperatures for a period of 2 hours. It is possible that the component of the fibre tension causing the different course of the first extension is chiefly thermo-elastic and may explain the more pronounced temperature dependence at a low degree of stretch found by JOSENHANS.

An inversion of the temperature dependence from length 144 was found by JOSENHANS and by WÖHLISCH and GRÜNING (1943). Since 44 per cent of stretch in a whole muscle containing fibres of different equilibrium lengths may well indicate that some of the fibres are stretched about 100 per cent, the inversion found does not disagree with the experiments on single fibres, in which the temperature coefficient was examined only up to length 180. The decreasing temperature dependence found with increasing degree of stretch does not exclude a point of inversion at higher stretch. The reversed temperature dependence may also, however, be due to the intramuscular connective tissue, which will play a more important rôle in a whole muscle than in a single fibre.

The elastic after-effect had a different temperature dependence in the muscle fibre than in rubber. As appears from the length-

tension diagrams in fig. 13 the hysteresis in the fibre bundle is larger at 21° C. than at 0° C. In the example shown in fig. 13 the increase and the decrease in length took 20 minutes. The hysteresis at 21° C. amounted to 22 per cent of the maximal tension and at 0° C., to only 14 per cent. We have found the

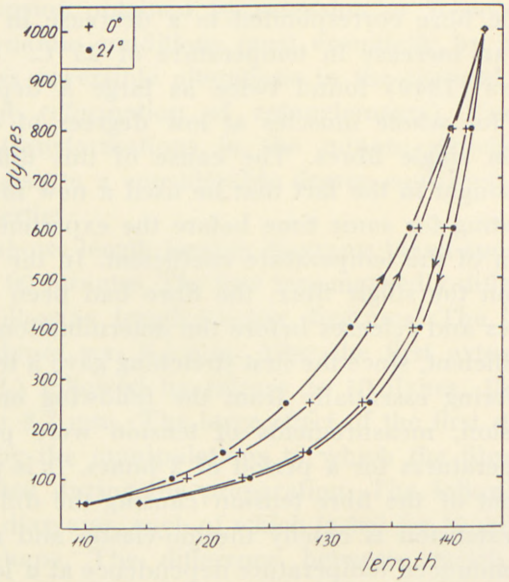

Fig. 13. Static length-tension diagrams recorded with increasing and decreasing tension. Duration of each cycle 20 minutes. First cycle 0°, second cycle 21°, and third cycle 0° C. Curve at 0° C. represents mean from the first and the third cycle.
ordinate: tension in dynes, P_0 = appr. 1000 dynes.
abscissa: length in per cent of L_0.

reverse to be the case for normally vulcanized rubber, the hysteresis at 25° C. being 16 per cent and at 0° C. 37 per cent of the maximal tension (L = 1200), while the hysteresis was larger—but less dependent on temperature—in undervulcanized rubber (stretched up to L = 650, 36 per cent at both 0° and 25° C.).

The hysteresis found in the length-tension diagrams of the muscle fibre may be due to permanent deformation (plasticity) and/or to elastic aftereffect. In order to decide between these two possibilities the slow adjustment to the stationary state after rapid changes in tension or length was investigated as a function of time under well defined experimental conditions. Such experiments are denoted *transient experiments* in what follows.

Transients.

1. The course of elongation following quick loading in the resting fibre (isotonic transient).

a) Initial adjustment (up to 20 msec.).

When the muscle fibre was subjected to a sudden increase in load (ΔP = 0.05 to 0.5 P_0),[1] its length increased as a function

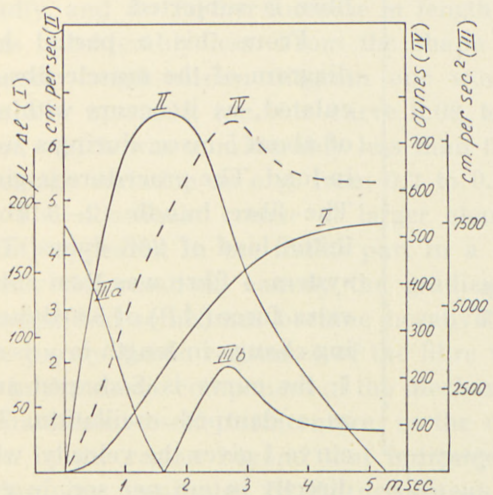

Fig. 14. Analysis of the time course of length, velocity, acceleration, and force after a sudden increase in load of 530 dynes in the resting muscle fibre. 0° C.
curve I: resulting change in length, ordinate I in μ.
curve II: velocity of change in length, ordinate II in cm per second.
curve III: positive (a) and negative (b) acceleration, ordinate III in cm per sec.^{2} or transformed to inertial force, ordinate IV in dynes.
curve IV: resulting force acting on muscle fibre itself, ordinate IV in dynes.
abscissa: time after increase in load in msec.

of time, first rapidly and then more and more slowly. The initial course was examined in a special series of experiments, in which the variation in length during the first 20 msec. was recorded through photoelectric transmission by a cathode ray oscilloscope (cf. p. 20). Since the initial course was markedly affected by the inertia of the system, the resulting effect on the tension had to be taken into account in the evaluation of the variation in length caused by the change in load.

When a force is introduced into a system having a given

[1] With regard to the size of ΔP applied to the isolated fibre compared with that examined in whole muscle, see p. 158.

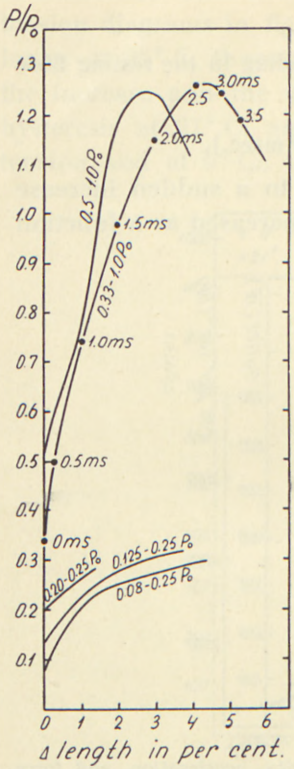

Fig. 15. *Partial length-tension diagrams.* Length as a function of load in the first 4 msec. during a sudden increase in load. Resting muscle fibre, 0° C. Different initial loads at final load 0.25 P_0 and 1.0 P_0. Initial and final value of load are denoted by the figures on the curves. The points of curve 0.33–1.0 P_0 indicate time in msec, after change in load.
ordinate: tension in units of P_0.
abscissa: elongation in per cent of L_0.

equivalent mass, elastic force, and damping resistance, a change in length is produced. From the extra load introduced, the recorded course of stretch, and the equivalent mass of the system it is possible to calculate the force of inertia, and hence the real tension to which the fibre is subjected.

From this a partial length-tension diagram of the muscle fibre can be calculated, as it occurs within an interval of about 5 msec. during a sudden change in load. The procedure is given in fig. 14. The fibre bundle (2—3 fibres) had an initial load of 266 dynes. The recording system + fibre was then subjected to an extra force (ΔP) of 530 dynes. The resulting change in length in μ is seen in curve I; the curve is S-shaped and continues as a damped oscillation. The slope of curve I gives the velocity, which is given directly in cm per sec. in curve II. The slope of the velocity curve corresponds to the acceleration, which acts on the system + fibre (curves IIIa and IIIb). Thus, knowing the acceleration and the equivalent mass of the system, the force of inertia could be determined. This was initially equal to ΔP (530 dynes). At 1.7 msec. the inertial force passed zero, the velocity simultaneously approaching its maximum. The extra force, which acted on the fibre, hence, was initially zero and increased gradually as the inertial force decreased. When the inertial force was zero, all 530 dynes thus acted on the fibre alone. After this, the velocity decreased, the inertial force reversed sign (curve IIIb) and therefore added to the external extra load so that the resulting force acting on the fibre ex-

ceeded 530 dynes. The course of the resulting force acting on the fibre as a function of time is given in curve IV. Thus, from curves IV and I the dynamic partial length-tension diagram can be plotted.

Partial length-tension diagrams for different initial loads are seen in fig. 15. It is characteristic of these diagrams that during the first increase in length up to about 1 per cent the tension increases rapidly, and for further increase in length the increase in tension was considerably less. From the shape of the static and semidynamic length-tension diagram one would expect a curvature concave upwards, i. e. for curve 0.08 to 0.25 P_0 an initial gradient, which was considerably less than the final one. A small percentage variation as e. g. from 0.2 to 0.25 P_0 gave a straight line. The non-linear course at larger changes in load ($>$ 20 per cent) appeared in the initial part in a manner suggesting a plastic deformation, namely the gradient of the resistance decreased and sometimes became negative with elongation. Thus the purely elastic resistance of the fibre was reduced. The decrease in the elastic component of the mechanical reaction of the fibre manifested itself, furthermore, in the course of the *after-oscillation* in the region beyond that indicated in curve I, fig. 14. The damping manifested by the decrement in the after-oscillation is most pronounced at high loads and large changes in length.

A further differentiation between elastic and viscous forces and plastic changes in the initial course was performed by comparing the fibre + recording system with a model which contains a known mass, elasticity, and damping. Fig. 16 shows the response (a = length, b = velocity) of the individual components as well as different combinations to a sudden change in load.

When a constant force acts on a *mass* (m), the change in length increases with the square of time and the velocity linearly with time. The effect of the force on an *elasticity* (G) causes an immediate increase in length, which in fig. 16 (a) appears as an increase in length constant with time and in fig. 16 (b) with velocity zero, apart from the instant at which the force is introduced, when the velocity is infinitely high.

If the force acts on *mass* and *elasticity* ($m + G$), the result is an oscillation with an amplitude varying between zero and twice the increase in length which the force could impose on the elasticity alone. The corresponding velocity is zero at the moment of loading and reaches

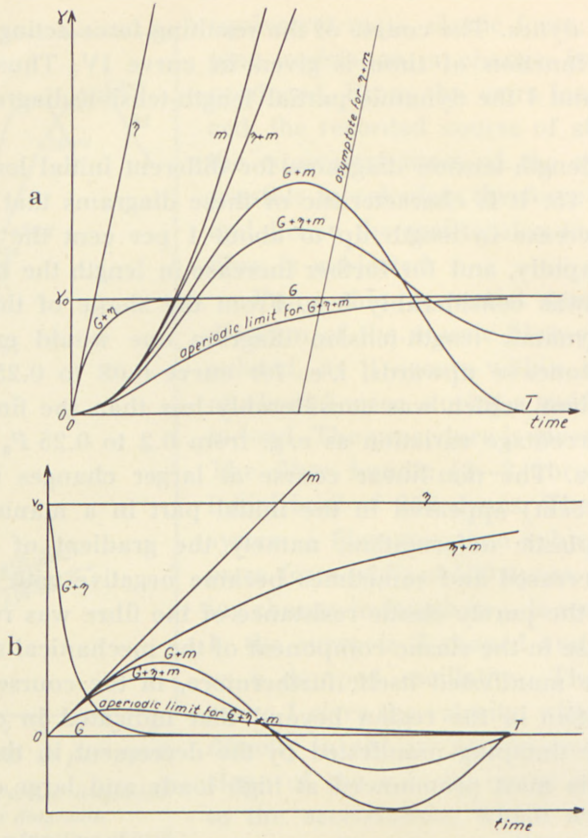

Fig. 16a and b. Course of elongation (a) and velocity (b) as a function of time in a mechanical system subjected to a sudden change in load (isotonic transient). System consisting of:
curve η: viscosity
curve m: mass
curve $m + \eta$: mass + viscosity
curve G: elasticity
curve $G + \eta$: elasticity + viscosity in parallel (Voigt-element)
curve $G + m$: elasticity + mass
curve $G + \eta + m$: Voigt-element + mass, oscillating and aperiodic course.
ordinate: (a) elongation, (b) velocity, linear scale.
abscissa: time, linear scale.
The viscosity η is adjusted so that the oscillation amplitude decreases to $\frac{1}{e}$ in the course of one oscillation period.

its maximum when the length has reached its point of inflection. At that time the velocity is $\frac{2}{\pi}$ times that which the mass alone would have.

A *damping resistance* (η) when it is acted upon by a constant force gives an increase in length which is linear with time, and a corresponding constant velocity.

When the force acts on a combination of *mass and damping resistance* ($m + \eta$), the change in length first follows that which the system would have had with mass alone, since the forces of inertia predominate as long as the velocity is low. With increasing velocity, the damping resistance increases, hence the acceleration decreases, the velocity becomes constant, and the length increases linearly with time. The velocity for this combination rises exponentially towards its maximum which is determined by the damping resistance.

If *mass, damping resistance and elasticity* ($m + \eta + G$) are combined and η and G are in parallel, an oscillating movement with decreasing amplitude is obtained. If the damping resistance exceeds a critical value, the oscillation becomes aperiodic. This is the case when $\eta^2 \geq 4\, m\, G$, i.e. $sr \geq 2$ (cf. p. 17).

The response of the muscle fibre to a sudden increase in load resembled the curve calculated for a combination of mass, elasticity, and viscosity. The first period of the oscillation indicated the presence of an almost aperiodically damped elasticity. However, this was followed by a small oscillation with a much smaller decrement than that corresponding to the first phase of the oscillation. At the same final load, varied between 0.25 and 1.0 P_0, it was furthermore found that the amplitude of the after-oscillation was practically independent of the size of the variation in load, although it might have been expected a priori that the amplitude of oscillation would increase with increasing ΔP. This was true as long as ΔP was < 50 per cent of the final load. When ΔP exceeded 50 per cent of the final load, a considerable increase was usually seen in the decrement of the after-oscillation. Thus, in the first half period of the oscillations an increasing proportion of the energy introduced in the transient was absorbed. The ratio between the total elastic energy and the dissipated losses decreased with the amount of energy introduced. This means that viscosity with rising ΔP dominated the mechanical reaction of the fibre increasingly, and must be interpreted as being caused by a "plastic" elongation, which always occurred when the variation in load exceeded 20—25 per cent of the final load. As long as ΔP was less than half the final load, the plastic yielding was completed within the first half period of the stretch. At higher variations in load it may continue and cause a completely aperiodic course.

In the cases in which the decrement of the after-oscillations

was so small that the period could be determined, the elastic component, i. e. the dynamic elastic stiffness was calculated on the basis of the simple spring-mass formula. In comparison with the magnitude of the dynamic stiffness measured during continuous vibrations of the same frequency and at stationary load the vibrational stiffness measured immediately after transient was 50—60 per cent higher. For example the experiment given in fig. 18 showed a relative stiffness calculated from the frequency of after-oscillations of 30 L_0^{-1}, while the stiffness obtained with continuous vibrations was 18—20 L_0^{-1} (0° C.). The cause of this difference is discussed on p. 104.

If instead of the initial course of length and tension (i. e. within 5 msec.) the elongation was measured which was attained 50 msec. after the transient change in load, the corresponding dynamic length-tension diagrams had an exponential course. Thus, as in static experiments, the differential quotient increased with increasing length and tension, but the gradient referred to the same tension was 3 to 5 times steeper than in static diagrams. An *increased initial* load, with the same extra load, resulted in a shorter elongation just as the gradient, i. e. the stiffness, was higher at a higher load. Table 1 shows the stiffness (expressed with P_0 as unit of tension and L_0 as unit of length) at different initial loads and variations in load. The dynamic stiffness measured

TABLE 1.

Dynamic stiffness in isotonic transient measured in $P_0 L_0^{-1}$ (0° C).

Initial load P/P_0	0.125	0.25	0.50	0.75
Stiffness at 2 % variation in length, time of adjustment 20 msec.	3.2 (16)	5.0 (14)	9.0 (14)	12.5 (14)
Stiffness at 5 % variation in length, time of adjustment 20 msec.	3.7 (14)	6.0 (13)	10.0 (13)	.. ..
Stiffness at 8 % variation in length, time of adjustment 20 msec.	4.5 (13)	8.25 (13)	.. ..	.. ..
Stiffness after a transient producing a variation in length of 2 %, time of adjustment 10 sec.	1.65 (9)	2.8 (9)	6.2 (10)	.. ..

The figures in brackets denote the relative stiffness (for definition see p. 59).

20 msec. after the change in load varied between 3.2 and 12.5 $P_0 \times L_0^{-1}$ (0° C.). At the *same initial* load the stiffness increased with increasing additional load. On account of the proportionality existing between both static and dynamic stiffness and load this increase was to be expected. However, referred to the mean load (Table 4, p. 61) the increase in stiffness in transient experiments is slightly less than proportional to the load (cf. also dynamic

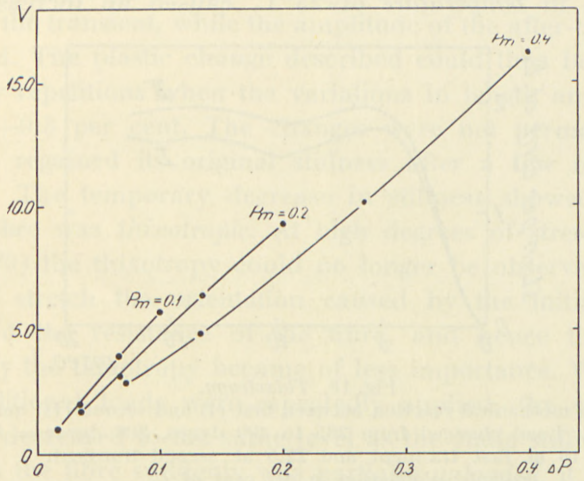

Fig. 17. *Maximum velocity of changes in length* in isotonic transients as a function of the change in load for different mean loads indicated in units of P_0 by the figures on the curves (0° C).
ordinate: maximum velocity in units of L_0 per sec.
abscissa: change in load in units of P_0.

elastic stiffness, p. 80). If the stiffness was measured from the elongation 10 sec. after the change in load, it was reduced to half. If the mean tension was taken into account (relative stiffness) the reduction was less pronounced and amounted to approximately 40 per cent (see also Table 4).

The *maximal velocity of the change in length* produced by different transient loadings as a function of the additional load is given in fig. 17. These curves are taken from a series of experiments in which we have varied both the initial load and the ratio between the additional and the final load. For a given mean load (P_m) the maximum velocity varied linearly with the transient load applied. The difference in slope at different values of P_m was due to the non-linear course of the length-tension

diagram. With the additional load equal to the initial load, the maximum velocity of elongation was attained on an average at a time at which the elongation was 37 per cent of the elongation at the start of the after-oscillations. This value was independent of the initial load. From these experiments it is seen that the tension changes with a decreasing gradient when the stretch is increased (cf. partial length-tension diagrams fig. 15).

A rise in *temperature* of 25° C. caused an increase in the

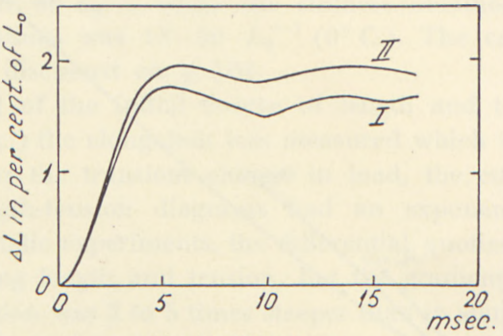

Fig. 18. *Thixotropy.*
Difference in mechanical reaction between first (I) and second (II) quick increase in load 0° C. Load changed from 285 to 400 dynes, 800 dynes = P_0; relative stiffness[1] = 19 at first transient and 22.5 at second transient.
ordinate: elongation in per cent of L_0.
abscissa: time after increase in load in msec.

initial change in length of 30 to 50 per cent as compared with that found at 0° C. In the range examined, the effect of the temperature did not vary appreciably with changes in the additional load and the initial load.

Thixotropy.

The plasticity or thixotropy which must be assumed in order to explain the mechanical reaction of the fibre in the dynamic phase of the transient experiment, was also obvious from the softening effect which repeated transients had within the same level of load. At an initial load of e. g. 0.25 P_0 and an additional load of 0.04 P_0 an increase of 0.24 per cent of the fibre length (0° C.) was observed at the first loading. The initial elongation increased with repeated loadings and at the fourth transient amounted to 0.38 per cent of the equilibrium length. Relative stiffness[1] calculated from the first transient was 52.0 and from

[1] Relative stiffness $= \frac{\text{stiffness}}{\text{load} + \text{stiffness-tension}}$ (cf. p. 59).

the fourth 33.0. A comparison of the present example with the one illustrated in fig. 18 shows the highest values of the relative stiffness, when the transient amplitude was small (cf. amplitude dependence of vibrational stiffness, p. 84 and stiffness measured by the period of after-oscillations p. 50). Apart from the increase in length amplitude, repeated loadings simultaneously caused an increase in the velocity of elongation in the initial phase of the transient, while the amplitude of the after-oscillations decreased. The plastic change described could thus be obtained by a few repetitions when the variations in length amounted to only 0.2—0.3 per cent. The changes were not permanent and the fibre regained its original stiffness after a few minutes of recovery. The temporary decrease in stiffness showed that the resting fibre was *thixotropic*. At high degrees of stretch (above length 170) the thixotropy could no longer be observed. In this range of stretch the orientation caused by the initial tension dominated the resistance of the fibre, and hence the change caused by the thixotropy became of less importance. When very high additional loads were repeatedly applied, the stiffness of the fibre decreased to the same level as the static stiffness.

When the fibre suddenly was partially *unloaded*, it shortened with about the same initial velocity as that which was measured during elongation between the same loads. At release, however, the high velocity was maintained over a variation in length which exceeded that observed during quick loading by about 50 per cent.

b) Prolonged creep (> 20 msec.).

At 20 msec. after transient there was still some distortion owing to the inertial force of the recording system. 50 msec. after the change in load this distortion (damped oscillation) had mainly disappeared and a smooth variation of length was obtained as a function of time.

Fig. 19 shows the effect of a change in load as a function of time. The units of the abscissa vary from curve to curve in the ratio 1:10. Curve I thus gives the course between 0 and 0.1 sec., curve II between 0 and 1 sec. and curve III between 0 and 10 sec. In the experiment shown the variation in load amounted to 50 dynes. In spite of the three different axes, the shape of the

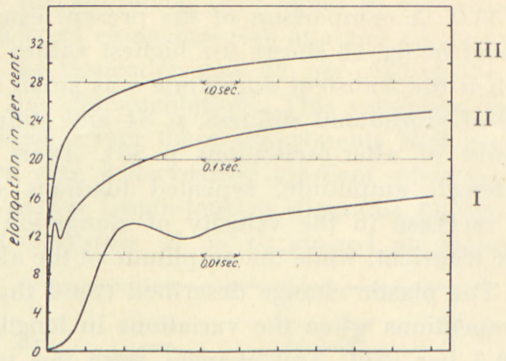

Fig. 19. Adjustment after a sudden change in load of 50 dynes, initial load 17 dynes. (P_0 = 1000 dynes), 0° C.
ordinate: elongation in per cent of L_0.
abscissa: curve I time in units of 0.01 sec.
curve II – - – - 0.1 sec.
curve III – - – - 1.0 sec.
The irregularity in the initial part of the curves between 0 and 50 msec. is due to the damped oscillation caused by the inertia of the recording system plus muscle fibre.

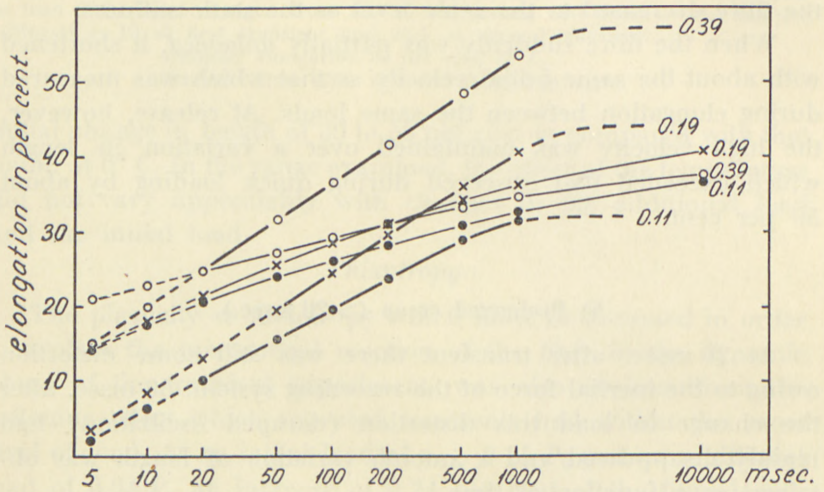

Fig. 20. Elongation after increase in load as a function of time in the resting fibre and during isotonic tetanic contraction, 0° C.
Different initial and additional loads. The figures on the curve denote the additional load in units of P_0. The initial load was $\frac{1}{3}$ of the additional load.
Thick lines: tetanic contraction.
thin lines: resting fibre.
ordinate: elongation in per cent of L_0.
abscissa: time after increase in load in msec., logarithmic scale.

curves was very nearly the same and this makes it natural to express the variation in length as a function of the logarithm of time. Fig. 20 gives for similar experiments the elongation in per cent of L_0 as a function of the logarithm of time, and it is seen that over a long range of time (2—3 decades) the lengths vary approximately linearly. In the example shown in the figure, the recording was finished after 10 sec. Other experiments with an observation time of more than 15 minutes showed that the elongation continued to be approximately proportional to the logarithm of time. The change in length can, therefore, be written in the form:

$$L(t) = L(1) + C_l \log t \qquad (23)$$

i. e.

$$v = \frac{C_l}{t},$$

where $L(1)$ denotes the length of the fibre at the time 1.

TABLE 2.

Changes in length and C_l in the resting muscle fibre as a function of time at different additional loads (0° and 25° C.).

Temp. °C.	$\frac{\Delta P}{P_0}$	ΔL at 0.02 sec.	ΔL at 0.14 sec.	ΔL at 1.0 sec.	C_l in per cent of the equilibrium length
0	0.05	10.0	17.65	25.0	4.00
25	0.05	20.5	25.85	30.6	2.91
0	0.10	17.3	25.45	33.5	4.21
25	0.10	20.6	26.00	31.35	2.80
0	0.20	22.0	31.45	40.6	4.77
25	0.20	27.8	35.7	43.1	4.19
0	0.50	26.6	33.35	40.0	3.52
25	0.50	38.0	40.75	43.8	1.46

$\Delta P = P_2 - P_1$, where P_1 is the initial and P_2 the final load. For increasing load $P_2 = 4\,P_1$ and for decreasing load $P_2 = \frac{1}{4}\,P_1$. The constants found are mean values for positive and negative values of $\Delta P/P_0$. The variations in length and C_l are expressed in per cent of the equilibrium length.

Table 2 gives values for the constant C_l which is the velocity at time 1 sec., for different additional loads at 0° C. and 25° C. As a function of $\Delta P/P_0$ C_l has a maximum between 0.1 and 0.5 at 0° C., and decreases rapidly with rising *temperature*. This fall in C_l is apparently paradoxical, since a higher velocity would

have been expected at higher temperature. The higher velocity is actually seen, but only in the initial course. As the total variation in length at a given variation in load is practically independent of temperature, the slow variation in length becomes less at high temperature and hence the reduction in velocity during the prolonged creep becomes comprehensible.

2. The course of stress-relaxation following sudden changes in length in the resting fibre (isometric transient).

a) Initial course, up to 1.5 msec.; development of tension.

When the fibre was stretched suddenly, the tension rose and reached its maximum when the extension was completed. Hereafter the tension fell off, first rapidly and then with decreasing velocity, but always approaching a final tension higher than the initial one. After 10 msec., according to the initial load, at 0° C. the decrease in tension amounted to 30 to 70 per cent of the maximal increase in tension. There was no significant difference in the relative course of stress-relaxation after quick stretches of 7 and 13 per cent of L_0.

By analogy with experiments with sudden changes in load an attempt was made to characterize the initial course by a dynamic partial length-tension diagram. Since the sudden change

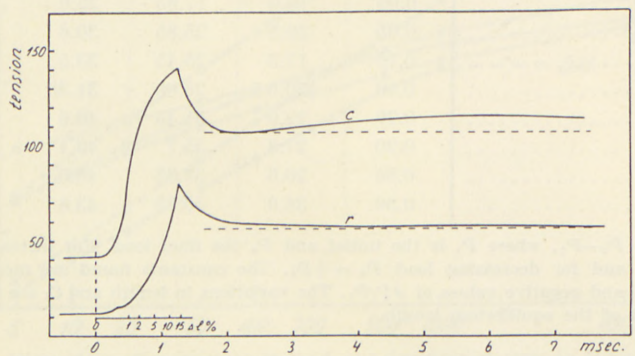

Fig. 21. Time course of tension during and after a quick increase in length of 13 per cent of L_0. 0° C.
r = in the resting fibre.
c = during isometric tetanic contraction.
ordinate: tension in arbitrary units, P_0 = 100 units.
abscissa (*below*): time after start of the increase in length in msec.
small scale above: elongation in per cent of L_0.

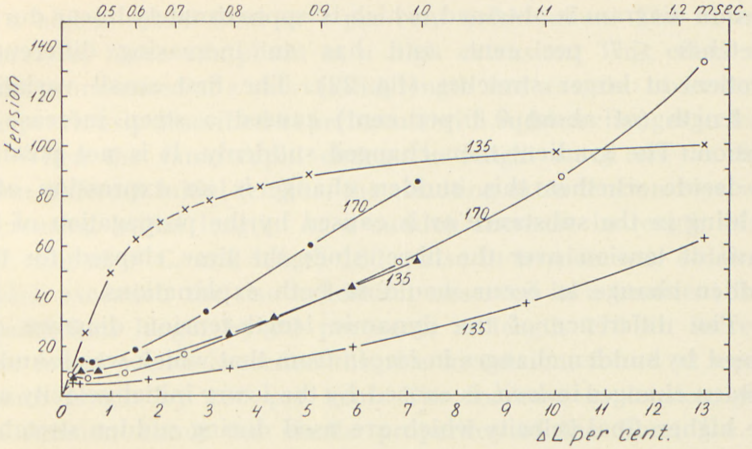

Fig. 22. *Partial length-tension diagrams* obtained from the initial course of isometric transients at rest and during contraction. 0° C. Duration of increase in length approximately 1 msec. The length is assumed to increase with t^3 (see text).

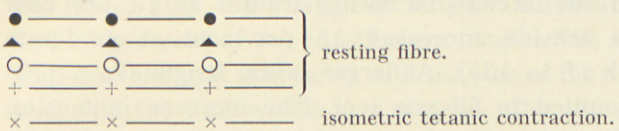

The figures on the curves denote the initial length in per cent of L_0.
ordinate: tension in arbitrary units, $P_0 = 75$ units.
abscissa: (below) elongation in per cent of L_0.
(above) time after the start of the increase in length in msec.
With regard to differences in the gradients of the length tension diagrams in curves with the same initial and different final length, see text (p. 58).

in length was introduced by means of an electromagnetic system, it proceeded with increasing velocity owing to inductance and inertia. However, considering that the electrical time constant of the moving system was approximately 10 msec., the moving force acting on the system within the first msec. could be assumed to increase linearly with time. Since the force exerted by the fibre did not exceed 1 per cent of the inertial forces, the motion governing the change in length will be practically that of a mass m subjected to a force increasing linearly with time. The velocity thus rose with the square and the change in length with the third power of time. The elongation in per cent, which was obtained during stretch, is given in fig. 21 by a scale above the abscissa.

If the change in length determined in this way is plotted against the corresponding values for tension, a dynamic length-

tension diagram is obtained, which is approximately linear during stretches ≤ 7 per cent, and has an increasing differential quotient at larger stretches (fig. 22). The first small variation in length (of about 0.3 per cent) caused a steep increase in tension. The gradient then changed suddenly. It is not possible to decide whether this sudden change is an expression of a yielding in the substance or is caused by the propagation of the wave of tension over the fibre, since the time elapsed for this sudden change to occur would fit both explanations.

The difference of the dynamic length-tension diagram obtained by sudden changes in *length* from that which was found at sudden changes in *load*, is caused by the lower initial velocity and the higher final velocity which are used during sudden stretches. The difference demonstrates how the shape of the length-tension diagram is affected by the velocity with which the stretch proceeds.

If the *sudden stretch* was increased from 7 to 13 per cent of L_0, the extra tension increased 15 per cent at moderate degrees of stretch ($L = 135$). At larger initial length ($L = 170$) the increase amounted to 50 per cent. The increase in tension caused by the elongation thus increased less than proportionally to the elongation, although the reverse would be expected according to the generally assumed length-tension diagram. It must, however, be considered that the length-tension diagrams obtained by an extension to 7 and 13 per cent did not coincide in the first part of the change of length, as would be expected. The previously mentioned change in slope occurred at a sudden elongation of 13 per cent at an earlier time and at a lower tension than in the curve for 7 per cent elongation, while the curves as a whole are similar. The different positions of the hump both in time, tension, and length in spite of the same initial tension and stiffness indicate a yielding in the substance. Furthermore, it is remarkable that the slope of the length-tension diagram despite the same initial length and load was steeper when the variation in length was 7 per cent, than when it was 13 per cent. This variation of the tension with the amount of stretch is an expression of the previously described *thixotropy*. The curves in fig. 22 represent a mean value for 4—5 repeated elongations taken at 20 sec. intervals. With the larger, repeated deformation (13 per cent) the thixotropy of the fibre will exert its influence

to a higher extent than at 7 per cent deformation. The fibre is, therefore, more compliant at a high extension. This effect was most pronounced at a short initial length and was also observed in the previously described experiments with sudden changes in load.

When the same rapid change in length acted on the fibre from different initial lengths, the resulting extra tension rose with increasing initial length. At a sudden increase in length of 13 per cent at 0° C. and length 130 a rise in tension was obtained, which exceeded the rise in tension observed in a transient from equilibrium length by 30 per cent; at length 170 an increase was found which exceeded the rise in tension, found at equilibrium length by 100 per cent. The increase in tension gives information about the elastic properties of the fibre, i. e. its stiffness, during relatively large and non-periodic changes in length.

Table 3 gives the stiffness after an isometric transient, 1 to 100 msec. after the change in length and at an elongation of 7 and 13 per cent of the equilibrium length. The stiffness increased with the load and decreased with the size of the variation in length and with the time which had elapsed after the change in length.

TABLE 3.

Stiffness in the isometric transients in $P_0 L_0^{-1}$.

Time after change in length in msec.	Change in length as percentage of equilibrium length	Initial load in units of P_0	0	0.025	0.045	0.200
		Initial length in units of $L_0 = 100$	100	125	135	170
1	7	..	..	..	7.9	12.0
1	13	..	..	..	4.8	10.0
20	13	..	1,6	3.3	4.3	6.2
100	13	..	1.3	3.0	..	5.8
10.000	13	..	(0.7)	(2.3)	..	(5.1)

The figures in brackets are extrapolated.

In order to compare the values of stiffness found by the different procedures, it is convenient to express the stiffness per unit tension (Table 4) in the following way:

$$\varkappa = \frac{G}{\left(\frac{P_m + P_{st}}{P_0}\right)} \qquad (24)$$

The stiffness (G) is defined as $\frac{\Delta P}{\Delta L}$ and measured in units of $P_0 L_0^{-1}$, P_m denotes $\frac{\text{initial } P + \text{final } P}{2}$, and P_{st} denotes the stiffness-tension (see p. 84). The advantage of introducing this *relative stiffness* is that its value is practically independent of the load. It appears from Table 4 that the stiffness referred to the same load, shows good agreement in the isometric and isotonic transient experiments. In both cases the relative stiffness decreased with increasing amplitude and increasing time of adjustment. The values of stiffness from isotonic transient given in Table 1 represent mean values from experiments of the same type as given in Table 4. In each experiment the stiffness was obtained as a mean from quick loading and unloading. When comparing the values of stiffness in the two tables it should be remembered that stiffness in Table 1 is given as a function of the initial tension. In Table 4 the stiffness is referred to the mean tension as defined above. Since the course of the variation in length with time is approximately symmetric in transient loading and unloading, the mean tension represents a reasonable parameter for reference when stiffnesses are compared which are obtained under different conditions.

The $\frac{\text{stiffness}}{\text{tension}}$ measured in vibration experiments, at a maximal amplitude of 2 per cent L_0 (peak to peak), is larger than the corresponding value obtained from isotonic transients, but less than the values found in isometric transient experiments at 7 per cent change in length. Considering that individual variations must occur in these 3 different series of investigations, it appears justifiable to conclude that the relative stiffness at the same load, the same amplitude of change in length, and the same velocity does not display significant differences in isometric transient, isotonic transient, and vibration experiments. Table 4 furthermore shows that the relative value of the dynamic stiffness is 3—4 times higher than the static stiffness, which was measured from the gradient of the length-tension diagram with a recording time of 30 minutes (15 minutes rising and 15 minutes falling tension). If this time interval is extended, still lower values are obtained for the static stiffness. At load zero the static modulus

of elasticity at 0° C. is $0.5—0.6 \times 10^6$ dynes $\times$ cm^{-2}. The cause of the difference in stiffness at different times of adjustment will be further discussed in connection with the spectra of retardation times (p. 74, 105).

Temperature dependence.

The additional tension (ΔP) produced by a sudden increase in length varied with the temperature. At equilibrium length ΔP decreased 40 per cent, when the temperature rose from 0° to 20° C. At an initial length 130, the additional tension decreased by 15 per cent with a rise in the temperature of 20° C., and at lengths of about 170 the variation in additional tension caused by the temperature was within the limits of experimental accuracy. The

TABLE 4.

Relative stiffness expressed as $\frac{\text{stiffness}}{\text{mean tension}^1 + \text{stiffness-tension}^2}$ in units of L_0^{-1} (0° C).

	Change in length in % of equilibrium length	Time in msec. after change in length or load					
		1	10	20	100	10000	10^6
Relative stiffness	2	..	..	14.7	..	8.9	..
from isotonic	5	..	..	13.7	..	..	..
transient	8	..	..	12.5	..	..	..
Relative stiffness	7	22.8	..	..	..	..	..
from isometric	..	..	..	..	..	..	..
transient	12	12.5	..	11.5	10.8	(10.0)[3]	..
Relative stiffness[4]	2	..	18—20	..	..	..	..
from vibration	..	..	..	..	..	..	..
experiments	..	..	..	..	..	..	..
Relative stiffness[5],	..	..	..	..	..	..	4.1
static	..	..	..	..	..	..	..

[1] mean tension $= \frac{\text{initial } P + \text{final } P}{2}$

[2] stiffness-tension $= 0.05\ P_0$.

[3] extrapolated.

[4] average of 25 experiments on 25 fibres measured in vibration experiments. Frequency 50 c.p.s. corresponding to 10 msec. after transient loading. Amplitude of vibration, peak to peak, 2 per cent.

[5] from gradients of the length-tension diagram, recording time 30 minutes.

same dependence on temperature was found for the stiffness determined in vibration experiments.

On the other hand, a comparison of the influence of temperature on the tension obtained in static and dynamic experiments showed considerable difference. In static experiments (p. 42), the tension *increased* according to the degree of stretch between 0 and 0.15 per cent per degree C. of increasing temperature (static stiffness practically unchanged). However, the alternating tension for a given vibrational amplitude *decreased* with increasing temperature, the variation being ten times higher than that of the static stiffness. In both cases the dependence on temperature is small at high degrees of stretch. The difference between the temperature dependence found in static and dynamic experiments is not surprising, since the former is determined by forces which are in equilibrium, while in dynamic experiments it is determined predominantly by the forces which cause the rearrangement of the structure, i. e. the forces which cause a deformation velocity.

Quick release.

A sudden *decrease in length* caused a reduced tension in the fibre. If the decrease in length was < 1.5 per cent of the equilibrium length, a course of tension was obtained at release of the same type as during extension, but which in agreement with the non-linear course of the length-tension diagram, had a smaller

TABLE 5.
Isometric transient

length	temp. °C	ΔL in % of L_0	$\log \frac{dP/P_0}{dt}$ at 10 msec.	$\log \frac{dP/P_0}{dt}$ at 32 msec.	$\log \frac{dP/P_0}{dt}$ at 100 msec.	Increase in tension in units of P_0 at 0 msec.	1 msec.	10 msec.	32 msec.	100 msec.
100	0	12	2.82	2.20	1.70	0.550	0.31	0.21	0.18	0.15
100	25	12	2.40	1.76	1.40	0.330	0.19	0.12	0.10	0.10
125	0	12	2.96	1.45	1.65	0.74	0.50	0.41	0.38	0.36
125	25	12	2.70	1.04	1.65	0.60	0.36	0.27	0.25	0.22
170	0	12	2.70	2.31	1.96	1.00	0.82	0.75	0.72	0.70
170	25	12	2.58	2.23	2.00	1.11	0.89	0.82	0.79	0.75

Velocity of change in tension in arbitrary units.

amplitude. If the decrease in length exceeded 1.5 to 2 per cent of L_0, zero tension was reached, and the fibre began to display a positive tension only after 20 to 50 msec. had elapsed after the moment of quick release. Obviously, when the amplitude of release exceeded a value which caused the tension to decrease to zero, the curves obtained were not suitable for an analysis of the course of tension.

b. Course of stress-relaxation within 100 msec. after length alteration.

Just as the length increased with time on a sudden increase in load, the tension decreased with time after a sudden increase in length. This variation proceeded rapidly immediately after the change in length (p. 56), and then with decreasing velocity. If the tension is plotted as a function of the logarithm of time, an approximately rectilinear course is obtained 1 msec. after the end of the stretch corresponding to the equation:

$$P(t) = P(1) - C_p \log t, \qquad (25)$$

where $P(1)$ represents the tension at time 1 (see fig. 23 and Table 5).

The increase in tension at low and moderate degrees of stretch was higher at 0° C. than at 20° C. At high degrees of stretch, however, the increase in tension was highest at 20° C.

The temperature dependence of the course of stress-relaxation is

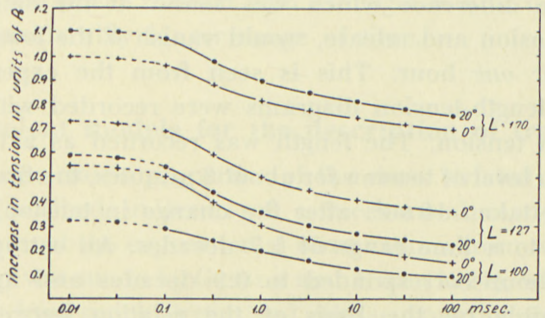

Fig. 23. *Adjustment of tension after a quick increase in length* (isometric transient). Resting fibre, 0° and 20° C. Increase in length 13 per cent of L_0. The figures on the curves denote temperature in ° C. and initial length in per cent of L_0.
ordinate: increase in tension in units of P_0.
abscissa: time after increase in length in msec.

seen from the values of the velocity of change in tension in Table 5. At length 100 an increase in temperature of 25° C. caused a decrease in stress-relaxation velocity of 33 per cent (measured 32 msec. after quick stretch). In whole muscle using quick stretches of the same order of magnitude as those applied here, HILL (1950) did not find any measurable variation of the course of stress-relaxation with temperature.

The formulas deduced for creep and stress-relaxation in isotonic and isometric transient indicate that the adjustment to a new state proceeds with about the same velocity, independent of whether the experiments are carried out at constant length or at constant tension.

The ratio between the increase in tension and in elongation (stiffness) is, as previously stated, identical after about 20 msec. in the experiments performed under isotonic and under isometric conditions (Table 4). At equilibrium length and at moderate degrees of stretch, the stiffness observed in both isotonic and isometric transients decreased with rising temperature (30—35 per cent per 20° C.). Creep and relaxation velocity had a similar temperature coefficient as well, the velocity of the change in length or tension after a transient decreasing approximately 30 per cent, when the temperature was increased from 0° to 25° C.

The transient experiments enable us to evaluate the type of the hysteresis occurring during the recording of the length-tension diagrams. This hysteresis was present regardless of whether the diagrams were recorded with rapid or very slow variations in length. The difference which was found at the same tension during extension and release, would vanish if the load was kept constant for *one* hour. This is seen from the experiments in which the length-tension diagrams were recorded with stepwise variation in tension. The length was recorded as a function of time at each level of tension for about 8 minutes, the first measurement being taken 10 sec. after the change in tension, thus corresponding to a time range of 1.7 decades. An extrapolation in time to 1 hour corresponded to 0.9 decades and appeared to be permissible on the basis of the relation between length-tension and time found in the creep and relaxation experiments. These experiments show that the hysteresis found in the static length-tension diagrams, including the very first extension

(fig. 12) is not due to plasticity, but to the delayed elasticity which manifested itself by the fact that over a wide range of time the fibre adjusts itself to variations in length and tension, approximately linearly with the logarithm of time. Only at extreme loads ($> 0.5\ P_0$ or length 170) did the fibre show irreversible changes in length, which, when repeated length-tension diagrams were recorded, amounted to 4 per cent per length-tension diagram (recording-time 15 min. each, maximum tension $= P_0$). The apparently plastic phase (thixotropy), which was found during the rapid change in length, cannot be seen in the static length-tension diagram.

To summarize, it can be concluded from the transient experiments that the mechanical properties of the fibre during the rapid phase of stretch indicate the presence of thixotropy, which appears partly as plasticity during elongation, and partly as decreasing stiffness during repeated stretches (fig. 18). This effect was most pronounced at low loads. The transient experiments showed furthermore that the length or tension adjust themselves approximately linearly with the logarithm of time. In isotonic experiments the change in length at rest was practically linear over a range from 20 to 10 000 msec., and in isometric experiments the change in tension was linear from 1 msec. up to at least 100 msec. Experiments with constant length thus give information about a time interval after transient, which escaped measurement in the isotonic experiments. Although in the present experiments only changes in length which occurred within 100 msec. were included, the linear relation with the logarithm of time extended over a considerably longer range of time.

Equivalent models for the description of transients.

The visco-elastic properties of the cross striated muscle fibre can be described in terms of a mechanical model. The first attempt to treat the experimental observations from whole muscle in this way was made by Gasser and Hill (1924), who described the results from quick stretch and release experiments by a model consisting of an elasticity in series with a viscosity (Maxwell-element). Levin and Wyman (1927) applying stretch and release with constant velocity demonstrated that this equivalent model

was unsuitable and suggested a system composed of three elements, a pure elasticity in series with a damped elasticity. The latter consists of a pure elasticity in parallel with a viscosity (VOIGT-element). However, this simple analogue cannot adequately describe the mechanical reaction of the isolated muscle fibre in the transient experiments. Therefore, it was necessary to develop a more complicated model[1] of the same type as used in high polymer physics. There are a number of different possibilities available for the description of the visco-elastic behaviour, but as pointed out by ALFREY and DOTY (1947) they are all *mathematically equivalent*.

An isotonic transient applied to a visco-elastic material is most conveniently described in terms of the *Voigt-model*, while an isometric transient is described most easily by the *Maxwell-model* (ALFREY, 1948). However, KUHN *et al.* (1947a, 1947b) have applied the Maxwell-model for the description of the effect of isotonic transients in caoutchouc. GROSS (1947, 1948) has derived the general transformation formulas connecting these two models.

The Voigt-model.

A Voigt-model consists of Voigt-elements (retarded elasticities), which are coupled in series. This series can contain an element which has "degenerated" to a pure elasticity (fig. 24). The single Voigt-element is characterized by a modulus of elasticity $\frac{1}{J_i}$ and a retardation time τ_i. The reaction of the Voigt-element to a change in load $\sigma(t)$ is determined by the equation of motion:

$$\frac{1}{J_i}\gamma_i + \frac{1}{J_i}\tau_i \frac{d\gamma_i}{dt} = \sigma(t), \tag{26}$$

where $\gamma_i(t)$ is the deformation.

The response of the element to a sudden change in load σ therefore is:

$$\gamma_i(t) = \sigma J_i \left\{1 - e^{-\frac{t}{\tau_i}}\right\}. \tag{27}$$

[1] JORDAN (1939) has suggested a complex mechanical system for the description of plastic properties of smooth muscle.

A discrete series of Voigt-elements, which contains a pure elasticity $\frac{1}{J_0}$ reacts to a *sudden constant change in load* according to the expression:

$$\gamma(t) = \sigma\left[J_0 + \sum_i J_i\left(1 - e^{-\frac{t}{\tau_i}}\right)\right]. \qquad (28)$$

A continuous distribution of Voigt-elements plus a pure elasticity $\frac{1}{J_0}$ reacts according to the expression:

$$\gamma(t) = \sigma\left[J_0 + \int_0^\infty J(\tau)\left(1 - e^{-\frac{t}{\tau}}\right) d\tau\right], \qquad (29)$$

where $J(\tau)$ is the distribution function for the retardation times. The final elongation becomes:

$$\gamma_\infty = \sigma\left[J_0 + \int_0^\infty J(\tau)\, d\tau\right]. \qquad (30)$$

Equation (30) expresses the linear relationship between static length and tension in the Voigt-model. The static length-tension diagram of the muscle fibre is approximately exponential, and this non-linearity will cause variations in the Voigt-model used here dependent upon the initial and the final state of length and tension. Thus, unless the deformation is small, J_0 and $J(\tau)$ will depend on both the initial and the final state of the fibre. This behaviour is illustrated in a later section which deals with the application of Voigt-models to the effect of isotonic transients (p. 72).

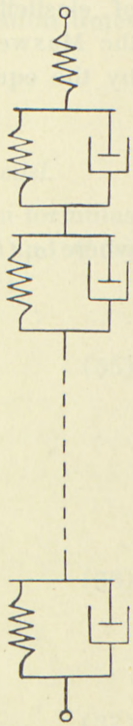

Fig. 24. *Voigt-model* (Kelvin model) see text.

The Maxwell-model.

A Maxwell-model consists of Maxwell-elements (an elasticity in series with a viscosity) which are coupled in parallel. One of these elements can "degenerate" so that it consists only of an

elasticity (fig. 25). This will prevent the model from flowing infinitely under an external load.

The single Maxwell-element is characterized by a modulus of elasticity G_i and a relaxation time τ_i. The response of the Maxwell-element to a change in length $\gamma(t)$ is determined by the equation of motion:

$$\frac{\sigma_i(t)}{G_i \tau_i} + \frac{1}{G_i}\frac{d\sigma_i}{dt} = \frac{d\gamma}{dt}, \tag{31}$$

where $\sigma_i(t)$ is the tension.

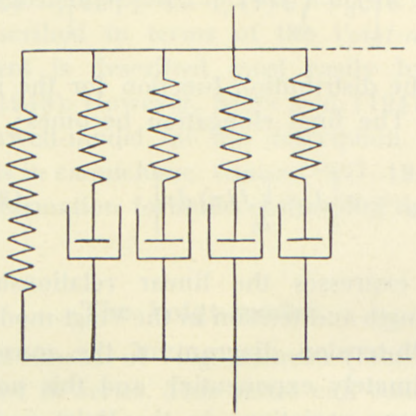

Fig. 25. *Maxwell-model*, see text.

The response of the element to a sudden change in length γ is therefore:

$$\sigma_i(t) = G_i \gamma e^{-\frac{t}{\tau_i}}. \tag{32}$$

This expresses the stress-relaxation. Hence, for a discrete set of parallel coupled Maxwell-elements containing a pure elasticity G_0 the stress-relaxation after a sudden change in length will be:

$$\sigma(t) = \gamma\left(G_0 + \sum_i G_i e^{-\frac{t}{\tau_i}}\right). \tag{33}$$

For a continuous set of Maxwell-elements we shall obtain:

$$\sigma(t) = \gamma\left(G_0 + \int_0^\infty G(\tau)\, e^{-\frac{t}{\tau}}\, d\tau\right), \tag{34}$$

where $G(\tau)$ is the distribution function for the relaxation times (non-normalized).

Transformation from Voigt-model to Maxwell-model.

Gross (1947, 1948) has derived the transformation-formulas connecting J_0 and $J(\tau)$ in the Voigt-model with G_0 and $G(\tau)$ in the Maxwell-model. These are in our terminology:

$$G(\tau) = \frac{J(\tau)}{\left[J_0 + \int_0^\infty \frac{J\left(\frac{1}{s}\right)}{s\left(s - \frac{1}{\tau}\right)}\, ds\right]^2 + (\pi\tau J(\tau))^2} \tag{35}$$

$$G_0 = \frac{1}{J_0 + \int_0^\infty J(\tau)\, d\tau} \tag{36}$$

and

$$J(\tau) = \frac{G(\tau)}{\left[G_0 + \int_0^\infty G(\tau)\, dt - \int_0^\infty \frac{G\left(\frac{1}{s}\right)}{s\left(s - \frac{1}{\tau}\right)}\, ds\right]^2 + (\pi\tau G(\tau))^2} \tag{37}$$

$$J_0 = \frac{1}{G_0 + \int_0^\infty G(\tau)\, d\tau}. \tag{38}$$

Application of a Voigt-model to the transient experiments.

When applying the Voigt-model and the Maxwell-model to the muscle fibre the purpose is to determine their parameters in such a way that the theoretical $\gamma(t)$ and $\sigma(t)$ from isotonic and

isometric transients agree as well as possible with the experimental findings.

In practice the changes in load or in length do not take place suddenly but occur within a certain time interval. This causes the initial course of creep and relaxation to be slightly different from those corresponding to ideal transients, but can be taken into account by correcting for the way in which the changes in load and length occur experimentally.

A. Isotonic transient.

In a series of experiments in which the change in load always was $+3$ or $-\frac{3}{4}$ times the initial load, creep curves (fig. 20 and Table 2) were recorded at rest and during tetanic contraction.

As already mentioned these curves were characterized by an approximate linearity with $\log t$. This gives a possibility for obtaining an approximate expression for the distribution function $J(\tau)$ defined in (29).

From (29) we obtain:

$$\frac{d\gamma}{d \log t} = \sigma \int_0^\infty J(\tau) \cdot \frac{t}{\tau} e^{-\frac{t}{\tau}} d\tau; \tag{39}$$

putting

$$J(\tau) = \frac{c}{\tau} \tag{40}$$

(39) gives

$$\frac{d\gamma}{d \log t} = \sigma c, \tag{41}$$

i. e. the elongation is linear with $\log t$.

The expression (40) for the distribution function has, however, like all expressions giving a linearity with $\log t$, the property that the final elongation γ_∞ becomes infinite

$$\gamma_\infty = \sigma \left[J_0 + \int_0^\infty \frac{c}{\tau} d\tau \right]; \tag{42}$$

(40) can, however, easily be modified to give both a practically linear course with $\log t$ over a suitably long time interval, and a finite final elongation. The following expression can be chosen:

$$J(\tau) = \begin{cases} \frac{c}{\tau} & \text{for} \quad \tau_1 \leqq \tau \leqq \tau_2 \\ 0 & \text{for} \quad \tau < \tau_1 \quad \text{and} \quad \tau > \tau_2 \end{cases} \tag{43}$$

in which it is assumed that

$$\frac{\tau_2}{\tau_1} \gg 1 . \tag{44}$$

With this expression (39) gives

$$\frac{d\gamma}{d \log t} = \sigma c \left[e^{-\frac{t}{\tau_2}} - e^{-\frac{t}{\tau_1}} \right]. \tag{45}$$

From this it can be seen that for

$$\tau_1 \ll t \ll \tau_2 \tag{46}$$

$\left(\text{e.g. } 3\,\tau_1 < t < \frac{\tau_2}{10} \right)$ the elongation varies practically linearly with $\log t$.

By substituting (43) in (29) the following expression for $\gamma(t)$ is obtained:

$$\gamma(t) = \gamma_0 + (\gamma_\infty - \gamma_0) \left[1 - \frac{-Ei\left(-\frac{t}{\tau_2}\right) + Ei\left(-\frac{t}{\tau_1}\right)}{\log \frac{\tau_2}{\tau_1}} \right], \tag{47}$$

where Ei denotes the integral logarithm, and

$$\gamma_0 = \sigma J_0$$

and

$$\gamma_\infty = \sigma \left[J_0 + c \log \frac{\tau_2}{\tau_1} \right] \tag{48}$$

denote the initial and the final elongation.

From the equations given above it must be expected that expression (43) for the distribution function $J(\tau)$ and the corresponding expression (47) deduced from it for the elongation $\gamma(t)$, will give a satisfactory approximation to the experimental course of elongation.

The spectrum of retardation times.

We shall now determine τ_1 and τ_2 for the different experimental curves and then compare the spectrum of retardation times (i. e. the distribution functions) for transient at rest at 0° C., for transient at rest at 25° C., and for transient during tetanic contraction at 0° C.

It is assumed that the elongation $\gamma_0 = \sigma \cdot J_0$ caused by the series elasticity J_0 is only very small (comp. vibration experiments). In the following calculations we shall assume that γ_0 amounts to 5 per cent of the final elongation γ_∞:

$$\gamma_0 = 0.05\, \gamma_\infty . \tag{49}$$

Substituting (49) in (47), τ_1 and τ_2 are then determined for the different courses of elongation in such a way that the theoretical elongation given by (47) is the same at $t = 20$ msec. and $t = 1$ sec. as the experimentally determined elongation. The results of these calculations are collected in Table 6.

TABLE 6.

Boundary values for the spectrum of retardation times.

	$\frac{\Delta P}{P_0}$	τ_1 msec.	τ_2 msec.
Rest 0° C.	0—0.2	0.1	10^5
	0.4—0.5	0.01	3×10^4
Rest 25° C.	0—0.2	0.01	3×10^4
	0.5	10^{-4}	10^4
Contraction 0° C	0.1—0.2	10	2000
	0.4	3	2000

The table shows a distinct difference in the spectrum of retardation times under the three different conditions. In fig. 26 $L(\log \tau)$, which is defined from the normalized distribution function $j(\tau) = \dfrac{J(\tau)}{\int_0^\infty J(\tau)\, d\tau}$ as:

$$L(\log \tau)\, d \log \tau = j(\tau)\, d\tau,$$

i. e.

$$L(\log \tau) = \tau \cdot j(\tau) \tag{50}$$

is given as a function of $\log \tau$.

From Table 6 and diagram fig. 26 it can be seen that the distribution function at 25° C. includes contributions from retardation times shorter than those found at 0° C. Differences in the contributions from long retardation times could not be demonstrated with our technique. *Contraction*, which was only investigated at 0° C., showed a reduction in the contribution from both short and long retardation times. Table 6 further-

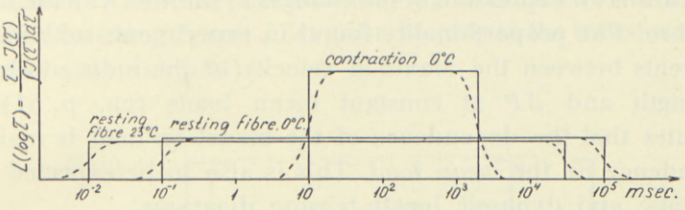

Fig. 26. *Spectrum of retardation times.*
ordinate: normalized distribution function of retardation times multiplied by the retardation time.
abscissa: retardation times in msec., logarithmic scale.
Note that the largest range of retardation times is present in the resting fibre at 25° C. The range is narrowed and displaced to longer durations at 0° C. and narrowed further during contraction. The stippled lines indicate the correction to the distribution which must be expected around the boundaries of the spectrum.

more shows a variation in the distribution function with load (cf. p. 67), the relative contribution of short retardation times increasing with increasing load and variation in load ΔP.

Apart from these changes in the boundary values of the spectrum of retardation times which were determined from the relative course of adjustment $\frac{\gamma(t)}{\gamma_\infty}$ alone, the constant c in the expression for the distribution function (43) also changes with the mechanical state of the fibre. These changes are obtained from the *absolute* values of the deformation $\gamma(t)$ and given in the following table:

TABLE 7.
Constant c in units of $L_0 \times P_0^{-1}$

ΔP in units of P_0.	resting fibre		contraction
	0° C	25° C	0° C
0.11	0.30	0.26	0.61
0.19	0.18	0.18	0.47
0.39	0.077	0.054	0.24

Together with the variations in the width of the spectrum of retardation times, the variation of the constant c with variations in ΔP and also with the mean load (on account of the constant ratio between ΔP and initial load in the experiments in question) expresses the dependence of the stiffness of the fibre on the load. Moreover, the difference in c at various temperatures and with contraction together with the accompanying changes in the width of the spectrum is an expression of the changes in stiffness with the state of the fibre. The proportionality found in experiments with isotonic transients between the maximal velocity of the induced changes in length and ΔP at constant mean loads (cp. p. 51) also indicates that the dependence of the model on load is mainly a dependence on the *mean load*. This is also to be expected from the static and dynamic length-tension diagrams.

It is assumed in the above calculations that the changes in load were sudden. In the experiments the changes in tension proceeded within a certain time and it can be assumed that the tension increased linearly within 2 msec. Calculations carried out to determine the effect of the linear increase of tension on the course of elongation showed that the distorting effect was negligible after about 5 msec. This distortion, therefore, cannot affect the curves used for the above calculations, since these refer to times > 20 msec.

Finally it might be emphasized that the application of a Voigt-model to a description of mechanical properties of the muscle fibre does not pretend to give a direct image of the minute structure, but seems to be a suitable way of illustrating with good approximation different and rather complex experimental findings. The structural basis of this equivalent model is represented by the general picture of minute structure as indicated on p. 42. Thus, it does not comprise quantitative assumptions with respect to the correlation between minute structural processes and their external manifestations as does e.g. the model conception developed for the visco-elastic behaviour of rubber by TOBOLSKY and EYRING (1943, see also Part IV, p. 229 of this paper).

B. Isometric transient.

Fig. 23 shows the course of stress-relaxation at 0° C. and 20° C. after a sudden change in length from different initial lengths.

The curves are approximately linear with $\log t$ for $t > 1$ msec., but the linearity is not as pronounced as is the case in isotonic creep. We shall now investigate how well the isometric curves agree with those to be expected from the Voigt-model (43) used for the description of the isotonic transients.

According to the Maxwell-model the decrease in tension $\sigma(t)$ after a sudden change in length is given by (34). The distribution function $G(\tau)$ and the pure elasticity G_0 to be used here are obtained by inserting J_0 and $J(\tau)$ given by (43) in the transformation formulas (35) and (36):

$$G(\tau) = \frac{\frac{1}{c}}{\tau\left[\left[\frac{1}{19}\log\frac{\tau_2}{\tau_1} + \log\frac{\frac{1}{\tau_1} - \frac{1}{\tau}}{\frac{1}{\tau} - \frac{1}{\tau_2}}\right]^2 + \pi^2\right]} \qquad (51)$$

$$\text{for } \tau_1 \leq \tau \leq \tau_2$$

$$G(\tau) = 0 \quad \text{for } \tau < \tau_1 \text{ and } \tau > \tau_2.$$

$$G_0 = \frac{1}{\frac{20}{19} c \log\frac{\tau_2}{\tau_1}}.$$

Just as $L(\log\tau) = \frac{\tau \cdot J(\tau)}{\int_0^\infty J(\tau)\,d\tau}$ was convenient for the description of the distribution of retardation times,

$$K(\log\tau) = \frac{\tau G(\tau)}{\int_0^\infty G(\tau)\,d\tau} \qquad (52)$$

is convenient for the description of the distribution of relaxation times. Fig. 27 shows $K(\log\tau)$ with $G(\tau)$ given in (51). For the ratio $\frac{\tau_2}{\tau_1}$ the value 10^6 is applied (cf. Table 6). It is seen from fig. 27 that about half the relaxation times are $< 10\,\tau_1$, i. e. according to Table 6 < 0.1—1 msec.

The course of stress-relaxation corresponding to $G(\tau)$ and G_0 given in (51) is very similar to the experimental, but the experimentally found ratios between the final and the initial increase in tension are appreciably higher than those expected theoretically. This is due to the fact that the change in length is produced within a finite interval of time (about 1 msec.) during which an essential relaxation can take place.

In caoutchouc Kuhn *et al.* (1947 a) have described the course

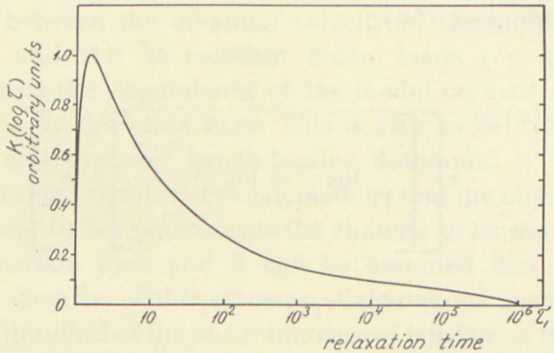

Fig. 27. *Distribution of relaxation times* in the Maxwell-model, which is equivalent to the Voigt-model for the resting fibre at 0° C., the distribution function of which is given in fig. 26.
ordinate: normalized distribution function multiplied by the relaxation time.
abscissa: relaxation time in units of τ_1.

of adjustment after an isotonic transient by means of a Maxwell-model. Over a long interval of time the elongation in this material varied linearly with $\log t$ (10^{-2} sec. $< t < 10^4$ sec.) (Brenschede 1943). Assuming an initial elongation zero, Kuhn on this basis found a distribution function which in the terminology used in the present paper is:

$$G(\tau) = \frac{1}{c} \cdot \frac{1}{\tau \left[\log\left(\frac{\tau}{\tau_0} - 1\right)^2 + \pi^2 \right]} \quad \text{for} \quad \tau > \tau_0 \tag{53}$$

$$G(\tau) = 0 \quad \text{for} \quad \tau < \tau_0. \tag{54}$$

Transformation of this expression to

$$G(\tau) = \frac{\frac{1}{c}}{\tau} \cdot \frac{1}{\left[\log \frac{\frac{1}{\tau_0} - \frac{1}{\tau}}{\frac{1}{\tau}}\right]^2 + \pi^2} \quad \text{for} \quad \tau > \tau_0 \qquad (55)$$

shows by comparison with (35) and (51) that the Maxwell-model applied by KUHN corresponds to a Voigt-model of the same type as that used here for the description of the mechanical properties of the muscle fibre. According to (51) and (55) the boundaries in KUHN's spectrum of retardation times are

$$\tau_1 = \tau_2 \quad \text{and} \quad \tau_2 = \infty. \qquad (56)$$

Furthermore, according to (35), (51), and (55):

$$J_0 = 0. \qquad (57)$$

The upper limit $\tau_2 = \infty$ indicates that KUHN's model flows ad infinitum.

2) Vibration experiments, resting and contracted fibre.

Transient experiments gave information about the transition from a dynamic to a static state by determining the velocity and degree of adjustment to a sudden change in length or tension. In this way the influence of the non-linear component on the total elastic reaction in the minute structure of the muscle fibre was studied. The procedure in these experiments, however, limited the range of measurements to processes which had a duration of more than 2 msec.

Further information about the mechanical properties of the fibre was obtained in vibration experiments.

These were previously performed by subjecting the fibre to a periodic change in *length* and measuring the change in tension produced (BUCHTHAL and KAISER, 1944). In experiments of this type it is important not to use too large an amplitude of vibration, since this may alter the mechanical reaction of the fibre during contraction. The effect of a periodic length amplitude of 2 per

cent (4 per cent peak to peak) on the tension developed during a single contraction can be seen in fig. 28, where it can be compared with the development of tension during a contraction without superposition of periodic vibrations. The mean tension *with* superimposed vibrations is only about 70 per cent of the mean tension in a twitch without vibrations. Curve II c shows how the fibre again approaches the original tension-time relation when

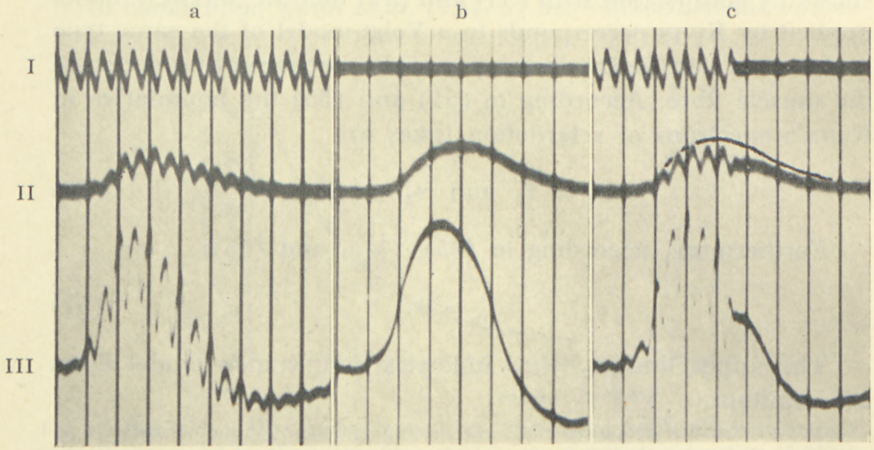

Fig. 28. *Isometric twitch with and without vibrations*, 15° C.
curve I: length alteration, amplitude peak to peak 4 per cent of L_0, 100 c.p.s.
curve II: tension in twitch as a function of time recorded with d. c. amplification and condenser myograph.
curve III: as II, but recorded with a. c. amplifier. (a) course of tension with and (b) without superimposed vibrations. Note that the vibrations stop in (c) after the maximum in tension. In curve II the upper contour of curve b for comparison is projected on curve c.

the vibrations are stopped during the contraction. At amplitudes of below 1 per cent, a decrease in the tension developed during contraction could no longer be observed.

In the present experiments a periodic alternating force acted on the fibre, and force and elongation were measured simultaneously. Lissajous figures such as those described in Part I were hereby obtained. An analysis of such a figure enables the determination of dynamic length-tension diagrams within a period of oscillation, which for the frequencies used was 10—30 msec.

Construction of dynamic length-tension diagrams. For a classically damped system the Lissajous figures produced by simultaneous values of force and amplitude are ellipses (comp. equations

(1) and (3) p. 17). However, the Lissajous figures obtained in vibration experiments, as fig. 7 shows, are not ideal ellipses, but more flattened in one half period than in the other. This deviation can be understood from the dynamic length-tension diagrams and the hysteresis which they show during

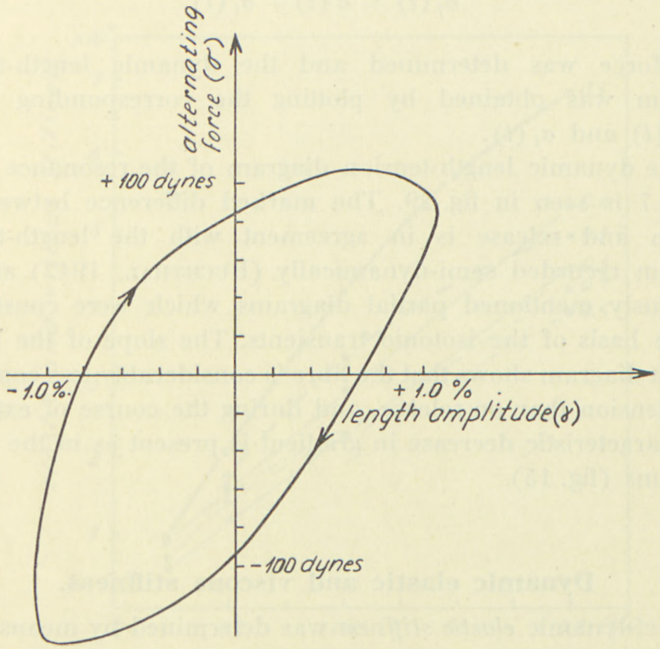

Fig. 29. *Dynamic length-tension diagram from vibrational experiments.* 0° C.
ordinate: change in tension in dynes.
abscissa: change in length in per cent of L_0.
The area described by the curve corresponds to the energy absorbed per oscillation period.

extension and release, and the Lissajous figures can be used to construct these length-tension diagrams. On account of the double differentiation of photographically recorded curves this can be only an approximate determination of the length-tension relation. However, the principal difference in the course of length produced by increasing and decreasing tension will appear with sufficient significance.

The external force $\sigma = \sigma_0 \cos \omega t$ varies sinusoidally with a known frequency. This enables us to plot the time on the x-axis and then to find the variation in length with time. By

differentiating twice, the acceleration of the movement ($\ddot{\gamma}(t)$) is obtained. Multiplication with the equivalent mass m finally gives the inertial force $\sigma_i(t)$. The force acting on the fibre σ_f is the difference between the external force and the inertial force:

$$\sigma_f(t) = \sigma(t) - \sigma_i(t). \tag{58}$$

This force was determined and the dynamic length-tension diagram was obtained by plotting the corresponding values for $\gamma(t)$ and $\sigma_i(t)$.

The dynamic length-tension diagram of the resonance ellipse in fig. 7 is seen in fig. 29. The marked difference between extension and release is in agreement with the length-tension diagram recorded semi-dynamically (BUCHTHAL, 1942) and the previously mentioned partial diagrams which were constructed on the basis of the isotonic transients. The slope of the length-tension diagram shows that the fibre is considerably less compliant on extension than on release, and during the course of extension the characteristic decrease in gradient is present as in the partial diagrams (fig. 15).

Dynamic elastic and viscous stiffness.

The dynamic *elastic stiffness* was determined by means of the resonance frequency arising from the elasticity of the fibre plus the mass of the system (cf. p. 18). The *viscous stiffness* was determined by the ratio between the alternating force acting on the fibre plus the recording system and the resulting maximal amplitude of vibrations. In the evaluation of the results obtained by this procedure it is necessary to examine to what extent resonance frequency and damping are unique standards, suitable for a complete characterization of elastic properties. In order to be able to define changes in the mechanical properties of the fibre, produced, e. g. by tension or temperature, it is necessary that the resulting changes in stiffness and viscosity are large compared with the change in these quantities which might result because of the necessary change in measuring frequency required by the experimental technique, i. e. the adjustment to a new resonance frequency when the stiffness and viscosity para-

meters vary. For example during transition from rest to contraction under isotonic conditions the resonance frequency at a given load rises from 40 to 56 vibrations per sec., with a corresponding increase in elastic stiffness of 100 per cent. If the measuring frequency applied to the resting fibre was increased from 40 to 56

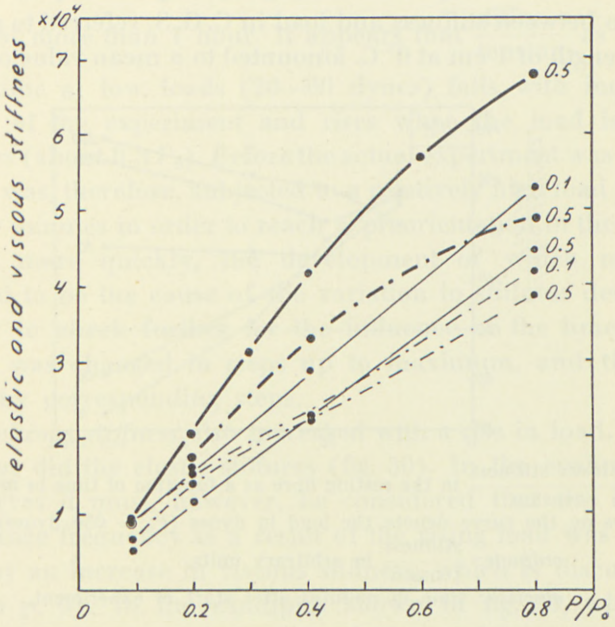

Fig. 30. Elastic stiffness (full lines) and viscous stiffness (stippled lines) in dynes × cm^{-1} as a function of load (1 $P_0 \times L_0^{-1}$ = 2800 dynes × cm^{-1}).
fibre at rest: thin lines.
contraction: thick lines.
The figures on the curves denote the vibrational amplitudes in per cent of the equilibrium length of the fibre (deflection measured from the mean position). 0° C.
ordinate: elastic and viscous stiffness in dynes × cm^{-1}.
abscissa: load in units of P_0.

vibrations per second, an increase in stiffness of only 0 to 10 per cent was found, so that at least 90 per cent of the increase in stiffness observed during contraction must be considered an expression of a change in elastic stiffness due to the contracted state. Thus, the frequency dependence of the elastic stiffness in the range of frequencies examined can be considered to have a second order significance.

Resting fibre.

The elastic stiffness increased in the fibre at rest approximately linearly with the load (fig. 30). At a load of 0.3 P_0 and an amplitude of the periodic changes in load corresponding to a length amplitude of 1 per cent of the equilibrium length (= 2 per cent peak to peak), the ratio between stiffness and load in C. G. S. referred to an equilibrium length of 1 cm at 0° C. amounted to a mean value of 18—20.

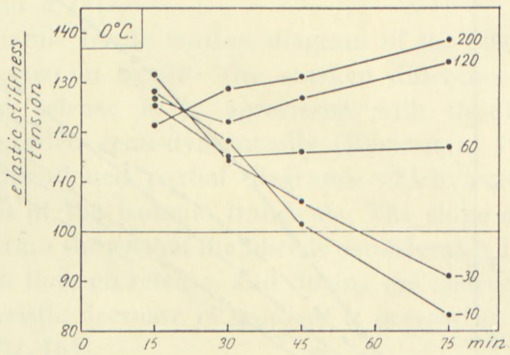

Fig. 31. $\frac{\text{Elastic stiffness}}{\text{tension}}$ in the resting fibre as a function of time in minutes. The figures on the curve denote the load in dynes (P_0 = 650 dynes). 0° C.
ordinate: $\frac{\text{stiffness}}{\text{tension}}$ in arbitrary units.
abscissa: time in minutes after start of experiment.

This value was independent of the cross section of the fibre within wide limits, the cross section in the present material varying between 0.05 and 0.5 mm in diameter, according to whether single fibres or small bundles of fibres had been examined. The results of these experiments, in which the load was varied and the change in stiffness measured, agree with the stiffness-tension relationship found in previous experiments, in which the changes in tension produced by periodic changes in length were used as a measure of stiffness (Buchthal 1942, Buchthal and Kaiser 1944). The variation of stiffness with load makes it an advantage to work at constant load when estimating changes in elasticity produced by factors other than the tension. When measuring at constant length, the tension varying with time will cause a concomitant change in stiffness. However,

even if measured at a constant load, the alterations in the texture of the fibre will bring about a variation in the stiffness with time when the fibre is exposed to different loads over a long time interval. This is illustrated in fig. 31 by experiments in which stiffness and tension in the resting fibre at constant temperature (0° C.) were measured at changing levels of load during an interval of more than 1 hour. It appears that $\frac{\text{stiffness}}{\text{tension}}$ as a function of time at low loads (20—60 dynes) falls with increasing duration of the experiment and rises when the load is above 200 dynes (about $0.3\,P_0$). Before the actual experiment was started, the fibre was, therefore, subjected to a relatively high load ($0.8\,P_0$) for a few minutes in order to reach a preorientation in the minute structure more quickly, the development of which must be presumed to be the cause of the variation in stiffness described. In order to check further for the influence of the time factor, the load was changed in steps up to maximum, and then decreased by corresponding steps.

The *viscous stiffness* also increased with a rise in load, but not linearly as did the elastic stiffness (fig. 30). In the evaluation of these curves it must, however, be considered that the increase in resonance frequency as a result of the rising load was accompanied by an increase in viscous stiffness, which is discussed in detail on p. 91. In the examples shown in fig. 30, which represents a mean curve for a series of 10 experiments, the viscous stiffness is of the same order of magnitude as the elastic. However, other experimental series, which were carried out under the same conditions, but at different times of the year showed remarkable uniformity for a given set of measurements, but a considerable variation in the ratio of viscous to elastic stiffness between the different groups. In a later section an attempt is made to correlate these variations with other properties of the fibre.

When viscous stiffness is expressed in terms of *viscosity*, the basic initial viscosity at equilibrium length of the fibre amounted to approximately 5×10^5 centipoise in the range of frequencies applied in the present experiments (25—150 c.p.s.). The viscosity of the structural elements exceeded that of the protoplasm of the fibre (29 centipoise) by 10^4. The latter was determined by measuring the migration velocity of an oil drop introduced into

the muscle fibre (RIESER 1949). Thus at the most, 0.01 per cent of the viscous stiffness may be caused by the sarcoplasm.

Dynamic stiffness as compared with static stiffness.

The dynamic stiffness of the muscle fibre always exceeded the static stiffness (BUCHTHAL 1942). With the vibrational frequencies employed in the present investigation the ratio $G_{dyn} : G_{stat}$ at the same load in different fibres varied between 3:1 and 5:1. With increasing load the ratio decreased slightly. As mentioned above, both static and dynamic stiffness increased linearly with load, the slope of the stiffness-tension diagram being three times steeper in dynamic than in static experiments. As the dynamic stiffness at tension zero exceeded the static 5 times, the ratio between the stiffness-tension[1] in dynamic and static experiments is $\frac{5}{3} = 1.7$. The *dynamic elasticity modulus* amounted with the resting fibre at equilibrium length at 0° C. to 2.5×10^6 dynes per cm^2. The vibrational amplitude applied was 1 per cent of L_0 and the frequency approximately 30 c.p.s.

The dependence of stiffness on the amplitude of vibration.

In addition to the load, there is a factor affecting the elastic and viscous stiffness which so far has not been considered. As long as an elastic body follows Hooke's law, the variations in length and tension are proportional $\left(\frac{\Delta \text{ tension}}{\Delta \text{ length}} = \text{constant}\right)$, i. e. a variation in the amplitude of the periodic changes in load used for stiffness measurements does not affect the result. In a body with a non-linear length-tension diagram, the stiffness will vary with the amplitude of the changes in load. From the dynamic length-tension diagram determined from the ratio between stiffness and tension, variations in stiffness of less than 1 per cent could be expected for the amplitudes of load used in the present experiments. A more detailed discussion of the influence of the exponential dynamic length-tension diagram on

[1] Stiffness-tension denotes the distance on the tension axis obtained by extrapolation of the stiffness-tension diagram to zero stiffness.

the dependence of stiffness on amplitude is found on p. 292. The experimentally found dependence of the stiffness on amplitude was, however, considerably larger than would have been expected on the basis of the non-linearity of the length-tension

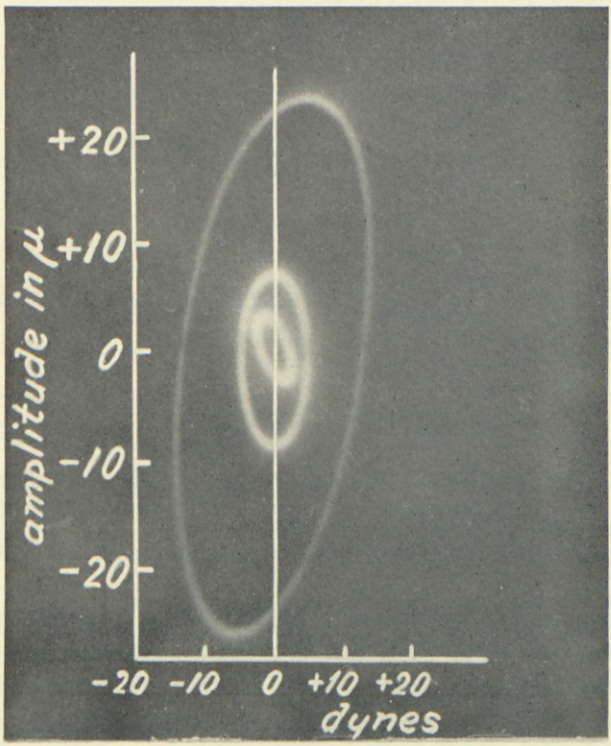

Fig. 32. Three Lissajous figures showing the relation between alternating force and alternating length at the same mean load and vibrational frequency, but three different alternating loads. 0° C.
ordinate: vibrational length amplitude in μ, measured as deflection from the mean position.
abscissa: applied alternating force in dynes.
The position of the intermediate ellipse indicates resonance, the smallest ellipse, corresponding to a decrease in amplitude, indicates an increase in stiffness and the largest ellipse (increase in amplitude) corresponds to a lower stiffness.

diagram. In the first experiments this deviation was assumed to be due to the recording system. In these experiments the electromagnetic coil was supported by pivots in which the frictional forces could vary with the amplitude of vibrations. Therefore, this recording device was replaced by a system with a knife-

edge suspension, and control experiments in which the muscle fibre was replaced by a very thin steel spring showed no measurable variation in resonance frequency with variation in vibrational amplitude within the range of frequency and amplitude used in the present experiments (cf. p. 23). Even when this system was used in which a lack of linearity due to possible play in the bearings of the recording system was eliminated, the muscle fibre showed a considerable variation of stiffness with the size

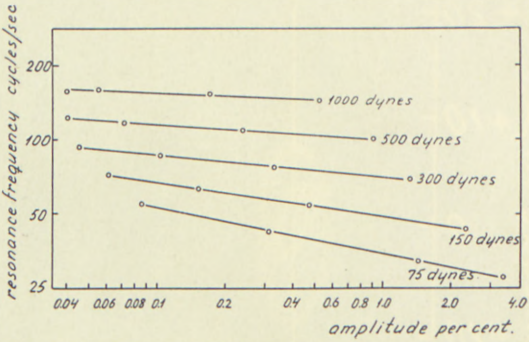

Fig. 33. Resonance frequency as a function of the alternating length amplitude. The figures on the curves denote the mean load in dynes (P_0 = 800 dynes). 0° C.
ordinate: resonance frequency in c.p.s.
abscissa: length amplitude in per cent of L_0 (peak to peak).

of the amplitude of vibrations. Fig. 32 shows 3 Lissajous figures which represent the correlation between alternating load and alternating amplitude for a fibre at different alternating loads (same measuring frequency and same initial load). The axes of the curve in the middle are parallel to the axes of the oscilloscope screen and indicate the presence of resonance at the frequency and amplitude in question. The deviation of the axes of the smallest ellipse (sloping to the left) and the largest ellipse (sloping to the right) shows that the resonance frequency of these ellipses was displaced to a higher and a lower value respectively. An example of the variation in the resonance frequency and hence of the elastic stiffness with the amplitude of vibrations is given in fig. 33. The logarithm of the resonance frequency varies linearly with the logarithm of the vibrational amplitude in such a way that the stiffness falls with increasing amplitude. This fall was relatively more pronounced the lower the load. Even a doubling of an amplitude of only 0.1 per cent of the equilibrium length

caused recognizable changes in stiffness. In the example shown in fig. 33, the decrease in stiffness was 20 per cent at a load of 150 dynes and a variation in amplitude from 0.15 to 0.30 per cent of L_0. The dependence on amplitude of the elastic stiffness at different loads can be seen in fig. 34. Independent of the load

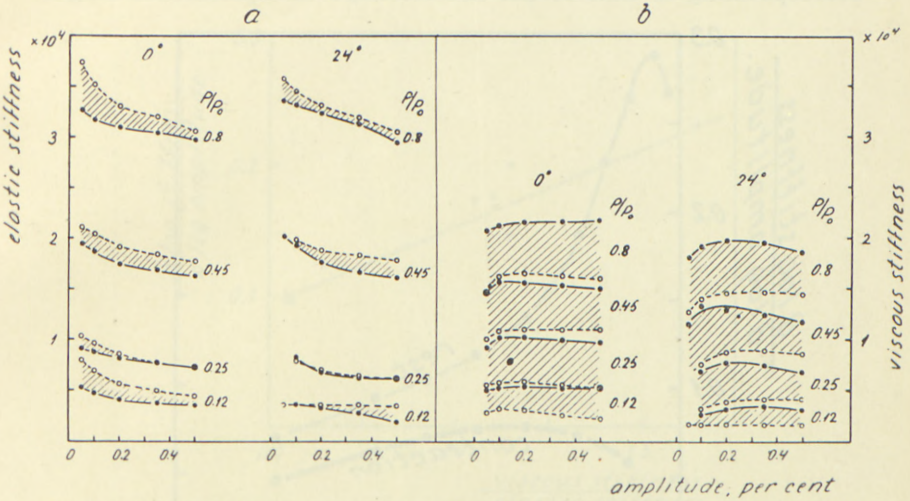

Fig. 34. Dynamic stiffnesses as a function of the alternating length amplitude at 0° and 24° C.

a) elastic stiffness, dynes $\times$ cm^{-1} (1 $P_0 \times L_0^{-1}$ = 2000 dynes $\times$ cm^{-1}).

b) viscous stiffness, dynes $\times$ cm^{-1} (1 $P_0 \times L_0^{-1}$ = 2000 dynes $\times$ cm^{-1}).

stippled lines: experiments with 16 times increased equivalent mass.

abscissa: alternating length amplitude in per cent of L_0, deflection measured from the mean position.

ordinate: elastic and viscous stiffness in dynes $\times$ cm^{-1}.

the absolute changes in stiffness are approximately of the same order of magnitude. This indicates that the relative variation of stiffness with amplitude decreased with increasing stiffness, and, on account of the stiffness-load relationship, also with increasing load.

For all the muscle fibres investigated, the influence of the vibrational amplitude, expressed by $\frac{d(\log \text{stiffness})}{d(\log \text{amplitude})}$ as a function of the load is shown in fig. 35. At a load of 0—0.1 P_0 the variation with amplitude was at maximum and decreased rapidly with increasing load. At 0.8 P_0 it amounted to only one fourth of the maximum.

In *rubber* we have found an amplitude dependence which was less than in the muscle fibre. In the unloaded state $\frac{d(\log \text{stiffness})}{d(\log \text{amplitude})}$ in undervulcanized rubber was 0.20 and in vulcanized rubber 0.14. At a load which produced an orientation corresponding to that of the muscle fibre at equilibrium length

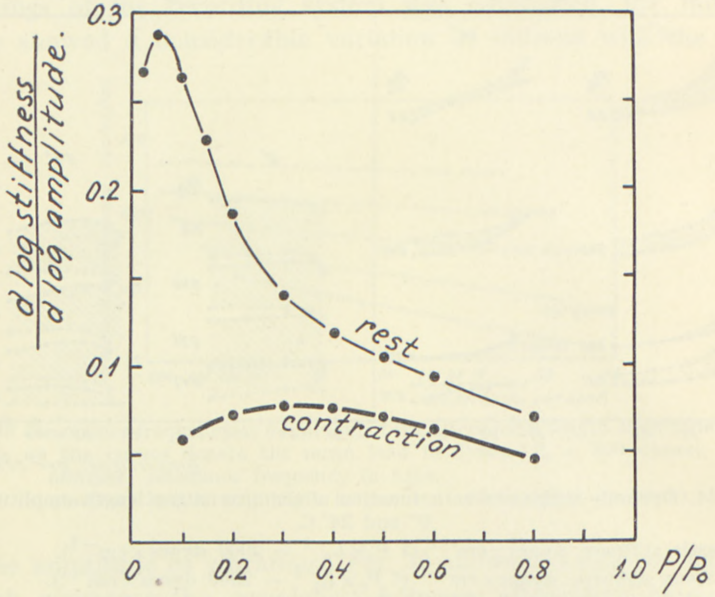

Fig. 35. Amplitude dependence of elastic stiffness as a function of load in the resting fibre and during isotonic tetanic contraction.
ordinate: $\frac{d\,(\log \text{stiffness}}{d\,(\log \text{amplitude})}$.
abscissa: load in units of P_0.
0° C., mean curve of all experiments.

($L = 300$ in rubber) the quotient decreased to one tenth of its value in the unloaded state.

The variation in viscous stiffness with a variation in vibrational amplitude had a course differing from that of the elastic stiffness, and showed a maximum in the amplitude range 0.1 to 0.4 per cent of L_0 (fig. 34b).

As previously mentioned, the ratio of viscous to elastic stiffness (sr) varied in different experiments. The varying ratio could not be related to variations in the elastic stiffness measured per unit of load, since this value showed only slight variations in the

different series of experiments. A relation to the size of the amplitude dependence was, however, found. Different experimental series referred to the same load (0.3 P_0) showed that the viscous stiffness was higher in the presence of a large amplitude dependence than when the amplitude dependence was small (fig. 36).

In order to obtain a quantitative expression of the interaction

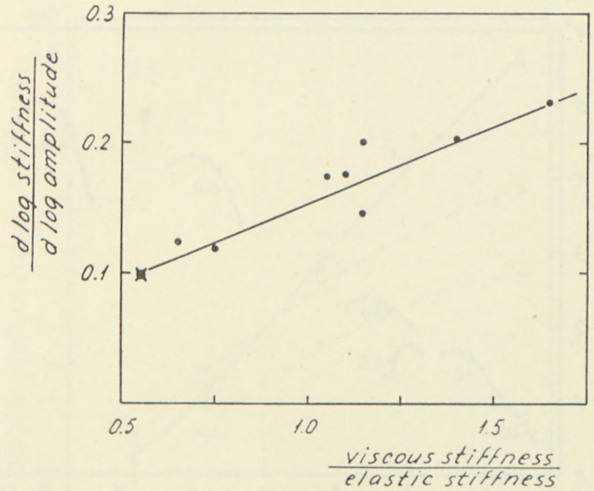

Fig. 36. Amplitude dependence of elastic stiffness plotted versus *sr* $\left(\frac{\text{viscous stiffness}}{\text{elastic stiffness}}\right)$, 0° C.

ordinate: $\frac{d\,(\text{log stiffness})}{d\,(\text{log amplitude})}$.

abscissa: $\frac{\text{viscous stiffness}}{\text{elastic stiffness}}$.

of the viscous and elastic forces, the viscous stiffness is plotted versus the elastic (fig. 37). A variation in the amplitude from 0.1 to 1 per cent of L_0 at the different loads produced a parabolic curve with the axis of symmetry parallel to the axis of the viscous stiffness. On increasing the load from 0.1 to 0.8 P_0 both elastic and viscous stiffness increased. The elastic stiffness decreased with increasing amplitude, which is indicated in the curves by the direction of the arrow. The maximum in these curves is caused by the changes in viscous stiffness with vibrational amplitude.

Both increasing vibrational amplitude and increasing fre-

quency caused a rise in the velocity of length variations. The maximal deformation velocity which was attained within a period of vibration is denoted as *velocity amplitude* ($\omega_0 \times \gamma_0$). In the example shown in fig. 33 illustrating the amplitude dependence of the elastic stiffness, the velocity amplitude varied between 0.25 and 6.0 L_0 per second.

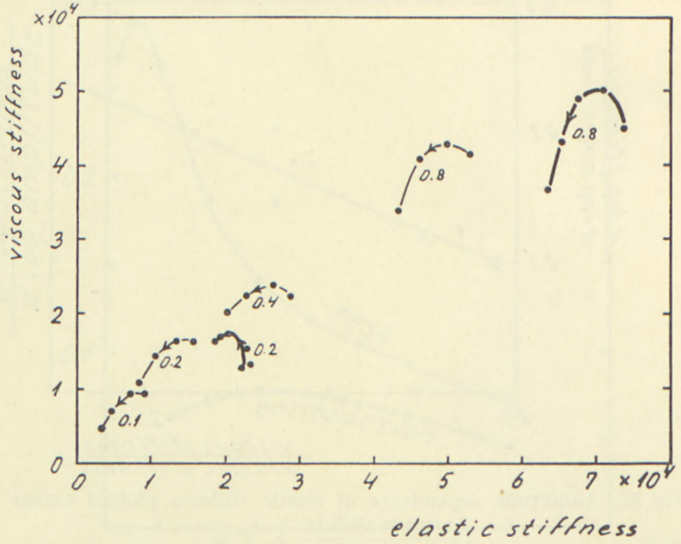

Fig. 37. Viscous stiffness plotted versus elastic stiffness. The figures on the curves denote the different levels of load in P_0.
Thin lines: resting fibre; thick lines: tetanically contracted fibre. The connected points denote in the direction of the arrow amplitudes of 0.1, 0.2, 0.5, 1.0 and during contraction also 2.0 per cent of L_0, deflection measured from the mean position. 0° C.
ordinate: viscous stiffness in dynes × cm^{-1} (1 $P_0 \times L_0^{-1}$ = 3500 dynes × cm^{-1}).
abscissa: elastic stiffness in dynes × cm^{-1} (1 $P_0 \times L_0^{-1}$ = 3500 dynes × cm^{-1}).

The *total stiffness* of the fibre (its "mechanical impedance"), defined as the Pythagorean sum of elastic and viscous stiffness ($\sqrt{G_{elast}^2 + G_{visc}^2}$), had a maximum at a low amplitude in the range of 0.2—0.4 per cent of L_0. In a special series of experiments, in which the fibre was subjected to forced changes in length with constant mean length (corresponding to former "isometric" experiments, Buchthal and Kaiser 1944), a similar decrease was found in the total stiffness with increasing amplitude. The range of amplitudes examined in these experiments was 0.5—2 per cent of L_0.

In the introduction to the present section it has been pointed out that the frequency of vibration may influence the results of the measurements. In order to investigate this effect further, a series of experiments was performed in which the equivalent mass of the recording system was increased by the introduction of an additional mass. This caused a reduction in the resonance frequency

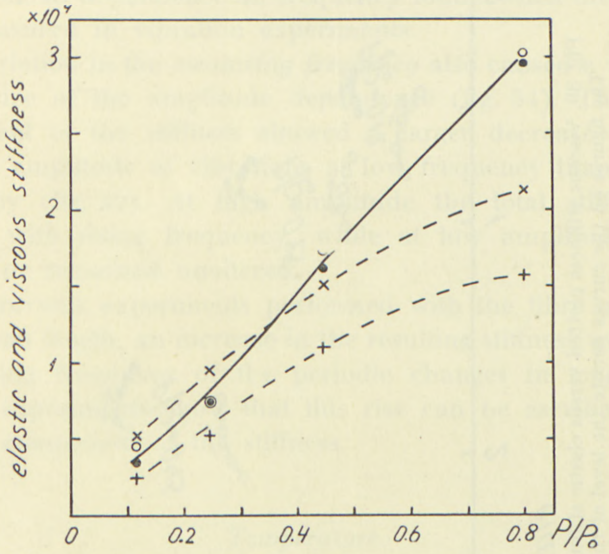

Fig. 38. Elastic (————) and viscous (— — — —) stiffness as a function of load without (• ×) and with (○ +) 15 times additional equivalent mass. Vibrational amplitude 0.50 per cent of L_0, deflection measured from the mean position. 0° C.

ordinate: stiffnes in dynes × cm^{-1} (1 $P_0 \times L_0^{-1}$ = 2000 dynes × cm^{-1}).
abscissa: load in units of P_0.

to approximately one fourth. The mean curve for these experiments showed that the elastic stiffness at a vibrational amplitude of 1 per cent of L_0 was not affected measurably (fig. 38). The viscous stiffness, however, decreased 16 per cent on the average, when the frequency was halved. This indicates that part of the increase in viscous stiffness, apparently caused by the load, is due to the change in resonance frequency. The total stiffness decreased approximately 5 per cent at load ca. 0.5 P_0, when the frequency of the vibrations was halved in the frequency range of 100 to 25 c.p.s. This frequency dependence corresponds to the variations in the stiffness found

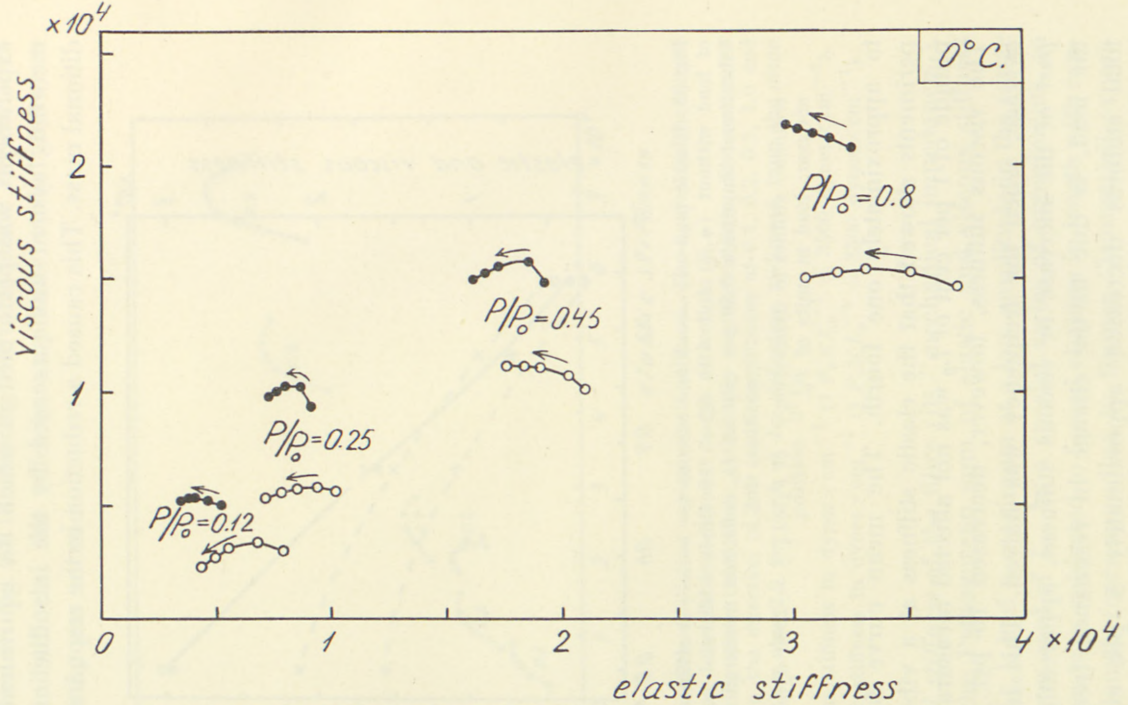

Fig. 39. Viscous stiffness plotted versus elastic stiffness at 0° C. in the resting fibre.
The figures on the curves denote the level of the mean load in units of P_0.
The connected points denote different vibrational amplitudes in the direction of the arrow: 0.05, 0.1, 0.2, 0.35, 0.5 per cent of the equilibrium length (measured as deflection from the mean position). • without and ○ with 15 times additional equivalent mass.

ordinate: viscous stiffness in dynes × cm^{-1} (1 $P_0 \times L_0^{-1}$ = 2000 dynes × cm^{-1}).

abscissa: elastic stiffness in dynes × cm^{-1} (1 $P_0 \times L_0^{-1}$ = 2000 dynes × cm^{-1}).

when it was measured at different times after a sudden change in length or load. A doubling of the time interval, elapsing after the change in load gave an increase in "softness" of 4 to 5 per cent (Table 4, isotonic transient). Thus, agreement can be expected between the distribution function for retardation times, calculated on the basis of transient experiments (fig. 26, p. 73) and the small dependence on frequency found when the stiffness was measured in vibration experiments.

A variation in the *measuring frequency* also caused a variation in the size of the amplitude dependence (fig. 34). The elastic component of the stiffness showed a larger decrease with increasing amplitude of vibrations at low frequency than at high frequency (fig. 39). At high amplitude the total stiffness increased with rising frequency, while at low amplitude it decreased or remained unaltered.

In previous experiments performed with the fibre at a constant mean length, an increase in the resulting stiffness was found with rising frequency of the periodic changes in length. The present experiments show that this rise can be ascribed to the viscous component of the stiffness.

Temperature.

Both the viscous and the elastic stiffness fell with rising temperature (fig. 40). This variation proceeded continuously with variation in temperature, but since the temperature range examined was naturally limited to 0°—25° C. and the variations in stiffness were relatively small, it cannot be decided whether this dependence follows a linear or e. g. a logarithmic function. At rest the *elastic stiffness* decreased by approximately 1 per cent per degree C. at low and moderate loads. At high loads no measurable changes in stiffness were observed, even for a maximal variation in temperature (25° C.). The *viscous stiffness* decreased appreciably more with rising temperature, i. e. 2 per cent per degree C. at a low load and 1 per cent at a high load. Viscous stiffness versus elastic stiffness at high and at low temperature is plotted in fig. 43. At a high load the increase in stiffness with falling temperature was caused exclusively by the viscous component.

The *elastic* stiffness versus amplitude relationship was not appreciably influenced by temperature in the range of 0° to 25° C. (fig. 34). The *viscous* stiffness versus amplitude relationship, however, changed with temperature such that the maxima were shifted to higher values of the amplitude with increasing temperature.

In earlier experiments in which the stiffness was determined

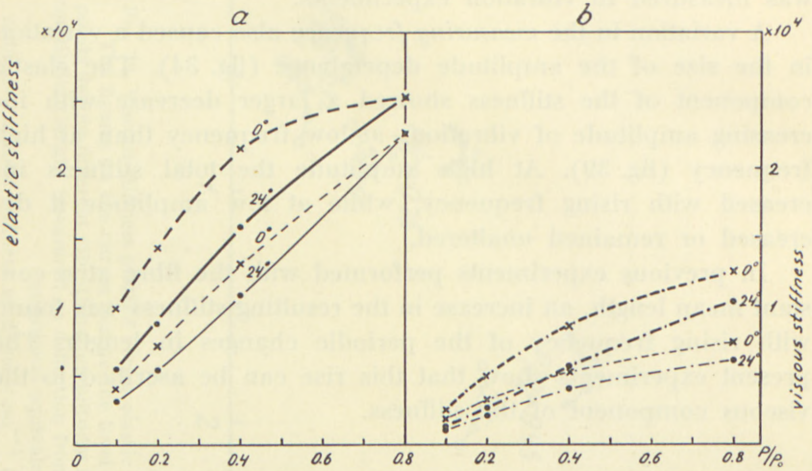

Fig. 40. Dynamic stiffnesses at rest (thin lines) and during contraction (thick lines) at 0° and 24° C. as a function of load.

ordinate: a) elastic stiffness in dynes × cm^{-1} ($1\ P_0 \times L_0^{-1} = 2000$ dynes × cm^{-1}).
b) viscous stiffness in dynes × cm^{-1} ($1\ P_0 \times L_0^{-1} = 2000$ dynes × cm^{-1}).
abscissa: load in units of P_0.
Vibrational amplitude 1 per cent of L_0, deflection measured from the mean position.

at constant length no significant variation in stiffness with temperature was found in the resting fibre (BUCHTHAL *et al.* 1944a). The relatively small changes in stiffness caused by the change in temperature were not observable with the low sensitivity used in these experiments, i. e. the sensitivity of the recording system was adjusted so that the amplifiers would not overload for the response of the system up to load P_0. Thus, in the region of small initial loads the sensitivity was too low. At a high degree of stretch, where the accuracy of the measurement was sufficiently high, the temperature dependence of the total stiffness, in agreement with the present experiments, was not significant and, therefore, was not observed.

The effect of hypotonic and hypertonic solutions on elastic and viscous stiffness.

When isotonic Ringer's solution was replaced by a 50 per cent hypotonic solution, no significant change was found in the viscous and elastic stiffness of the fibre. The average increase in the muscle fibre diameter in these experiments amounted to 30 per cent. 100 per cent hypertonic Ringer's solution, however, caused a doubling of both the elastic and the viscous stiffness. The decrease in diameter averaged 12 per cent and occurred in the course of few minutes.

Example: equilibrium length of fibre 6 mm. Load: 0.3 P_0.

concentration of Ringer in m. equivalents per l.	elastic stiffness 10^4 dynes × cm^{-1}	viscous stiffness 10^4 dynes × cm^{-1}	diameter in per cent
250	3.34	2.68	100
125	3.30	2.70	133
500	8.10	7.50	89

The effect of hypertonic Ringer's solution was reversible and at the end of the experiment the fibre was often still excitable. An increase in the water content of the fibre, obtained by placing it in hypotonic environment, did not affect the structural elements which are responsible for the elastic and viscous stiffness, and these elements must be assumed to be maximally hydrated. As a decrease in the water content increased the stiffness of the structure, this must indicate that part of the structural water acts as "softening agent" in the same way as plasticisers in high polymers.

Elastic and viscous stiffness in isotonic tetanic contraction.

In the range of loads investigated the elastic stiffness in isotonic tetanic contraction was higher than that at rest. This was also the case at 1.0 P_0, where the tension at rest and in contraction coincided, i. e. where no more extra tension could be developed by contraction. At 0° C. and with a vibrational amplitude of 0.5 per cent of L_0, the increase in stiffness during contraction amounted

to 50—100 per cent with its maximum at 0.3 to 0.4 P_0 (fig. 30). In fig. 41 stiffness and tension at rest and in contraction are given as a function of the degree of stretch. In this series, determinations of stiffness, tension, and length in *isotonic* and *isometric* contraction were carried out alternately on the same fibre. The stiffness varied steeply in the range of length below equilibrium

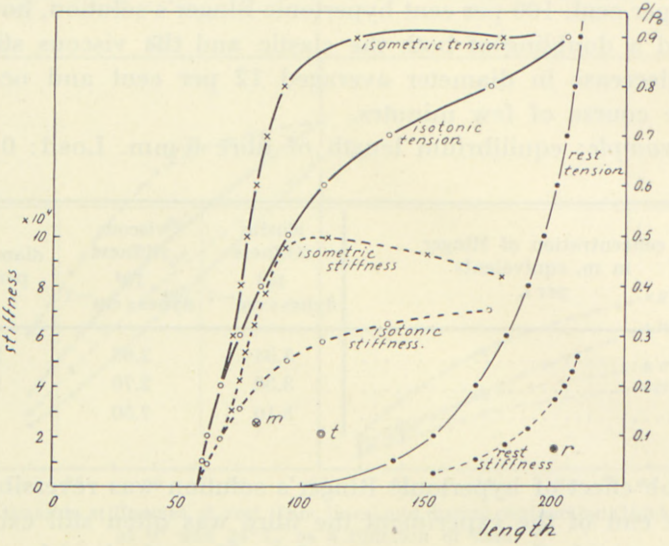

Fig. 41. Tension (P/P_0) and dynamic stiffnesses as a function of length. 0° C.
Full lines: tension.
Dashed lines: elastic stiffness.
$\odot_r$ viscous stiffness at 0.6 P_0 at rest.
$\otimes_m$ viscous stiffness at 0.6 P_0 during tetanic isometric contraction.
$\odot_t$ viscous stiffness at 0.6 P_0 during tetanic isotonic contraction.
left ordinate: stiffness in dynes $\times$ cm^{-1} (1 $P_0 \times L_0^{-1}$ = 2500 dynes $\times$ cm^{-1}).
right ordinate: tension in units of P_0.
abscissa: length in per cent of L_0.

length. Corresponding to the higher tension reached in the curve for the isometric maxima, the dynamic stiffness determined in isometric contraction, referred to the *same length*, was 50 to 100 per cent higher than that found in isotonic contraction. However, when referred to the *same tension*, the stiffness was highest when the length of contraction was least, i. e. in isometric contractions ($L_{\text{rest}} > 100$) or in stop ("anschlag") contractions ($L_{\text{rest}} < 100$). The difference between isotonic and "isometric" stiffness at the

same tension was proportional to the difference in length during contraction. For a decrease in length of 2.5 per cent an increase in elastic stiffness of 1 per cent was measured in "isometric" contraction as compared with isotonic contraction at the same tension. This means that in isotonic contraction the variation of stiffness with load can be described by a family of curves, where each curve

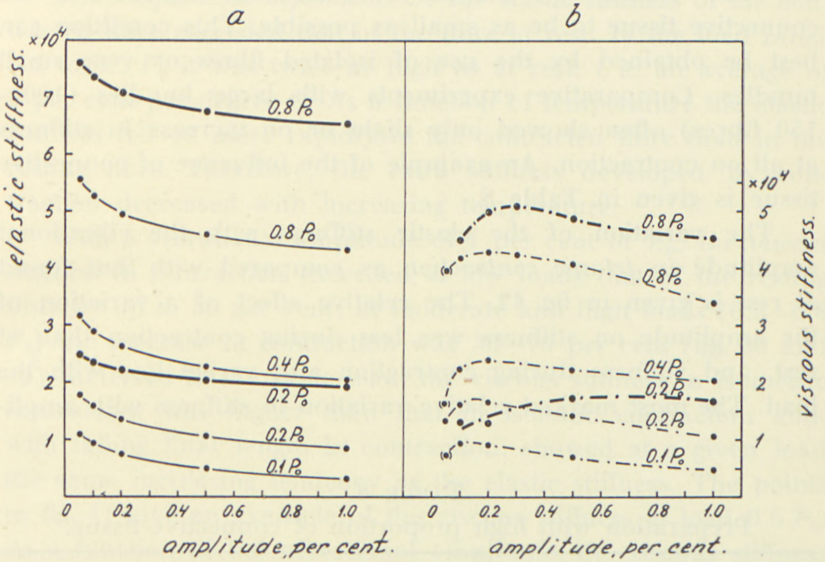

Fig. 42. Dynamic stiffnesses as a function of vibrational amplitude at rest (thin lines) and during contraction (thick lines). The figures on the curves denote the load in units of P_0. 0° C.

a) elastic stiffness (left ordinate) in dynes × cm^{-1}, 0° C, (1 $P_0 \times L_0^{-1}$ = 3600 dynes × cm^{-1}).

b) viscous stiffness (right ordinate) in dynes × cm^{-1}, 0° C, (1 $P_0 \times L_0^{-1}$ = 3600 dynes × cm^{-1}).

abscissa: alternating length amplitude in per cent of L_0, measured as deflection from the mean position.

represents the stiffness-load relation for a certain initial length. A similar dependence was also found under isometric conditions (Buchthal and Kaiser 1944). The length dependence of the stiffness-load relation is not necessarily an expression of a variation in the intensity of the contraction process, since the increase in cross section and the shortening in itself must be expected to give increased stiffness. The stiffness during tetanic contraction is determined exclusively by the length and tension of the fibre,

regardless of whether the contraction was an isometric, an isotonic, a stretch or a release contraction. Even after complete relaxation after a tetanic contraction the stiffness was still found to be higher than before contraction. This increase practically disappeared within 0.5 to 1 minute at 0° C.

In order to be able to measure an increase in stiffness of the order found, it is necessary for the shunting effect of the connective tissue to be as small as possible. This condition can best be obtained by the use of isolated fibres or very small bundles. Comparative experiments with large bundles (100—150 fibres) often showed only slight or no increase in stiffness at all on contraction. An example of the influence of connective tissue is given in Table 8.

The variation of the elastic stiffness with the vibrational amplitude *in tetanic contraction* as compared with that found at rest is given in fig. 42. The relative effect of a variation of the amplitude on stiffness was less during contraction than at rest, and stiffness during contraction also varied less with the load. The most marked relative variation in stiffness with ampli-

TABLE 8.

Preparation with high proportion of connective tissue.

Initial length in per cent of L_0	load in dynes	state	resonance frequency c. p. s.	shortening in per cent of L_0	change in stiffness in per cent
100	64	contraction	64	18	..
118	64	rest	63.5	..	—4
100	64	contraction	64.5	18	..
118	64	rest	69	..	..
122	120	rest	91	..	..
104	120	contraction	85	18	—11
104	120	contraction	87.5	22	..
126	120	rest	91.5	..	..
116	300	contraction	128	19	..
136	300	rest	128	..	0
116	300	contraction	128	19	..

equilibrium length = 5 mm. Referred to L_0 = 1 cm, $\frac{\text{stiffness}}{\text{tension}}$ = 50—60, i. e. 2.5—3 times the value found in the isolated fibre or in a small bundle.

tude was seen at moderate loads. At low loads (0.1 P_0) the amplitude dependence of the stiffness in contraction was only $\frac{1}{5}$, at load 0.25 P_0 $\frac{1}{2}$, and at loads exceeding 0.5 P_0 $\frac{2}{3}$ of that found at rest (fig. 42). The fact that contraction stiffness decreased less with amplitude than stiffness at rest implies that the increment in stiffness due to contraction increases with increasing amplitude.

The temperature dependence of the elastic stiffness of the contracted fibre exceeded that of the fibre at rest. In the load range 0.1 to 0.5 P_0 it was twice as high as at rest, i. e. an average of 2 per cent per degree C. As a function of temperature the elastic stiffness fell off more rapidly in the contracted fibre than in the resting fibre. Therefore, the extra stiffness developed by contraction decreased with increasing temperature.

With a vibrational amplitude of 1 per cent of L_0, *the viscous stiffness in contraction* exceeded at low loads that of the resting fibre by up to 30 per cent; at moderate and high loads (0.3—0.8 P_0) the increase in contraction was 30—70 per cent (fig. 30 and 42). Referred to the same load, the viscous stiffness in isometric contraction was higher than that in isotonic contraction and, with falling final length in contraction, showed at a given load the same increasing tendency as the elastic stiffness. The points in fig. 41 give an example of the viscous stiffness at load 0.6 P_0. As a function of the vibrational amplitude, the viscous stiffness during contraction only increased very slightly with the load in the range of amplitude 0.1 to 0.5 per cent of L_0 (fig. 42).

The *temperature dependence* of the viscous stiffness in contraction displayed the same behaviour as the elastic stiffness, viz. it fell off faster with temperature than in the resting fibre. In the range of load 0.1 to 0.5 P_0 the temperature coefficient of viscous stiffness amounted on the average to 2.2 per cent per degree C. (fig. 40). In contrast to the elastic stiffness, the temperature dependence of the viscous stiffness only decreased slightly with a rising load (up to 0.8 P_0). In earlier experiments with isometric contractions a considerable temperature dependence was also found for the total stiffness.

The plot of simultaneous values of viscous and elastic stiffness shows that the increase in total stiffness during an isotonic *tetanic contraction* is caused predominantly by the elastic component (fig. 37). It is also seen that a variation in the vibrational am-

plitude gave parabolic curves for each load for contraction as well, but in contraction the variation in viscous stiffness was relatively larger at low amplitudes (see also fig. 42 b). The rising part of the curve is therefore more clearly defined.

Fig. 43 shows viscous stiffness plotted versus elastic stiffness in another series of experiments. This series also showed that the increase in stiffness during contraction at a low load was chiefly

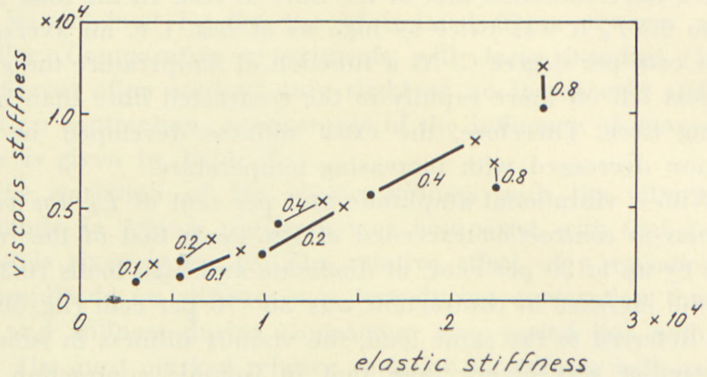

Fig. 43. Viscous stiffness plotted versus elastic stiffness at rest (thin lines) and during contraction (thick lines). The figures on the curves denote the load in units of P_0.
× = 0° C., • = 24° C.
ordinate: viscous stiffness in dynes × cm^{-1} (1 $P_0 \times L_0^{-1}$ = 1000 dynes × cm^{-1}).
abscissa: elastic stiffness in dynes × cm^{-1} (1 $P_0 \times L_0^{-1}$ = 1000 dynes × cm^{-1}).
Vibrational amplitude 1 per cent of L_0, measured as deflection from the mean position.

due to the elastic component, while the viscous component dominated the increase at a high load. The change in stiffness during contraction caused by the temperature (2 per cent per degree) was up to 0.4 P_0 caused mainly by an increase in elastic stiffness, and at a high load (0.8 P_0) by the viscous component.

The values given for the increase of stiffness during contraction are valid for non-fatigued fibres only. With increasing degree of *fatigue* the increase in stiffness fell, and especially at low vibrational amplitudes a *decrease* in stiffness of 10—30 per cent, accompanying the reduced shortening, could be measured in the fatigued fibre.

We have performed preliminary experiments in order to determine the course of stiffness under isotonic conditions *during*

the transition from rest to contraction. An alternating force was introduced on the fibre and the resulting amplitude was recorded, in addition to the course of shortening. In these experiments the stiffness was found to be maximal about 0.1 second after the elapse of the latent period. This agrees with the findings in transient experiments during contraction (p. 163) and with earlier vibration experiments under isometric conditions (BUCHTHAL and KAISER 1944). However, the procedure previously applied for the determination of stiffness had the limitation that the changes in the phase angle were not known, hence it was not possible to differentiate between viscous and elastic stiffness. In addition, knowledge of the change of their mutual relation during the development of shortening was inadequate and consequently the time of the exact position of the maximum could not be ascertained with any great accuracy in these experiments.

Elastic and viscous stiffness in threads of actomyosin.

In a series of experiments we have investigated elastic and viscous stiffness in actomyosin threads. The preparation of the actomyosin was described in a previous paper (BUCHTHAL *et al.* 1949). In these threads the stiffness increased with the load, but the dependence was not linear, as was the case in the muscle fibre (fig. 44a). The increase in stiffness for both elastic and viscous stiffness was relatively largest at small loads. With a constant load the elastic stiffness also increased with time in the actomyosin threads and the increase amounted to about 10 per cent within 15—20 minutes. The viscous stiffness, however, tended to decline.

The viscous stiffness was about one fifth of the elastic. A variation in stiffness with the amplitude of vibration was also found in actomyosin threads (fig. 44b), but this variation *was only 10—20 per cent* of that found in the resting muscle fibre, and was independent of the load. $\frac{d(\log \text{stiffness})}{d(\log \text{amplitude})}$ for actomyosin threads had a mean value of 0.025 (cf. p. 88). The dependence on amplitude in actomyosin threads was of the same order of magnitude as that found in normally vulcanized rubber. Both the elastic and viscous stiffness fell by about 1 per cent per degree C. with

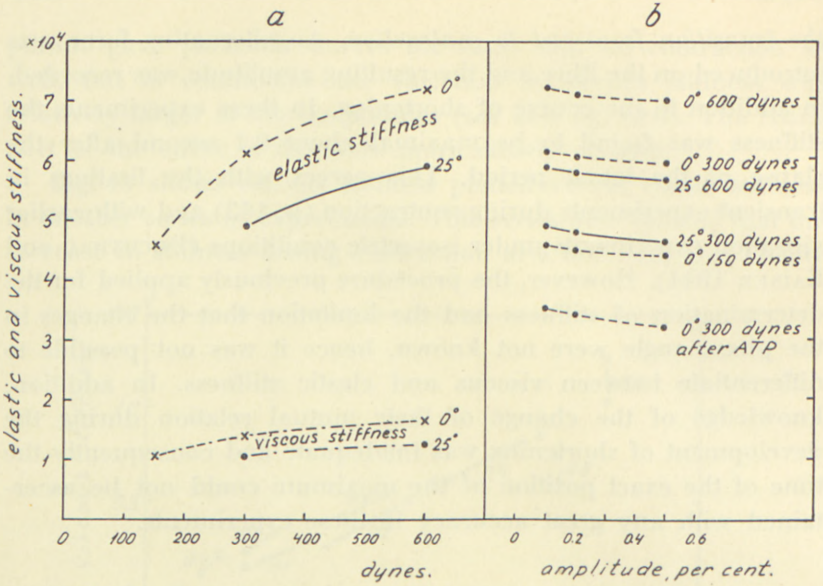

Fig. 44. Elastic and viscous stiffness in an actomyosin thread (a) at 0° and 25° C. as a function of load in dynes. (b) elastic stiffness in an actomyosin thread at 0° and 25° C. with different loads (dynes) as a function of vibrational amplitude (in per cent of the equilibrium length). The lowest curve shows the reduced stiffness and its increased amplitude dependence after treatment with Na-adenosine triphosphate(3×10^{-6} mol/ml).
ordinate: stiffness in dynes $\times$ cm^{-1}.
left abscissa: load in dynes.
right abscissa: alternating length amplitude in per cent of L_0, deflection measured from the mean position.

falling temperature. In contrast to the findings in muscle the temperature dependence of elastic and viscous stiffness was identical. In agreement with earlier experiments we also found in this series that adenosine triphosphate (ATP, 3×10^{-6} mol/ml) caused a decrease in stiffness of almost 50 per cent.[1] The relative decrease was the same for both elastic and viscous stiffness. After treatment with ATP the stiffness of the actomyosin threads was independent of changes in temperature (0°—25° C.), but a larger variation was found with varying amplitude of vibration.

[1] Obviously this deviates from the behaviour of the living muscle fibre during contraction, e. g. released by application of ATP. According to Szent-Györgyi (1949) and Varga (1950) glycerol extracted muscles displayed a mechanical reaction after application of ATP which in several respects resembles that of the living muscle fibre. However, in recent experiments we found the decrease in stiffness after application of ATP in glycerol extracted muscle fibres as well (Buchthal and Knappeis).

Dynamic elastic and viscous stiffness as an expression of minute structure.

In the interpretation of the structural viscosity a general picture has been indicated of the minute structure of the muscle fibre (p. 41). Its mechanical reaction is considered to be the result of the properties of the minute structural elements themselves and of the texture in which they are organized. The mechanical changes which occur in the elements are transmitted along the molecular architecture which constitutes the fibrillar system. While the changes in these elements will occur fast and dominate the dynamic properties, the adjustment of the texture will take time. As the alignment of the texture is far from complete (see X-ray diffraction and birefringence) a considerable portion of the minute structural elements can be assumed *not* to be under tension. These elements therefore cannot attack the points of entanglement in the texture and do not contribute to the resulting stiffness. In terms of the model of the texture with entanglements of minute structural elements given in fig. 90, this means that the stiffness of the substance is determined by the stiffness between the points of entanglement of the texture, which is again dependent on the stiffness of the contractile elements themselves. The latter can, however, only exert its influence when the chains are aligned by loading. It must thus be assumed that with an increasing load more and more chains are caused to take up part of the load and then contribute to the external stiffness. Simultaneously the elements which were previously orientated on account of the increased stretch, give a further contribution to the stiffness as well, because of their intrinsic non-linear properties.

The result of these interactions between the texture and contractile chains is that (1) the stiffness increases with increasing load and (2) the stiffness decreases with increasing vibrational amplitude. The cause of this amplitude dependence of stiffness is a delay in the adjustment of the textural pattern and corresponds to the previously mentioned *thixotropy* (see p. 53). With increasing velocity of deformation the number of disrupted points of entanglement per second will increase. Assuming that the reformation of points of entanglements varies proportionally

to the number of latent possibilities for entanglements, under stationary conditions the ratio of latent and real points of entanglements will vary proportionally to the velocity-amplitude ($\omega_0 \times \gamma_0$). Therefore, the number of points of entanglement will decrease with increasing velocity-amplitude which implies a corresponding decrease in stiffness.

Apart from thixotropy another factor will be of importance which is treated quantitatively in a later section (see p. 295). Owing to the delay in the adjustment of the texture the *number of minute structural elements* which are under tension, will vary *within* a period of oscillation. Therefore, the stiffness of the fibre is maximal during only part of the period of vibration and this part decreases with increasing vibrational amplitude. That a delay in the adjustment of the texture is an essential factor for the amplitude dependence of stiffness, is also indicated by the finding that high values of sr[1] are associated with a high degree of amplitude dependence.

As previously described (p. 50), an increased vibrational stiffness was found in transient experiments 20 msec. after the change in load, as compared with the vibrational stiffness at approximately the same frequency when the same tension had been allowed to act for a few seconds. The cause of this difference is similar to that described above, in that immediately after the change in load a greater number of elements are under tension than during stationary load, as the texture has not yet reached its stationary adjustment.

The resulting external stiffness is affected by a variability in the points of entanglement of the textural pattern. In the same way as for other high polymers, it can also be assumed for muscle fibres that some of the points of entanglement disappear while others are reformed by chance as a result of thermal agitation. This fluctuation in the points of entanglement gives the stiffness a viscous character. A change in load will thus initially cause a tendency towards a new level of orientation, which, however, can only develop gradually as the pattern adjusts itself. The rise in the dynamic stiffness with falling temperature expresses the longer time taken for regrouping in the texture with falling

[1] $sr = \dfrac{\text{viscous stiffness}}{\text{elastic stiffness}}$.

temperature. This adjustment is not only restricted to the points of entanglement, but must also be assumed to occur within the chains themselves. The fact that the dynamic stiffness is 3 to 5 times higher than the static, indicates that the adjustment is incomplete within a vibrational period. In dynamic experiments the deformation caused by the vibrations is therefore determined mainly by the events in the minute structural elements themselves, while in static experiments it is essentially influenced by the orientation of the texture.

The increase in stiffness accompanying a decrease in the water content of the fibre can be interpreted as being due to the increased number of points of entanglement in the texture which occur when the distance between the minute structural elements is reduced.

Dynamic elastic and viscous stiffness rose in isotonic *tetanic contraction*. This rise is attributed to the interaction of the following factors:

(1) The stiffness of the contractile chains themselves is gradually increased by contraction.
(2) The quick shortening in previously slack chains aligns a considerable number of chains which thereby contribute to stiffness.
(3) The increased alignment accompanying contraction will cause an increased probability for the formation of new points of entanglement.

These changes are reflected in part in the spectrum of retardation times by a reduction in the density of very short and very long times. If we investigate stiffness by the deformations produced by vibrations of high frequency (i. e. frequencies corresponding to the shortest retardation times) these are not represented during contraction and, therefore, we here find a higher stiffness. Measuring at a low frequency (i. e. frequencies corresponding to the longest retardation times) the deformation during contraction will include *all* the retardation times represented, while at rest there still will be low retardation times which cannot participate in the deformation. Therefore, we can have the peculiarity that static (= semidynamic) stiffness may decrease during contraction (Buchthal 1942).

The essential reduction of the amplitude dependence of the vibrational stiffness in contraction can be explained by the improved alignment of the structure in the activated fibre. Thereby the prerequisite for a significant change of stiffness with amplitude (slack chains) is no longer present.

In dynamic experiments the increase in stiffness during contraction is dominated by an increase in elastic stiffness at a low load, while the viscous component apparently dominates at a high load. It should, however, be remembered that viscous stiffness varies with the vibrational frequency to a higher degree than the elastic stiffness (cf. p. 91). With higher load the resonance frequency increases and the increase in frequency can account for the differences in behaviour of the viscous stiffness found at high and at low loads.

We have so far considered the dynamic stiffness at the isotonic maximum, i. e. under approximately stationary conditions, which are characterized by a definite dependence between stiffness and load. *On transition from rest to contraction, special conditions apply.* The relative stiffness $\left(\frac{\text{stiffness}}{\text{tension}}\right)$, which at rest is independent of the tension and the change of which must be considered an expression of an essential alteration in the structure of the fibre caused by contraction, increased initially rapidly and had its maximum before the tension reached its maximal value. Among the factors which must be assumed to be the cause of the change in stiffness on contraction, the maximum must be referred to those mentioned in (2). The rapid shortening of the slack, long chains gives a contribution to the stiffness at the beginning of the contraction (see p. 163). As the shortening in the active substance gradually proceeds, the internal forces will increase up to a certain value. Then the pattern will "give", thereby partly compensating the initial rise in stiffness. In addition, the fact that the influence of changes in the vibrational amplitude is considerably less during contraction than at rest, must be interpreted as indicating that the number of slack chains is reduced during contraction, thereby causing a greater number of chains to participate more equally in bearing the load within the period of deformation. The change in the diffraction spectrum likewise indicates the better alignment of minute struc-

tural elements caused by contraction (BUCHTHAL and KNAPPEIS 1940).

In a later section, an attempt is made to give an approximately quantitative treatment of the mechanical effect of inter- and intramolecular rearrangements.

Voigt-model and vibration experiments.

In the definitions on p. 18 of dynamic elastic and viscous stiffness as measured in vibration experiments we used for the description of the mechanical reaction of the muscle fibre a *single Voigt-element* (a retarded elasticity) but emphasized that this model is only of approximate validity and can only be used for suitably high frequencies (> 50 c.p.s.) and amplitudes $<$ about 2 per cent of the equilibrium length of the fibre. In the interpretation of the isotonic transient experiments a *Voigt-model* was applied, i. e. a *series* of Voigt-*elements* with different retardation times.

The Voigt-model is characterized by the distribution function $J(\tau)$ and the series elasticity $\frac{1}{J_0}$ (comp. p. 67). Interpreted in terms of the minute structure $J(\tau)$ and J_0 describe the delayed and instantaneous adjustment of the fibre structure to a transient change in load or length. According to the picture of the fibre structure indicated above, the cause of this delay is the finite velocity with which entanglements in the texture are broken and reformed. An infinitesimal range in the distribution function around a fixed retardation time can be considered a Voigt-*element* and corresponds to changes in the fibre structure which proceed with a delay corresponding to this retardation time.

When applying the Voigt-model derived from the course of adjustment in isotonic transients to vibration experiments it must be kept in mind that the distribution function $J(\tau)$ (43) was determined from the prolonged creep alone, i. e. from changes in length occurring more than 20 msec. after the transient change in load. Therefore, the part of the spectrum of retardation times lying appreciably below 20 msec. is rather poorly determined. Furthermore, the deformations in the prolonged creep experiments used to determine the spectra of retardation times were large, up to 30—50 per cent of the equilibrium length of the fibre, so that they are of quite another order of magnitude than the small deformations in the vibration experiments. The vibrational frequencies were 25—150 c.p.s. corresponding to periods of 7—40 msec. Consequently, they partly go down to times within the poorly determined section of the spectrum of retardation times.

When a Voigt-model is subjected to an external alternating force: $\sigma(t) = \sigma_0 \cos \omega t$, the stationary motion of the system will, just as for the single Voigt-element, be of the type: $\gamma(t) = \gamma_0 \cos(\omega t - \varphi)$.

Therefore, dynamic elastic and viscous stiffness for a Voigt-*model* in forced vibrations can be defined as the elastic and viscous stiffness for the Voigt-*element* which when acted on by the same alternating force performs the same movement as the Voigt-*model*. While for a Voigt-element the elastic stiffness is independent of the frequency and the viscous stiffness is proportional to the frequency, both stiffnesses for the Voigt-*model* depend on frequency and the viscous stiffness is not simply proportional to the frequency. The ratio $\frac{\gamma_0}{\sigma_0}$ between the deformation amplitude and the external force amplitude which acts on the system, varied experimentally with the frequency in approximately the same way as it does for a single Voigt-element. However, the phase did not vary in the expected manner. If a Voigt-*model* is applied the experimental changes in phase can be appropriately described as well. For a Voigt-model with the distribution function $J(\tau)$ and the series elasticity $\frac{1}{J_0}$ it is found (cp. e. g. ALFREY 1948, p. 189 ff.):

$$G_{\text{elast}}(\omega) = \frac{J_0 + \int_0^\infty \frac{J(\tau)\,d\tau}{1+(\omega\tau)^2}}{\left(J_0 + \int_0^\infty \frac{J(\tau)\,d\tau}{1+(\omega\tau)^2}\right)^2 + \left(\int_0^\infty \frac{\omega\tau J(\tau)\,d\tau}{1+(\omega\tau)^2}\right)^2} \tag{59}$$

and

$$G_{\text{visc}}(\omega) = \frac{\int_0^\infty \frac{\omega\tau J(\tau)\,d\tau}{1+(\omega\tau)^2}}{\left(J_0 + \int_0^\infty \frac{J(\tau)\,d\tau}{1+(\omega\tau)^2}\right)^2 + \left(\int_0^\infty \frac{\omega\tau J(\tau)\,d\tau}{1+(\omega\tau)^2}\right)^2} \tag{60}$$

If the Voigt-model is coupled with an inertia m, the resonance frequency ω_0, i. e. the frequency at which the phase displacement between the external alternating force and the deformation caused by it is $\frac{\pi}{2}$, is determined by:

$$m\omega_0^2 = G_{\text{elast}}(\omega_0). \tag{61}$$

Therefore, the stiffnesses measured depend upon the measuring frequency, which is influenced by the inertia m.

By introducing the distribution function (43) and the different boundary values τ_1 and τ_2 (Table 6) in the formulas (59) and (60) we obtain elastic and viscous stiffness as a function of the frequency. Fig. 45 shows these quantities and the total stiffness (cf. p. 90) for the Voigt-models corresponding to the resting fibre and to the tetanically contracted fibre at 0° C. The curves for the Voigt-model which corresponds

to the resting fibre at 25° C. are very similar to those for the model of the resting fibre at 0° C. While for the Voigt-model corresponding to the resting fibre elastic, viscous, and total stiffness increase with frequency in the frequency range of interest for the vibration experi-

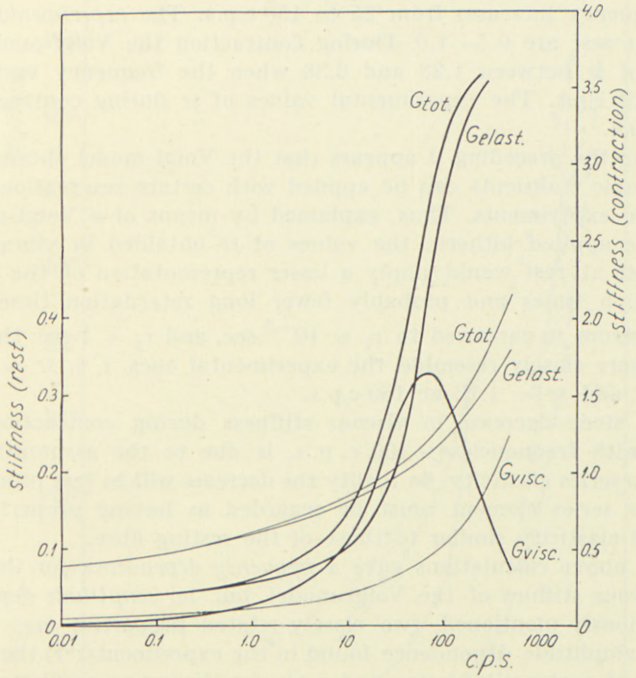

Fig. 45. Elastic, viscous, and total stiffness as a function of vibrational frequency in the Voigt-model developed from isotonic transients (cf. fig. 26 0° C.).
Thick lines: model corresponding to contraction, right ordinate.
Thin lines: model corresponding to resting fibre, left ordinate.
ordinate: stiffness in units of c^{-1} (cf. equation 43).
abscissa: frequency in c.p.s.

ments (25—150 c.p.s.), conditions are more complicated for the Voigt-model corresponding to the tetanically contracted fibre (comp. fig. 45). Here elastic and total stiffness increase with frequency, while viscous stiffness first increases to reach a maximal value at about 70 c.p.s. and then decreases.

In experiments on the resting fibre in which the resonance frequency was varied by altering the equivalent mass of the recording system (cp. p. 91) a reduction of the frequency by a factor 4 caused a slight *in*crease in the elastic stiffness (at most 10 per cent) and a *de*crease in the viscous stiffness by 50—25 per cent according to the tension on the fibre. In the Voigt-model given in fig. 45 a reduction in frequency to one fourth in the frequency range 25—150 c.p.s. results

in a *de*crease in elastic stiffness of 20 per cent and viscous stiffness *de*creases 45 per cent.

"Stiffness ratio", $sr = \frac{G_{visc}(\omega)}{G_{elast}(\omega)}$ *calculated* for the Voigt-model corresponding to the resting fibre varies between 0.32 and 0.49 when the frequency increases from 25 to 150 c.p.s. The *experimental* values for *sr* at rest are 0.5—1.0. During contraction the Voigt-model gives values of *sr* between 1.28 and 0.38 when the frequency varies from 25 to 150 c.p.s. The experimental values of *sr* during contraction are 1.0 to 0.4.

From the preceding it appears that the Voigt-model obtained from the isotonic transients can be applied with certain reservations to the vibration experiments. Thus, explained by means of a Voigt-model of the type applied hitherto the values of *sr* obtained in vibration experiments at rest would imply a lesser representation of the shortest retardation times and probably fewer long retardation times. When the spectrum is narrowed to $\tau_1 = 10^{-3}$ sec. and $\tau_2 = 1$ sec. the values for *sr* more closely resemble the experimental ones, i. e. $sr = 0.64$ at 25 c.p.s. and $sr = 1.13$ at 150 c.p.s.

The steep decrease in viscous stiffness during contraction which occurs with frequencies > 100 c. p. s. is due to the assumption of a Hookean series elasticity. In reality the decrease will be less pronounced, since the series element must be regarded as having properties of a retarded elasticity similar to those of the resting fibre.

The above calculations gave a *frequency dependence* for the elastic and viscous stiffnes of the Voigt-model, but *no amplitude dependence.* As previously mentioned, two closely related properties may account for the amplitude dependence found in the experiments: 1) the varying number of contractile chains under tension during an oscillation period and 2) the delayed adjustment caused by thixotropy (cf. p. 52). The former possibility is treated in detail in Appendix II.

3) The significance of the sarcolemma for the length-tension diagram of the resting muscle fibre.

In the evaluation of the length-tension diagram and transient experiments in the resting fibre, it is essential to know whether the mechanical properties investigated are localized in *potentially active,* i. e. contractile substance, or in passive elements. Passive substance constitutes part of the fibre content and the surrounding sarcolemma.[1] The question of the part played by the sarcolemma in the length-tension diagram has been disputed.

[1] Histological investigations indicate that the sarcolemma consists of two layers, a plasma membrane and an outer layer of reticular fibres (Long 1947 and Sitaramayya 1951). The reticulum has been demonstrated in electron micrographs (Draper and Hodge 1949, Rozsa *et al.* 1951). In the following we denote by sarcolemma both structures.

According to RAMSEY and STREET (1940, 1947) the tension in the resting fibre is considered to be caused exclusively by the sarcolemma. Hence, the length-tension diagram of the contractile

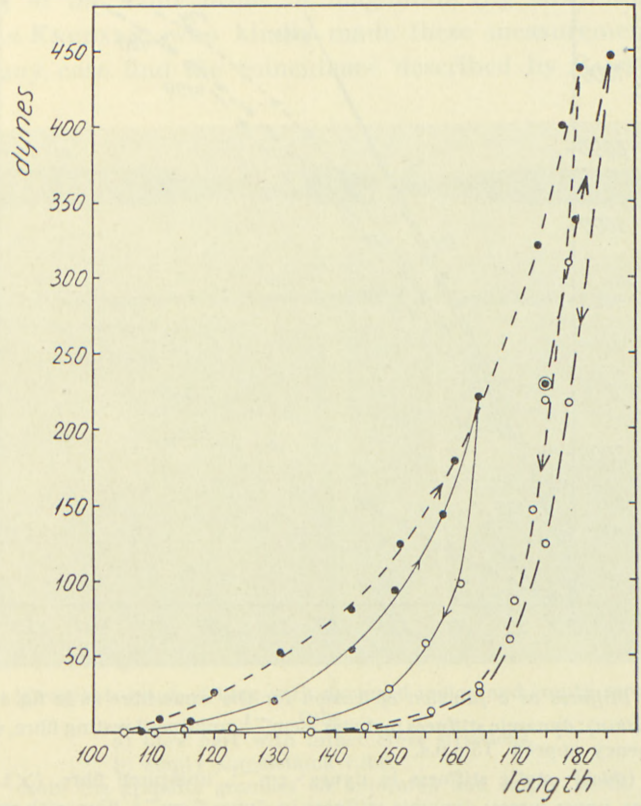

Fig. 46a. *Length-tension diagram* recorded with increasing (•) and decreasing (○) length in an uninjured isolated fibre (full lines) and in the same fibre with empty sarcolemma tube (broken lines). In the latter the increase and decrease was performed twice; 0° C., fibre diameter at equilibrium length (L_0) 160 μ, L_0 = 0.8 cm (STEN-KNUDSEN).
ordinate: load in dynes.
abscissa: length in per cent of L_0.

substance can only be represented by the course of the extra tension as a function of the length of the fibre, with the exception of the length at maximal shortening, where the sarcolemma tube can limit the shortening which is accompanied by an increase in the cross section of the fibre. RAMSEY and STREET support their hypothesis with experiments which showed that the tension developed by the intact fibre practically coincided with the

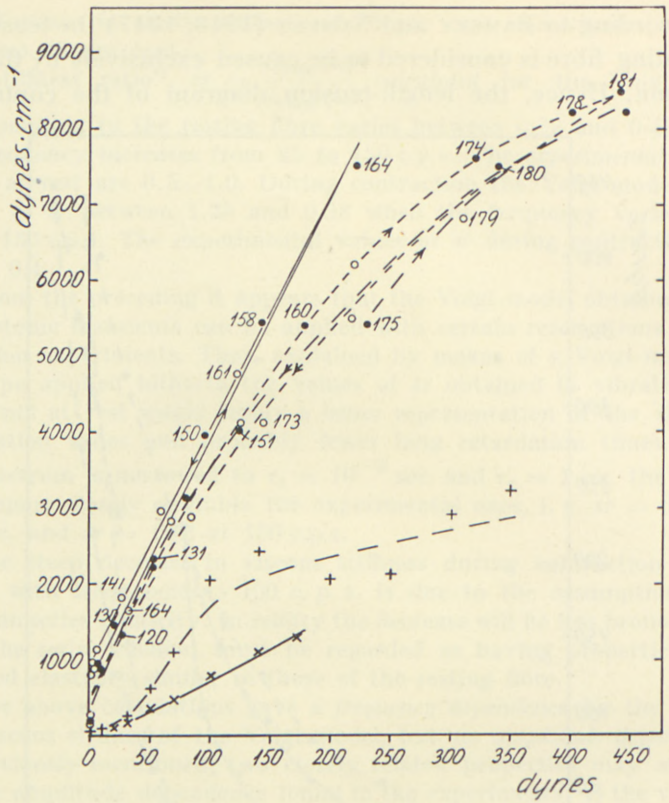

Fig. 46b. *Stiffness as a function of tension* for the same fibre as in fig. 46a. 0° C.
Full lines (thin): dynamic stiffness in dynes × cm^{-1}, uninjured resting fibre, vibration frequency approx. 15 c.p.s.
full lines (thick): static stiffness in dynes × cm^{-1}, uninjured fibre. (×).
broken lines, upper curves: dynamic stiffness in dynes × cm^{-1}, fibre with empty sarcolemma tube.
broken lines, lower curves: static stiffness in dynes × cm^{-1}, fibre with empty sarcolemma tube. (+).
The figures on the curves denote the length in per cent of L_0.
● increasing length, ○ decreasing length.
(Sten-Knudsen)
ordinate: stiffness in dynes × cm^{-1}.
abscissa: load in dynes.

tension which was developed at the same length by a sarcolemma tube alone, emptied of the fibrillar contents. In a previous paper it has been pointed out (Buchthal 1942) that this coincidence is surprising on account of the elongation of 50 to 70 per cent, which was measured for the sarcolemma tube after retraction of the fibre content (cf. Bairati 1937).

A comparison of the length-tension diagram of an intact fibre with that of the same fibre after lesion, showed, in agreement with RAMSEY and STREET (1940, 1947), that the tension in both cases is of the same order of magnitude (fig. 46a). However, Dr. STEN-KNUDSEN, who kindly made these measurements, did not in any case find the coincidence described by RAMSEY and

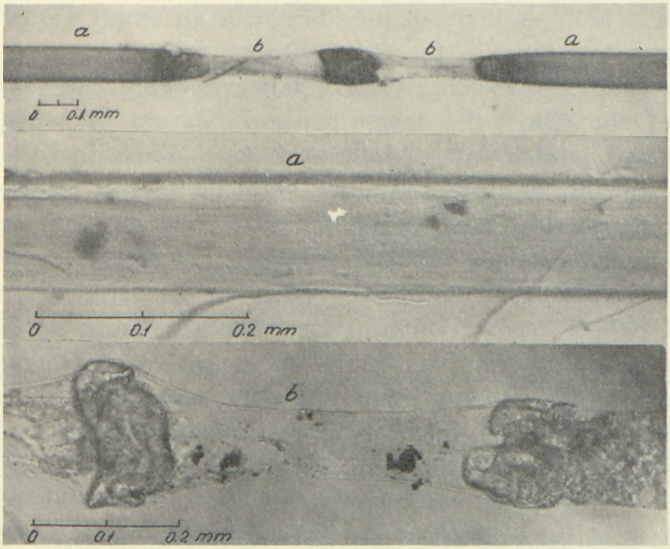

Fig. 47. Microphotograph of fibre with damaged region and empty sarcolemma tube.
a) fibre part with intact cross striations.
b) empty sarcolemma tube.
Note the graphite granules on uninjured and empty parts.

STREET. A considerable difference was seen especially at the first extension, when the lesion (which was produced by local compression) and the retraction of the fibre content occurred at low degrees of stretch. It can be seen that the tension here at the same length was considerably higher, probably as a result of shrinkage of the sarcolemma at the retracted region; and only after repeated stretches could reproducible values be obtained for the length-tension diagram of the injured fibre.

After retraction of the fibre content, the diameter of the sarcolemma tube decreased to about 60 per cent of the original diameter, while the length was only increased by about 40 to 50 per cent (fig. 47). Hence the volume enclosed by the sarcolemma

tube was diminished by about half. The decrease in volume became more marked with increasing degree of stretch (fig. 49). Since this reduction in volume did not result in a corresponding increase in those parts of the fibre to which the fibre content had retracted, it must be assumed that part of the water left the fibre, either as a result of pressure or changed osmotic activity within the fibre. After the first extension had been completed, hysteresis and plasticity in the fibre with an empty sarcolemma tube was less than in the intact fibre.

The empty sarcolemma tube, however, only extended over part of the fibre, the length-tension diagram of which was determined, and it was of interest to carry out direct measurements on the part of the fibre with the empty sarcolemma tube in comparison with its intact parts. By placing small graphite grains on different parts of the fibre before injuring it, it was found (Casella 1951) that the lesion, which was performed at 40 per cent stretch of the intact fibre, caused an increase in equilibrium length of the injured part of on an average 46 per cent. This increase in equilibrium length occurred equally in the empty sarcolemma tube and in the adjoining region of the fibre, which showed only disintegration of the cross striations. The static stiffness of the empty sarcolemma tube was considerably higher than that of the portion of the fibre with *intact* cross striations. Measuring the change in length by the distance between two groups of graphite grains placed on the sarcolemma tube and the intact fibre section, it was found that the length of the sarcolemma tube increased on an average 2.4 times less than that of the fibre section with intact cross striations. This indicates that the relative static stiffness is 1.65 times higher than in the intact fibre, referred to the same tension and to the equilibrium length of the sarcolemma in the intact fibre. Fig. 48 shows, for 8 fibres, the relative length of the empty sarcolemma tube with its new equilibrium length as unit length plotted versus the relative length in an intact fibre section.

The maximal length of the sarcolemma tube reached before rupturing was on the average 135. Considering that the previously mentioned elongation caused by the injury, amounted to $0.46 \pm 0.03\ L_0$, the ordinate value 100 in fig. 48 corresponds to length 146 (referred to the length of the sarcolemma at the equili-

brium length of the intact fibre). The breaking length of 135 thus becomes 197 (135×1.46).

In contrast to the increased static stiffness, the *dynamic stiffness* determined in vibration experiments (10—12 c.p.s) and compared at the same tension decreased when the fibre was injured (fig. 46b). Up to length 140—150 the decrease in stiffness

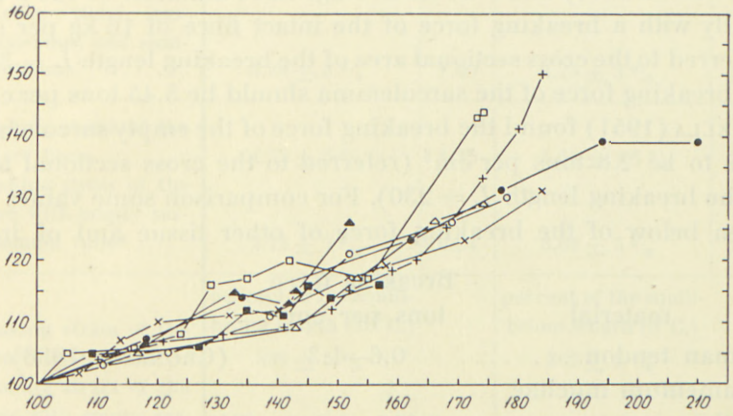

Fig. 48. Length of the empty sarcolemma tube plotted versus the length of the fibre region with intact cross striations during stretch. Tensile force identical in intact and empty regions (second stretch). The different signatures indicate experiments on different fibres (20° C.). (CASELLA 1951).
ordinate: length of the sarcolemma tube in per cent of its L_0
abscissa: length of the fibre part with intact cross striations in per cent of L_0 of the intact fibre.

was slight, but since only part of the fibre had been transformed to the emptied state, an appreciable decrease in dynamic stiffness must have occurred in the injured part of the fibre. At longer initial length the decrease was considerably more pronounced and the linear dependence between stiffness and tension, characteristic of the intact fibre, could no longer be observed. At a load of 100 dynes the dynamic stiffness of the fibre before injury was 5 times higher than the static. After injury the static stiffness rose simultaneously with the dynamic stiffness and, referred to the same tension, the difference now was only a factor of 2. This must mean that the elasticity of the injured fibre is less influenced by viscosity than the mechanical reaction of the intact fibre.

The mean values of breaking length and breaking stress for

intact fibres and fibres with empty sarcolemma sheaths, and values for the maximal specific tension developed in isometric tetanic contraction are given in Table 9 (CASELLA 1951).[1]

Both the sarcolemma of the intact fibre and the empty sarlemma tube must have a considerable strength. Reckoning with a thickness of the sarcolemma wall of 0.1 μ (BARER 1948, JONES and BARER 1948) and with an average fibre diameter of 125 μ and finally with a breaking force of the intact fibre of 16 kg per cm^2 (referred to the cross sectional area of the breaking length $L = 300$) the breaking force of the sarcolemma should be 5.45 tons per cm^2. CASELLA (1951) found the breaking force of the empty sarcolemma tube to be 2.8 tons per cm^2 (referred to the cross sectional area at the breaking length $L = 230$). For comparison some values are given below of the breaking force of other tissue and of iron:

material	Breaking force tons per cm^2	
Human tendon	0.6—1.3	(CRONKITE 1936)
Ligamentum muchae (cattle)	0.012—0.042	(WÖHLISCH *et al.* 1927)
Cast iron	1.2	
Steel	6—7	

CASELLA (1951) has shown that the breaking length and breaking stress in the fibre with an empty sarcolemma tube was considerably lower than in the intact fibre. The fact that the sarcolemma in the intact fibre did not break before a relatively long length was reached, is probably due to the extra deformation arising in the cross section of the empty sarcolemma tube on stretching and not by accidental "weak spots". The decrease in the diameter of the empty sarcolemma tube on stretching was more pronounced than that occurring in the intact fibre or on stretching a rubber tube. A stretching of the intact fibre or of a thin-walled rubber tube of 40 per cent is accompanied by a decrease in diameter of 15 per cent. A corresponding stretch of the empty sarcolemma tube caused a decrease in diameter of 60 to 85 per cent. Assuming a constant volume of the sarco-

[1] WALTER (1944–1947) determined the breaking stress of whole muscle (frog's gastrocnemius) to 4–9 kg per cm^2 (20° C). Since this value is of the same order of magnitude as the breaking stress of the isolated fibre, the intramuscular connective tissue can only be of minor importance.

TABLE 9.

Breaking stress and breaking strain (CASELLA 1951).

	$\times 10^6$ dynes/cm^2 20° C.	Units of P_0 20° C.	$\times 10^6$ dynes/cm^2 0° C.	Units of P_0 0° C.
Maximal tetanic tension, isolated fibre from anterior tibial, gastrocnemius, and semitendinosus	3.29 ± 3 %	1.00	2.75 ± 3 %	1.00
Breaking stress of the intact fibre.....	4.35 ± 5 %	1.35	5.51 ± 4.5 %	2.00
Breaking stress of the fibre with empty sarcolemma tube*	2.72 ± 7 %	0.84	3.64 ± 5 %	1.33
	per cent of the equilibrium length (20°C.)		per cent of the equilibrium length (0°C.)	
Breaking strain of the intact fibre.....	339 ± 5 %		302 ± 5 %	
Breaking strain of the fibre with empty sarcolemma tube	200 ± 1.5 %		229 ± 2 %	

* Referred to the area of the intact fibre at equilibrium length.

lemma during the stretch, this considerable decrease in diameter must be accompanied by a corresponding increase in the thickness of the sarcolemma wall.

When the fibre content had retracted after injury, the diameter decreased, and at equilibrium length the diameter of the empty sarcolemma tube was only 55 per cent of the diameter of the intact fibre. The fibre content must therefore have been subjected to a radial pressure arising from tangential elastic forces in the sarcolemma tube. At equilibrium length of the *fibre*, this pressure must have caused an elongation and orientation of the fibrils in the fibre in such a way that they react as if they were acted upon by an external longitudinal force. At the equilibrium length of the sarcolemma tube ($L = 146$) the tangential force will give rise to a hydrostatic pressure inside the tube, whose components along the longitudinal axis of the fibre will act to counteract an externally applied load. Thus, when the longitudinal

tension arising intrinsically in the sarcolemma is just compensated by the longitudinal force arising from the intrinsic tangential elastic forces in the sarcolemma, then the net-contribution with respect to the external longitudinal force becomes zero. This must be assumed to occur at a length slightly longer than the equilibrium length of the sarcolemma. Only at a length longer than the latter can the sarcolemma give a positive contribution to the total fibre tension. At equilibrium length of the fibre, there must be equilibrium between the three factors giving rise to an external longitudinal force, i. e. the longitudinal force of the fibrils, the longitudinal force of the sarcolemma, and the tangential force of the sarcolemma. It is impossible to decide with certainty whether the equilibrium length measured for the empty sarcolemma tube (146 compared with 100 for the fibre) and the corresponding diameter (55 per cent of that of the intact fibre) is actually the equilibrium length of the sarcolemma in the intact fibre. The occurrence of an irreversible plastic change in the texture of the sarcolemma on retraction of the fibre contents cannot be excluded.

The marked transverse contraction on stretching showed that, in addition to the tangential force caused by the smaller equilibrium diameter of the sarcolemma as compared with that of the fibre, a tangential force also arose as a result of the stretch. This, however, was not very large. The length-tension diagram of the empty sarcolemma tube did not differ significantly from that of the sarcolemma tube filled with disorganized fibre substance. In this portion the diameter was equal to that of the intact fibre. Thus, an only insignificant work of deformation accompanies the reduction in the cross section. Since the deformation itself is relatively large, the resistance of the sarcolemma to the tangential deformations must have been slight. As regards the efficiency of the fibre this flexibility in the sarcolemma implies that unnecessary work of deformation is minimized during the changing cross section, which accompanies the shortening of the muscle fibre.

The experiments on the empty sarcolemma tube reported here, do not confirm the hypothesis of RAMSEY and STREET (1940, 1941) that the sarcolemma alone is responsible for the tension of the fibre at rest. There are two possible interpretations of the present experiments. One interpretation is that the sarcolemma tube, as already mentioned, is so much altered in its

structural properties that it is not justifiable to draw any conclusions with regard to the properties of the sarcolemma in the intact fibre. The other possibility is that the contribution of the sarcolemma tube to the total tension of the muscle fibre at rest is of minor importance. The latter alternative is illustrated by the re-

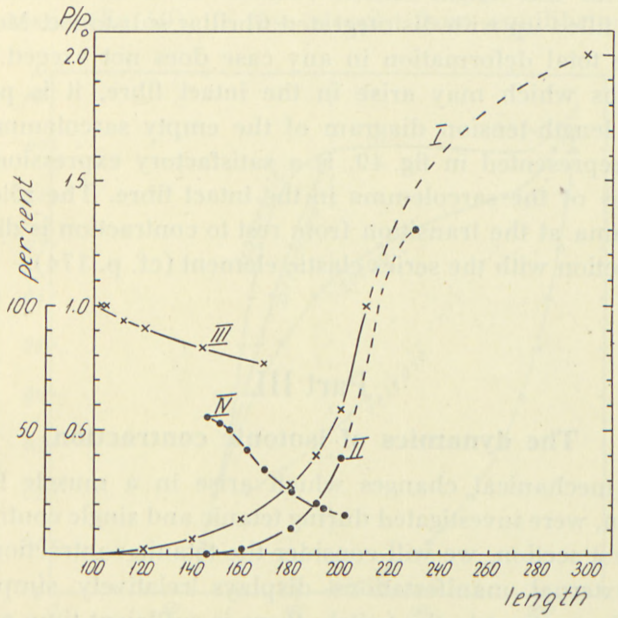

Fig. 49. Tension and diameter as a function of length in the uninjured muscle fibre and its empty sarcolemma tube.
curve I: length-tension diagram of uninjured resting fibre, interpolated to the breaking point.
curve II: length-tension diagram of the empty sarcolemma tube from tension zero to the breaking point.
curve III: diameter of uninjured fibre as a function of length.
curve IV: diameter of empty sarcolemma tube as a function of length.
left ordinate: diameter in per cent of the diameter of the uninjured fibre at equilibrium length.
right ordinate: load in units of P_0.
abscissa: length in per cent of L_0.
(CASELLA 1951).

construction of the length-tension diagram of the sarcolemma (fig. 49). This is based on the following experimental findings: (1) the equilibrium length of the empty sarcolemma tube on an average was 46 per cent above that of the intact fibre; (2) the static stiffness of the empty sarcolemma tube was 1.65 times that of the intact fibre section, referred to the same load. The curves

in fig. 49 show that the sarcolemma only gives a positive contribution to the total tension of the fibre at rest, above a length of 150. At shorter lengths its contribution to the tension is zero or negative.[1]

The deformation of the cross section in the empty sarcolemma tube has no significant effect on the length-tension diagram as compared with the length-tension relation in a sarcolemma tube which is filled up with disintegrated fibrillar substance. Moreover, since the total deformation in any case does not exceed the deformations which may arise in the intact fibre, it is probable that the length-tension diagram of the empty sarcolemma tube, as it is represented in fig. 49, is a satisfactory expression of the properties of the sarcolemma in the intact fibre. The rôle of the sarcolemma at the transition from rest to contraction is discussed in connection with the series elastic element (cf. p. 174).

Part III

The dynamics of isotonic contraction.

The mechanical changes which arise in a muscle fibre on activation, were investigated during tetanic and single contractions. In the first section, we will consider the tetanic contraction which in its external manifestations displays relatively simple properties. In contrast to the twitch, there is sufficient time available for a mechanical adjustment of the substance to the changes caused by the contraction process. As mentioned in the Introduction, in the present material stress is laid on an analysis of the mechanical properties under isotonic conditions. This gives the important advantage that pure elasticities which are in series with the contractile components do not change their lengths and hence do not exert a varying influence on the length of the fibre during transition to an active state.

[1] The findings in the present experiments, divergent from those of RAMSEY and STREET (1940), cannot be explained on the basis of differences in the length-tension diagrams of the non-injured fibre. If the slope of Ramsey's length-tension diagrams had been much flatter than the slope in the diagrams of our intact fibres, the tension obtained at the natural length of the empty sarcolemma tube would only be of minor importance as initial tension. However, at this length (L = 146) in RAMSEY's experiments the fibre tension amounted to 8 and 25 per cent of the maximal tension developed in contraction (1940, figs. 3 and 4), as compared with a fibre tension of 10 per cent in the present experiments.

Tetanic contraction.

Curve of isotonic maxima.

The maximal shortening obtained for a given load in isotonic tetanic contraction is called an *isotonic maximum*. The curve of isotonic maxima as a function of load displayed an S-shaped characteristic (fig. 50). It rose steeply from equilibrium length

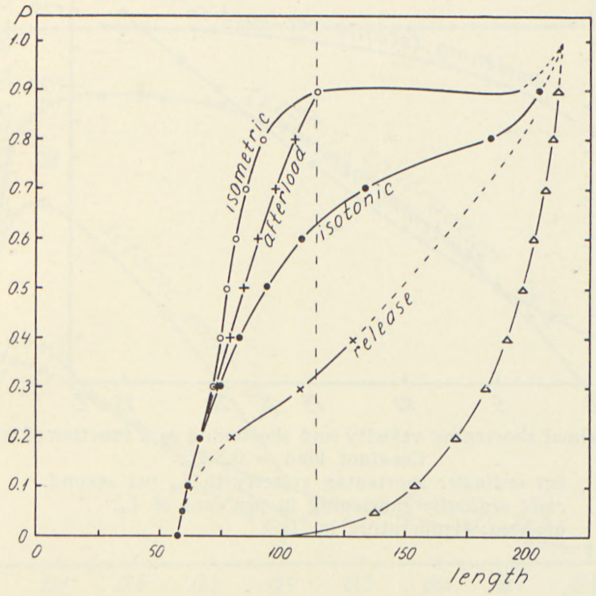

Fig. 50. Length-tension diagram of the isolated fibre at rest, during isometric tetanic contraction, isotonic contraction, afterload contraction, and during release contraction to the same tension as at rest. 0° C. Vertical broken line indicates the position of the stop in afterload contractions.
ordinate: tension in units of P_0.
abscissa: length in per cent of L_0.

during contraction (length 50—60) and the shortening (difference between length at rest and during contraction at the same load) was maximal at 0.4 P_0, amounting to about 100 per cent of L_0 at 0° C. At 0.75 P_0, the S-shaped curve had its point of inflexion, and the contraction curve then gradually approached the resting curve.

The shortening in tetanic contraction increased with rising *temperature*. The temperature range examined was naturally limited to temperatures between — 2° and + 26° C. Fig. 51 shows

the shortening as a function of the temperature during tetanic contraction at low load (0.1 P_0). The shortenings given are mean values obtained by continuous cyclical changes in temperature from —2° to +26° C. The cyclical measurements show that the shortening during rising temperature was less than the corresponding shortening during falling temperature. This hysteresis

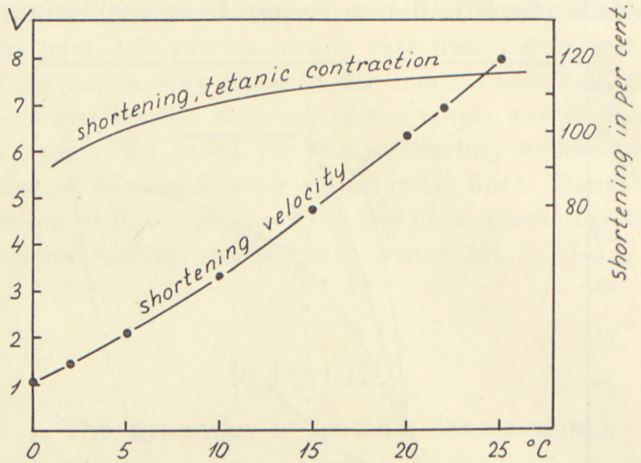

Fig. 51. Maximal shortening velocity and shortening as a function of temperature. Constant load = 0.3 P_0.
left ordinate: shortening velocity in L_0 per second.
right ordinate: shortening in per cent of L_0.
abscissa: temperature in °C.

was not due to incomplete equilibration of temperature between the Ringer's solution and the muscle fibre. It must be caused by a slow adjustment of temperature-dependent equilibria in the structure. In other experiments we have examined the effect of two extreme temperatures, 0° and 26° C., and waited until temperature equilibrium was obtained at the different loads examined. On each fibre, at least three experiments were carried out, one at 0° C., one at 26° C., and repetition of the experiment at 0° C. Only experiments which showed agreement in the two series carried out at 0° C., were included in the material. The curves in fig. 52 show an example of the shortening at 0° C. and at 26° C. as a function of the load. The curve at 0° C. is a mean value of the first and last series. At low loads, the shortening at 26° C. was about 25 per cent higher than the shortening at 0° C.

The difference increased with rising load, the shortening at 0° C. decreasing rapidly with the load. This decrease in shortening may be more or less pronounced as can be seen by comparing the present example with the mean curve in fig. 57.

Compared with the temperature dependence of the length of the resting fibre (maximally 1 per cent per 25° C.), the temperature dependence of the active fibre was 25 times larger at the load at which the shortening at 0° C. was at its maximum (fig. 52).

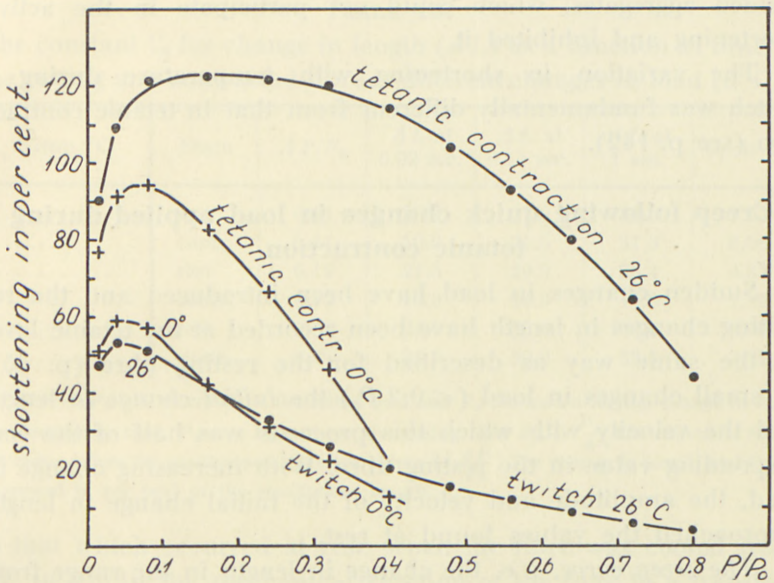

Fig. 52. Maximal shortening in an isotonic twitch and tetanus as a function of load. 0° C. and 26° C.
ordinate: shortening in per cent of L_0.
abscissa: load in units of P_0.

While increasing load caused decreasing temperature dependence at rest, the reverse was true during contraction.

If extrapolation is performed on the curve for the data at 0° C. a value for P_0 would be obtained which would seem to indicate that it was $\frac{1}{2} P_0$ at 26° C. However, the small difference in P_0 obtained in isometric contraction shows that extrapolation is not permissible in this region. In fact the curve for 0° C. must intersect the abscissa (fig. 52) at higher values than indicated by an extrapolation. The tension rose only 1 per cent per degree rise in temperature, the average value of isometric tension at 0° C. being

$2.75 \pm 0.095 \times 10^6$ dynes per cm^2 and at 20° C. $3.27 \pm 0.100 \times 10^6$ dynes per cm^2 (temperature coefficient $9.8 \times 10^{-3} \pm 2.4 \times 10^{-3}$, CASELLA 1951[1]). The relatively small change in P_0 accompanying a change in temperature, as compared with the rapid decrease of the shortening with decreasing temperature indicated that the shortening tended to be inhibited at low temperature and high load. It must be assumed that these conditions offered good possibilities for "crystallizations", i. e. that the contractile substance formed aggregates, which could not participate in the active shortening and inhibited it.

The variation in shortening with temperature during a twitch was fundamentally different from that in tetanic contraction (see p. 142).

Creep following quick changes in load applied during tetanic contraction.

Sudden changes in load have been introduced and the resulting changes in length have been recorded at the tetanic level in the same way as described for the resting fibre (p. 45). At small changes in load ($< 0.2\ P_0$) the *initial change in* length and the velocity with which this proceeds was half of the corresponding value in the resting fibre. With increasing change in load, the amplitude and velocity of the initial change in length approached the values found at rest.

The creep curve, i. e. the change in length in the range from 20 to 1000 msec., had an approximately linear course as a function of the logarithm of time (fig. 20). The creep velocity was about twice that found at rest. At large changes in load ($> 0.4\ P_0$) the final change in length was larger and at small changes in load ($< 0.1\ P_0$) less than at rest, and at changes in load of between $0.1\ P_0$ and $0.4\ P_0$ the creep curves for rest and contraction intersect.

The almost linear course of the change in length as a function of the logarithm of time justifies characterizing the curve by means of a constant C_1, as in the resting curve (cf. p. 55). C_1 is considerably higher in contraction than at rest, and the difference which is largest at high loads is at least 50 per cent.

[1] From experiments of RAMSEY and STREET, BULL (1945) calculated a temperature coefficient for the isometric tension of $8.4 \times 10^{-3} \pm 3.6 \times 10^{-3}$.

However, during contraction the change in length approached rapidly a limiting value after a few seconds; this did not occur at rest.[1]

Table 10 shows that at 0° C. the creep velocity was higher in the contracted than in the resting fibre while contraction reduced the initial velocity and the amplitude of the change in length. The difference between rest and contraction corresponds

TABLE 10.

The constant C_l for change in length (ΔL) as a function of time in the resting and contracted fibre at different changes in load (0° C.).

Temp. °C	State	$\Delta P/P_0$	ΔL at 0.02 sec.	ΔL at 0.14 sec.	ΔL at 1 sec.	C_l in %
0.....	rest	0.11	20.4	27.0	32.6	3.67
0.....	contr.	0.11	10.0	21.5	31.3	6.06
0.....	rest	0.19	21.5	29.9	36.4	4.87
0.....	contr.	0.19	13.0	26.9	40.9	7.19
0.....	rest	0.39	24.6	30.0	34.6	3.00
0.....	contr.	0.39	24.9	39.0	53.5	7.12

$\Delta P = P_2 - P_1$ where P_1 is the initial load and P_2 the load after the change in load. For increasing load, $P_2 = 4\,P_1$ and for decreasing load $P_2 = \frac{P_1}{4}$. The constants found are mean values for positive and negative values of $\frac{\Delta P}{P_0}$. The change in length and C_l are expressed in per cent of the equilibrium length.

to that which occurred at rest, when the fibre was cooled from 25° to 0°. In the mechanical reaction of the fibre to a transient change in load the resistance is increasingly dominated by viscous forces as the temperature falls and even more so when the fibre is thrown into the contracted state.

The transient course recorded here showed good agreement with the measurements of dynamic and static stiffness. The smaller initial change in length, which was found at a given change in load, as compared with rest indicates that the *dynamic stiffness* rises during contraction. The higher creep velocity as

[1] Similar to HILL's estimate of the elastic energy liberated by sudden release of contracted whole muscle (1950 b) we have calculated this quantity for the isolated fibre. At release from 0.5 P_0 during the first 20 msec. an energy corresponding to 0.03 $P_0 \times L_0$ was transmitted to the recording system. Later on (interval 20 to 200 msec.) the energy rose to 0.05 $P_0 \times L_0$ and increased approximately linearly with the logarithm of time (fig. 20). The continuous way in which the elastic energy is liberated in the isolated fibre indicates that it will hardly be possible to distinguish between purely elastic and retarded components.

compared with rest, and the larger final change in length on contraction especially at high load, indicate that the fibre is considerably more fluid and has a smaller *static stiffness* on contraction than at rest. The elongation reached *shortly* (2—10 msec.) after a change in load corresponds to the high values for the dynamic stiffness, which were found in vibration experiments, with frequencies of about 200 to 50 c.p.s. The elongation after a *longer* interval (20—200 msec.) corresponds to the lower values for stiffness found at frequencies of about 10 to 2 c.p.s.

As already mentioned in the discussion of transient experiments on the resting fibre, creep during contraction can be described by means of a Voigt-model. Fig. 26 gives the distribution of the retardation times calculated on the basis of the experimentally determined course of elongation at rest and on contraction. The spectrum of the retardation times during contraction had a smaller representation of short retardation times and the long times, found at rest, were completely missing on contraction. The high dynamic stiffness found during contraction,

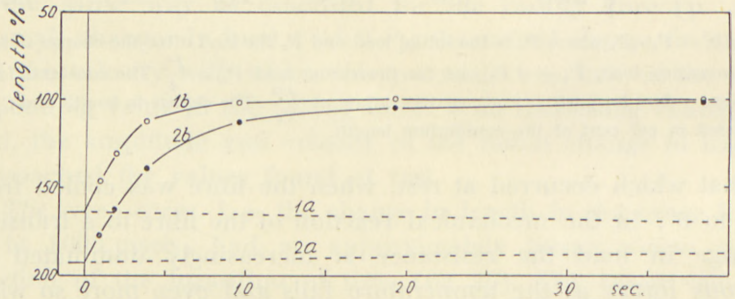

Fig. 53. Adjustment of length at 0.1 P_0 as a function of time after a short decrease (curve 1a and 1b) or a short increase (curve 2a and 2b) in load.
a: rest, b: isotonic tetanic contraction. 0° C. See fig. 54.

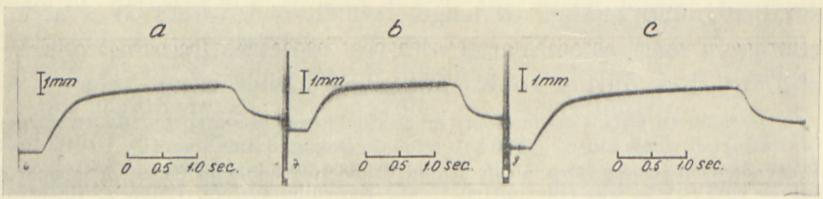

Fig. 54. Adjustment of length in isotonic tetanic contraction at constant load (0.1 P_0). Curves a and c after a preceding increase, curve b after a preceding decrease in load. L_0 = 4 mm. 0° C.
Duration of the stimulation is indicated by the broader line of the myogram.

as compared with rest, is interpreted as an expression of the smaller representation of shorter retardation times, and the more rapid approach to a stationary state after a transient must be interpreted as an expression of the absence of long retardation times which are replaced by the more numerous retardation times of intermediate size.

Thus, the change in the retardation time spectrum on contraction can illustrate the observation that a contraction is able to extinguish the influence of mechanical effects, to which the fibre has been subjected at rest. An adjustment towards equilibrium, which on contraction was reached within 3 seconds, required about 1 minute at the same load at rest. Fig. 53 shows the course of adjustment at rest (curves 1a and 2a) and during contraction (curves 1b and 2b), the latter obtained from the curves in fig. 54. The change in the length of the fibre at rest (fig. 53, curve 2a) was produced by a transient application of an additional load. The difference in length at the same tension was retained at rest during a relatively long period, i. e. it was reduced to about 60 per cent in 3 seconds. A tetanic contraction lasting 3 seconds reduced the difference in length to only 10 per cent.

The curves for the isotonic and isometric maxima.

It was natural to assume that the curve for the isotonic maxima in the length-tension diagram would coincide with the curve for the isometric maxima. However, this was only the case from load 0 to 0.2 P_0, i. e. at a length at which an "isometric" contraction was initiated about 30 per cent below the equilibrium length of the isolated fibre. Obviously, this was no true isometric contraction, the fibre shortening without tension until it was straightened out. The range of length from equilibrium to the shortest length obtained in contraction corresponds to a stop ("anschlag") contraction. After the fibre had taken up the slack, the contraction then proceeded isometrically. The tension for the same length was less during stop contraction than in the corresponding isometric contraction (Reichel 1936, 1938), and therefore it is not surprising that the "isometric" contraction at low tension coincided with the isotonic. If, at the beginning of the contraction, the fibre had been kept slightly compressed in the

longitudinal direction to a length below the equilibrium length, higher values of tension should have been expected for the fibre actually under isometric conditions. From load $0.2\ P_0$, the tension in isometric contraction for the same length was up to 50 per cent higher than the tension in isotonic contraction. The difference was largest in the range about length 100.

In order to be able to make a comparison as described above, it is of course necessary, both for isometric and isotonic contraction, to wait until complete equilibrium is obtained, i. e. constant tension or constant length. In isotonic contraction, the presence of possibly undamped inactive series elasticities in the muscle fibre are without significance for the course of adjustment, since the elasticities retain a constant length, on account of the constant load. On the other hand, these series elasticities will influence the development of tension in isometric contraction, since the contractile elements, in spite of external isometry of the fibre, must work against a certain velocity of elongation of the inactive series elements during the rise in tension. The shortening velocity which arises in the active elements in compensation of the lengthening of the inactive elements causes the resulting tension to be lower than the truly isometric tension would be (cf. force-velocity relation p. 148, 177). A series elastic element, therefore, can cause differences in the course of adjustment, in isotonic and isometric contraction, but it cannot explain the higher stationary value of tension, which was found in isometric contraction.

Before the difference in the length-tension dependence found for the isotonic and isometric maxima could be considered as real, it was necessary to ensure that the difference was really due to a peculiarity in the behaviour of the contractile substance. In order to exclude the possibility of *fatigue and plastic elongation*, which could have exerted its influence in different ways in isotonic and isometric contraction three special series of experiments were carried out:

Three successive curves were recorded from the same fibre in the sequence, isotonic, isometric, and isotonic. A comparison between the two isotonic curves permits an evaluation of the presence of possible fatigue and plastic yielding as compared with the intermediate isometric curve. Experiments on fibres in

which the first and the last curves recorded for the isotonic maxima coincided, still showed the considerable difference in length-tension dependence between isotonic and isometric contraction.

This difference was also seen in other experiments, in which isotonic shortening and isometric tension were recorded alternately for each length at rest; an isotonic control measurement at moderate load ($0.3\ P_0$) was performed at regular intervals, in order to control the possible occurrence of fatigue or plastic elongation. As a further control of the possible influence of fatigue, which could be expected to be especially marked after isotonic contraction, where the initial length even at moderate load approached 200, we carried out a series of experiments with continuous repetition of a cycle of alternating isotonic and isometric contractions. Comparing values of equal tension in isotonic and isometric contraction, the corresponding differences in length could be determined. The fibre was brought to isometric contraction at a low initial length, and an isotonic contraction was then initiated at the same tension as that reached in the isometric contraction, etc.

By all these procedures the same result was obtained, that is the curve for the isotonic maxima lies considerably below the curve for the isometric maxima (fig. 50), and this difference is not due to incomplete adjustment, fatigue, or plastic elongation.

The area which lies between the curve for the isometric and the curve for the isotonic maxima, can be examined by means of stop-contractions, or, as we have done, by means of afterload contractions (v. Kries (1880), Sulzer (1930), Hill (1938), and Reichel (1936, 1938)). The first phase of an afterload contraction proceeds isometrically up to the point at which the tension developed by the fibre is sufficiently high to overcome the external load. The fibre then shortens isotonically against the external load.

In afterload contractions the length of the muscle was limited by means of a stop (n, fig. 2) to, for example, length 115. The load required at rest to stretch the muscle to this stop was denoted P_r. At loads $< P_r$ the muscle fibre worked isotonically, since it had not reached the stop. At loads $P > P_r$, the muscle was stretched to the stop and the tension rose isometrically from

P_r to P. The fibre then shortened under the load P. When the fibre worked at loads varying between P_r and P_0, a curve for the *maxima of the afterload contractions* was obtained, the end-points of which were the isotonic point at load P_r and the corresponding isometric point at load P_0 at the length determined by the stop, i. e. 115. For each fibre length determined by the position of the stop there was an afterload curve connecting the isometric maximum with a point on the curve of the isotonic maxima at a considerably lower length and tension. Thus, it can be seen that for different stop lengths, i. e. for different values of P_r, there will be described a family of afterload curves starting from the isometric maximum and sloping downwards to the left (fig. 50) terminating on the curve of the isotonic maxima. The curves for the maxima of the afterload contractions are approximately linear. Afterload contractions with isometric and isotonic contractions as limiting cases thus allow in a well defined way a combination of the latter conditions and show that there is a continuous transition in length and tension between isotonic and isometric contraction.

In evaluation of the difference found between the curves for the isotonic and isometric maxima it was important to establish whether factors other than the resting length and tension determined the length reached during maximal tetanic contraction. During the recording of the curves for the isotonic and isometric maxima we have, therefore, inserted *release contractions* at different resting lengths. The fibre was stimulated at a given initial length under isometric conditions until tension P_0 was reached. Then the fibre was released during continuous stimulation to the same tension which it had at rest. The resulting stabilized shortening was considerably less than an isotonic shortening, at loads above 0.1 P_0 (Buchthal 1942).

In agreement with our findings for isotonic and release contractions Reichel (1936), using whole muscles, has shown that from the same resting length smaller or larger shortenings are obtained at the same tension, according to whether the contraction proceeds isometrically-isotonically (afterload) or isotonically-isometrically (stop).

Texture and elastic locking.

From the *same* initial length and tension, different values are thus obtained for the final length attained in contraction, according to the length-time or tension-time course, which the fibre has undergone during the contraction. The explanation of the differences in the length-tension diagrams under different conditions is to be found in the previously described elastic locking (BUCHTHAL 1942). However, on the basis of the present experiments the textural pattern is assumed to be the site of the locking in the structure and not—as previously assumed—the minute structural elements themselves.

The random cross-linking of chains establish the condition that part of the contractile substance will not be under load in the fibre at rest (slack). *Upon activation* the fibre changes in two ways: (1) the minute structural elements begin to shorten, and (2) the stiffness will increase. The increased stiffness is an expression of an alteration of the minute structural pattern produced by changes in its elements. Part of the resulting increase in stiffness is localized to the minute structural elements themselves and part to the texture in which they are organized. The quick shortening which will occur in the chains not under tension will cause a continuously increasing fraction of the structure to participate in bearing the load, thereby producing an increased stiffness. Finally, because of the better alignment in the structure, the probability of new points of entanglement to be formed will increase. Both factors contribute to the rise in stiffness. The more rigid textural pattern will be formed relatively soon during the development of shortening and will limit the latter. Thus, in order to shorten appreciably, it is necessary for the fibre to be able to contract considerably before the pattern is finally established. In isotonic contraction a fibre with a load of 0.7 P_0 (fig. 50) will shorten from length 200 to length 140. A corresponding tension in isometric contraction is reached at length 85. The reason for the smaller shortening under isotonic conditions is the more rigid textural pattern which arises during shortening. This limits the shortening to length 140. The even smaller shortening observed in release contraction as compared with that obtained in isotonic contraction at the same tension,

can be explained by the relatively long time allowed for the isometric contraction to persist before release. The rigid texture characteristic of the contracted state in release contraction becomes established at the high initial length, while during an isotonic contraction this happens when the fibre is in the process of attaining a smaller length. The textural pattern which is established during an isometric contraction may be partially broken and then reformed at a longer length under the influence of vibrations with $>$ 2 per cent length amplitude. Thereby the extra tension is reduced. This yielding in the texture was seen in the experiments illustrated by fig. 28 when high frequency vibrations (100 c.p.s.) were applied and also during development of the isometric tension when low frequency vibrations were imposed on the fibre (5—10 c.p.s., Buchthal *et al.* 1944a). Therefore, in vibration experiments it will be advisable to apply as low a vibrational amplitude as possible.

The experiments hitherto described all showed that the stationary tension for the same length obtained in contraction depended on the previous experimental treatment both as regards tension and length at rest and during contraction (cf. Blix 1895 a and b). For the same length the highest tension was obtained in isometric contraction.

In isotonic contraction the tension was lower and the afterload contractions which contained both an isometric and an isotonic phase lay in between. In release contraction, defined as release during stimulation from isometric contraction to the same tension as at rest, the tension of contraction for the same length was even lower than in isotonic contraction.

Comparison between length and tension in maximal contraction of the single fibre and whole muscle.

Shortening in a whole muscle varies considerably with the equilibrium length of its fibres, and with the geometric arrangement of the fibres in relation to the direction of pull of the muscle. The shortest relative length which could be reached during contraction did not differ appreciably from that obtained in the single fibre.

TABLE 10.

Maximum force developed in contraction of whole muscle and isolated fibre.
(Calculated from experiments made by CASELLA (1951)).

Maximal tetanic tension	number of muscles	mean weight mg.	L_0 cm.	20° C. force/g.	20° C. $P_0 \times L_0/M$ (2)	20° C. $\times 10^6$ dynes/cm.^{2} (3)	20° C. $\times 10^6$ dynes/cm.^{2} (1)	0° C. force/g.	0° C. $P_0 \times L_0/M$ (2)	0° C. $\times 10^6$ dynes/cm.^{2} (3)	0° C. $\times 10^6$ dynes/cm.^{2} (1)
Whole semitendinosus (ventral head)	10	39.5	1.81	1275	2320	2.28 ± 3.3 %	1.48 ± 5 %	940	1695	1.66 ± 3.8 %	1.09 ± 6 %
Whole anterior tibial (medial head)	10	50.5	2.07	2210	4480	4.40 ± 2.5 %	2.50 ± 4 %	1500	3180	3.12 ± 3.9 %	1.71 ± 5 %
Isolated fibre from semitendinosus, anterior tibial, and gastrocnemius	38	—	0.8	3.29 ± 3 %				2.75 ± 3 %			

(1) Tension determined at length 110—120.
(2) L_0 = equilibrium length, M = mass of the muscle, P_0 maximum force in g.
(3) Calculated from (2) as $P_0 \times L_0/M \times 981$.

As regards the *specific tension* CASELLA (1951) in this laboratory has carried out a systematic comparison between the maximal tension developed in the fibre and in the respective muscle (Table 10). As seen from the table force × length per g. weight ($P_0 \times L_0/M$, HILL 1950 b) for the semitendinosus was of the same order of magnitude as HILL found for frog and toad sartorius. $P_0 \times L_0/M$ for the anterior tibial muscle is considerably greater, a finding which can be understood when considering the bipennate fibre arrangement of this muscle, whereby the length of the muscle no longer represents a measure of the length of the fibres. With $P_0 \times L_0/M$ as a basis for calculation the specific force developed in a whole muscle as compared with that of the isolated fibre is approximately 40 per cent lower. In the case of the isolated fibre, measurements of the cross sectional area could be performed with sufficient accuracy and, therefore, the force was determined directly per cross sectional unit. In the table values are also given for the specific tension of whole muscle calculated on the basis of a direct measurement of cross section. These values were about 35 per cent lower than those arrived at by calculating specific force from $P_0 \times L_0/M$. This difference is obviously caused by deviations from a cylindrical shape which was not taken into account when measurements were made of the maximal diameter only.

The difference between the specific tension in the single fibre and the whole muscle (calculated from $P_0 \times L_0/M$) is so large that it cannot be explained merely on the basis of the different equilibrium lengths of the different fibres and the subsequent differences in degree of stretch. Moreover, the small spread found for the mean values of the tension excludes the possibility that the difference could be due to an accidentally higher activity in some of the single fibres examined. Neither can variations in the cross sectional area in that part of the muscle (ab. $\frac{1}{2}$) where the fibres can move freely during stretch without hindrance from the tendon sheath, account for the difference. This part of the muscle is approximately cylindrical. The cause of the difference must mainly be the fact that only part of the cross sectional area of the muscle consists of active substance. Although the fibres are plastic, they are not tightly packed, and the interspaces are filled with connective tissue, blood-vessels and lymph-

vessels, nerves, and tissue fluid. A comparison between the *specific birefringence* of the single fibre and the whole muscle can give a measure of the amount of active substance. The mean value for the birefringence of the isolated fibre was $2.01 \pm 0.048 \times 10^{-3}$ (Buchthal and Knappeis 1938)[1] and for large bundles from semitendinosus muscles consisting of 100—200 fibres 1.41×10^{-3} with a minimum value of 1.23×10^{-3} and a maximum value of 1.65×10^{-3}. The specific birefringence was thus 30 per cent less in large cylindrical bundles than in the isolated fibre, indicating a correspondingly smaller amount of active substance. The difference found by measurements of birefringence was twice as large as the values found by Boyle and Conway (1941) for the volume of the intercellular space by studying the distribution of inulin (13 per cent). This discrepancy must be assumed to be an indication that part of the inactive substance in muscle cannot take up inulin.

These experiments show that the considerable difference in P_0 per unit area for whole muscle and single fibres can be explained chiefly by the contribution of the inactive substance to the cross section. The passive substance reduces the specific P_0 for whole muscle in two ways: 1) by contributing as an important factor to the cross sectional area and 2) by part of it acting as series elasticity to the fibres. In spite of external isometry, contraction of the fibres may thus be accompanied by a shortening. Owing to this shortening the fibres cannot develop their maximal force (see elastic locking p. 131).

The higher specific tension which apparently was found in an anterior tibial muscle as compared with the semitendinosus muscle, in spite of the fact that the single fibres in both muscles developed the same maximal tension during contraction, was doubtless due to the difference in the geometric arrangement of the fibres. The physiological cross section in the anterior tibial is larger than the anatomical, while in the semitendinosus this difference is considerably less. It is, therefore, more appropriate to compare the single fibre and whole muscle in the case of a semitendinosus than in that of an anterior tibial.

When the fibre is stimulated at equilibrium length, it can

[1] Regarding the correction for difference in diameters see Höncke (1947) and Knappeis (1948).

shorten without tension to about 60 per cent of the equilibrium length. This shortening apparently is less than that found by HILL (1949 e) for whole muscles, which is reported in his papers to be 40 per cent of the "natural length". The difference, however, presumably lies only in the definition of the length unit used. "Natural length" corresponds to length 135—165 in our length units, and in these units the shortening found by HILL therefore corresponds to a length of contraction of 54—66. RAMSEY and STREET (1940) found a reversible shortening down to a length of 60 to 70 per cent at the "resting length". At larger shortening they found irreversibility (δ state). In the present experiments we have obtained reversible shortenings amounting to a maximum of 50 per cent at the equilibrium length, which corresponded to a shortening to length 40 in RAMSEY's units. We have not found a δ state (for a critical evaluation of the δ state see BUCHTHAL 1942 and HILL 1949 e).

A considerable difference was found between single fibres and small bundles on the one hand, and whole muscles on the other with regard to the shortest initial length at which a contraction could be initiated. If a whole muscle was placed so that the distance between the tendon ends was about half of the natural length of the muscle, the latent period, which initially was long (approximately half of the duration of the shortening period) decreased successively at repeated twitches and values were obtained equal to those found in the straightened muscle (HILL 1949 e). This is interpreted as a disappearance of slack, i. e. an adjustment of the fibres to a shorter length than the muscle originally had in the unloaded state. This experiment cannot be performed on the single fibre. When the fibre contracts from a tensionless state it straightens after the cessation of stimulation almost as quickly as a fibre under load. In the length range 100—200 no significant shortening of the latent period was found in the single fibre with increasing load.

The fundamental difference between whole muscle and the fibre lies in the fact that the former can be "compressed" and obtain lengths below 100 without curling or folding to any considerable extent. In the presence of many parallel fibres a curling is improbable, since during shortening it would make necessary a larger amount of work of deformation than is the case when

the fibres can be compressed. In the single fibre a decrease of the distance between the ends of the fibre to a length below the equilibrium length will cause curling without real shortening in the minute structure. A comparison can be made with the deformation which would occur on compressing a rubber stopper, and the curling which arises when a thin rubber fibre cut from the same stopper is compressed. The finding of a constant duration of the latent period in the isolated fibre independent of the degree of stretch between lengths 100 and 200 indicates that slack in a fibre is never complete, i. e. there are always a number of elements which are straightened out. On the other hand, in a whole muscle, in which there is a possibility for "compression", there can occur complete slack which manifests itself by an increase in the latent period.

As previously mentioned, the intrinsic resistance developing in the muscle texture during contraction decreases with decreasing initial length (cf. elastic locking p. 131, 155). Therefore, it seems natural to assume that in a muscle which has been "compressed" at rest, the intrinsic forces developing at the transition from rest to contraction will be less than in a muscle which contracts from equilibrium length. Since whole muscle in its resting state is compressible to length below equilibrium length the elastic aligning forces will be less than in a fibre. Therefore better conditions will exist in the whole muscle for the hysteresis in the texture and in the connective tissue to maintain the muscle tensionless in a shortened state.

The course of stress-relaxation when quick changes in length are applied to the tetanically contracted fibre.

When a tetanically contracted fibre was suddenly stretched, the change in tension as a function of time proceeded differently than at rest, both during the rise in tension and during the adjustment. While the tension in the resting fibre following a quick stretch increased with rising gradient, the increase in tension following a quick stretch applied during contraction had an S-shaped course (fig. 21). The increase in length applied was

approximately 13 per cent of the equilibrium length and its final value was reached within 1.2 msec. The difference in the initial course of tension at rest and during contraction can be clearly seen when the increase in tension is plotted as a function of the elongation (fig. 22). At rest half of the additional tension is reached after 1 msec., at 8.5 per cent elongation. During contraction half of the additional tension was reached after 0.5 msec., at an elongation of less than 1 per cent. Referred to the same length the increase in transient tension was larger than at rest if the extra tension in contraction was low, while the reverse was true when the extra tension was high.

The course of the *initial* part of the increase in tension was always steeper during contraction than at rest, corresponding to the higher dynamic stiffness during contraction which was found when the stiffness was determined with vibrations of small amplitude. The finding of a smaller total rise in the tension during high tensions of contraction than at rest indicates the occurrence of a sudden yielding when the extension had reached a certain critical amplitude (comp. the S-shaped tension-time diagram, fig. 21 and the length-tension diagram with falling gradient, fig. 22).

When the stretch transient had attained its final value, tension first began to fall quickly and then more slowly. After about 1 msec. the tension reached a minimum value and then rose towards a new maximum within the next 5 msec. This secondary rise in tension was not due to an incomplete tetanic contraction and was most pronounced when extra tension was high. A possible explanation of this course is that part of the contractile elements are inactivated by the sudden change in length (yielding) and thus contract again under the influence of the continuous stimulation.

During *quick release* the initial course of the tension was equal to that found in the resting fibre and the secondary rise in tension characteristic of quick stretch was not observed. At release amplitudes of more than 2 per cent of L_0, the tension fell to zero.

The effect of the frequency of stimulation and of a limited number of successive stimuli.

The contractions in the experiments described above were maximal tetanic contractions. The strength of the stimuli was 3—7 times the threshold value, at a stimulation frequency of 25 per sec. and an impulse duration of 10 msec. at 0° C. As is well known, the size of the shortening at maximal stimulation varies with the number of stimulations per second and with the total number of impulses (duration of stimulation). Fig. 55 shows the maximal shortening as a function of the frequency of stimulation from a twitch to a tetanic contraction produced by a stimulation frequency of 30 per sec. which gave optimal shortening. Even at an impulse frequency of 1 per sec. at 0° C. a shortening could be obtained which was halfway between the peak of shortening in a twitch (50 per cent of L_0 at 0.3 P_0) and the maximal shortening in a tetanic contraction (90 per cent of L_0 at 0.3 P_0). In previous experiments performed under isometric conditions an extra tension halfway between that developed in a twitch and in a

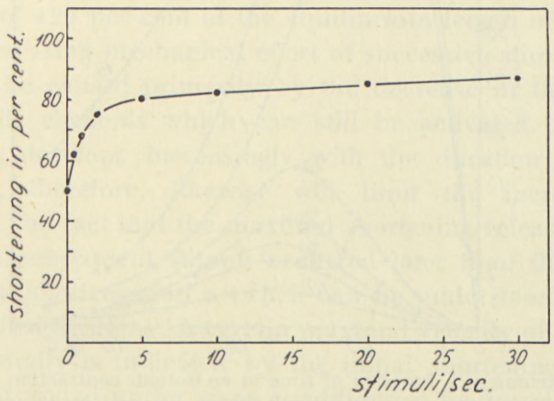

Fig. 55. Shortening as a function of stimulation frequency. Constant load 0.3 P_0. Duration of the single stimulus 5 msec. 0° C.
ordinate: shortening in per cent of L_0.
abscissa: number of stimuli per second, 0 indicates single stimulus.

tetanic contraction was reached at a frequency of 12 impulses per sec. (20° C., Buchthal 1942) and in mammalian fibres at a frequency of 40—45 impulses per sec. (37° C., Höncke 1947). The fact that half of the difference between twitch and tetanic con-

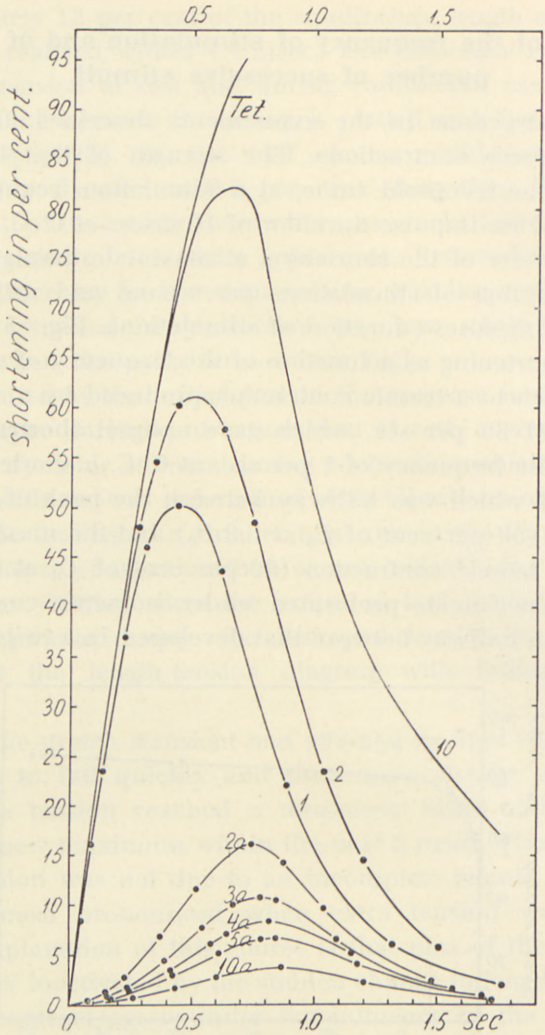

Fig. 56. Shortening as a function of time in an isotonic contraction, by 1 stimulus (curve 1), 2 stimuli (curve 2), 10 stimuli (curve 10), and by tetanic stimulation (curve Tet), distance between stimuli 30 msec. Curves 2a–5a give the net increase in shortening caused by the second to the fifth stimulus, curve 10a the net increase for the tenth stimulus. Load 0.2 P_0. 0° C.

ordinate: shortening in per cent of L_0.

abscissa: time in seconds (0 corresponds to the end of the latency period).

traction was reached at considerably higher frequencies, when the contraction occurred at high temperatures, must be due to the large temperature dependence of the relaxation.

In experiments with *constant* stimulation frequency of 30 per sec. the influence of the duration of stimulation was investigated. It was varied from single stimuli to tetanic stimulation lasting 16 sec. Fig. 56 shows the effect of 1 stimulus (curve 1), 2 stimuli (curve 2), 10 stimuli (curve 10), and tetanic stimulation (curve Tet) as a function of time in seconds at 0° C. Zero marks the end of the latent period. The increment in shortening produced by each successive stimulus is given for the range 2—10 stimulations in curves 2a—10a. Curve 4a, for example, shows the difference in shortening as a function of time obtained by 3 and 4 stimuli. Note that the stimuli are always separated by 30 msec. in time. The zero point for these curves is referred to the time for the preceding stimulus. The effect of the single stimulus decreased with increasing number of preceding stimuli. The peak of shortening for 2—10 stimuli was 0.3 to 0.4 seconds later than for the twitch, i. e. 60 to 100 per cent later than the time for the maximum of shortening in a twitch.

Stimulation of longer duration caused a further shortening. A single stimulus at load $0.2\,P_0$ and 0° C. thus produced a shortening of 50 per cent, and a 4 sec. tetanic stimulation, a shortening of 120 per cent of the equilibrium length of the fibre.

The decreasing mechanical effect of successive stimuli is considered to be caused primarily by the decrease in the number of contractile elements which can still be activated. Moreover, the locking develops increasingly with the duration of stimulation and, therefore, likewise will limit the increment in shortening. The fact that the maximal shortening released by the second and subsequent stimuli occurred later than the time of the maximal shortening in a twitch can be understood from the following considerations: A certain maximal velocity of activation which externally is indicated by the initial shortening velocity, cannot be exceeded under given conditions of load and temperature. Upon release of a subsequent stimulus (for example the second stimulus) "the stimulation factor" will already be present and the energy liberated by the second stimulus will only be able to exert its influence gradually as the effect of the first stimulus no longer maintains maximal shortening velocity. The effect of the stimulus 2 will thus be delayed in relation to the time at which it is released and can be "stored" until the mechanical

conditions for its use are present. In a later section experiments are described indicating that a transient change in the mechanical conditions can cause storing of the effect of stimulation as well (cf. p. 161).

In addition to its effect on the shortening, the duration of the stimulation also affects the course of relaxation, an effect which is already known from experiments on whole muscles (HARTREE and HILL 1921) and its effect on single fibres is described in a later section (p. 183).

Isotonic twich.

Isotonic shortening during a twitch at 0° C., expressed in per cent of the equilibrium length, is given as a function of the load in fig. 57. With increasing load the maximum in shortening decreased more rapidly than in tetanic contraction. At a low load and 0° C. the shortening in a twitch amounted to up to 60 per cent of the equilibrium length, and to 50—80 per cent of the

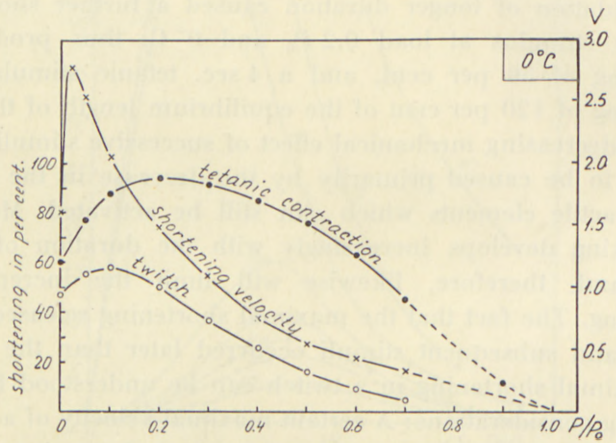

Fig. 57. Maximum shortening and shortening velocity in tetanic contraction and in a twitch as a function of load. 0° C.
left ordinate: shortening in per cent of L_0.
right ordinate: maximal shortening velocity in L_0 per second.
abscissa: load in units of P_0.

shortening in tetanic contraction. At a load of 0.5 P_0 the shortening fell to 20—40 per cent of the tetanic shortening.

Early investigations (cit. EVANS 1947) on whole muscles under isometric conditions showed a decrease in the extra tension in a

twitch with rising *temperature*, while the extra tension in tetanic contraction increased. Under isotonic conditions an increasing shortening was found with rising temperature in these experiments, both in tetanic contraction and in the twitch. However, this increasing shortening in the twitch has been assumed to be caused by inertial forces in the recording system.

In the present experiments on single fibres and small bundles of fibres the inertia of the recording system was so small that it did not cause any appreciable distortion of the shortening or the shortening velocity, despite the relatively small forces concerned.

In the isolated fibre the shortening in a twitch varied considerably less with the *temperature* than the shortening in tetanic contraction. Fig. 52 and fig. 60 show the shortening as a function of load at 0° and 24° or 26° C. in both cases. Dependent upon the load the temperature coefficient of the shortening in the twitch may be either positive or negative in the same fibre. At a low load the shortening always increased with decreasing temperature. In tetanic contraction increasing shortening was found with increasing temperature over the whole range of loads.

The difference found in temperature dependence in the twitch and the tetanic contraction is due to the fact that a stationary value for the shortening is not obtained in the twitch. The high temperature dependence of the relaxation velocity can partly explain the paradoxical difference in temperature de-

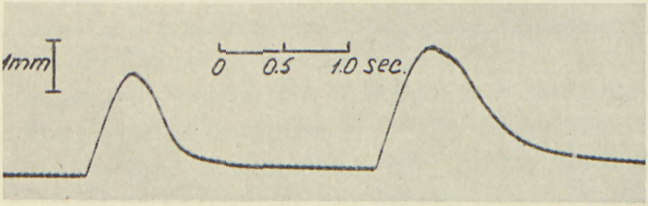

Fig. 58. Two twitches released with an interval of 2.2 seconds. Constant strength of stimulus. 0° C., 0.15 P_0, L_0 = 5 mm. Curarised fibre. Note the enhancement of shortening and duration of the second contraction.

pendence between the twitch and the tetanic contraction. In a later section a correlation will be discussed between the size of the shortening in a twitch and a tetanic contraction and the velocities of shortening and relaxation (see p. 188).

In addition to load and temperature, the shortening in a twitch is affected by a preceding contraction (HARTREE and HILL 1921 for whole muscles and RAMSEY and STREET 1941 for single fibres, isometric conditions). The isotonic twitch showed increased shortening for a subsequent twitch, i. e. the first, second, and third twitch showed a gradual increase in the peak of shortening (fig. 58). This effect was most pronounced at a low load, when the velocity of relaxation had low values. The increased shortening was characterized by an increase in the velocity of shortening, a reduced velocity of relaxation, and an increased duration of contraction.

Shortening as a function of time.

Apart from the maximum shortening as a function of the external conditions as discussed above, the mechanical response of the fibre is characterized by the *time course* of the shortening or the tension. In an isotonic *twitch* the shortening rose almost linearly during the first three quarters of the change in length (fig. 59), and at 0° C. the maximal shortening was reached 0.4 to 0.7 seconds after the end of the latent period. The time for

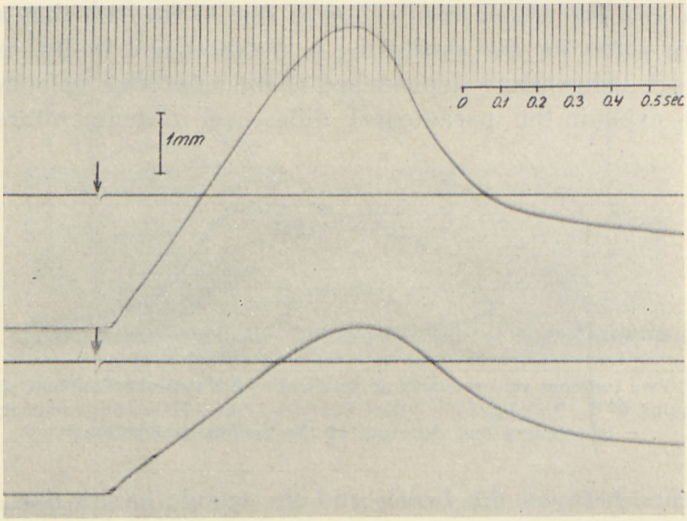

Fig. 59. Isotonic twitches with a load of 60 dynes (upper curve) and 120 dynes (lower curve). Shortening 56 per cent (upper curve) and 30 per cent (lower curve). P_0 = 800 dynes, L_0 = 9 mm. Maximum shortening 0.65 sec. after the end of the latency period. Stimulus at arrow. 0° C.

the maximal shortening varied up to 30 per cent with the load. At low and high loads the maximum occurred earlier than at intermediate loads of 0.3 to 0.5 P_0 (fig. 60 and fig. 61). At 0° C. the whole contraction lasted 1 to 1.5 sec. In tetanic contraction at the same temperature half of the maximum shortening was reached 0.1 to 1 sec. after the end of the latent period, depending on the size of the load. Fig. 60 shows the course of shortening

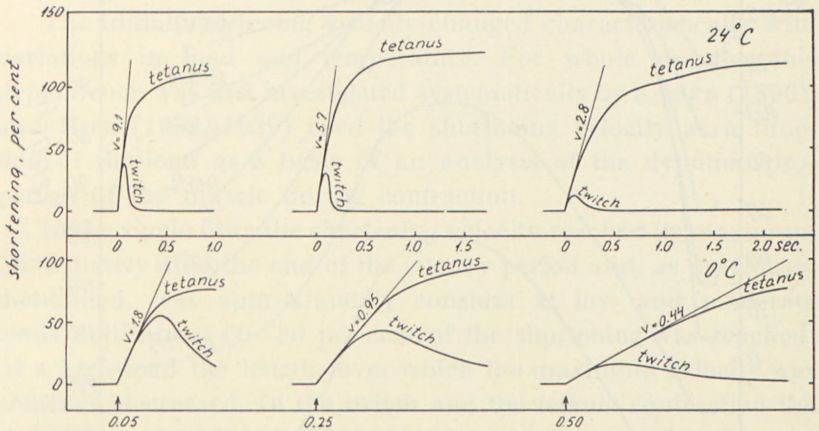

Fig. 60. Course of shortening in isotonic twitches and tetanic contractions. Upper curves 24° C., lower curves 0° C. The values of the maximal shortening velocity (V) are given on each curve. The figures at the arrows denote the different loads, 0.05, 0.25 and 0.50 P_0.
ordinate: shortening in per cent of L_0.
abscissa: time in seconds.

in a twitch and a tetanic contraction for the same fibre at three different loads and at 0° and 24° C.

A comparison between the *time course* of the twitch under *isotonic* and *isometric* conditions showed, in agreement with the findings for whole muscles (Fick 1871, 1882, Schenck 1895, Fenn 1936, Hill 1949 d), that at all the loads examined the peak of tension was obtained before the peak of the shortening. In the single fibre this time difference on an average amounted to 200 msec. (0° C.). An example of the course of the tension and the shortening for the same fibre is given in fig. 61. The fibre was stimulated at different initial loads, alternately under isotonic and isometric conditions. It is seen from the figure that the shortening still proceeds during part of the relaxation phase

of the isometric twitch. An analysis of the cause for this time difference based on the shortening velocity and of its dependence on the load is attempted in a later section (see p. 172).

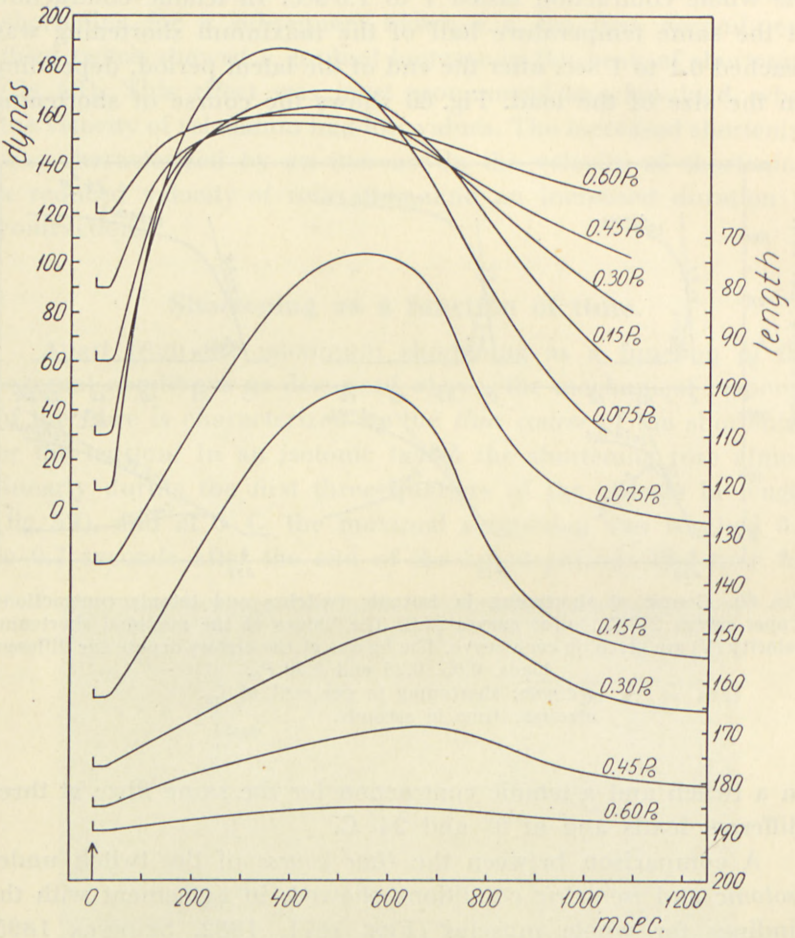

Fig. 61. *Isotonic and isometric twitches* alternatively recorded from the same muscle fibre.

The five lower curves represent length in isotonic contraction and the five upper curves tension in isometric contraction as a function of time. The figures on the lower curves denote the isotonic load and those on the upper curves the initial tension both in units of P_0. 0° C.

left ordinate: isometric tension in dynes, 200 dynes = P_0.
right ordinate: length in per cent of L_0.
abscissa: time after stimulus in msec.

The shortening velocity.

Since the absolute velocity with which a fibre shortens depends on its length, the relative velocity (V) is used as a measure of the development of the shortening:

$$V = \frac{\text{shortening velocity in cm./sec.}}{\text{equilibrium length in cm.}}.$$

The initial shortening velocity changed characteristically with variations in load and temperature. For whole muscles this dependence was first investigated systematically by KAISER (1896), and HILL (1938, 1939) used the shortening velocity as a function of the load as a basis of an analysis of the dynamic properties of the muscle during contraction.

In the single fibre the shortening velocity reached its maximum immediately after the end of the latency period and, as previously mentioned, was approximately constant at low and moderate loads until about 60—80 per cent of the shortening was reached. At a high load the length, over which the maximum velocity was constant, decreased. In the twitch and the tetanic contraction the shortening coincided at different loads at 0° C. over a time interval of 0.2 sec. after the end of the latent period. Fig. 62 shows an example of the maximal shortening velocity at different loads during alternating twitch and tetanic contraction. The frequency of stimulation in a frequency range of 0.5 to 60 stimuli per sec. did not affect the initial velocity of shortening, provided the stimulation was always maximal.

The abrupt development of shortening has been considered to indicate that at the end of the latent period the contractile mechanism is already fully active (HILL 1949d, ABBOTT and RITCHIE 1951b). However, the fact that the shortening velocity quickly attains its maximal value, in our interpretation can only indicate that the *rate* and not the degree of activation quickly attains a maximum. The steep beginning of shortening must actually be considered the result of an interaction between shortening caused by contraction and elongation caused by the *latency relaxation*[1] (SANDOW 1944, ABBOTT and RITCHIE 1951a).

[1] The existence of a latency relaxation in the isolated fibre has recently been demonstrated by MAURO (1951).

The resulting course of shortening is delayed by this initial elongation. Thereby, using a sensitivity which allows to record the peak tension of the twitch, the course of shortening appears very abrupt.

In the initial phase of the shortening, especially at a high load,

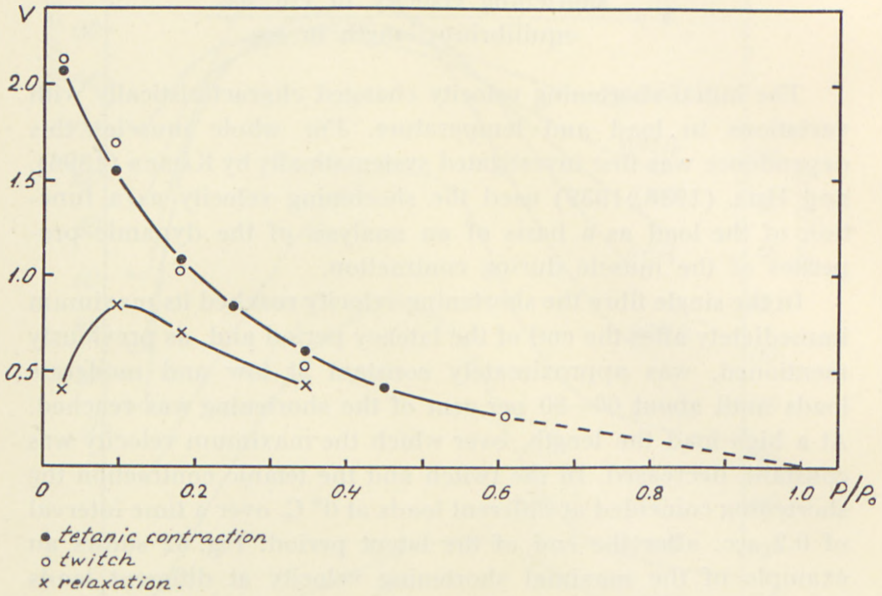

Fig. 62. Maximal *shortening velocity* in isotonic twitches and tetanic contractions and maximum relaxation velocity in tetanic contractions as a function of load. 0° C.
ordinate: velocity in L_0 per second.
abscissa: load in units of P_0.

a maximal velocity may occur at the beginning of the shortening, which exceeded the later constant velocity. This deviation was not caused by the inertia of the recording system, since it extended over an interval which was at least 10 times longer than the oscillation period for the recording system plus fibre.

As a function of the load, the shortening velocity in the fibre decreased with increasing load and the course of the curve in the range 0.03—1.0 P_0 was of the same type as that described by HILL (1938) for whole muscles. However, at loads below 0.03 P_0, the course of the force-velocity relation for the fibre differed from that found in whole muscles, since the curve had a maximum at 0.02 P_0 (Table 11). The lower velocity, which occur-

TABLE 11.
Force-velocity relation.

Load mA	Load dynes	Load in units of P_0	Relative V
2.0	9.0	0.007	2.53
5.0	22.5	0.017	2.92
20.0	90.0	0.067	2.41
60.0	270.0	0.200	1.62
100.0	450.0	0.333	1.03
150.0	675.0	0.500	0.63
200.0	900.0	0.667	0.41

P_0 = 300 mA total (each fibre half = 150 mA) = 1350 dynes (2 fibres) 1 mA = 4.5 dynes.
Equilibrium length of the 2 fibres = 6 mm; effective L_0 in the apparatus = $\frac{6}{2}$ = 3 mm.

red at loads near the equilibrium length, is probably caused by the incomplete alignment in the fibrillar structure and corresponds to the lesser shortening, which was found during contractions from equilibrium length as compared with, for example, contraction occurring at lengths 110—120. In experiments on whole muscles great difficulty will be encountered in the analysis of correspondingly low loads. The longer equilibrium length of the whole muscle causes higher absolute velocities and hence larger inertial forces than in the single fibre, and these may distort the initial course of the curve. In the first phase of the movement the retarded reaction of the recording system will cause a summing up of elastic energy which is later released. Thereby the system will be accelerated to a velocity which exceeds the natural shortening velocity. In addition, the inhomogeneous internal state of tension in the muscle, due to the different equilibrium lengths of the fibres and the connective tissue, will conceal the initial decrease in velocity. However, the decrease found in the single fibre at low loads makes it doubtful whether it is justified to extrapolate the velocity in force-velocity diagrams for whole muscles to load zero (HILL 1938, 1939, RALSTON *et al.* 1947, 1949).

The relative velocities found in the single fibre or in small bundles from the semitendinosus muscle at loads above 0.03 P_0 are considerably higher than those found for the corresponding whole muscle (fig. 63). This is true both of semitendinosus and

sartorius muscles from the same animal, examined with the same system as that used for experiments on the single fibre. The force-velocity diagrams found in these experiments for sartorius muscle showed agreement with those found by HILL (1938, 1939) for the same muscle. The cause of the difference

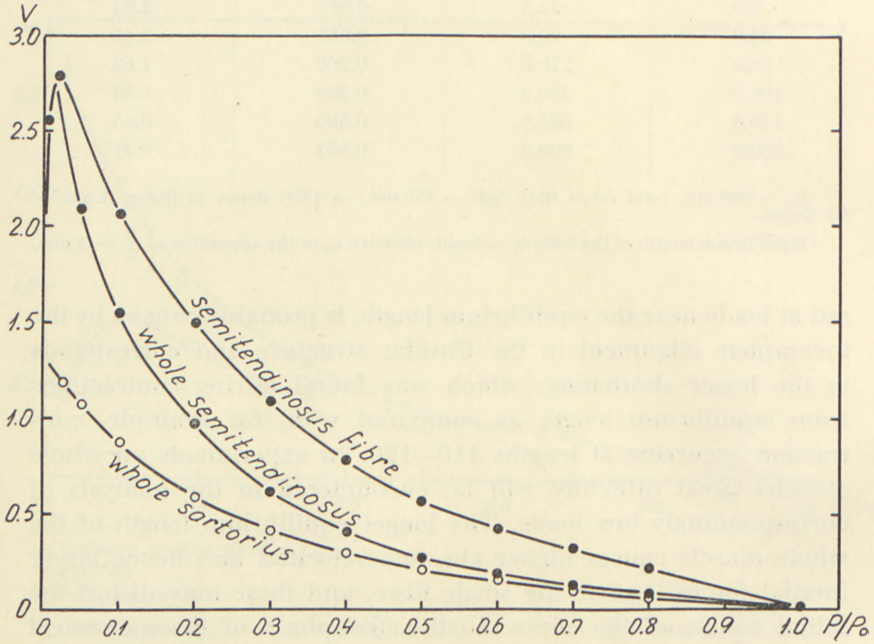

Fig. 63. Maximal shortening velocity in a whole muscle (sartorius, semitendinosus) and the isolated fibre of the same semitendinosus. Average of 10 muscles. 0° C.
ordinate: shortening velocity in L_0 per second.
abscissa: load in units of P_0.

between fibre and whole muscle lies presumably in the distribution of the different fibre lengths and in the resulting non-uniform state of stretch of different fibres in a whole muscle. This is accounted for quantitatively in a later section (Appendix III., p. 298).

Shortening velocity during different external mechanical working conditions for the muscle fibre.

Since the tension developed in contraction for a given length to a large extent depends on the mechanical conditions under

which the contraction proceeds, it was of interest to investigate whether the relative shortening velocity is likewise affected by mechanical factors other than the load. We have, therefore, compared the shortening velocity in isotonic contraction with 1) the velocity during afterload contractions, 2) the shortening velocity which occurs when the fibre is allowed to shorten

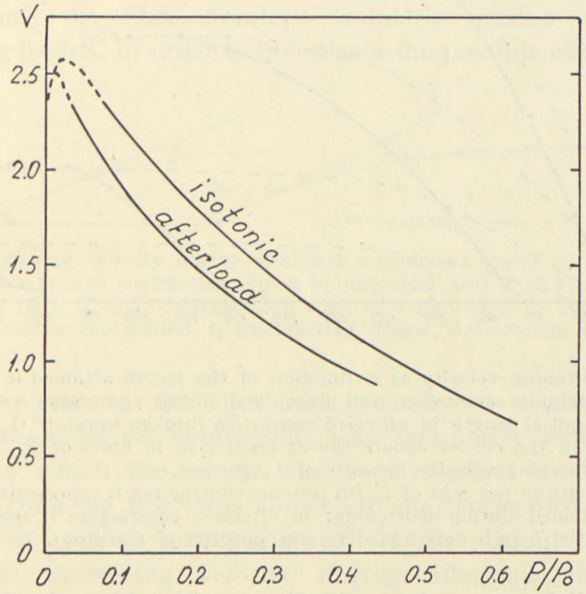

Fig. 64. Force-velocity relation during afterload from length 114 (L_0 = 100) and in isotonic contraction. Isolated fibres, 0° C.
ordinate: shortening velocity in L_0 per second.
abscissa: load in units of P_0.

from its isometric tetanic maximum against a given load, and 3) the shortening velocity following a sudden change in load applied during a twitch.

1) *Shortening velocity as a function of load during afterload and isotonic contraction* is shown in fig. 64. During afterload the velocity is always lower than under isotonic conditions. In the load range between 0.1 and 0.5 P_0 the difference between afterload and isotonic contraction was about 20 per cent in the example shown in fig. 64, and may amount to a maximum of 30 per cent. The difference between the shortening velocities under these two conditions, though statistically significant, is

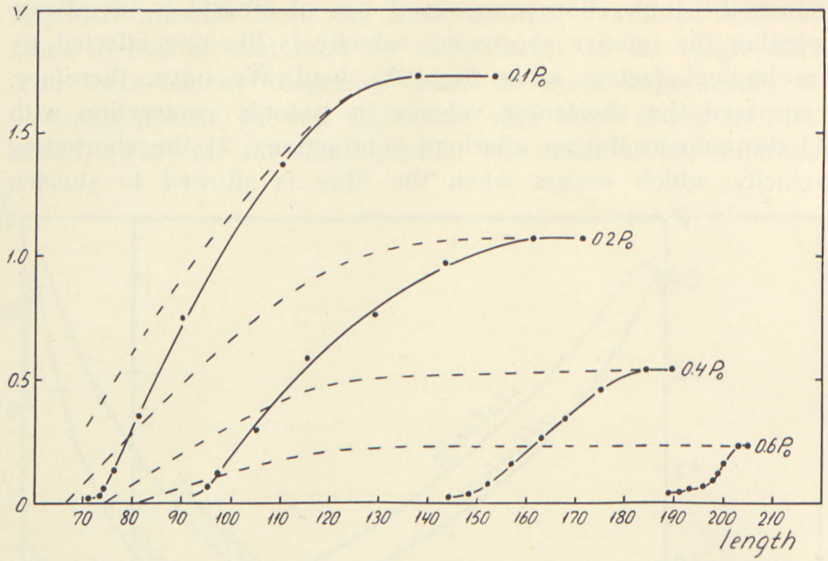

Fig. 65. Shortening velocity as a function of the length attained in the course of *isotonic* tetanic *contraction* (full lines) and initial shortening velocity as a function of initial length in *afterload contraction* (broken lines). 0° C. The figures on the curves denote the external load in units of P_0.
ordinate: shortening velocity in units of L_0 per sec.
abscissa: length in per cent of L_0 (in isotonic contraction it represents the length attained during shortening; in afterload contraction it represents the initial length determined by the position of the stop).

quite small in comparison with the considerable reduction found in the change in length during afterload contraction as compared with isotonic.

Shortening velocity as a function of shortening in isotonic contractions at four different loads is seen in fig. 65. The dashed lines represent the initial shortening velocity in afterload contractions at the same load as a function of the initial length. In view of the finding that the force-velocity relation is valid during the major part of the course of shortening (see below), it seems justified to compare the initial velocity in afterload contractions with the velocity at the same length and load in isotonic contraction. Referred to the same length and load, the velocity in isotonic contraction is less than the velocity in afterload contraction, while the reverse is the case of the initial velocities.

2) *The shortening velocity during release from isometric tetanic contraction.*

The difference found in the shortening velocity during isotonic contraction and afterload contractions may be caused by the differences of the initial length at rest in these conditions or by the different initial phase of contraction where, during afterload contractions, the fibre develops isometric tension until the shortening begins. In order to investigate the possible effect of this

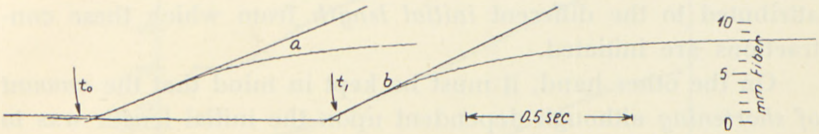

Fig. 66. Shortening velocity during afterload contraction (curve a) and release from isometric tetanic contraction (curve b). Identical load (0.15 P_0) and initial length (L = 150). 0° C. t_0 indicates the start of stimulation in both afterload and isometric contraction, t_1 the start of release, 0.8 seconds after t_0.

isometric phase on the shortening velocity at a given initial length, the afterload contraction was compared with a contraction in which the length was kept constant until P_0 was reached. Then the fibre was allowed to shorten against the same load as that applied during afterload. In the example shown in fig. 66 the shortening velocity during afterload contraction (curve a) at load 0.15 P_0 and 0° C. amounted to 1.25 L_0/sec. On release from the isometric tetanic maximum under the same load the velocity was 1.37 L_0/sec. This velocity was determined over an interval of 0.15 sec. after the elastic hump, which occurred when the fibre was released from isometric contraction. The change in length, corresponding to the hump which amounted to 4.5 per cent of the equilibrium length of the fibre at rest (L_0) was probably not entirely completed during this interval of time. Assuming that the hump was caused by a series elasticity of the same dynamic properties as the resting fibre, it would give an increase in the shortening velocity of 0.08 L_0 per sec.[1] The

[1] The ratio between the initial change in length and the change in length which occurred between 20 and 140 msec. amounted to about 0.2 at large variations in length at rest (see transient experiments, Table 2). Therefore, at an initial change in length of 4.5 per cent the change in length between 20 and 140 msec. is about 0.9 per cent. This corresponds to a mean velocity of $\frac{0.009\ L_0}{0.12\ \text{sec.}} = 0.075\ L_0$/sec.

shortening velocity in the active elements therefore is 0.08 L_0 per sec. less than the directly measured velocity, i. e. 1.29. Thus, the corrected shortening velocity was approximately of the same order of magnitude during afterload and during release from isometric contraction. Therefore, the results of these experiments indicated that the isometric phase in an afterload contraction can scarcely be responsible for the lower velocity of shortening found under these conditions as compared with isotonic contraction, and, moreover, the difference in velocity must be attributed to the different *initial length* from which these contractions are initiated.

On the other hand, it must be kept in mind that the *amount of shortening* although dependent upon the initial length was to a large extent a function of the isometric phase which preceded the shortening (cf. p. 130). *The change in the mechanical working conditions of the fibre, which at the same load caused large changes in the stabilized length of contraction, thus gave only small or no changes in the initial relative shortening velocity of the fibre.* The cause of this difference must be sought in the previously described "elastic locking" of the contractile substance. It gives rise to different stabilized lengths in contraction initiated under different conditions, but it does not affect the shortening velocity until a certain deformation in the structural pattern of the fibre has taken place, i. e. after a certain shortening has been reached.

In order to obtain some idea of the size and course of the internal tension which arises in the structure during "locking" the progressive shortening during development of an isotonic tetanic contraction is treated from the following point of view:

During the development of an isotonic tetanic contraction the shortening velocity decreases. This decrease may be caused by an internal resistance against the shortening which arises by the elastic "locking". During the *isotonic* contraction the initial length is determined by the load (i. e. the length-tension diagram of the resting fibre). By the introduction of an *afterload* (cf. p. 129) it is possible at a given load by means of the adjustment of the stop-screw (fig. 2, n) to vary the initial length between the length at rest and the length during isometric contraction at the same load. Thus, the initial shortening velocity could be examined at the same load as a function of the initial length. In the very

first phase of contraction the elastic locking is assumed still to be of subordinate importance and the external load therefore corresponds to the load acting on the contractile elements. Hence, the initial shortening velocity in afterload contractions represents the "*pure*" *velocity* which arises for a given external load. Referred to the *same length and load* the shortening velocity

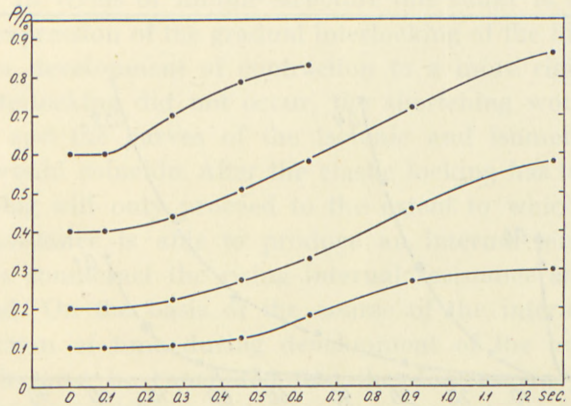

Fig. 67. *Internal tension* as a function of time during development of the isotonic tetanic shortening calculated from the data in fig. 65. 0° C. Different external loads (0.1 to 0.6 P_0). *ordinate:* internal tension in units of P_0. *abscissa:* time in seconds.

in isotonic contraction decreases with increasing shortening as compared with the "pure" velocity (fig. 65). This difference in velocity is attributed mainly to the internal mechanical resistance which arises by the change in the texture (elastic locking). In the example given in fig. 65 we see that an isotonic contraction was released at load 0.2 P_0 from length 171 and had an initial velocity of 1.14 L_0 per sec. When shortening had proceeded for about 0.8 sec. to length 108, the velocity had decreased to 0.39 L_0 per sec. At the same load and at length 108 the initial shortening velocity in an afterload contraction was 0.79 L_0 per sec. In an afterload contraction a velocity of 0.39 L_0 per sec. was obtained at twice the load, viz 0.4 P_0. Supposing that the relation between shortening velocity, load, and length is not essentially changed by a duration of the contraction of 0.8 sec., the difference in shortening velocity indicates an internal resistance developed during shortening of the order of magnitude of 0.2 P_0.

The assumption that the force-velocity relation remains unaltered by the duration of contraction is supported by the experiments illustrated in fig. 66.

Fig. 67 shows the internal tension in the contractile elements as a function of time estimated on the basis of the difference between shortening velocity in isotonic contraction and the initial

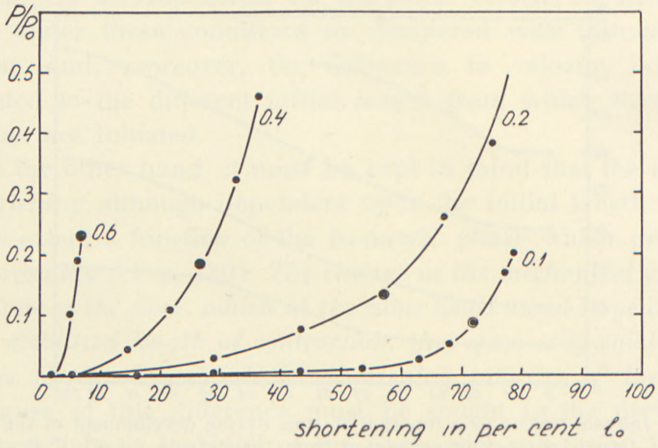

Fig. 68. Calculated *internal resistance* against shortening during the development of an isotonic tetanic contraction as a function of the shortening. 0° C. External load 0.1, 0.2, 0.4, and 0.6 P_0.
◉ indicates the internal tension after a shortening of 0.63 second.
ordinate: internal resistance in units of P_0.
abscissa: external shortening in per cent of L_0.

velocity in afterload contraction. The internal structural resistance, i. e. the tension in the contractile elements minus the external tension, as a function of shortening is given in fig. 68. The specially marked points denote the size of the internal resistance at different initial loads at a given time (0.63 sec.) after the start of shortening. In spite of the decrease in shortening the resistance is higher at high loads than at low loads. For example, at load 0.4 P_0 it is twice that of load 0.1 P_0. This difference indicates an increased tendency to locking with increasing load, produced by the decreasing cross-section of the fibre and tighter packing of the minute structural elements on the one hand and a longer time necessary to give a certain shortening on the other.

At 0° C. the internal resistance arising during isotonic tetanic shortening 0.5 sec. after the start of stimulation corresponds to one

third of the initial load. As the maximum of shortening in a twitch occurs approximately 0.5 sec. after the stimulus, the upper limit of the internal resistance counteracting shortening in a twitch will not exceed 30 per cent of the initial load.

In an equivalent system the internal resistance developed during contraction is described by a shunt of elastic and viscous elements. In terms of minute structure this shunt is considered to be an expression of the gradual interlocking of the fibre texture during the development of contraction to a more rigid pattern. If this interlocking did not occur, the shortening would not be inhibited and the curves of the isotonic and isometric tetanic maxima would coincide. After the elastic locking has taken place a shortening will only proceed to the extent to which the contractile substance is able to produce an internal tension large enough to counteract the rising internal resistance and the external load. On the basis of the course of the internal tension as a function of time during development of the tetanic contraction, it must be concluded that the decrease in shortening velocity is due chiefly to this shunting element.

The resistance from a shunting element, which is developed during contraction could also be demonstrated under isometric conditions (Buchthal *et al.* 1944a, fig. 4). In these experiments a periodic vibration (amplitude 1 per cent of L_0) was superimposed on a stationary tetanic isometric contraction (20° C.). The stiffness was determined by measuring the resulting periodic changes in tension. Immediately after the maximal tension had been reached in tetanic contraction, the stiffness still increased. It was found to be at maximum 0.4 sec. after the tension had reached P_0. The lower stiffness which initially was observed at the maximum in tension of the isometric tetanus was interpreted as being caused by a yielding in the textural pattern produced by the altered state of loading during contraction. Due to the low vibrational frequency the initial increase in stiffness which is discussed in detail in a later section (cf. p. 163, 189) did not manifest itself in these recordings.

In the preceding section the mechanical reaction of the fibre under constant external load has been analysed in the hope that the load on the contractile elements would be equal to the external load. The results of these experiments, however, show that this

is *not* the case and that the load in the contractile elements varies despite external isotonic conditions. In the experimental series to be described here, we have introduced changes in load during a twitch in order to obtain further information about the extent to which the relation found between load and velocity is generally valid.

3) *The shortening velocity following a transient change in load during a twitch.*

Experiments, corresponding to those performed by GASSER and HILL (1924) and HILL (1949 d) on whole muscle under *isometric* conditions, were carried out during *isotonic* contraction of the single fibre by introducing sudden changes in load at different times during the course of the contraction. The quick loads applied to single fibres in these transient experiments (0.1—0.8 P_0) were less than those used in experiments on whole muscles (HILL 1949 d). In whole muscle at the end of the latent period the changes in load resulting from the transient change in length, were of the order of magnitude of P_0.

The mechanical reaction of the fibre during a change in load can be interpreted as consisting of a rapid elastic change in length, superimposed on a change in the shortening velocity. This change in velocity appears to correspond closely to the change which could be expected according to the known relation between load and shortening velocity.

Fig. 69 shows a twitch at load 0.20 P_0 (0° C., curve 1) and at load 0.40 P_0 (curve 3). Curve 2 shows the effect of a sudden increase in load of 0.2 P_0, lasting 0.12 sec., introduced 0.15 sec. after the end of the latent period. During the 0.12 sec. the load was thus the same as that in curve 3, after which it continues as in curve 1 at 0.2 P_0. The change in load could be introduced at different times between the end of the latent period and the end of the relaxation by means of an adjustable system of switches (HELMHOLTZ pendulum). Between every other contraction *with* change in load, a contraction was recorded with constant load, corresponding to curves 1 and 3; hence, the mechanical reaction of the fibre with and without change in load was carefully controlled in this way. Data from a series of experiments of the

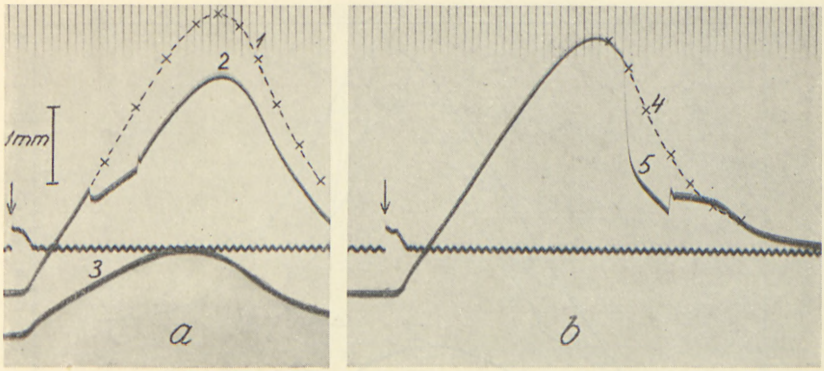

Fig. 69. *Transient change in load applied during an isotonic twitch.*
curve 1 and 4: twitches at load 0.2 P_0, projected on curves 2 and 5.
curve 3: twitch at load 0.4 P_0.
curve 2 shows the effect of a sudden increase in load of 0.2 P_0, introduced 0.15 sec. after the end of the latency period and lasting for 0.12 seconds (a).
curve 5 shows the effect of the same increase in load (0.2 P_0) introduced when shortening is maximal (b).
L_0 = 13.5 mm. 0° C. Distance between time marks 20 msec. Stimulus at ↓.

type described are given in fig. 70. The increase in load of 0.2 P_0 was introduced at different times during a twitch (0° C.) which began and ended at load 0.2 P_0. Curve I represents the shortening at 0.2 P_0, curve II, the shortening at 0.4 P_0, and curve III, the difference between the curves for 0.2 and 0.4 P_0.

The effect of the change in load introduced from 0.15 sec. to 1 sec. after the end of the stimulus, is seen in curves a—k. In curves a—d the quick loading causes a rapid change in length of about 1 per cent of the equilibrium length; this is superimposed by a damped oscillation, and it can be seen that this part of the change in length has elastic character. The fibre then began to shorten again with a velocity nearly equal to that which would have occurred at the same time if the contraction had been introduced with a load of 0.4 P_0. When the fibre was released again after 0.12 sec., it shortened at first elastically and then with the same velocity which it would have had at the constant load 0.2 P_0 at the same time after stimulation (curves a—c). Shortly before the shortening reached its maximum, the mechanical reaction to quick load became essentially different from that occurring during the shortening phase. The change in length was 5—6 times larger and no longer of an elastic character. Only during

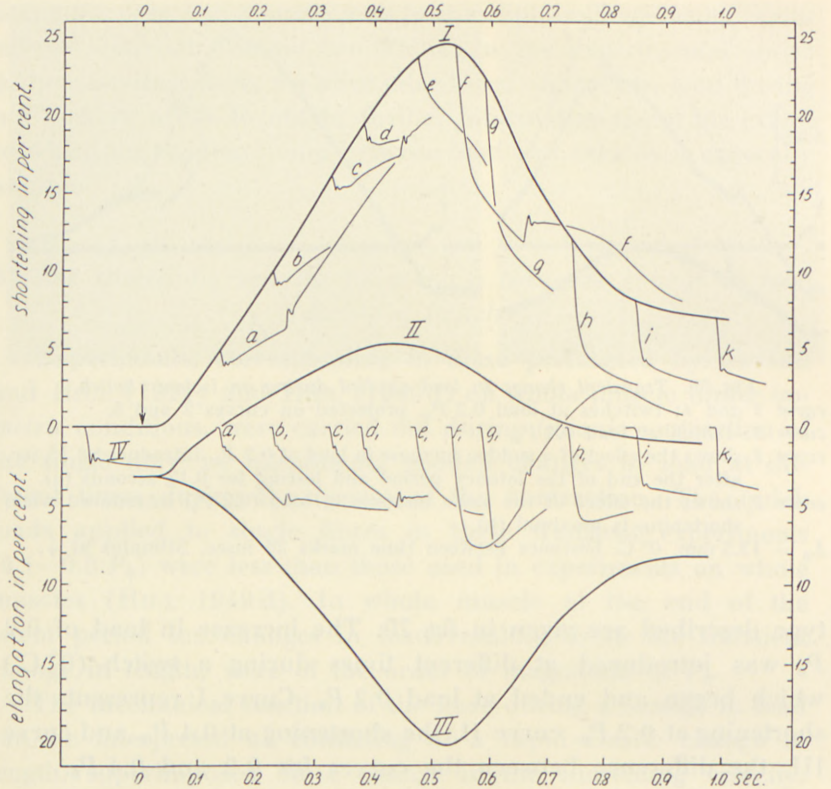

Fig. 70. *Transient increase and decrease in load applied at different times in the course of an isotonic twitch, 0° C.*

curve I: shortening in a pure isotonic twitch at load 0.2 P_0.
curve II: shortening in a pure isotonic twitch at load 0.4 P_0.
curve III: difference between curve I and II.
curve IV: effect of transient change in load in the resting fibre.
curves a—k: effect of an additional load of 0.2 P_0, lasting 0.12 sec. and imposed on curve I.
curves a_1—k_1: difference between curve I and curves a—k (net effect of transient).
ordinate: shortening and elongation in per cent of L_0.
abscissa: time after stimulus in seconds.

the following relaxation could the effect of the elasticity again be demonstrated, as can be seen from curve f, fig. 70, and from fig. 69. The course of length after the unloading, in this case intersects curve I. This indicates that after quick loading, introduced at the maximum of shortening, a shortening could be attained during the subsequent quick unloading exceeding that which would be possible at a constant load. The forced elon-

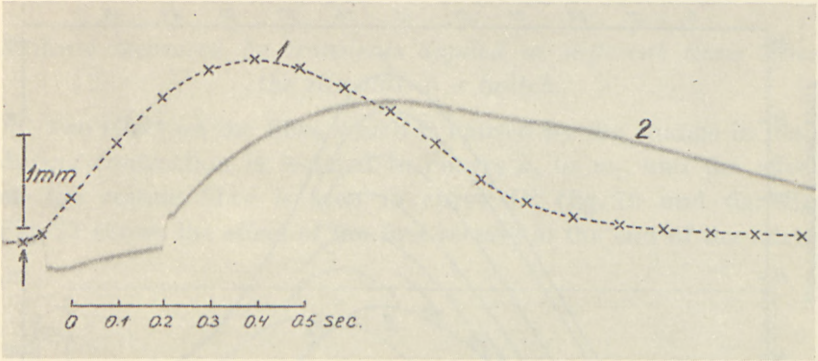

Fig. 71. *Effect of transient additional load on time course of isotonic twitch, 0° C.* ("storing").
curve 1: isotonic twitch, load 0.2 P_0 projected upon curve 2.
curve 2: isotonic twitch, initial load 0.2 P_0; 0.04 second after the end of the latency period an additional load of 0.6 P_0 is introduced for 0.26 sec.

gation thus caused an extra-shortening instead of a lasting elongation.

The example shown in fig. 71 shows clearly how transient loading and unloading of 0.6 P_0 can cause a displacement in the time course of the shortening. At a time when the relaxation in the twitch is complete (load 0.2 P_0 curve 1), a considerable displacement of the shortening can be seen as a consequence of a transient quick load (curve 2) introduced immediately after the end of the latent period for about 0.25 sec. After 0.75 sec. curve 1 and curve 2 intersect. It may be emphasized that after the transient loading the load in curve 2 was identical with that in curve 1, and it is seen that the transient prolonged the effect of the stimulus considerably.

The increase in duration in the *isometric* twitch, which could be caused by an increased initial degree of stretch corresponds to the effect of an increase in load described here. The fact that this cannot always be observed may be due to different reactions in the series element described later (see p. 172).

The constant relation between load and shortening velocity, regardless of the change in load introduced at rest or at different times during the shortening, was also obvious from experiments with quick unloading. In the experiments shown in fig. 72, the initial load was 0.34 P_0, which was released to 0.17 P_0

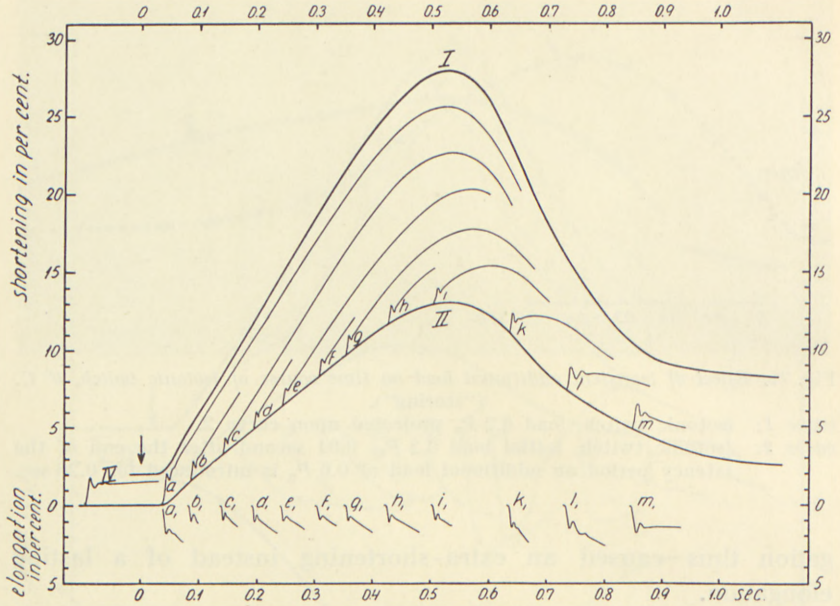

Fig. 72. Effect of a transient decrease in load applied at different times after the stimulus during the course of shortening in an isotonic twitch, 0° C.

curve I: pure isotonic twitch, load 0.17 P_0.

curve II: pure isotonic twitch, load 0.34 P_0.

curve IV: effect of a transient decrease in load from 0.34 to 0.17 P_0 in the resting fibre.

curves a—m: effect of a transient decrease in load from 0.34 to 0.17 P_0 during the twitch.

curves a_1—m_1: difference between curves a—m and curve II (= net effect of transients a—m).

ordinate: shortening and elongation in per cent of L_0.

abscissa: time after stimulus in seconds.

and the contraction continued against a load of 0.17 P_0. Here the initial shortening had a pronounced elastic component regardless of the time during the contraction at which the release was introduced. Nearly up to the maximum in shortening the slow change in length following the initial one corresponded exactly to the velocity which would arise at the same *constant* load. At the maximum of shortening and during the first part of relaxation, the fibre continued to shorten and in contrast to the findings with a quick *increase in load* it could only be made to coincide with the curve for constant load by a parallel displacement to an earlier phase of the contraction.

Stiffness measured by transients applied at different times after the stimulus in a twitch.

The effect on the fibre which is caused by the change in load during contraction is isolated in curves a_1 to m_1, and the effect on the resting fibre is seen in curve IV (fig. 70 and fig. 72). Fig. 72 shows the effect of the first release at the end of the latent

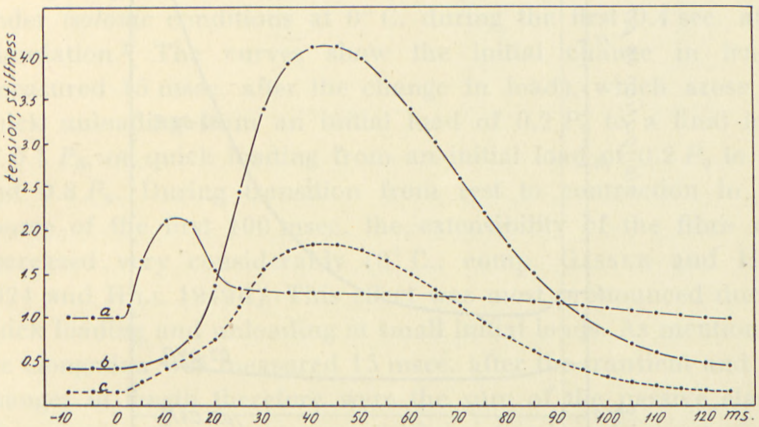

Fig. 73. Initial increase in stiffness in isometric contraction.
b = tension in an isometric twitch (15° C.).
c = vibrational stiffness, frequency 100 c.p.s.
$a = \frac{G}{P + P_{st}}$, where P_{st} = stiffness-tension, for definition see p. 84.
ordinate: tension, stiffness, and relative stiffness in arbitrary units.
abscissa: time in msec.

period (curve a_1). Here the change in length is of the same order of magnitude as at rest, but from the superimposed oscillation, the period of which is reduced and the damping increased, it can be seen that the state of the fibre has changed. The course of the curve indicates that the increase in stiffness began to develop in the latter part of the transient. In curves b_1 to i_1 the initial change in length was reduced to about half the value at rest. In curve k_1 the amplitude of the initial change in length increased again, and the velocity of the slow change in length rose (the velocity of relaxation was compensated for). The oscillation period in the damped oscillation was still unchanged, although the initial change in length in the transient

manifested itself at this time only by *large* changes in length. The initial change in length in curve l_1 was the same as that in curve k_1, but the period of oscillation was larger and corresponded approximately to the value found at rest. Shortly afterwards, as

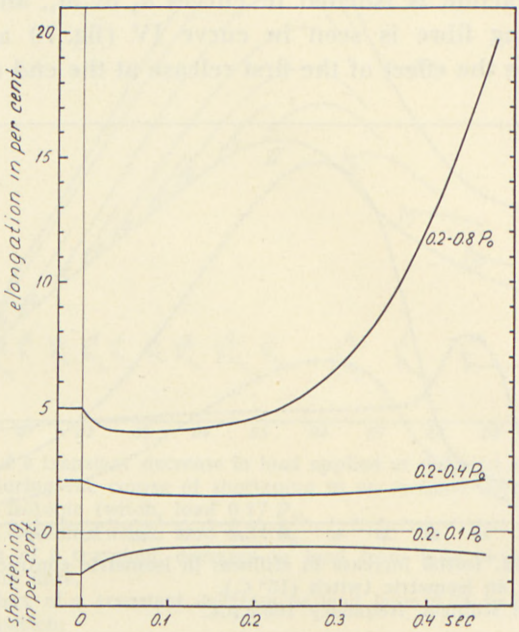

Fig. 74. *Initial* net increase and net decrease in length caused by different transient variations in load applied at different times in the initial phase of contraction (0° C.). The figures on the curves indicate the variations in load in units of P_0. Variations in length measured 15 msec. after introduction of change in load (not corrected for the alterations in shortening velocity produced by the change in load occurring within these 15 msec.).
ordinate: elongation and shortening in per cent of L_0.
abscissa: time after stimulus in seconds.

indicated by m_1, the stiffness for both large and small changes in length displayed the same value as that at rest.

The early maximum in stiffness found in these experiments could also be observed in experiments with the fibre under "*isometric*" conditions (Buchthal and Kaiser 1944). In these experiments periodic vibrations of 100 c.p.s. with an amplitude of 1 per cent of the equilibrium length (20° C.) were superimposed on the fibre. The stiffness was measured by recording the resulting periodic changes in tension at rest, during a twitch,

and a tetanic contraction. Fig. 73 shows the course of the tension, the stiffness and $\frac{\text{stiffness}}{\text{tension}}$ during a twitch of a muscle fibre from the semitendinosus muscle. While the tension during the first 20 msec. rose approximately exponentially, the stiffness increased linearly and the *ratio* between stiffness and tension had a maximum 10—15 msec. after the stimulus (15° C.).

Fig. 74 gives a survey of the resulting change in length obtained under *isotonic* conditions at 0° C. during the first 0.4 sec. after stimulation.[1] The curves show the initial change in length (measured 15 msec. after the change in load), which arose on quick unloading from an initial load of 0.2 P_0 to a final load of 0.1 P_0, or quick loading from an initial load of 0.2 P_0 to 0.4 and 0.8 P_0. During transition from rest to contraction in the course of the first 100 msec. the extensibility of the fibre was decreased very considerably (0° C., comp. GASSER and HILL 1924 and HILL 1949d). This effect was most pronounced during quick loading and unloading at small initial loads. As mentioned, the elongation was measured 15 msec. after the transient and the changes in length therefore were the sum of the passive elastic changes and the active ones, which occurred on account of the variation in the shortening velocity caused by the different load. The latter change in length amounted to 0.4—0.5 per cent of L_0 within 15 msec. and the passive change in length was therefore 0.4—0.5 per cent of L_0 less than the values measured after 15 msec. The time for the appearance of the maximal stiffness (corrected in this way) and the value of the corresponding shortening in per cent of the maximal shortening at load P_1 (initial load) are given in Table 12. The time taken for the propagation of the contraction over the fibre is of secondary importance in this connection (see p. 34).

After the maximum in stiffness was passed, the extensibility increased again and at the maximum of shortening reached or exceeded that of the resting fibre. Also, in experiments in which the stiffness was measured by periodic vibrations, the stiffness in the later course of a twitch was seen to attain values lower than those at rest.

[1] The sensitivity employed in the present experiments would not permit the recording of a latency relaxation (SANDOW 1944, 1947, see p. 147).

TABLE 12.

The time for the occurrence of the maximum in stiffness.

P_1	P_2	time for the occurrence of maximal stiffness in msec.	shortening in per cent of maximal shortening
0.20	0.10	250	50
0.20	0.40	200	35
0.20	0.80	70	14
0.40	0.20	300	69
0.07	0.26	250	75

P_1 denotes the initial load and P_2 the load after transient.

On account of a "give" in the structure, the higher the quick load, the earlier the minimum in extensibility was passed during contraction. Thus, the relative increase in stiffness during transition from rest to contraction, measured at the time for maximal stiffness, was lowest at high loads. The stiffness was higher during quick *unloading* than during quick loading.

Length-tension diagram for the passive series element, calculated and measured.

By means of the corrected initial "transient" change in length, caused by the quick load, it is possible to determine points on a *dynamic length-tension diagram* for the passive component of the structure during contraction and at rest. This is of special interest in connection with the interaction between the series elasticity and the contractile elements, described by HILL (1949d). Fig. 75 gives values for elongation and shortening in per cent of the equilibrium length, when the load was increased or decreased suddenly from initial load 0.2 P_0 (curve 1). The change in load was introduced 100 msec. after the stimulus, and the change in length measured was corrected for the effect of the shortening velocity due to contraction. The values given in curves 1 and 2 are final values measured 15 msec. after the transient. Curve 2 shows the dynamic shortening or elongation in the resting fibre recorded under the same conditions as curve 1 which represents values for the contracted fibre. From the ratio between increase in tension and increase in length it can be

seen that the stiffness $\left(\frac{\Delta P}{\Delta L}\right)$ during contraction was higher at small loads than at high loads, in contrast to the findings at rest. This is reflected in the fact that curve 1 (contraction) is concave towards the abscissa, while curve 2 (rest) is convex. However, at all loads the stiffness during contraction was higher than the

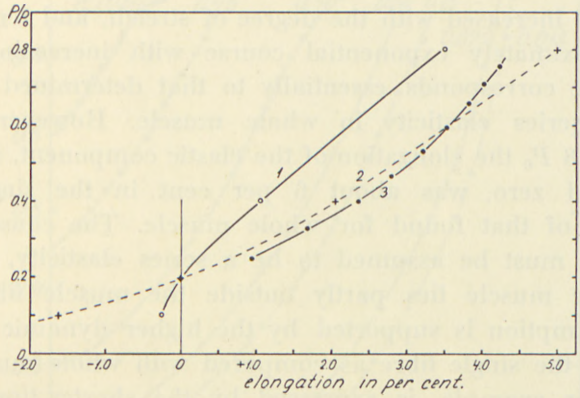

Fig. 75. *Dynamic length-tension diagrams of the series elastic element in a muscle fibre*, 0° C.

curve 1: determined from transient changes in load introduced 0.1 sec. after the stimulus during an isotonic twitch, initial load 0.2 P_0 (compare fig. 74; but in the present example values were corrected for the change in shortening velocity caused by the change in load occurring within 15 msec.).

curve 2: obtained as 1, on resting fibre.

curve 3: calculated from the course of isometric tension and the force-velocity relation, initial load 0.2 P_0.

ordinate: tension in units of P_0.

abscissa: elongation in per cent of L_0.

stiffness at rest. The points of curve 1 and 2 in fig. 75 correspond to the end points of the *partial* length-tension diagrams illustrated in fig. 15.

To summarize, the experiments with transient changes in load applied during an isotonic contraction showed that:

1) the relation between shortening velocity and load was valid when the load was changed suddenly during contraction;

2) the stiffness was maximal at an early stage in the course of shortening (70—300 msec. after the stimulus at 0° C.);

3) the stiffness in the passive series elements was larger during contraction than at rest, and, contrary to the behaviour

at rest, the stiffness during contraction was highest at low loads.

According to HILL (1949d), a *length-tension diagram for the passive series elasticity* can be calculated from the course of the tension in isometric contraction and the force-velocity relation. A length-tension diagram calculated on this basis for the isolated fibre at initial load 0.2 P_0 is given in curve 3, fig. 75. The gradient of tension increased with the degree of stretch, and tension had an approximately exponential course with increasing length. The curve corresponds essentially to that determined by HILL for the series elasticity in whole muscle. However, with a load of 0.8 P_0 the elongation of the elastic component, measured from load zero, was about 6 per cent in the single fibre, i. e. half of that found for whole muscle. The cause of this difference must be assumed to be a series elasticity, which in the whole muscle lies partly outside the muscle fibre itself. This assumption is supported by the higher dynamic modulus found in the single fibre as compared with whole muscle, and which, for example, is expressed by the shorter time (30 per cent) necessary for the isometric maximum to be reached in the single fibre.

Fig. 76 shows calculated length-tension diagrams for the passive series elasticity in the single fibre at different initial loads, obtained from the isotonic and isometric contractions shown in fig. 61. The curves for the different initial loads cannot be made to coincide by a simple displacement in length, which indicates that the gradient for the same tension is different for the different curves. The single points on the curves are separated by a distance corresponding to 10 msec., and it can be seen that the gradient in the length-tension diagram is steepest when the tension rises quickly as a function of time. If, e. g., the length-tension course in the range 0.45—0.6 P_0 (fig. 61) is compared for initial loads of 0.015 and 0.45 P_0, an elongation of 0.55 and 1.30 per cent of the equilibrium length is obtained respectively. This elongation is reached for an initial load of 0.015 P_0 in 27 msec. and for an initial load of 0.45 P_0 in 62 msec. In the curve which started with an initial load of 0.45 P_0 the change in length thus was 0.75 per cent larger and the time interval required for this increase in length was 35 msec. By comparing the increase

in length and the increase in time a relative velocity of elongation of 0.21 L_0 per sec. was obtained.

A systematic investigation in the same fibre of the gradient at the same load, but at different *velocities of rise in tension*, showed

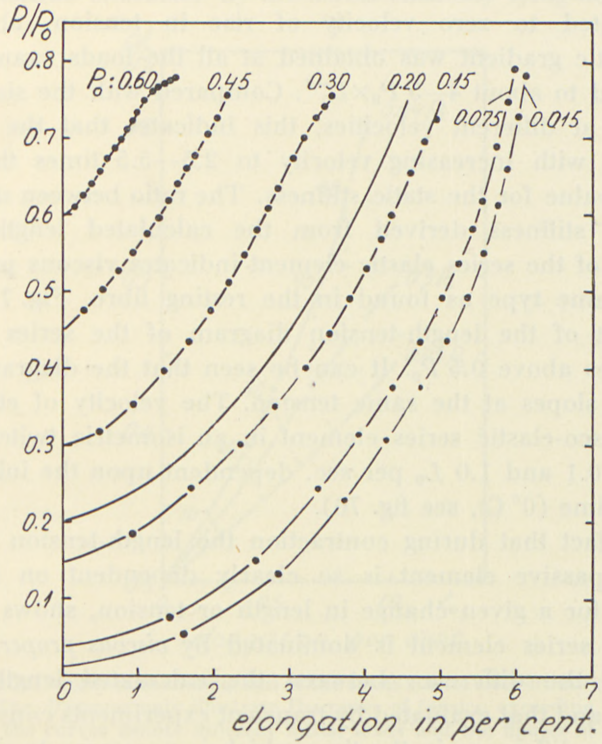

Fig. 76. *Length-tension diagrams of the series elasticity in a muscle fibre*, calculated from the course of tension in isometric twitches and the force-velocity relation. 0° C.
The figures on the curves denote the different initial loads in units of P_0 (curve for 0.2 P_0 interpolated).
ordinate: tension in units of P_0.
abscissa: calculated elongation in per cent of L_0.

that the gradient varied approximately linearly with the velocity of rise in tension. For example, at a load of 0.5 P_0, the following values were obtained for the velocity of rise in tension and the stiffness $\left(\frac{\Delta P}{\Delta L}\right)$:

Velocity of rise in tension in P_0 per sec.	2.2	3.7	4.3	5.9
Length-tension gradient in $P_0 \times L_0^{-1}$	10.6	16.3	18.0	23.5

If the gradients for the different length-tension diagrams were extrapolated to zero velocity of rise in tension, about the same static gradient was obtained at all the loads examined; it amounted to about 4—5 $P_0 \times L_0^{-1}$. Compared with the size of the gradient at different velocities, this indicates that the stiffness increases with increasing velocity to 2.5—5.5 times the extrapolated value for the static stiffness. The ratio between static and dynamic stiffness derived from the calculated length-tension diagram of the series elastic element indicates viscous properties of the same type as found in the resting fibre. Fig. 77 shows *that* part of the length-tension diagram of the series element which lies above 0.5 P_0. It can be seen that the diagrams have different slopes at the same tension. The velocity of elongation of the visco-elastic series element in an isometric twitch varied between 0.1 and 1.0 L_0 per sec. dependent upon the initial load and on time (0° C., see fig. 76).

The fact that during contraction the length-tension diagram for the passive element is so clearly dependent on *the time* elapsing for a given change in length or tension, shows that the assumed series element is dominated by *viscous properties.* The cause of the difference between the calculated length-tension diagram and that evaluated by transient experiments consequently lies in the difference in the time which is necessary to obtain the data of length and tension. In the diagram measured from transients a given change in length was reached within 10 msec., in the calculated diagram the same change was developed within about 200 msec. (curve 1 and 3, fig. 75). Although the mechanical properties of the series element thus have a predominantly viscous character within the range so far mentioned (up to 300 msec. at 0° C.), the level during a tetanic contraction shows that the elongation of the series element approaches a limiting value. The series element, therefore, essentially can be described by a Voigt-element (or better a series of Voigt-elements), i. e. a viscosity which dominates during quick transients shunted by an elasticity which limits the change in length.

The findings of HILL (1949 d) on whole muscles of a satisfactory agreement between the calculated length-tension diagram and a diagram obtained at quick release during isometric contraction, can probably be explained by the partial concealment of the viscous character by the series elasticity lying outside the

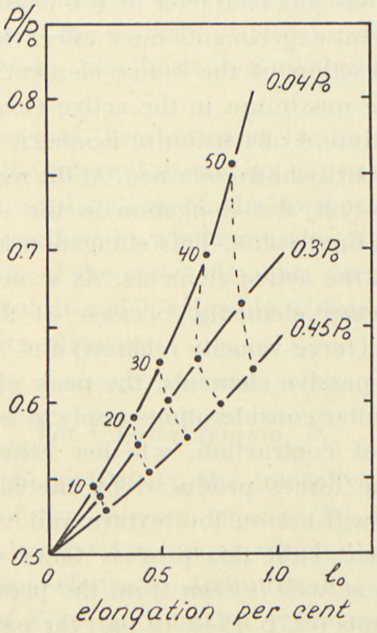

Fig. 77. Partial length-tension diagrams of the series elastic element during isometric twitches. The diagrams only illustrate the range of tension exceeding 0.5 P_0. The figures on the curves denote different initial loads and the figures at the broken lines denote time in msec. after the tension 0.5 P_0 has been passed. (0° C).
Mean velocity of rise in tension:
curve 0.04 P_0 = 5.1 P_0 per sec.
curve 0.30 P_0 = 3.3 P_0 per sec.
curve 0.45 P_0 = 2.4 P_0 per sec.
ordinate: instantaneous load in units of P_0.
abscissa: elongation in per cent of L_0.

fibres. HILL (1950 b) considers the series element in whole muscle to be an undamped elasticity and does not assume viscous properties to be of importance in the range of the velocities examined.

The analysis of the length-tension diagram of the series element in the single fibre gives, in the same way as HILL (1949 d) has shown for whole muscles, an explanation for the difference

in the time course between a contraction under isometric and one under isotonic conditions, i. e. it helps to understand the fact that the shortening maximum in a twitch occurred at a later point in time than the peak of tension in an isometric twitch.

The markedly viscous character of the passive series element found in the present experiments must affect the views regarding the mechanical reaction of the *active* element. The assumption that the shortening maximum in the active elements coincides in time with the maximum of tension in isometric contraction (Hill 1949 d) thus can hardly be maintained. At the maximum of tension in an isometric twitch, the elongation in the series element has not yet reached its final value. This elongation is compensated for by a shortening in the active elements. As soon as the shortening velocity in the active elements, because of the relatively high tension, decreases (force-velocity relation) and becomes less than the velocity of the passive elements, the peak of the external tension is passed. Similar considerations apply to *isotonic contraction.*

At the onset of contraction, whether initiated isometrically or isotonically, the forces produced by the increase in tension or the shortening will act on the texture and tend to reorganize the textural pattern. That this process takes considerable time during contraction as well is seen from the previously mentioned transient experiments (cf. p. 124). In part the pattern of the texture will behave as a series element to the contractile substance. Its adjustment which proceeds during shortening will effect that even at constant load and at the maximum of shortening the contracting elements still shorten, counteracting the viscous lengthening of the series element. Thus, although the external shortening velocity is zero, this implies that the internal shortening velocity in the active elements is equal to the velocity of elongation in the passive series element.

Hence, the explanation of the *displacement in time of the maximum of tension and shortening* in a twitch, according to the above, is as follows: At the peak of the isometric tension and at the peak of the isotonic shortening the velocity of the viscous elongation in the passive elements is equal to the shortening velocity in the active elements. During the isometric twitch the tension rises rapidly and the viscous series element, which still can be stretched

considerably, elongates rapidly. The velocity of shortening in the active elements is therefore compensated at an early stage by the velocity of elongation in the series element, and an early maximum is obtained. During the isotonic twitch, in which the series element is under an approximately *constant load*, the velocity of elongation is low and at the peak of shortening the compensating influence of the velocity of viscous elongation is of less importance. Therefore, the shortening maximum is displaced to a later time.

The assumption that the shortening in the active elements is not maximal until the external shortening has passed its maximum, may serve as an explanation of the humps in the course of relaxation, also described in whole muscle (HARTREE and HILL 1921). The viscosity of the series elements may cause this hump to occur at the point at which relaxation (desactivation) actually begins in the active elements.

The internal tension, P_i.

According to HILL (1949 d), the intensity of activity is defined by means of the *internal tension* (P_i) in the contractile elements. P_i denotes the tension at which the active elements neither shorten nor elongate. Assuming an undamped series elasticity, values of P_i in the isometric twitch can be determined by the maximum of tension, and in the isotonic twitch, by the maximum of shortening. However, the viscous character of the series element makes it difficult to determine P_i in this way, since the active elements must still be assumed to shorten at the maximum of tension or shortening.

If P_i is determined as a function of time from the maximum of the shortening, then ambiguous values are obtained, i. e. a high and a low value. The shortening maximum at low and high loads was earlier than at intermediate loads (see e. g. fig. 61). If the viscous elongation in the passive series elements is taken into consideration, unambiguous values may be expected for P_i at different loads, and the different positions of the shortening maximum as a function of load in the isotonic twitch can be understood. Assuming that relaxation sets in later when the load is high, it would follow that the shortening maximum also occurs at a later time with a rising load. This assumption is supported by the observation illustrated in fig. 71,

where it is seen that a sudden rise in load in the first phase of an otherwise isotonic twitch caused a considerable delay in the time for the appearance of the relaxation. However, the yielding of the series element will influence the occurrence of the peak of shortening with time in the opposite direction. Hence, the low shortening velocity at a high load is compensated earlier by the velocity of elongation of the passive elements, and the shortening maximum in an isotonic twitch at a high load occurs earlier than at an intermediate load. The time required for the shortening maximum to develop in a twitch thus increases with increasing initial load until the velocity of elongation of the passive elements begins to exert its influence and causes this time to be decreased. Since, as mentioned, the load itself affects the time at which the maximum of shortening occurs, it must be assumed that the relative course of the internal tension as a function of time also varies at a high and at a low load.

Viscous properties of the series elastic element have been shown to account for differences in the gradients of its length-tension diagram which exist at a given load. Moreover, the shape of the computed length-tension diagrams of the visco-elastic series element gives information as to the rôle of the sarcolemma for the mechanical properties of the resting fibre. The fact that the *initial* gradient of the length-tension diagram of the series element increases considerably with load indicates the existence of an interdependence between external stress and orientation of the series element at the moment of stimulation. An increase in load from 0.03 to 0.6 P_0 is associated with an increase of the initial gradient of five times (fig. 76). This increase in orientation requires that external work is invested in the structure which represents the series element at rest. Obviously, this conclusion is incompatible with the assumption that the fibrillar substance does not contribute to the length-tension diagram of the fibre at rest (cf. the discussion of the rôle of the sarcolemma p. 110).

At the onset of contraction the stiffness of the visco-elastic series element amounts to approximately $15\ P_0 \times L_0^{-1}$ and increases during the further development of contraction to about twice this value, i. e. the stiffness is of the same order of magnitude as that found in dynamic experiments on the transition from rest to contraction. Hence, the stiffness in the visco-elastic series element in the range of loads investigated (up to 0.5 P_0) represents the essential part of the total stiffness which develops during contraction, and at the transition from rest to contraction the

stiffness which can arise from the sarcolemma will only be of secondary importance.

Thus, from the discussion above it can be seen that the visco-elastic series element whose presence was demonstrated under isometric conditions, exerts its influence under isotonic conditions as well. It can explain the variation with load in the time required to obtain peak shortening. As long as the value for the lengthening velocity of this element is unknown, it is impossible to determine P_i by the shortening maximum in the isotonic twitch.

The initial shortening velocity as a function of temperature.

The initial shortening velocity depends chiefly on two factors: 1) load, discussed previously, and 2) temperature. The velocity increases with rising temperature. In experiments in which, for each temperature, sufficient time was allowed for complete thermal equilibrium as well as structural changes brought about

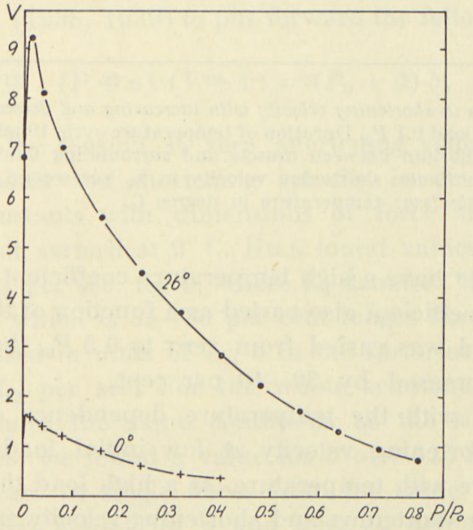

Fig. 78. Force-velocity relation at 26° and 0° C., isolated fibre. *ordinate:* maximum shortening velocity in L_0 per second. *abscissa:* load in units of P_0.

by temperature variation, an increase in the velocity of shortening of 4 to 8 times was found for a difference in temperature of 26 degrees. If the initial velocity as a function of temper-

ature is examined for a series of fibres, one finds a family of curves which converges at some upper temperature (26° C.). This permits the conclusion that the spread of temperature coefficients is not random but a systematic property inherent in the physiological mechanism of different fibres, i. e. fibres with a low initial

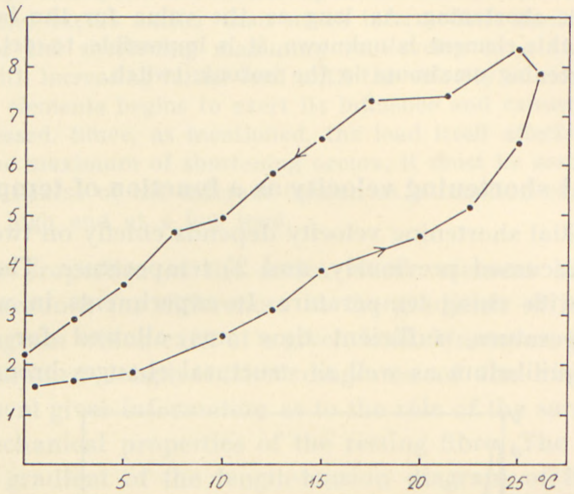

Fig. 79. *Hysteresis in shortening velocity with increasing and decreasing temperature,* isotonic twitches, load 0.1 P_0. Duration of temperature cycle 10 minutes. Regarding temperature equilibrium between muscle and surrounding fluid see text.
ordinate: shortening velocity in L_0 per second.
abscissa: temperature in degree C.

velocity tend to have a high temperature coefficient (fig. 78). The temperature coefficient also varied as a function of the initial load. When the load was varied from zero to 0.5 P_0, the temperature coefficient increased by 30—40 per cent.

Compared with the temperature dependence of shortening, the initial shortening velocity at low initial loads varied considerably more with temperature. At a high load the temperature coefficients for shortening and shortening velocity are of the same order of magnitude.

Measurement of the shortening velocity during continuously rising and continuously falling temperature showed, at the same temperature, higher velocity of shortening during falling than during rising temperature. This difference might amount to half of the total variation in velocity in the range 0° to 25° C.

A series of experiments carried out with temperatures rising from 0° to 25° C. within 5 minutes and falling back to 0° within the next 5 minutes showed a hysteresis which could not be explained on the basis of an incomplete temperature equilibrium between the Ringer's solution and the fibre, since the time for thermal equilibrium of the fibre did not exceed 1 second (fig. 79). The cause of the hysteresis must be sought in a delay in the temperature-dependent adjustment in the minute structure. A hysteresis in the adjustment of the structure caused by variations in the temperature is well known from plastics. A similar hysteresis was also found in the muscle fibre in measurements of the membrane potential (BUCHTHAL and LINDHARD 1936).

Hill's equation.

The fact that the variation in the initial shortening velocity with the load represents one of the best reproducible expressions for the dynamic properties of the muscle during contraction, has led HILL (1938, 1939) to put forward the following equation:

$$(P + a) \cdot (V + b) = (P_0 + a)\, b, \qquad (62)$$

where P_0 is the tension at zero shortening velocity and P the load. V denotes the shortening velocity in cm per sec. and a and b constants with dimensions of force and velocity respectively. For sartorii at 0° C. HILL found values of 0.25 P_0 for a and 0.33 L_0' per sec. for b, where L_0' denotes "natural" length, i. e. a length which is 35—50 per cent longer than the L_0 of the fibre. Expressed in units of L_0, b in the sartorius, therefore, becomes 0.45 L_0 per sec. For the whole semitendinosus muscle, examined under the same conditions as the single fibre and small bundles, we found a value for a of 0.125 P_0 and for b of 0.38 L_0 per sec. In single fibres from the same muscles values of 0.30 P_0 were found for a and 0.92 L_0 per sec. for b. The values for a and b in isotonic contraction were about twice as large as the constants measured for the same fibre during afterload contraction. Three experimental series of this type thus gave:

$$\frac{\text{a (isotonic)}}{\text{a (afterload)}} = 1.87 \quad \text{and} \quad \frac{\text{b (isotonic)}}{\text{b (afterload)}} = 1.93.$$

In a whole muscle, in which the length during contraction under isotonic conditions is limited by the shunting connective tissue or by a small number of fibres, which on account of a small equilibrium length are maximally loaded, the rest of the fibres work under afterload. Hence, it cannot be expected that afterload conditions for the whole muscle will give a similar difference in the constants of the equation as that found in the single fibre.

For whole sartorius muscles HILL (1938) found that the value of a corresponds to the heat of shortening. If the same were true for semitendinosus, a transformation of the values found for a in whole muscle and single fibre to g/cm^2 by means of the values for P_0 listed in Table 10 would give a heat of shortening in the single fibre which is four times that in whole muscle, i. e. for the fibre $a = 841$ g/cm^2 and for whole muscle $a = 213$ g/cm^2 (0°C). Even when the value of a for whole muscle is corrected for the 30 per cent passive substance, we still have so large a difference between a in the fibre and in the muscle that it is incompatible with the assumption of a as shortening heat.

On account of the different values found for the constant a in isotonic and afterload contractions one might expect that the heat of shortening in the fibre during isotonic contraction would be nearly twice as large as that during afterload. Hence, in the case of the single fibre the constant a can hardly be considered to correspond to the heat of shortening, but can only be interpreted as an arbitrary constant in the empirical relation between load and velocity.

The constants *a* and *b* in the single fibre and in whole muscle.

The difference in the mechanical reaction between the single fibre and the corresponding muscle may be due to the factors: (1) different equilibrium lengths of the single fibres in the muscle, causing different degrees of stretch, and (2) shunting connective tissue. In the semitendinosus muscle, in which the fibres run from tendon to tendon, the shunting connective tissue can be assumed to act only slightly as a limiting factor for the shorte-

ning velocity. However, a difference in length between the different fibres was found.

We have examined the distribution of the fibre lengths in a semitendinosus muscle. For this purpose the muscle was fixed at its natural length. 15 per cent nitric acid (ROMEIS 1928) was used for fixation and was allowed to act for 2—3 hours. The muscle was then washed in water and the single fibres with their

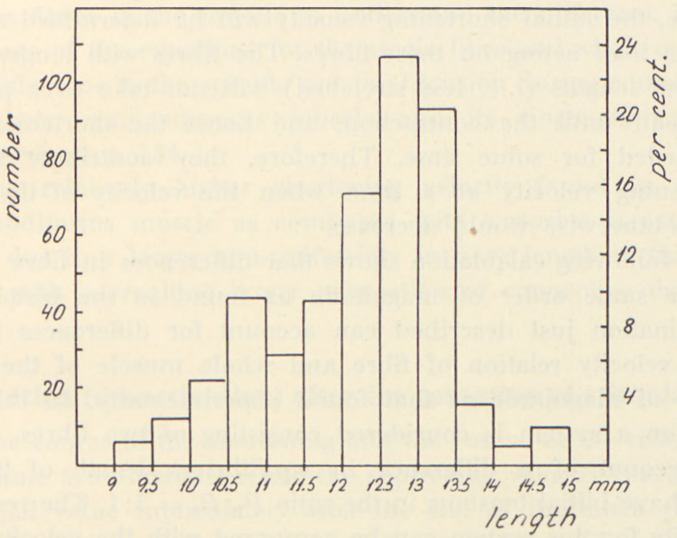

Fig. 80. Distribution of fibre lengths in the semitendinosus, Rana temporaria.
left ordinate: number of fibres in the different ranges of length.
right ordinate: number of fibres in per cent.
abscissa: length in mm.

corresponding tendon ends could easily be isolated. The number of fibres in the muscle examined was 515, of which a length determination could be carried out on 458. The length varied between 9 and 15 mm with a mean value of 12.25 mm and a standard deviation of 1.14 mm (fig. 80). According to this distribution, the average difference in length for two fibres selected at random was 1.25 mm, corresponding to a difference in length of 10 per cent. There is a 30 per cent probability of a difference in length of > 2 mm, corresponding to more than 15 per cent of L_0.

The resulting inhomogeneous state of stretch can explain the

difference between the force-velocity curve for single fibre and whole muscle. It follows from the approximately constant tension in the curve for the isometric maxima over a large range of lengths that a non-uniformity in stretch will hardly affect P_0. At load P_0 the shortening velocity is zero and the diagrams for fibre and muscle coincide, just as the curves have the same starting point when the shortening proceeds without load. The shortest fibres will be subjected to a relatively greater part of the load. Hence, the initial shortening velocity will be determined mainly by the load acting on these fibres. The fibres with longer equilibrium lengths (i. e. less stretched) will not take over part of the load until the contraction, and hence the shortening, has proceeded for some time. Therefore, they contribute to the shortening velocity at a time when the velocity of the short fibres otherwise would decrease.

A following calculation shows that differences in fibre length of the same order of magnitude as found in the histological examination just described can account for differences in the force-velocity relation of fibre and whole muscle of the same order of magnitude as that found experimentally. In this calculation a system is considered consisting of two fibres, which on account of a difference in equilibrium length of 20 per cent have initial tensions in the ratio $P_1 : P_2 = 3 : 1$. The resulting velocity for this system can be compared with the velocity of a whole muscle. In the calculation HILL's equation was applied to the fibres in the range of loads up to P_0. At loads of above P_0, where the shortening is actually an elongation, the velocity as a function of the load, has an almost horizontal course (KATZ 1939), which has been taken into account in the calculations.

In Appendix III, p. 298, the calculations are given of the shortening velocity of the system mentioned above, corresponding to a whole muscle assuming for its fibres: $a = 0.30\ P_0$ and $b = 0.92\ L_0$ per sec. If the computed force-velocity curve is approximated by a hyperbola, we obtain:

$$a_m = 0.145\ P_0 \text{ and } b_m = 0.445\ L_0/\text{sec.}$$

or

$$a_m = 0.120\ P_0 \text{ and } b_m = 0.360\ L_0/\text{sec.}$$

according to the way in which the hyperbola is fitted to the calculated resulting velocity.

The experimental values for a and b from whole semitendinosus muscle were:

$$a_m = 0.125\ P_0 \text{ and } b_m = 0.38\ L_0/\text{sec.}$$

Thus, it is possible from the different state of stretch for the various fibres in the muscle to understand the difference in the constants of the equations for the single fibre and whole muscle. The difference in the specific maximal tension during contraction for whole semitendinosus muscle and its single fibres was discussed on p. 134.

The relatively higher shortening velocity found in whole semitendinosus muscle as compared with sartorius is assumed to be due to a larger non-uniformity in fibre length in the sartorius with a resulting larger proportion of connective tissue.

Relaxation (desactivation) after the cessation of stimulation.

The course of the shortening and the course of the relaxation with time are different. While the shortening velocity reached its maximal value immediately after the end of the latent period, the relaxation velocity did not reach maximum until some time after the cessation of stimulation. In the first phase of shortening, the shortening velocity was approximately constant, while the change in length after the interruption of stimulation followed an S-shaped curve. Therefore, the relaxation velocity rose slowly, reached a maximal value and then decreased slowly again. In tetanic contraction at 0° C., the time interval between the interruption of stimulation and the maximal relaxation velocity was 0.3 sec.

When characterizing in the following the mechanical course of the relaxation by the maximal relaxation velocity (V_d), we are well aware that this is only an approximate description of the whole course of relaxation. The relaxation might also be characterized by the interval elapsing between the interruption of stimulation and the occurrence of maximal velocity. However, since the *maximal relaxation velocity* showed characteristic

variations caused by shortening, load, temperature, duration of contraction, and fatigue, it was convenient to use this parameter in discussing relaxation.

Shortening: At the same load, temperature, and duration of contraction, the maximal relaxation velocity depended on the

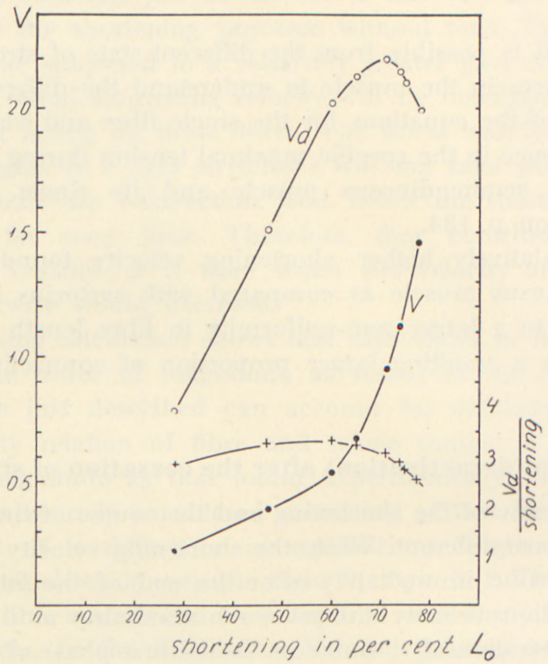

Fig. 81. Maximal shortening velocity (V = •), lengthening velocity (V_d = O) during relaxation, and velocity constant (+) plotted versus maximum shortening during and after different degrees of isotonic tetanic contraction. 0° C., load 0.17 P_0, different strength of stimulation, completely curarized muscle fibre.
left ordinate: velocity in L_0 per second.
right ordinate: velocity constant $\left(\frac{V_d}{\text{shortening}}\right)$ in sec.$^{-1}$.
abscissa: shortening in per cent of L_0.

amount of shortening. A variation of the shortening at the same load could be obtained by varying the strength of the tetanic stimulation from threshold value to three times the threshold value. Fig. 81 shows that the maximal velocity of relaxation increased approximately proportionally with the shortening up to 75 per cent of the maximal shortening, i. e. a shortening of approximately 60 per cent of L_0.

Duration of contraction: Different durations of contraction were obtained by varying the number of stimuli from 1, 2, 3, 4 stimuli up to tetanic contraction lasting 3—10 sec. The duration was defined as the time elapsing between the first sign of shortening and the time at which the relaxation velocity was maximal.

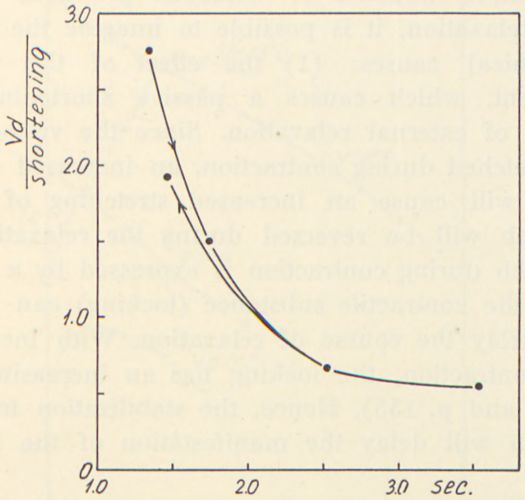

Fig. 82. Decreasing relaxation velocity, expressed as velocity constant, with increasing duration of the isotonic, tetanic contraction, 0° C., load 0.15 P_0. *ordinate:* ratio between maximum lengthening velocity after interruption of stimulation and maximum shortening ("velocity constant" in sec.$^{-1}$). *abscissa:* duration of contraction in seconds.

Since the maximal relaxation velocity was also affected by the shortening, the course of relaxation was described by the *maximal velocity of relaxation per unit of shortening* (in sec.$^{-1}$). Within the range of proportionality between shortening velocity and shortening this "*velocity constant*" expresses the effect of the duration independent of the shortening reached. The velocity constant decreased with increasing duration of contraction (fig. 82) and the effect was most marked during transition from a twitch to a tetanic contraction. The duration of contraction required for the velocity constant to approach constant values varied inversely with the load in the different experiments, i. e. for high and low loads the extreme values were 3 and 8 sec. respectively. That the effect on the relaxation velocity was not caused by fatigue was seen from control contractions of short

duration released 1—2 sec. after a tetanic contraction of long duration. The controls *immediately* showed high relaxation velocity.

The decreased velocity of elongation occurring with increased duration of contraction may be due to different factors. Apart from a possible influence of metabolic products, which may counteract relaxation, it is possible to imagine the two following mechanical causes: (1) the effect of the visco-elastic *series* element, which causes a passive shortening reducing the velocity of external relaxation. Since the visco-elastic element is stretched during contraction, an increased duration of contraction will cause an increased stretching of series elements, which will be reversed during the relaxation. (2) the process which during contraction is expressed by a mechanical *shunt* over the contractile substance (locking) can also be assumed to delay the course of relaxation. With increasing duration of contraction, the locking has an increasing influence (see p. 131 and p. 155). Hence, the stabilization in the structural pattern will delay the manifestation of the internal relaxation.

Fatigue: Numerous repetitions of contractions of the same duration gradually caused a reduction of the relaxation velocity to about the same extent as the shortening itself was reduced. Thus, the velocity constant was not significantly affected by fatigue. Both the relaxation velocity and the shortening were more affected by fatigue than the shortening velocity. When relaxation velocity and shortening during fatigue had fallen to 35 per cent of the initial values, the shortening velocity was only reduced to 60 per cent of the initial value.

Load: As a function of the load, the relaxation velocity after tetanic contraction always had a maximum at 0.2 to 0.4 P_0 (fig. 62 and 83). The maximum value of the relaxation velocity varied considerably from fibre to fibre and, when referred to the same load, could even exceed the shortening velocity by 20 to 25 per cent.

Temperature: It is well known from experiments on whole muscles that over a considerable range of loads the temperature dependence of the relaxation velocity is larger than that of both the shortening velocity and of the shortening. Fig. 83 shows the

shortening and relaxation velocities as a function of the load during tetanic contraction at 0° C. and 26° C. At loads $> 0.2\ P_0$ the temperature dependence of the relaxation velocity was always larger than that of the shortening velocity. This difference in-

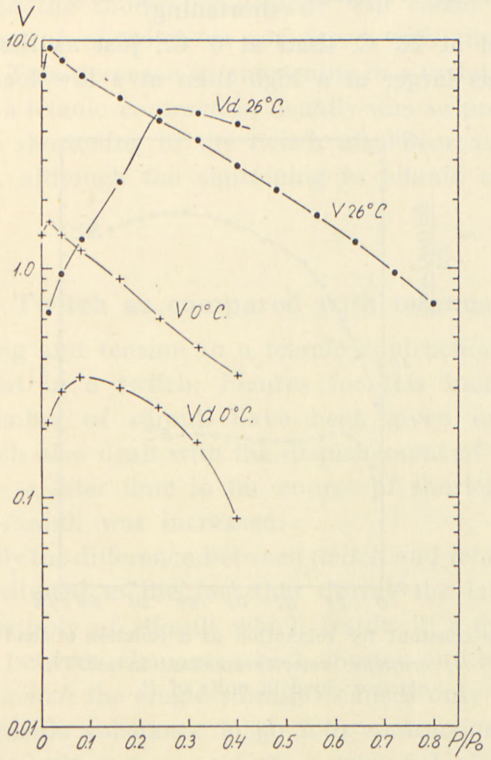

Fig. 83. Maximal shortening velocity (V) and lengthening velocity (V_d) during and after isotonic tetanic contraction (duration approximately 1 second), 0° and 26° C.
ordinate: velocity in L_0 per second, logarithmic scale.
abscissa: load in units of P_0.

creased with increasing load. At load $0.25\ P_0$ the relaxation velocity thus increased 20 times and the shortening velocity 7 times, when the temperature rose from 0° to 26° C.; at $0.4\ P_0$ V_d increased 50 times and the shortening velocity only 8 times for the same rise in temperature. In the range of load 0 to $0.2\ P_0$, where V_d increased rapidly with load, the temperature dependence was less than at high loads, and at loads $< 0.1\ P_0$ it may be less than the temperature dependence of the shortening velocity.

The experiments at 26° C. also showed a maximum for the relaxation velocity as a function of the load. This maximum occurred at higher loads than the maximum in experiments at 0° C. The velocity constant $\left(\frac{Vd}{\text{shortening}}\right)$ varied more markedly with the load at 26° C. than at 0° C., just as the temperature coefficient was larger at a high than at a low load (fig. 84).

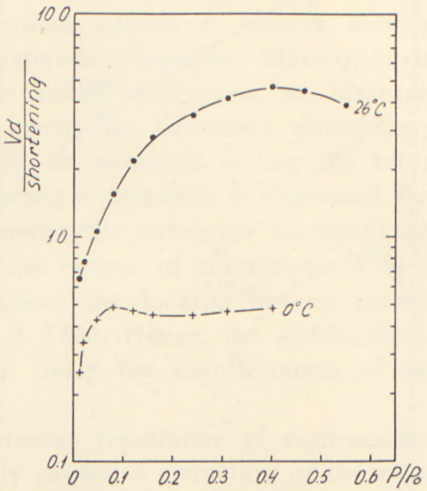

Fig. 84. Velocity constant for relaxation as a function of load at 0° and 26° C.
ordinate: velocity constant in sec.$^{-1}$.
abscissa: load in units of P_0.

The larger temperature dependence found for the relaxation velocity, as compared with the shortening velocity, supplies an explanation for the difference in the influence of temperature on the shortening in a twitch and in a tetanic contraction. As previously mentioned, the shortening in tetanic contraction increased markedly with rising temperature, while the shortening in twitch increased much less, or decreased. Both in a twitch and in a tetanic contraction the relaxation appears externally *after* the end of the stimulation. In a twitch this occurs so early that a considerable shortening velocity can still be present. At the peak of the twitch the external shortening velocity is zero, but that of the active elements is compensated for by the velocity of elongation in the visco-elastic series element.

At high relaxation velocity and high velocity of stretch in the passive elements, the shortening velocity is compensated at an early time and hence the maximal shortening is reduced. The fact that relaxation velocity rises more rapidly with rising temperature than the shortening velocity will cause a decrease in the shortening of a twitch as compared with that of a tetanic contraction. This decrease in shortening in a twitch as compared with that in a tetanic contraction usually was so pronounced that the absolute shortening in the twitch also decreased with rising temperature, although the shortening in tetanic contraction increased.

Twitch as compared with tetanus.

Shortening and tension in a tetanic contraction considerably exceeded that in a twitch. Figures for this increase with increasing number of stimuli have been given in a preceding section, which also dealt with the displacement of the shortening maximum to a later time in the course of shortening when the number of stimuli was increased.

Essentially the difference between *twitch* and *tetanic contraction* must be attributed to the fact that during the latter there is a continuous supply of stimuli which results in a quasi-stationary equilibrium between elements which shorten and elements which relax. In a *twitch* the single stimulus causes only a limited part of the contractile substance to go into contraction, since relaxation has desactivated part of the contracted elements already before the shortening maximum has been arrived at. In addition, when a single stimulus is applied the limited possibility of activation might also be a limiting factor. Thus, shortening in a twitch often comprises only a minor fraction of that attained in tetanic contraction. This is true even when the relaxation velocity is low as compared with the shortening velocity, due consideration being given to the more limited time available for the development of a twitch.

It remains to explain why the initial shortening velocities during a twitch and a tetanic contraction following maximal stimulation are identical. Apparently this finding is in contradiction with the assumption that relaxation starts to act in a twitch

before the maximum in shortening has been reached. However, there are a number of observations which indicate that there is an upper limit for the velocity with which contractile substance can be activated, regardless of the number of stimuli applied. Hence, the stimuli will only be effective gradually. Examples for this "storing" of stimuli with a following delay in the

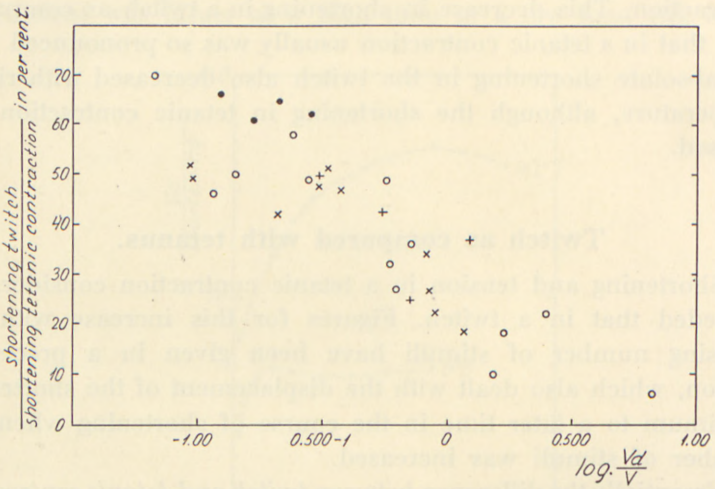

Fig. 85. Correlation between the ratio of shortening in the isotonic twitch and tetanus and the ratio of relaxation and shortening velocity.
ordinate: peak shortening of twitch in per cent of the shortening in tetanic contraction.
abscissa: ratio between maximal relaxation velocity and shortening velocity in tetanic contraction, logarithmic scale.

maximum of activation have been given in a previous section (cf. p. 141).

The reduced shortening found in a twitch as compared with a tetanic contraction at different loads and temperatures can be explained roughly by the joint effect of shortening and relaxation velocities and of a limited possibility of activation by virtue of the single stimulus applied.

The external shortening and relaxation velocities can, with certain reservations, be considered to correspond to the same quantities in the contractile elements themselves. On this basis, an attempt has been made to correlate the ratio of the peak shortening in a twitch and the maximal shortening in a tetanic contraction with the ratio of the relaxation and shortening velocities in a tetanus.

Each point in fig. 85, where the abscissa denotes the logarithm of $\frac{V_d}{V}$ and the ordinate the ratio between shortening in a twitch and in a tetanic contraction, corresponds to a mean value from experiments on at least five different muscle fibres or small fibre bundles. The points include experiments at high and at low temperature, and at high and low load in non-fatigued fibres and at different degrees of fatigue. Regardless of these different experimental conditions, the *relative shortening in the twitch as compared with that of the tetanic contraction* decreased with increasing $\frac{V_d}{V}$. For a fixed value of this ratio, shortening in a twitch as a fraction of the shortening in a tetanic contraction varied on an average 8 per cent and at most 15 per cent. This spread must be attributed to the fact that $\frac{V_d}{V}$ in the active substance can only be reflected with approximation in the external reaction of the fibre. A direct transfer of changes in length and tension in the contractile elements is prevented by their organization in the texture. Furthermore, as mentioned above, the external relaxation velocity is the sum of relaxation and shortening velocities in the contractile component.

Initial total activation or gradual activation?

The present explanation of the difference between twitch and tetanus deviates essentially from that suggested by HILL (1949c). We assume a continuously increasing degree of activation with increasing shortening. Hence, the shortening velocity is considered to be an expression of the velocity with which the contractile elements are activated. According to HILL the degree of activation (contraction intensity, P_i) is practically maximal at the onset of shortening or tension. This implies that the whole contractile substance simultaneously is thrown into contraction.

The finding that the increase in stiffness develops much faster than both tension and shortening has been considered one of the main indications of the early and total activation. However, as previously described, in the isolated fibre both longitudinal and torsional stiffness did not reach their maximum values until

$\frac{1}{3}$ to $\frac{1}{2}$ of the time necessary for the attainment of the shortening maximum had elapsed. Also in whole muscle GASSER and HILL (1924) and HILL (1949 d) have demonstrated that maximal stiffness is reached only about twice as fast as the maximum in tension.

According to HILL the early maximum in stiffness indicates an initial maximum activation of the contractile component. Its activity is transmitted through a passive series element which does not give external manifestations of stiffness until some shortening has developed and has stretched the series element. The explanation suggested here assumes a gradual development of activation in contractile chains which are more or less aligned (slack). The question is, however, whether the fact that the maximum in stiffness occurs earlier than the maximum in tension, is consistent with the assumption of a gradual activation of the contractile substance during the development of contraction. In a homogeneously aligned contractile substance it should be expected that the stiffness increases proportionally with the degree of activation. Our suggestion that not all contractile elements contribute simultaneously to the onset of tension would imply an *initial* rise in stiffness as well. Under *isometric* conditions the slack chains, as their lengths become comparable with the taut ones, will contribute to the *stiffness* in finite increments, so that as a function of time the stiffness builds up quite rapidly as more and more slack chains are recruited. Moreover, remembering the general property that stiffness increases with rising tension, as the tension in the various chains increases, so will their stiffness and thereby the total stiffness will increase as well. On the other hand, the *tension* contributed by each chain as its slack is taken up will not occur in steps, but will gradually rise from zero.

Similarly, under *isotonic* conditions on account of their higher shortening velocity, the slack chains will catch up with the loaded ones and contribute stepwise to the total stiffness, whereas they only gradually assume their share in the load, and, thus again the rate of the increase in stiffness will be greater than that of the shortening. The finite initial contribution of a chain to stiffness will be equal to the stiffness present in it in the state at which it is "captured" by the load. With the tension rising in the whole texture the intrinsic forces will increase and with progressing

contraction cause a "give" in the contractile elements which will tend partially to diminish the mechanical effect of the rise in stiffness (cf. also BUCHTHAL *et al.* 1944a). In the equivalent system the yielding which occurs during contraction both under isometric and isotonic conditions is symbolized by the viscous series element previously mentioned (cf. p. 170).

The assumption of a non-uniform state of internal tension in the contractile elements as a cause of the early maximum in stiffness is supported by the finding that the maximum is most pronounced at a small initial load. There the slack is most pronounced in the resting fibre. The same mechanism can explain the previously described changes of elastic and viscous stiffness with vibrational amplitude (cf. p. 102). If one assumes that the disappearance of slack is the main cause of the initial rise in stiffness, the course of stiffness with time can hardly prove or disprove an initial total activation.

The early development of *heat of activation* within the latent period is used as an argument in favour of an initial maximal activation (HILL 1949c, 1950a). However, the time course of heat of activation can also be attributed to the heat production which accompanies the shortening in slack chains (cf. p. 283). HILL's (1950c) finding that heat of activation develops more slowly when contraction is initiated at high loads than at low loads can also be explained by assuming a gradual activation.

As discussed in detail in Part IV, the interpretation suggested in the present paper gives a suitable basis for a quantitative explanation of the variation of shortening velocity with load, a finding difficult to understand from the assumption of a total initial activation. It can also help to understand the previously mentioned "storing" of the effect of successive stimuli.

Active or passive relaxation.

From the analysis of the course of relaxation as a function of load and temperature, it is possible to discuss certain aspects of the problem of relaxation. An *active* relaxation implies the assumption that the contracted state is a state of equilibrium for the contractile substance, and that the resting length is reached by an active extension of the contractile elements after the

cessation of stimulation. Contraction may be interpreted as the removal of a "barrier" to shortening, and the potential energy decreases during the shortening and is then rebuilt during the active relaxation. A *passive* relaxation, on the other hand, means that the process of contraction is active, since the mechanical energy is not stored in the minute structure of the resting fibre. During transition from rest to contraction the energy content of

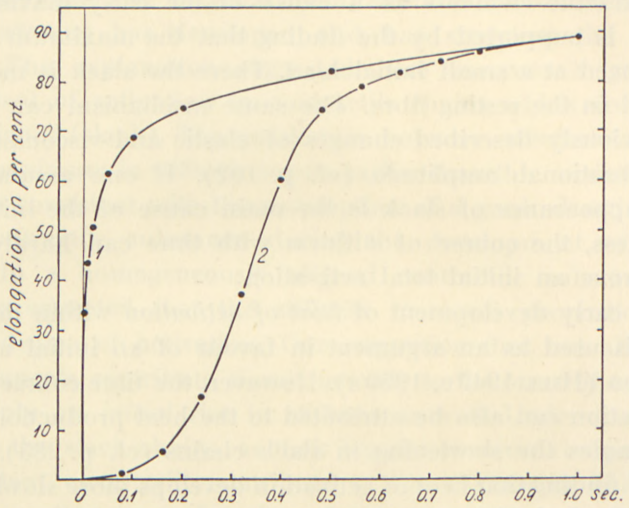

Fig. 86. Comparison between the course of adjustment in the resting fibre and during relaxation from isotonic tetanic contraction. 0° C.
curve 1: resting fibre, initial load 0.05 P_0, suddenly loaded by 0.2 P_0.
curve 2: relaxation of isotonically contracted fibre after interruption of stimulation (load 0.2 P_0).
ordinate: elongation in per cent of L_0.
abscissa: time in seconds.

the fibre increases. Hence, the beginning of relaxation only indicates the end of the state of contraction, whereupon the elasticity of the contractile substance acts to reestablish the resting length of the entire texture. In passive relaxation, the transition from contraction to rest denotes the time at which the external load begins to pull out the shortened—but desactivated—minute structural elements to the resting length. The velocity with which this stretching occurs can be determined with good approximation by applying a sudden load to the resting fibre (transient). An unavoidable source of error in the evaluation of these experiments consists of non-contractile, elastic series

elements, which also are present in the fibre, although to a less extent than in whole muscle. Hence, before comparing a transient at rest and the elongation during relaxation it will be necessary to investigate to what extent the deformation during transient on the resting fibre takes place in the *contractile* elements. This information is provided by the length-tension diagrams. A fibre which had contracted without tension and then was loaded with $0.5\ P_0$ was stretched by about 15 per cent of L_0. When the fibre was loaded at rest, the corresponding increase in length amounted to about 100 per cent of L_0. Therefore, it must be concluded that the essential part of the stretch in the resting substance occurred in the contractile elements. Consequently, the transient course shown in fig. 86 (curve 1), illustrating the effect of quick loading with $0.2\ P_0$ in a resting fibre with small initial load, is essentially an expression of the mechanical reaction of elements which participate actively in the contraction (for the rôle of the sarcolemma see p. 110). Curve 2 in the same figure shows the course of relaxation after isotonic contraction at the same load ($0.2\ P_0$, 0° C.) as applied during transient extension at rest. A comparison of these two curves, in which the same passive shunting elasticities were involved, shows that the visco-elastic resistance to elongation, as it manifests itself in transient experiments, can only be an insignificant delaying component in the course of relaxation after contraction.

The difference in the course of the curves, however, cannot be interpreted as evidence of an active relaxation, since it can equally well mean that the process of contraction does not disappear abruptly at the end of stimulation, and that some substance still is found in the contracted state some time after stimulation has been interrupted. The S-shaped course of the relaxation curve thus expresses the statistical distribution of the times for the transition of the different elements from contraction to rest. The course of the curve does not permit a decision whether this time is due to active or passive processes.

Since KÜHNE (1859) described that a muscle contracted on a surface of mercury, i. e. without influence of external deforming forces, does not straighten again, relaxation in a tensionless muscle has been of importance in the discussion of active or passive relaxation. KAISER (1900) repeated these experiments and re-

duced the friction of the muscle by surrounding it with a film of olive oil and found that the muscle rapidly regained its equilibrium length after the end of stimulation. The muscle returned so rapidly to its original shape that KAISER considered this to be caused by elastic forces. However, in experiments on whole muscle HILL (1949e) was recently able to confirm the findings of KÜHNE that the muscle retains its contracted length after the end of stimulation. Using the latent period as indicator, which in spite of the short length is not increased, HILL concludes that the short length at rest is caused by a real shortening of the fibre and not by "slack".

The single fibre, which at rest hangs tensionless in a loop between two suspension points in Ringer's solution and shortens during contraction, regains its original length immediately after the end of the stimulation (RAMSEY, cit. from FENN 1945). This observation, however, can hardly give any contribution to the problem of active or passive relaxation. The contractile substance itself must be assumed to have a natural length to which it returns after the end of the contraction.

The unloaded length of the fibre is determined by the equilibrium between the tension in the fibrils and the longitudinal forces arising in the sarcolemma (see p. 117). Thus, the equilibrium length of the fibrils is not necessarily identical with the equilibrium length of the fibre. A radial pressure exerted by the sarcolemma at equilibrium length will normally be sufficient to elongate the fibre after a contraction in the tensionless state.

HILL (1949d) has calculated the straightening elastic force which e. g. can arise on account of differences in the colloid-osmotic pressure in the fibre and the surrounding fluid, and found that this force, which is of the same order of magnitude as the weight of the fibre, would be sufficient to explain the spontaneous alignment found by RAMSEY. This interpretation, however, cannot apply to experiments which we have performed with the fibre suspended in Ringer with the same colloid-osmotic pressure as plasma; also in these experiments we found that the fibre resumed its initial length immediately after the end of stimulation. Experiments in which the elastic forces in the resting fibre (length 110—120) were measured in Ringer's solution and in a moist chamber in air, demonstrated the presence of an

aligning force in the single fibre and in small fibre bundles large enough to cause return to the resting length. With the fibre bundle in Ringer at a low load, a stiffness could be measured which was up to 40 per cent higher than the stiffness of the fibre in the moist chamber in air (p. 28). The difference in stiffness corresponds to a change in load equal to several times the weight of the fibre. These experiments show that a force large enough to cause alignment really occurs when the fibre is in Ringer's solution. When the fibre is placed in air, this force is probably counteracted by the surface tension in the Ringer film, which still surrounds the fibre. The fact that a whole muscle does not show the spontaneous relaxation means that the aligning force cannot, as in the fibre, overcome the mechanical hysteresis. The lack of an external elongation may consequently be due to an increased hysteresis or decreased forces of alignment. A deformation in the pattern of the connective tissue during shortening can cause an increased resistance to elongation. On the other hand, the fact that the fibres of the whole muscle can be compressed without curling (see p. 136) may cause a decreased resistance to shortening by the locking, and consequently weaker forces will be present for an elongation during relaxation.

An important argument, apparently in favour of passive relaxation, is HILL's (1949b) finding that heat production during relaxation of a tensionless contracted muscle is zero, and that heat production during a relaxation proceeding under load, does not measurably exceed the energy which is introduced from outside (increase in length × tension).

As previously described during the discussion of "locking" (see p. 155), a marked internal resistance which considerably exceeds the external forces, develops in a contracting fibre. This tension must cause a large internal work of deformation, which may appear as heat during relaxation. During the tensionless relaxation it might, therefore, be assumed that the external heat production is zero, because the expected heat of deformation is compensated for by a negative heat production, assumed to be connected with the process of relaxation. Also during relaxation under tension a considerable internal work of deformation must be released as heat, in addition to the work of deformation introduced from outside.

Apart from the "spontaneous" relaxation after the end of stimulation, described here, there are indications that during tetanic stimulation an additional relaxation may be enforced by a load considerably in excess of P_0 (HILL 1939). This relaxation similarly might be assumed to be connected with a negative heat production. The heat production during stretching of an activated muscle with a tension between P_0 and $2\,P_0$ is less than the work involved (HILL 1937, 1938, FENN 1923, 1924, AUBERT 1948). Thus, it is possible to measure a negative heat of shortening, which according to the considerations given here, corresponds to the negative heat of relaxation. The unexpectedly low heat production on stretching means that part of the mechanical energy introduced increases the potential energy of the structure or becomes transformed into chemical energy. Part of the heat released in the muscle as initial heat must thus be expected to be re-absorbed in the relaxation phase.

It is obvious from the preceding discussion that neither the study of mechanical properties nor the measurement of heat production can give an unambiguous answer to the problem of active or passive relaxation. On the other hand, in view of the theory for the mechanism of contraction developed in a later section of this paper, it seems rather doubtful that this is a pertinent question when dealing with the problem of relaxation. According to this hypothesis the contractile substance is assumed to consist of minute structural chains with elements which may occur in two states of equilibrium, a short and a long one. The energetic potential of these two states will be of the same order of magnitude. Contraction is defined as an increase in probability of the occurrence of short linkages in proportion to the long modification. Hence, contraction and relaxation are considered only to be consequences of changes in probability of these two states. On this basis it will hardly be meaningful to talk about active or passive relaxation.

Work and rate of work production.[1]

The area between the length-tension diagram at rest and the curve for the isometric maxima represents theoretically the upper

[1] A preliminary report of these experiments has been given in Acta neurol. psychiat. 1949, **24**. 333.

limit for the net work which a fibre is able to perform during a cycle of work, i. e. stretching from zero tension to maximal tension at the indifference point (negative work) followed by active shortening (positive work). However, this would be valid only if the tetanic shortening followed the curve for the isometric maxima (with due regard to the elastic aftereffect). This, how-

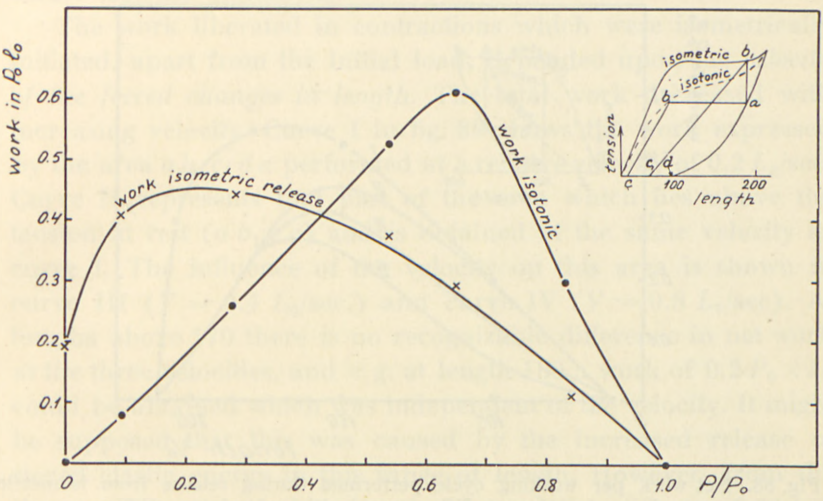

Fig. 87. Work as a function of the load in isotonic tetanic contraction and in release from isometric tetanic contraction, release velocity 0.2 L_0 per second, 0° C. The inset length-tension diagram in the right corner shows the areas for work beginning at the resting point *a*. Work during isotonically started contraction corresponds to the area within points *a b c d a*, work during release contraction to the area *a* b_1 c_1 *d a*.
ordinate: work in units of $P_0 \times L_0$.
abscissa: initial load at rest in units of P_0.

ever, is not the case. Even if sufficient time is allowed for complete adjustment of the tension to the new length, the tension during release is considerably lower than that reached in the isometric maximum (locking, see length-tension diagram during release, p. 130).

In the following section an account is given of the part played by the mechanical conditions present at the onset of contraction for the net amount of external work. For this purpose a comparison has been made between the external net work in *isotonically* started contraction (corresponds to *a—b* in fig. 87) and an *isometrically* attained contraction (corresponding to *a*—b_1). The

initial phase of the isotonic contraction is characterized by a constant tension and shortening velocity, and hence work is produced with constant velocity. When initiated isometrically the contraction is characterized in its initial phase by constant length, increasing tension, and storage of elastic energy. In the subsequent release phase (b_1—c_1 and b—c) the remaining part of

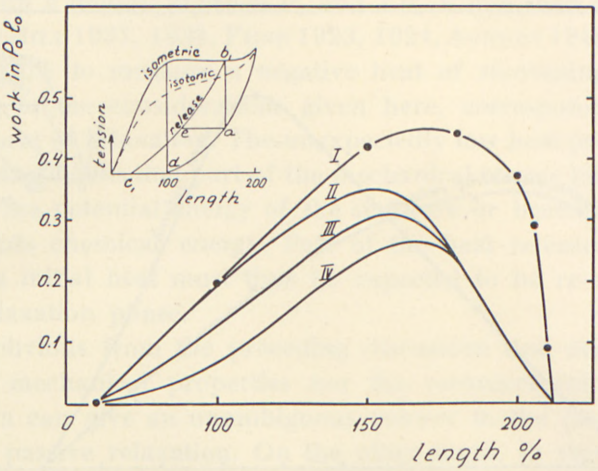

Fig. 88. Net work per working cycle performed during release from isometric tetanic contraction at different velocities of release. 0° C.
curve I: net work at total release, work represented by area $a\ b_1\ e\ c_1\ d\ a$ in inset length-tension diagram. Release velocity 0.2 L_0 per second.
curves II—IV: work during release from isometric tetanic contraction to the same tension as initially present at rest (area $a\ b_1\ e\ a$).
release velocities: curve II 0.2 L_0 per second, curve III 0.4 L_0 per second, curve IV 0.8 L_0 per second.
ordinate: work in units of $P_0 \times L_0$.
abscissa: initial length in per cent of L_0.

the work is liberated which contraction can produce. It consists partly of stored elastic energy, and partly of energy originating from continuation of the contraction process during continued stimulation. In contraction which is evoked during isotonic conditions the net work corresponds to the area of $a\ b\ c\ d\ a$, and in isometric release contraction to the area $a\ b_1\ c_1\ d\ a$. Fig. 87 shows the work under these conditions as a function of the initial load and with a release velocity of 0.2 L_0 per sec.

At a high initial load the net work was largest during a contraction which was started isotonically. The curve had its maximum at 0.65 P_0 and the work, in units of $P_0 \times L_0$, was 0.60. The position of

the maximum here corresponded to length 200. At a load 0.4—0.5 P_0 the work was the same during both types of contraction, and at a low load the work was largest during an isometrically induced contraction. In this case the maximum occurred at an initial load of 0.25 P_0, corresponding to a length of 180 and was 25 per cent lower than the maximal work during contraction started under isotonic conditions.

The work liberated in contractions which were isometrically initiated, apart from the initial load, depended upon the *velocity of the forced changes in length*. The total work decreased with increasing velocity. Curve I in fig. 88 shows the work expressed by the area $a\,b_1\,c_1\,d\,a$ performed at a relative velocity of 0.2 L_0/sec. Curve II represents that part of the area which lies above the tension at rest ($a\,b_1\,e\,a$) and is obtained at the same velocity as curve I. The influence of the velocity on this area is shown in curve III ($V = 0.4\ L_0$/sec.) and curve IV ($V = 0.8\ L_0$/sec). At lengths above 170 there is no recognizable difference in net work at the three velocities, and e. g. at length 180 a work of 0.2 $P_0 \times L_0$ could be obtained which was independent of the velocity. It might be supposed that this was caused by the increased release of stored elastic energy in this range of length. However, from the linear stiffness-load relation and with a relative stiffness of 30 L_0^{-1} at most a work of 0.015—0.03 $P_0 \times L_0$* could be expected. During sudden release of whole muscle HILL (1950) found tension over only 2—3 per cent of the "natural length", i. e. 3—5 per cent of L_0. The work obtained hereby is only 0.015—0.025 $P_0 \times L_0$, hence, considerably less than the work which does not vary with the velocity (see also p. 125). The fact that part of the work is independent of velocity (fig. 88) can be explained by assuming

* Assuming a stiffness-load relation:

$$\frac{dP}{dL} = \varkappa (P + P_{st})$$

the work W liberated during release from load P_1 to P_2 will be:

$$W = \frac{1}{\varkappa}\left(P_1 - P_2 - P_{st} \log \frac{P_1 + P_{st}}{P_2 + P_{st}}\right)$$

Putting $\varkappa = 30\ L_0^{-1}$ and $P_{st} = 0.05\ P_0$ one obtains for $P_1 = P_0$ and $P_2 = 0$:

$$W = 0.028\ \ P_0 \times L_0$$

and for $P_1 = P_0$ and $P_1 = 0.5\ P_0$:

$$W = 0.0155\ P_0 \times L_0.$$

that there is less time for the manifestation of locking, the higher the release velocity. Thereby the inhibiting influence on the amount of work released is concealed. At lower initial length the velocity of the contraction process itself begins to influence the amount of energy released, probably because locking is developed more slowly at lower length (fig. 67). The decrease in the total external work with rising release velocity is in agreement with the observation that the shortening velocity decreased with increasing load. This relation implies on the other hand, that the muscle force—and hence also the work performed—must decrease with increasing velocity.

As a special type of work performed partly under isotonic conditions, the work produced in *afterload contractions* was examined. Here the total shortening, referred to the isotonic load, was less than during isotonic contraction (see p. 130). Hence, the net work was less than the work which started under isotonic conditions, and the difference was relatively greater, when the length was limited at low degrees of stretch and when the load was high.

The amount of work absorbed when a tetanically contracted fibre was stretched, exceeded essentially that liberated in isotonic tetanic contractions or afterload contractions. The tension in the former slightly exceeded P_0, i. e. rose above the curve of the isometric maxima. Thus, the work absorbed in stretch during contraction was considerably larger than $P_0 \times \Delta L$.[1] In isotonic contraction and in release contraction from initial load $0.5\ P_0$ the total work produced was approximately $0.45\ P_0 \times L_0$ with a change in length of 100 per cent of L_0 (0° C., fig. 87). For the same change in length the work absorbed in stretch during tetanic contraction was $1.2\ P_0 \times L_0$. Thus, in order to perform the same amount of work in isotonic or afterload contraction on the one hand and in stretch contraction on the other, in the latter only 40 per cent of the fibre mass is necessary as compared with the former.

The force-velocity relation (Hill 1938), even when corrected for forces $> P_0$ (Katz 1939), can only account for a minor part of the difference between the two types of work. This is illustrated by the following example:

Comparing the work done by the brachial biceps during raising

[1] ΔL = elongation.

and lowering of the body in two subjects we found that the lowering, which was performed with the same velocity as the raising (within 5 sec.), was carried out at least three times more easily, using fatigue or the integrated number of action potentials as a measure. In recent experiments ASMUSSEN (1951) has demonstrated a difference of the same order of magnitude when the oxygen consumption was used as a measure of the intensity of work. To simplify the comparison, the differences in torque during different phases of the work were disregarded and constant load was assumed during both raising and lowering. Assuming that the change in length of the biceps muscle during raising and lowering of the body maximally is 30 per cent and the time allowed for the movement in each direction was 5 seconds, the mean velocity will be 0.06 muscle lengths per second. With $\frac{P_0}{a} = 4$ and $b = 1$ muscle length (HILL 1940) the tension during body raising will be 0.93 P_0 and during body lowering 1.40 P_0. During lowering of the body some of the fibres go out of action and the remaining fibres, for a longer or shorter period, are under a load $> P_0$. In this comparison it is taken into consideration that for $P > P_0$ the force-velocity relation no longer follows HILL's equation, the slope of the curve being considerably reduced (KATZ 1939). Thus a difference in work of maximally 50 per cent can be accounted for. However, actually the difference is at least 200 per cent and, as mentioned above, it can be explained without difficulty by the differences in the length-tension relation during afterload contraction (body raising) and stretch contraction (body lowering). The former proceeds along a length-tension diagram which is considerably lower than that of the isometric maxima. Therefore, in order to lift the load, a larger number of fibres must be put into action. During lowering, fewer fibres can equilibrate the same load.

Rate of work production.

In *isotonic* contraction the rate of work production (measured in $P_0 \times L_0$/sec.) was calculated as the product of shortening velocity (V) in relative units and the corresponding relative load.

A discussion of the maximal shortening velocity as a function of load and temperature was given in an earlier section (see p. 148, 175). The maximum of the rate of work production lay at load 0.3 to 0.4 P_0, i. e. at half the load required for maximal total work.

During *isometric release contraction* with constant *forced* release velocity, the determination of the velocity of work is encumbered with difficulties. During release work is liberated partly on account of active shortening and partly on account of stored elastic energy accumulated during the rise in tension in the initial isometric phase. Since it is impossible to distinguish between these two effects during release, the *mean velocity of work production* was used as a measure of the rate of work production. The mean rate of work production is defined as the total work divided by the time taken to perform this work. The time necessary for the isometric increase in tension (0.1 sec.) was also included in this time. A comparison between the rate of work production in isotonic contraction and in isometric release contraction, necessitates investigation of the *mean* rate of work production in isotonic contraction as well. In the isotonic contractions we have used a contraction period of the same duration as that used in isometric release contraction (0.5 sec.). In both isotonic contraction and isometric release contraction, the maximal mean rate of work production was reached at an initial load of 0.3 to 0.4 P_0. The rate of work production amounted to about 0.3 $P_0 \times L_0$ per sec. Fig. 89 shows the way in which the rate of work production decreased during isometric release, when lower relative velocities were used (0.4 and 0.2 L_0 per sec.). On release with velocities of $< 0.2\ L_0$ per sec. the rate of work production decreased linearly with the release velocity. Independent of the release velocity, the rate of work production had its maximum at an initial load of 0.3 to 0.4 P_0.

The rate of work production in *whole* muscles determined during isotonic contraction, varied as a function of the load similarly to that found in single fibres or small bundles. The maximum also lies at 0.3 to 0.4 P_0, but the maximum in a whole semitendinosus muscle is only 0.2 $P_0 \times L_0$ per sec. However, this is higher than the maximum in sartorius muscle, for which we found a maximum rate of work production of 0.125 $L_0 \times P_0$ per

sec. These results show that, at the same load, the rate of work production in the single fibre, is considerably higher than in whole muscle. The difference between fibre and whole muscle decreases the more uniform the fibres of the muscle are with regard to relative

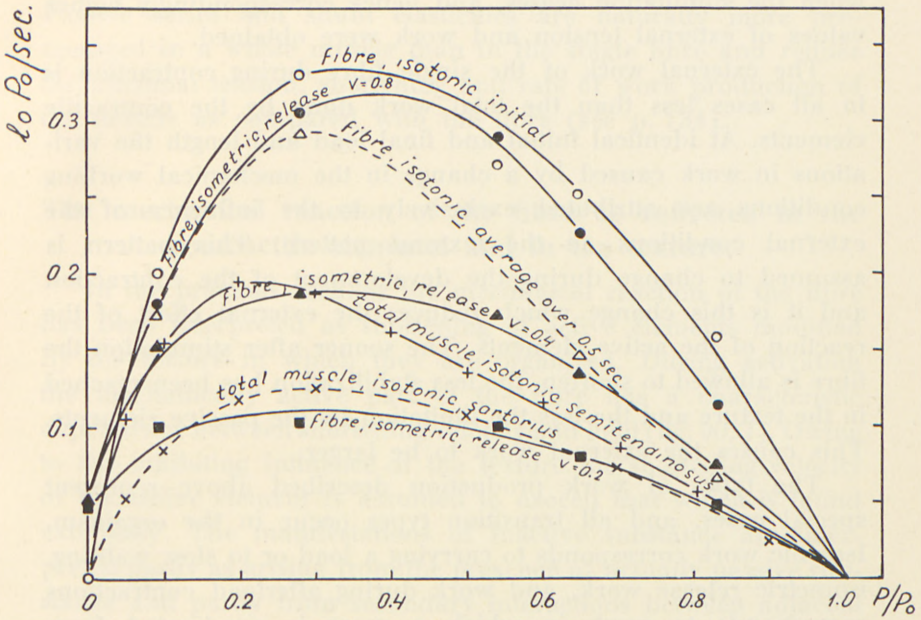

Fig. 89. *Rate of work production* in a single fibre (from m. semitendinosus) and in the total muscle (m. semitendinosus and m. sartorius). Release from isometric tetanic contraction with different velocities of release (0.2, 0.4 and 0.8 L_0 per second) averaged over the first 0.5 seconds of a contraction. 0° C.
O — — — O — — — O isolated fibre, isotonic contraction,
initial rate of work calculated from initial shortening velocity.
× — — — × — — — × whole sartorius, isotonic contraction,
initial rate of work calculated from initial shortening velocity.
ordinate: rate of work in units of $L_0 \times P_0$ per second.
abscissa: initial load in units of P_0.

length and the more of the fibres are aligned in the longitudinal direction at equilibrium length.

The results shown in fig. 87 and fig. 89 were obtained on the basis of shortening and tension in experiments with *continuous* tetanic contraction. Previous experiments have shown that an increase in the yield of work of up to 50 per cent could be obtained when the stimulation was interrupted for a short period during a release contraction. This additional work was obtained in spite of the fact that the fibre was desactivated during

part of the total period of work (BUCHTHAL 1942). The cause of this difference was considered to be the limiting influence which the locking had on shortening in a continuous cycle of work whereby the yield of work is reduced. The locking is interrupted when the stimulation ceases, and hence correspondingly higher values of external tension and work were obtained.

The external work of the single fibre during contraction is in all cases less than the total work done by the contractile elements. At identical initial and final load and length the variations in work caused by a change in the mechanical working conditions are attributed exclusively to the influence of the external conditions on the textural pattern. This pattern is assumed to change during the development of the contraction and it is this change which reduces the external effect of the reaction of the active elements. The sooner after stimulation the fibre is allowed to shorten, the less stabilization has been reached in the texture and the less the limitation by the passive elements. This causes the external work to be larger.

The types of work production described above represent special cases, and all transition types occur in the organism. Isotonic work corresponds to carrying a load or to slow walking, isometric release work, and work during afterload contractions corresponds to work in which a mass is accelerated from velocity zero, e. g. as in a jump. The maximum for both types of work investigated lies at a high degree of stretch (length 180 and length 200). Even if there are whole muscles which in nature cannot attain this elongation, some of their individual fibres which often do not run through the whole length of the muscle may exhibit the degree of stretch necessary to obtain maximal values of work. An elongation of the whole muscle of 50 per cent may thus correspond to an elongation of 100 per cent or more of some of its fibres.

Comparing the isolated fibre with the whole muscle, the geometric arrangement of the fibres and their relation to the pattern of connective tissue has to be taken into account. In the cases in which connective tissue shunts contractile substance, the types of contraction at a definite degree of stretch may be changed from an isotonic to an "internal" afterload contraction. The stiffness of the connective tissue acts as a stop for the length of

the fibres. The connective tissue which occurs in *series* with the contractile substance causes the velocity of development of tension in isometric contraction to be delayed by the work which the fibres must perform in order to stretch the passive substance. Passive series and shunt elasticities are naturally more pronounced in a whole muscle than in the single fibre and reduce the maximal tension, shortening and rate of work production of the muscle as compared with the fibre (see p. 134).

The mechanical reaction of the fibre as reflected in the contractile elements and in the texture.

In the previous sections the mechanical reaction of the fibre has been interpreted as shortening of active elements modified by the texture in which they are organized. During activation the mechanically active part of the fibre has a characteristic dependence between shortening velocity and load (fig. 90, *1*). Owing to the inhibiting influence of the texture the shortening velocity of the active element is assumed to exceed that which is found externally. The manifestations of inactive substance are interpreted partly as arising from the presence of actually passive substance and partly from secondary interactions between adjacent chains of contractile elements (entanglements, fig. 90, 2). These points of entanglement are distributed at random and slack chains (4) occur between the points. On activation the slack chains will tend to catch up with the taut ones (3). Hereby the intrinsic tension in the structure will increase both longitudinally and transversally. This increase in the tension will cause a higher resistance towards both an increase in length and in cross-section, i. e. it will impede shortening. The gradual disappearance of slack which occurs on activation will by the better alignment of the structure cause an increase in longitudinal orientation (a_1). Simultaneously chains which are orientated transversely (a_2) when activated will cause an increase in transverse stiffness. The initial rise in the ratio between the transverse and longitudinal moduli which occurs at an early time after the onset of contraction indicates that the resulting effect is an initial decrease in longitudinal orientation (Sten-Knudsen 1950). Thereafter the longitudinal orientation increases. This increase which occurs with deve-

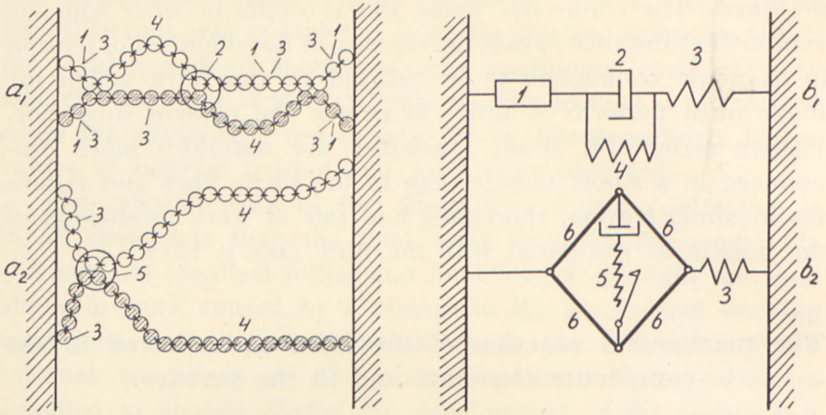

Fig. 90. Pattern of minute structure in a muscle fibre and its mechanical analogue.

a_1: two contractile chains with long range elasticity with three points of entanglement, one example marked with circle 2.
(1) and (3) parts of the chains under stress,
(4) part of the chain with slack.

b_1: (1) corresponds to contractility in chains under stress (1 and 3 in a_1),
(2) symbolizes viscosity caused by rearrangement in points of entanglement (e. g. 2 in a_1),
(3) longitudinal elasticity in elements under stress (1 and 3 in a_1),
(4) shunt elasticity caused by the variation in slack (4 in a_1),
(2), (3) and (4) act as series components to the contractile component (1).

a_2: molecular pattern accounting for shunt elasticity during contraction. Two contractile chains entangled at (5).
(3) part of chain which gives rise to strong transverse structural forces, when the fibre diameter increases during shortening.
(4) parts of the chains with slack.

b_2: bar-polygon (6) symbolizing the resistance against an increase in cross section converted to a shunt element impeding shortening.
(5) catch mechanism with series viscosity symbolizing entanglement (5 in a_2),
(3) series elasticity in the catch mechanism (corresponding to the elasticity 3 in a_2).
b_2 acts as a shunt to b_1 impeding its mechanical reaction.

loping contraction is considered to be caused by the "slip" in the texture which occurs with increasing intrinsic tension. Thereby a better alignment of elements will be produced and a sharp decrease in transverse stiffness relative to the longitudinal one.

On account of the practically constant volume, the shortening is accompained by a corresponding increase in cross-section. In the equivalent diagram the transmission between transverse forces and longitudinal forces is symbolized by a rhombic structure

with articulating joints (6) which represents the increase in diameter on shortening.

When new points of entanglement are loaded during the development of contraction, disruptures occurring at random will cause an increase in orientation and length by rearrangements, and hence be shown externally as series elasticity (2, 4, and 3 in a_1 and b_1, fig. 90.) and as shunting elasticity (3 and 5 in a_2 and b_2) of a markedly viscous character. The viscosity is a result of the time necessary for regrouping. The difference in the textural pattern shown in the diagram between series (a_1) and shunt (a_2) elasticities is schematic. In reality, as mentioned above, a random mixture of more or less longitudinally and transversely orientated structural elements must be considered. In connection with points of entanglement, slack causes a viscous series elasticity (longitudinal orientation, a_1, b_1) at one point of the structure and an increased shunting stiffness at *another* point (transverse orientation, a_2, b_2).

According to the interpretation given here, the stiffness during contraction is a complex quantity and is the result of an interaction of the following three factors: a change in the geometric pattern of the texture during activation, a rise in the number of activated elements, and a rise in the stiffness of the contracting elements themselves. Hence, the early maximum in stiffness cannot be considered to be an indication of an initial maximum intensity of activation.

Chemical findings likewise suggest the establishment of a more rigid textural pattern during contraction. (Dubuisson 1950 a, b). This is concluded from the change in extractibility of the structural proteins. In the contracted state myosin β and protein y are non-extractable by 0.6 M KCl, which extracts these proteins in the resting muscle. Moreover, a new protein (myosin γ = "contractin") appears. These changes are considered to indicate the formation of new and more solid linkages between the components of the structural proteins.

Summary of Experimental Results.

The object of the present paper is a study of rheological properties of the resting and the activated muscular substance. The experiments were performed on *isolated fibres* or small bundles of frog's semitendinosus representing the smallest functioning unit which can be isolated from a living striated muscle. In spite of the fact that the isolated muscle cell undoubtedly is examined in an environment different from the physiological, the influence of which it is difficult to evaluate, the study of the isolated muscle fibre involves many obvious advantages. Thus, in the analysis of mechanical properties part of the complications are avoided which naturally arise from the pattern in which the fibres are organized in the whole muscle, such as the transmission of the mechanical effects to the outside, a non-uniform state of stretch in different fibres, connective tissue, etc. Moreover, it is possible to select fibres with a constant cross sectional area and the small diameter of the fibre allows fast transmission of heat and fast diffusion from or to the surrounding medium. Consequently, the use of isolated fibres brings about essential advantages both experimentally and in the evaluation of the experimental results.

The study of rheological properties comprises *static* experiments, *transient*-experiments, i. e. an analysis of the course of adjustment after quick stretch or quick loading, and *vibration* experiments, i. e. the application of periodic changes in length or load with different frequencies of vibrations. The temperature used in most of the experiments was 0° C., being referred to as a standard condition.

The resting muscle fibre.

The tension of the resting muscle fibre increases exponentially with increasing load. Therefore, the static stiffness $\left(\frac{\Delta P}{\Delta L}\right)$ increases linearly with the load. Within a range of elongation which must be assumed to represent physiological conditions, i. e. up to 70 per cent of stretch, the tension of the fibre is essentially the result of the fibrillar substance. The sarcolemma hardly contributes to tension until stretch exceeds 50 per cent of the equilibrium length (Casella 1951).

The stationary value of tension increases with increasing temperature, the increase being maximal at 20 per cent of stretch (BUCHTHAL *et al.* 1944a). In the application of simple thermokinetical considerations it is necessary to remember that the temperature coefficient is always less than that which corresponds to a proportionality to the absolute temperature.

The *hysteresis* in the mechanical properties as it is revealed e. g. in recording the length-tension diagram with increasing and decreasing load was systematically investigated by applying sudden changes in load or length to the fibre (transients). The variation in load (ΔP) as compared with the initial load (P) was examined for values which varied between 0.1 and 3, the maximal value of ΔP being 0.5 P_0 and the minimum value 0.04 P_0. It could be demonstrated in these experiments that the time delay in the mechanical adjustment, i. e. the elastic aftereffect, can account quantitatively for the hysteresis. Over a large interval of time the velocity with which the new length adjusts itself after a quick loading or unloading varies approximately in inverse proportion with time. This course of adjustment, which can be followed from less than 10 msec. to several minutes after the transient, is described by means of a distribution of retardation times in a Voigt-model. The spectrum of retardation times extends over several decades. There is good agreement between the changes in length after a sudden increase and after a sudden decrease in load, the constants characterizing the course of adjustment in both cases being approximately identical. At *a high temperature* (25° C.) the adjustment within the first 10 msec. after the transient occurs faster than at 0° C. and thereafter more slowly. In the Voigt-model this behaviour corresponds to an increased representation of short retardation times.

However, even when small changes in load are applied, there are properties which cannot be appropriately described by a Voigt-model. The fibre exhibits *thixotropy*, both in the initial phase of stretch during a transient loading and in the effect of repeated transients on the stiffness. In the initial phase of a transient loading the mechanical reaction of the fibre is dominated more by a viscous resistance than by elasticity as compared with the vibrational elasticity measured with the same change in load. Repeated quick loadings cause a transient decrease in stiffness.

The original stiffness is regained after a recovery period of a few minutes.

In *vibration experiments* performed at a constant mean load ("isotonic") it was possible to differentiate accurately between elastic and viscous components in the mechanical reaction. As a measure of these properties we have used *elastic* and *viscous stiffness* determined at the resonance frequency of the oscillating system, in which the muscle fibre provides the directional force and the inertia corresponds to the equivalent mass of the recording system at the point of attachment of the fibre. The damping is produced by the "viscous resistance" of the fibre. At resonance the inertial forces of the system equilibrate the elastic forces of the fibre. Therefore, *elastic stiffness* is $m \times \omega_0^2$, where ω_0 represents the cyclic vibrational frequency at resonance and m the equivalent mass. At resonance the viscous resistance of the fibre is in equilibrium with the external force applied and *viscous stiffness* is defined as the ratio between the external force and the vibrational amplitude produced by it. The vibrational stiffness was found to be of the same order of magnitude as that found from the initial elongation produced by *small* transient changes in load. Immediately after a sudden change in load the vibrational stiffness exceeds its adjusted value by approximately 50 per cent. This final value is obtained in the course of several seconds. *Elastic stiffness increases linearly with the load.* Over the range of frequencies examined (25—150 c.p.s.) it varies only insignificantly with the vibrational frequency, while viscous stiffness increases with increasing frequency. A decrease in vibrational frequency to one fourth causes a decrease in viscous stiffness of 25 to 50 per cent.

In a standard fibre 1 cm long the dynamic elastic stiffness at 0° *C. amounts to 18—20 dynes* cm^{-1} *per dyne load* (vibrational amplitude[1] 1 per cent of L_0, frequency 25—100 c.p.s.).

The elastic stiffness decreases with increasing *amplitude of vibrations.* Expressed by $\frac{d\,(\log \text{ stiffness})}{d\,(\log \text{ amplitude})}$ the amplitude dependence for vibrational amplitudes of 0.5 to 2 per cent[1] of the equilibrium length at low loads amounts to 0.3 and at high loads decreases to 0.1. The amplitude dependence cannot be accounted for by

[1] $\frac{\text{peak to peak}}{2}$.

the non-linear course of the length-tension diagram, but is explained by assuming that the number of loaded minute structural elements varies *within* the period of vibration. The average number of elements participating in the load during the oscillation will decrease with increasing vibrational amplitude, i. e. slack will occur in a larger part of the period of oscillation. Thixotropy originating from slack will enhance this effect.

The dynamic elastic stiffness varies considerably more with *temperature* than the static tension. With increasing temperature the elastic stiffness decreases on an average 1 per cent per °C.

Dynamic viscous stiffness is of the same order of magnitude as the elastic stiffness, but its temperature coefficient is twice as large (2 per cent per °C.). The temperature dependence is most pronounced at low loads. Viscous stiffness increases with increasing load as well, but less than proportionally to the load. As a function of the amplitude, viscous stiffness has a maximum around amplitudes of 0.1—0.4 per cent of the equilibrium length.

A decrease in the *water content* of the fibre causes an increase of both elastic and viscous stiffness, while an increased water uptake does not produce significant variations in these quantities. This means that at the normal osmotic concentration that part of the structure which is deformed by the mechanical vibrations is fully hydrated and water acts as a "plasticiser". The viscosity measured by vibrations or in transient experiments is a structural viscosity, the resistance produced by the viscosity of the sarcoplasm (Rieser 1949) being more than 10000 times less. The sarcolemma tube as such gives hardly any significant contribution to the viscous component of the structural stiffness, delayed elasticity being here much less pronounced than in the intact fibre. Moreover, the difference between static and dynamic stiffness is less in the sarcolemma tube than in the intact fibre. In the latter dynamic stiffness (vibrational frequency 25—150 c.p.s.) exceeds the static by 3—5 times. The static stiffness is measured by differentiation of the adjusted length-tension diagram and the *static modulus* of the resting fibre at equilibrium length amounts to $0.50—0.63 \times 10^6$ dynes per cm^2. The *dynamic modulus* with the resting fibre at equilibrium length was 2.5×10^6 dynes per cm^2 (0° C., vibrational frequency ca. 30 c.p.s., vibrational am-

plitude 1 per cent of L_0). The *difference between dynamic and static* stiffness decreases with increasing load. The transition from dynamic to static conditions can be derived from the course of adjustment in transient experiments and is described by the Voigt-model mentioned above.

The analysis of the mechanical reaction of the resting muscle fibre thus reveals that there are delayed mechanical adjustments with retardation times extending over an interval from 0.1 msec. to several minutes. The slow adjustment is considered to arise exclusively from transitions in the *texture* of the fibre, i. e. the pattern in which the minute structural elements are organized. The short retardation times taken together with the relatively high degree of orientation in the unloaded fibre indicate that the adjustment occurs *within* the minute structural elements as well.

The muscle fibre has rubber-like elasticity, and the organization of its minute structure involves the assumption of transverse forces. Their existence is proved by measurements of torsional stiffness. This exceeds that of an ideally parallelized anisotropic substance without points of entanglement by twenty times at low degrees of stretch and by 5 times at length 200 (STEN-KNUDSEN 1950). Thus, in the muscle fibre there are essential deviations from a pure parallel orientation of the structure. Compared with the longitudinal modulus the torsional modulus in a muscle fibre is ten times less than in a randomly orientated isotropic body (STEN-KNUDSEN 1948).

The transverse forces are considered to arise from deformations in the structure between its points of entanglement in the incompletely parallelized substance. These points of entanglement cause a non-uniform distribution of tension in the different minute structural elements and under certain conditions only part of the structure will participate in the load. Especially at low loads an essential part of the structure will consist of *slack elements*. With increasing elongation the number of loaded elements will increase, slack will decrease, resulting in a higher degree of mechanical anisotropy. In the range of small loads the increase in stiffness with load can be accounted for by an increase in the number of minute structural elements which participate in the load. Assuming the presence of slack, it is possible to account quantitatively for the large variation of

elastic and viscous stiffness with the vibrational amplitude. The fact that this amplitude dependence increases with increasing sr[1] indicates moreover that an increasing viscous stiffness prevents adjustment of the slack which arises *within* an oscillation period. Finally, on this basis it is possible to explain the mechanical and thermal changes which occur at an early time after the activation.

The contracted muscle fibre.

The length-tension diagram of the isolated fibre in the tetanic contraction, i. e. the curves of the isometric and isotonic maxima have an S-shaped course. The isotonic maxima always lie below the isometric, and the curve of release contractions[2] is still lower than that of the isotonic maxima. These differences are not the result of an incomplete *final* adjustment caused by insufficient time to adjust (cf. also the difference between afterload and stop-contractions). The reduced external tension obtained when the fibre shortens as compared with the tension which develops under isometric conditions is explained by an internal resistance arising from the stabilization of the textural pattern in the development of a contraction (elastic locking). Thereby the shortening is inhibited. Thus, differences in the *initial* adjustment during contraction determine the tension arising under the different conditions for contraction. The increased resistance in the texture develops gradually during contraction and is most pronounced when tension is developed over a long period of time before the fibre is allowed to shorten and when shortening occurs slowly. The maximal tension in tetanic contraction at 0° C. amounts to 2.75×10^6 dynes per cm^2 and increases approximately 1 per cent per degree C. with rising temperature. The shortening at 0° C. in tetanic contraction amounts to approximately 100 per cent of the equilibrium length (load 0.1 P_0) and increases 20 per cent when the temperature rises to 25° C. The temperature dependence of shortening increases with increasing load. The variation in shortening, produced by a change in temperature occurs with a significant delay in time. This hysteresis is not due to delayed temperature transmission to the fibre substance,

[1] $sr = \dfrac{\text{viscous stiffness}}{\text{elastic stiffness}}$.

[2] Release from isometric contraction to the same tension as at rest.

but indicates a delayed adjustment of temperature-dependent equilibria in the texture.

Adjustment to the new length after *quick loading* or unloading applied *during contraction* displays a smaller initial change and a larger and faster creep as compared with the adjustment after a transient in the resting fibre. A change in length, arising in the resting fibre from a preceding loading or unloading is neutralized much faster by a contraction than would be the case if the adjustment continued in the resting fibre. Expressed by the spectrum of retardation times, the course of adjustment after a transient applied during contraction is characterized by a Voigt-model with retardation times which extend over a smaller interval than in the resting fibre.

During contraction *dynamic elastic and viscous stiffness* referred to the same tension as in the resting fibre always exceed that of the resting fibre by approximately 100 per cent (frequency of vibration 25—150 c.p.s.). Static stiffness measured by the slope of the reversible release diagram from isometric contraction can be less during contraction than at rest (BUCHTHAL 1942). The distribution of retardation times in the spectrum for the resting and the contracted fibre helps to understand this difference between static and dynamic stiffness during contraction as compared with that in the resting fibre. With increasing load dynamic stiffness increases during contraction, but approaches rest at a high load. The *temperature dependence* of elastic stiffness during contraction exceeds that of the stiffness in the resting fibre; it amounts to 2.0 per cent increase when the temperature falls 1 degree C. Viscous stiffness varies only slightly more with the temperature in the contracted fibre than at rest (2.2 per cent per °C.).

The dependence of stiffness on the amplitude of vibration is considerably less in the contracted fibre than at rest. It amounts to one fifth of the maximal value found in the resting fibre and, in contrast to what is the case at rest, in the contracted state it does not vary significantly with the load. The decrease in the amplitude dependence of the stiffness during contraction is considered a sign of the shortening of slack minute structural elements, which thereby become aligned. Therefore, the distribution of tension in the contracted fibre is more homogeneous than at rest. An increase in mechanical anisotropy at the level of tetanic con-

traction is also indicated by the change in the torsional modulus which decreases as compared with the longitudinal modulus (STEN-KNUDSEN 1950).

Both vibrational experiments and transients applied at different times after stimulation show that stiffness develops faster than tension and shortening. This initial course of stiffness is interpreted as being due to the disappearance of slack by the fast contraction of unloaded chains. Thereby more and more elements contribute to the external stiffness and always with a finite initial stiffness. The fact that stiffness does not continue to rise with the further development of tension or shortening, but passes a maximal value early in the course of contraction is explained by a yielding in the texture which occurs when the internal tension passes a critical value. Direct signs of this "give" in the structure have been observed (1) when the fibre is stretched during contraction, (2) in the development of the vibrational stiffness on the tetanic level of an isometric contraction, and (3) in the decrease of the contraction tension when the vibrational amplitude exceeds a critical value (4 per cent of the equilibrium length, peak to peak). Therefore, the maximum in stiffness can hardly be considered a suitable expression of a *maximum intensity* of activation, which exists in the initial stage of the contraction.

The *shortening velocity* of the isolated fibre decreases with increasing load according to a hyperbolic function and follows essentially HILL's equation (1938), but with different values for the constants a and b as compared with those found for whole muscle. These constants vary both with temperature and with the initial mechanical conditions for the contraction. If the temperature rises from 0° to 25° C., the velocity increases 4—8 times according to the initial value of the shortening velocity. As was the case with shortening, shortening velocity adjusts itself with a time delay to changes in the temperature of the surrounding medium.

The non-uniform state of stretch in whole muscle can account quantitatively for the differences in the values for the constants a and b found in the fibre and the whole muscle.

The relation between shortening velocity and load is valid even when changes in load are introduced before or during

shortening. This is demonstrated by quick loadings applied at different times after the stimulus during the course of a twitch.

Tension in isometric contraction develops faster than shortening under isotonic conditions. In agreement with HILL (1949 d) this difference is explained by the effect of a passive element acting in series with the contractile substance. The mechanical reaction of this element as calculated from the force-velocity relation as compared with its reaction at transient loadings indicates that *viscous properties* dominate this element in the initial phase of contraction. Hitherto, this element was considered to correspond practically to an undamped elasticity (HILL 1949 d, 1950 b). The finding of a visco-elastic element acting in series with the contractile elements makes it impossible to determine the internal tension (P_i) at the peak of tension or shortening in a twitch. In the conception of minute structure arrived at in the present paper the properties of the series element are attributed partly to the elasticity of the contractile substance, and partly to the external effects of transitions in the texture subsequent to a change in load or to activation.

In spite of the identity of the initial shortening velocity in a twitch and in a tetanic contraction, the maximal shortening in a *twitch* amounts to only half the shortening attained during tetanic contraction. In contrast to the assumption that contraction also initially is maximal in a twitch and that shortening here is less because relaxation enters before the tetanic level is reached (HILL 1949 d), the present experimental findings are interpreted by assuming that contraction develops approximately proportionally to time and that relaxation enters about simultaneously with contraction. The gradual development of contraction is reflected in the course of shortening with time. Thus, large loads will inhibit the development of contraction (= decreased shortening velocity) and high temperature will facilitate contraction (= increased shortening velocity). A single stimulus is considered to represent a limited possibility of activation (= shortening). This assumption is supported by experiments in which a transient load is applied to the fibre after the latent period for an interval of time which corresponds to half the time necessary to reach the peak of shortening in an isotonic twitch (0° C.). While the load acts on the fibre, the course of shortening is

interrupted, but continues *displaced in time* after the load again is removed, as if the stimulus had been given essentially later ("storing" of activation). Furthermore, the limited possibility of activation inherent in each stimulus is indicated by experiments in which twin stimuli are applied within the latency period. As is well-known from experiments on whole muscle, thereby a summation is caused of the effect of the second stimulus which is displaced in time. The resulting shortening attains its maximum in the middle of the relaxation period of the twitch which is elicited by the first stimulus. This effect is studied under isotonic conditions at a low load and thus cannot be explained by the delaying influence of a series element. The evidence has been mentioned above which indicates that the course of stiffness can hardly *prove* an initial maximum intensity of contraction. Moreover, the time course of initial heat production (HILL 1950c) is not inconsistent with the assumption of a gradual activation during the development of the contraction. Heat of activation is supposed to arise from the shortening of slack minute structural elements, i. e. a heat production which externally will be associated with an increase neither in tension nor in shortening. The delayed development of heat of activation at high loads (HILL 1950c) could correspond to an alignment of these slack elements.

Relaxation after the cessation of stimulation is interpreted as a gradual desactivation. A transient change in load applied to the resting fibre, which has the same magnitude as the tension developed in contraction produces a change in length different in type and of much higher velocity than the elongation which is associated with the desactivation after the stimulation is interrupted.

As a function of load, the maximal *relaxation* velocity determined after a tetanic contraction under isotonic conditions has a maximum. At the load at which this maximum is attained, the relaxation velocity is of approximately the same order of magnitude as the shortening velocity. The relaxation velocity varies over a large range of shortening about proportionally to shortening, but decreases with increasing duration of contraction. *Fatigue* depresses both the shortening and the relaxation velocity to a much higher degree than it reduces the shortening velocity.

At the peak of external shortening (e. g. in a twitch) there

is equilibrium between a finite shortening velocity and a finite relaxation velocity. This interpretation is supported by the correlation which under all conditions examined was found to exist between shortening velocity and relaxation velocity on the one hand and the ratio between shortening in a twitch and in a tetanic contraction on the other. Independent of load, temperature, and degree of fatigue, the shortening in a twitch can be predicted from the shortening velocity, the relaxation velocity, and the shortening in a tetanic contraction. That a high shortening velocity facilitates the shortening in a twitch while a high relaxation velocity has the opposite effect, is likewise seen from the paradoxical variation with temperature which can be observed for the shortening in a twitch. While tetanic shortening increases with temperature, shortening in a twitch either decreases or changes insignificantly with rising temperature. This finding can be explained by the 3—4 times higher temperature coefficient of the relaxation velocity as compared with that of the shortening velocity.

Active and passive relaxation are discussed and it is concluded that mechanical investigations can hardly give a pertinent contribution to the understanding of this problem. However, in view of the conception developed in the last part of this paper for the description of the process of contraction, the problem as such no longer seems to be meaningful.

A comparison of the *net work* produced by the muscle fibre during contraction from different initial conditions shows that the largest amount of work is liberated in isotonic contraction at an initial load of 0.6 to 0.7 P_0. This load corresponds to about 100 per cent elongation in the resting fibre. The maximum amount of work produced in an isometric release contraction with a release velocity of 0.2 L_0[1] per second is found at an initial load of 0.3 P_0, corresponding to 80 per cent of stretch. The amount of work produced decreases with increasing velocity of release. The difference between eccentric (negative) and concentric (positive) work is derived from the differences between the length-tension relation for stretch during contraction and afterload contraction. The static length-tension diagram of the former exceeds slightly that of an isometrically contracted fibre (Buchthal 1942) and is much higher than that of isotonic or afterload contractions. The diffe-

[1] L_0 = equilibrium length.

rence is explained by the stabilization in the texture which characterizes an isometric contraction (elastic locking). An attempt is made to give a quantitative estimate of the internal resistance produced in the development of contraction.

As a function of the initial load the *mean rate of work production*, defined as the total amount of work divided by the time during which it is performed, has a maximum at 0.2 to 0.4 P_0. The highest rate was observed in isotonic contraction and amounted to 0.3 $P_0 \times L_0$ per second (0° C.). The relative rate of work production of the isolated fibre exceeds considerably that of the corresponding whole muscle.

Part IV.

Minute structure and interpretation of mechanical properties.

1. Review of experiments on direct minute structure analysis.

Before an attempt is made to interpret the mechanical investigations on muscle fibres in terms of conceptions which have been developed for the understanding of the rheology of rubber-like substances and high polymers, a short review is given of the results obtained with other methods of minute structural analysis. These results must form the basis of an estimation of the level in the structure at which the deformations can be assumed to occur.

Examination of the isolated living fibre with the *ordinary microscope* indicates that apart from the cross striations, there is a longitudinal orientation, i. e. a fibrillar structure with a diameter of 1—2 μ (Buchthal *et al.* 1936). In electron microscopy which implies the use of dehydrated material, the diameter of these fibrils was found to vary between 0.2—3.2 μ, with a maximum occurrence of fibrils with a diameter of 1 μ (Draper and Hodge 1949). These fibrils are made up of fine threads, *protein filaments*, the diameter of which varies according to the different investigators, but is of the order of magnitude of 100—160 Å. Owing to the technique of preparation and maceration the length of these filaments, as they appear in the preparations for the electron microscope, varies considerably. However, in view

of the fact that fragments with a length of 2—3 μ are frequently met with, the assumption seems justified that the filaments pass uninterrupted through one or more compartments (HALL *et al.* 1946, DRAPER and HODGE 1949, ROZSA *et al.* 1950).

The protein filaments show fine transverse lines, with a periodicity of 250—400 Å comparable to that found in collagen and nerve fibrils. This pattern occurs in the filaments both in the A and in the I substance. *There are no indications of an increased orientation of the filament in the anisotropic substance.* Possibly the region between two of these fine stripes can be considered the fundamental functional unit of the fibre, but the detailed structure of this region, the resolving of which approaches the borders of the electron microscope, is mostly a matter for speculation. DRAPER and HODGE (1949) assume it to be made up of at least 3 macromolecules of different structure arranged in a definite pattern. Since the fine stripes often disappear during the preparation, ROZSA *et al.* (1950) considered them to be caused by a material which periodically is glued to the filament, and which can be washed off. It also seems wise to be cautious in accepting the assumption that the filaments represent tubular structures filled with some fluid material. Obviously, the preparative treatment of the fibre can give rise to a number of artifacts and ROZSA *et al.* did not find any indications of this tubular structure. As mentioned above, for the time being electron microscopical analysis does not give any pertinent information concerning changes in structure accompanying the deformation occurring with stretch and during contraction. On the other hand, the results from the analysis with the electron microscope make it necessary to revise the interpretation of measurements of birefringence in the muscle fibre.

By immersing the fibre in substances with different refractive indices it has been established that birefringence in the muscle fibre is the result of a form (rod) component and a crystalline component (STÜBEL 1923, NOLL and WEBER 1934, WEBER 1934 a, b). This differentiation is only possible on fixed fibres. In the living muscle fibre of the frog the resulting birefringence amounts to $2.0 \times 10^{-3} \pm 0.05 \times 10^{-3}$ (BUCHTHAL and KNAPPEIS 1938, KNAPPEIS 1948) and varies 1 per cent per 10 per cent of stretch. In fixed mammalian fibres FISCHER (1947) found a 2—3

times larger effect of stretch on birefringence. Provided that the results from fixed fibres can be applied to the living fibre, the crystalline birefringence increases about as much with stretch as the form birefringence. However, it is essential to point out that the increase in birefringence with stretch under all circumstances is small in muscle as compared with caoutchouc and actomyosin threads.

The approximately parallel longitudinal orientation of protein filaments revealed by the electron microscope would be sufficient as such to account for the degree of birefringence found in the muscle fibre. However, considering that there are no signs of differences in orientation in the protein filaments corresponding to the anisotropic and isotropic segments, and in view of the fact that the filaments pass uninterrupted through one or more compartments, the origin of the resulting birefringence must be reconsidered. It may be looked for either in a substance with negative birefringence in the I segment which compensates for the positive birefringence of the fibril itself, or in positive birefringent substances surrounding the fibrils in the anisotropic segments. The former assumption is supported by the histo-chemical finding of lipoid material in the I layer (Dempsey *et al.* 1946) and by the extraction of a material with negative birefringence from muscle (Matoltsi and Gerendás 1947). However, the question seems far from settled and, as pointed out by Draper and Hodge (1949), one might just as well assume the filaments throughout their whole length to be covered with a substance the negative birefringence of which could compensate their positive birefringence. Thereby, the I substance would appear isotropic and the substance surrounding the fibrils in the A segments might account alone for the resulting positive birefringence.

The amount of material present in the muscle fibre apart from the filaments is assumed to be localized essentially in the A segment, the space in the isotropic part being very restricted. Assuming this to be a well established fact it is of interest to note the work of Casparsson and Thorell (1942), whose findings indicate that nucleotide is localized in the I segments. During contraction or contracture the anisotropic substance is assumed to migrate towards the I segment. However, these

assumptions do not give a quantitative explanation of the systematic changes found in the distribution of the length of the A and I substance during isometric and isotonic contraction and during stretch (Buchthal *et al.* 1936, Buchthal and Knappeis 1943).

In isotonic contraction of whole muscle birefringence decreases (Fischer 1936, 1944, 1947). In isometric contraction the results obtained are somewhat conflicting. Von Muralt (1932, 1934) has found a slight negative fluctuation with two peaks, while Bozler and Cottrell (1937) found a decrease, an increase, or no change at all depending on the initial tension. Obviously, the complicated mechanical changes accompanying isometric contraction in whole muscle make the interpretation of these findings rather difficult. In the isolated fibre a tetanic isometric contraction is followed by a decrease in birefringence (10—20 per cent, Buchthal and Knappeis 1938). The decrease is not present if a contraction is released in a fibre poisoned with monoiodoacetic acid. It is found also in contractions released by minute amounts of adenosine triphosphate, but is absent when contraction is released by inorganic triphosphate (Buchthal *et al.* 1944b). For technical reasons no information is available as yet concerning the changes *during* isometric or isotonic contraction of the isolated fibre.

The evidence hitherto available indicates that the deformations caused by stretch or contraction must occur at the molecular level of the structure.

X-ray diffraction analysis which has contributed important results to the understanding of protein structure has been applied to myosin, muscle, and similar fibrous structures (Böhm 1931, Astbury 1931, 1936, Böhm and Weber 1933). It has revealed that there is a *fibre diagram* both in the living and in the fixed and dried muscle. These fibres contain a more or less irregular mass of protein chains which are so perfectly arranged in the crystalline protein molecule, and fibrous substances may be compared with a kind of "oakum of protein strands" (Bragg 1948). Owing to the rather imperfect arrangements of molecular fragments they give more diffuse X-ray diffraction effects and must be considered "unsatisfactory witnesses" (Bragg 1948). In analogy to findings on other fibrous proteins, especially keratin and myosin, Astbury (review 1947) has suggested a way in which polypeptide chains

could be folded, and assumed the presence of chains also in muscle which occur in a short (α) and a long (β) modification. However, this is an analogy and the transformation from an α to a β-form by stretch has not hitherto been found in *living* muscle. Only in dried muscles which were reimmersed and stretched, spacings corresponding to a longer modification have been demonstrated.

The reproducible spacing corresponding to the intramolecular foldings is 5.1 Å, while a spacing of 10—11 Å is considered to indicate a periodicity in the transverse direction, i. e. corresponding to the mean distance *between* the molecules. Recent investigations have shown that the 1.5 Å reflexion from planes perpendicular to the fibre axis which characterizes a number of polypeptide chains (PERUTZ 1951) also occurred in dried muscle (HUXLEY and PERUTZ 1951). It was present in the relaxed, stretched, and contracted state. These subdivisions are considered to indicate a spacing corresponding to the repeat of the amino acid residues along the polypeptide chains and correspond to the helix with 3.7 residues per turn suggested by PAULING *et al.* (1951).

In an important series of papers which has appeared very recently PAULING and COREY (1951) have treated the fundamental structure of proteins. They suggest two main configurations of polypeptide chains, viz. the α helix with 3.7 residues per turn and the pleated sheet consisting of a layer of chains with the same orientation. According to their assumptions the α helix is present in α keratin and α myosin, while the pleated sheet occurs in β keratin and β myosin.

PAULING and COREY (1951 a) characterize contraction of muscle by the transition from a pleated sheet configuration to layers of packed cylindrical helices subsequent to the disrupture of a number of the hydrogen bonds. Provided that the mechanical forces between larger units are of a similar nature as those acting between the individual chains, an assumption which seems reasonable, the conception of structural changes given by PAULING and COREY can account a. o. for the decrease in transverse forces that occurs in a tetanic contraction as indicated by the changes in the torsional modulus mentioned above (p. 205).

The estimations of mechanical tension and heat produc-

tion made on the basis of the structural data are difficult to evaluate. However, there seems to be a discrepancy between the calculated values for heat and for force developed by the muscle. Thus, a calculated tension of 1.53 kg per cm^2 per g. muscle and a calculated shortening of 54 per cent result in a work of 0.018 cal per g. muscle and not in a work of 0.18 cal per g. muscle, the figure given by PAULING and COREY. The reason for this discrepancy is not obvious from the assumptions made and the calculations given by the authors. However, a value of 0.018 cal per g. muscle would be in good agreement with the experimental values for the maximum work which can be obtained in a tetanic contraction of a muscle fibre (0.036 cal per g. muscle).

X-ray diffraction of living muscle showed clear signs of an *incomplete* longitudinal molecular orientation within the filament. Stretch caused an improvement of this orientation. In the evaluation of results from X-ray diffraction it must be recognized that essential deformations of the structure may be applied without evoking corresponding changes in the pattern. Thus, the diffraction pattern of stretched hair which was allowed to shorten 20 per cent, remained unaltered with respect to spacing and signs of different orientation. The pattern in an isotonically contracted smooth muscle (mytilus, shortening 50 per cent) showed no deviation from the resting muscle, while iodoacetic acid contracture in frog's sartorius was accompanied by an increase in orientation and in scattering near the centre of the diagram. That the increase in orientation is moderate cannot be surprising in view of the relatively high degree of orientation present already in the resting muscle. The increase in scattering around the primary spot of the diagram is interpreted as being caused by the formation of amorphous irregular aggregates, which bring about certain distortions of the filaments. An isotonic iodoacetic acid contracture is associated with scattering to larger angles. Investigations of the normal type of contraction in living fibres with a proper technique are still scarce.

Optical methods, other than measurements of birefringence, have been applied to the living muscle fibre and have given information about structural properties and their changes by deformations. *Light-transparency* is only to a minor degree caused by true absorption. The fibre acts as a scattering body and ab-

sorption is 20—40 times less than the decrease in the light intensity of the primary ray caused by the muscle fibre. The specific absorption remained unaltered by stretch and increased by 0.8 per cent in the isometric twitch. The transparency decreases both during stretch and isometric contraction corresponding to an increase in scattering. The close packing of minute structural elements during contraction is assumed to cause light-interference of neighbouring rod-shaped particles (*increased aggregation*). These results were interpreted as an *improvement* in minute structural orientation which accompanies both stretch and contraction (Buchthal *et al.* 1939). A transient *increase* in transparency has been found at an early time after stimulation, simultaneously with the latency relaxation (D. K. Hill 1949). This increase is an indication of a decrease in true absorption and does not occur at quick stretch of other highly elastic substances.

The cross striations of the fibre give rise to a diffraction pattern (Ranvier 1874, Sandow 1936, Buchthal and Knappeis 1940). Even with a beam which is circular in cross section, the spectra do not form sharply limited round spots as is the case in a Rowland grating. The images of 0. to IV. order have no sharp limit and they are elongated in the vertical direction. These "tails" indicate the presence of diffraction phenomena in the longitudinal structures of the fibre. The intensity maxima which have been observed in the tails indicate a periodicity in these longitudinal structures. The histological correlate is the grouping of fibrils in columns of 5—7 μ in diameter (fig. 1). The tail which has a fan-like spreading in the resting fibre, is closed to a pointed narrow stripe both by stretch and by contraction. This also indicates an improvement of the parallel orientation by stretch and contraction (Buchthal and Knappeis 1940).

Although many important details of minute structure in the muscle fibre still remain unrevealed, there are a number of common trends which have come out from electron microscopical, X-ray, and optical analysis. The muscle fibre has a relatively good, but by no means complete longitudinal orientation. This orientation is improved by stretch and by contraction. The mechanical deformations must mainly be looked for on the molecular level. Both X-ray diffraction and transparency measurements give indications of an increased aggregation of the minute structure in contraction.

2. Minute structural interpretation of mechanical properties.

In the present investigation of the structural elements of striated muscle accessible in a living state we have mainly dealt with the isolated fibre, whose mechanical reactions are considered to be the nearest expression of the minute structure. The parallelized organization existing for the fibres of a muscle is repeated in its fibrils and protein filaments. Therefore, after a certain degree of adjustment has been obtained, equivalence can be assumed in the mechanical reactions of the fibre and its filaments. The minute structural investigations referred to in the preceding section have revealed that on the molecular level of the fibre structure we might also reckon with an orientation, though incomplete, nevertheless predominantly along the longitudinal axis of the fibre. The deformation obtained by stretch or contraction must be attributed to changes in the structural proteins, which consist of long molecular chains with a high molecular weight ($1—17 \times 10^6$, Weber 1934b, Bergold 1946).

As is the case with other high polymers it is improbable that these long chains exist as fixed units. The incomplete orientation will facilitate the interaction between adjacent units, and thermal agitation will cause local deformations which are distributed at random in time and space. In order to explain the large elastic extensibility (change in length 1:4) it is necessary to look for a minute structural mechanism dealing with forces which act over a large distance, i. e. *long range forces* as in high polymeric substances.

When the properties of the fibre are looked upon in a general way their complex mechanical reactions found under various conditions display both phenomena which occur quickly and reactions whose adjustment takes a considerable time. The adjustment can be described by a distribution of retardation times and/or relaxation times in a mechanical equivalent system.

The kinetic theory of rubber-like substances.

At an early state of the development of high polymer physics mechanical properties of highly elastic substances, especially rubber, have been explained by assuming the presence of loosely

curled chain molecules (Ostwald 1926). A few years later Busse (1932) clearly defined the properties which characterize the minute structure of a highly elastic material. Rubber is assumed to be built up from chain molecules of long length. Their primary valency linkages are considered to be strong enough to resist the tension when deformed. Between the adjacent molecules secondary linkages are assumed to exist which are broken and reformed by thermal agitation and thus allow movement of the chains in relation to each other. Moreover, a minor number of main-valency transversal linkages are supposed to be present in the reversibly elastic structure. This interlocking forms a more or less permanent pattern of a three-dimensional network. According to the kinetic theory (Meyer *et al.* 1932, Wall 1942, Treloar 1943, 1949, 1951), the individual links of the chains have a relative freedom of motion. Therefore, the chain molecules can assume a large variety of different configurations, each having in principle the same probability at zero load. The mechanical forces arise from the thermal movements, which cause different states of contraction by curling of the molecular chain as a whole. The length of the chain or its degree of orientation is determined by the ratio between the disorganizing thermal forces and the external aligning forces acting on the chain. If the chains with respect to their terminals have a certain degree of orientation, an internal curling up will result in an external shortening of the substance in the direction of its orientation and it will display elastic properties. Thus, according to the kinetic theory, shortening (e. g. as it occurs in rubber with an increase in temperature) is considered to be caused by a change in the thermo-kinetic conditions. It is an essential consequence of the kinetic theory that the elastic tension in a highly elastic substance which is stretched to a given length increases proportionally to the absolute temperature.

With the development of the theory for the mechanical (thermoelastic) properties of highly elastic materials corresponding kinetic considerations were applied to biological substances (Meyer and Ferri 1936, Wöhlisch 1939).

The anomalous behaviour of elastic tension with temperature, which in muscle as in rubber at constant length shows increasing tension with rising temperature, the finding of delayed elasticity

and the demonstration of phenomena such as yielding, elastic locking, and thixotropy indicate that also in muscle there is an organization of minute structural elements in a network, a *texture* which is similar to that assumed for other high polymers. This assumption is supported by the demonstration of variable cross-linkages in measurements of torsional elasticity and its variation during stretch and contraction (Sten-Knudsen 1950). However, although disrupture and reformation of points of entanglement between minute structural elements of the texture can explain part of the mechanical reactions of the muscle fibre, by no means can it account for all their peculiarities. Changes in the textural pattern implying the occurrence of slack chains, can explain the differences between isotonic and isometric contraction (locking), the amplitude dependence of dynamic elasticity, the maximum in stiffness which occurs in an early phase of contraction, and finally the finding of thixotropy in the mechanical reaction of the fibre.

The kinetic theory can account satisfactorily for the static properties of rubber. However, the S-shaped length-tension diagram which can be expected in a substance with kinetic elasticity and which in fact is found, does not apply to the resting muscle fibre. The deviation occurs especially at small degrees of stretch where an increase in length *in the muscle fibre* is associated with a low gradient of tension, while the gradient is high in the curve which is determined by kinetic elasticity. In the latter the initial stiffness, i. e. the stress gradient, exceeds that present at a moderate load. Although in the case of e. g. rubber this deviation could be explained on the basis of the work performed in order to attain the degree of preorientation which in muscle already exists at zero load, there are, apart from orientation, other quantitative differences in the mechanical reaction between muscle and rubber:

The proportionality between static tension and absolute temperature (T) characterizing orientated rubber, which as mentioned is a direct consequence of the kinetic theory, does not apply to the muscle fibre. The temperature coefficient of the isolated muscle fibre amounts at most to only one third of a kinetically caused temperature dependence (Buchthal *et al.* 1944a). This is in conflict with Meyer and Picken's results (1937) from

experiments on whole muscle. The higher temperature coefficient of the "static" tension which even exceeds that corresponding to a proportionality with absolute temperature might be explained by the greater difficulty in attaining equilibrium of temperature and mechanical adjustment of the structure in a whole muscle.

Eyring and Tobolsky's theory.

The kinetic theory in its simplest formulation, however, met rather early with difficulties. Although this theory can account for the static properties of rubber, it is unable to explain the viscous effects, such as the slow changes in length observed at constant load, delayed elasticity, and the decrease in tension at constant stretch. For an explanation of these phenomena, TOBOLSKY and EYRING (1943) and TOBOLSKY *et al.* (1943) suggested that the chain molecules of rubber have cross-linkages with a relatively low energy content. These cross-linkages are broken and reformed by thermal agitation. Thereby flow properties of the substance will emerge, adjacent molecules continuously changing position in relation to each other. A flow unit moves from one position of equilibrium to another by overcoming a *potential barrier*, the energy necessary being derived from thermal agitation. The shape and position of the potential barrier changes slightly with the external load. Certain points of entanglement will resist and not be disrupted, then only displaying crystalline elasticity, while others will give and yield in steps. This results in a visco-elastic reaction of the material.

On the basis of these reaction-kinetic considerations EYRING *et al.*[1] have introduced the 3-element model consisting of an elasticity shunted by a generalized Maxwell-element to describe the mechanical behaviour of rubber and certain textile fibres. Also in cellulose fibres the stress-relaxation can be adequately described by this theory (ANDERSEN 1951). The elasticity of the Maxwell-element has linear properties while the viscosity is non-linear and its resistance determined by the following equation:

$$\sinh r \cdot \sigma = r \cdot \eta \frac{d\gamma}{dt}, \qquad (63)$$

[1] HALSEY, WHITE, and EYRING 1945, HALSEY and EYRING 1945, EYRING and HALSEY 1946, STEIN, HALSEY, and EYRING 1946, HALSEY and EYRING 1946a, HOLLAND, HALSEY, and EYRING 1946, REICHARDT and EYRING 1946.

where σ denotes the resistance, $\frac{d\gamma}{dt}$ the velocity of flow, η corresponds to the viscosity, and r is a constant. However, the mechanical reaction of wool fibres could not be satisfactorily described on the basis of EYRING's simple 3-element model (HALSEY and EYRING 1946 b), and it was necessary to introduce non-linear elasticities in this model, so that its correlation to the basic minute structural reaction becomes extremely complex. Also in the case of muscle this type of theory seems hardly adequate to describe the mechanical reactions.

As regards *dynamic mechanical properties* of muscle they display essential differences from rubber as well. For example the difference between static and dynamic elasticity in the muscle fibre exceeds considerably that found in rubber. In the former the dynamic stiffness exceeds the static by 300—500 per cent. In normally and under-vulcanized rubber which we have examined under the same conditions as the muscle fibres, the dynamic elasticity exceeds the static on an average by 50 per cent and at most by 100 per cent. Therefore, the mechanical reactions of the muscle fibre are dominated to a higher degree by retardation phenomena than is the case in rubber. The large difference between static and dynamic elasticity found in the muscle fibre indicates that time enters as an essential factor in the length-tension relation. The delay in time corresponds to the presence of a viscous component, though it does not behave as a classic Newtonian viscosity.

In search of a cause of the non-Newtonian delay one might think of changes in the degree of hydration of the elastic minute structural elements. The liquid which surrounds and imbibes these elements might alter their mechanical dimensions owing to differences in the pressure gradient which might arise from mechanical deformations. Although an assumption of this type might seem near at hand when discussing a cellular structure, it seems less probable in the case of the muscle fibre. The dimensions of the elastic filaments are so small that the time necessary for diffusion would be extremely short. Thus, possible fluid displacements will hardly influence to a measurable degree the variations of tension with time which extend over seconds to minutes.

The slow adjustment to a new stationary state after a change in length indicates that the structural changes do not occur instantaneously but with a certain limited velocity. As mentioned

above, this flow is considered to be due to a discontinuous interaction between the molecular chains thereby accounting for the variations of viscosity under different conditions. A Newtonian viscosity is independent of the load and its resistance varies proportionally to the velocity of deformation. In a muscle fibre the viscous resistance increased with increasing load and/or degree of orientation. To an essentially lesser degree the same was the case both in vulcanized and under-vulcanized rubber. The viscous reaction of the muscle fibre is attributed chiefly to properties of the texture in which the minute structural elements are organized, i. e. it is interpreted as a structural viscosity caused by a delayed adjustment to altered mechanical conditions. Its increase with increasing degree of stretch is interpreted in the following way: The orientation of the texture increases with increasing load. With a small degree of orientation disrupture of a point of entanglement will cause a high increase in length while at high degrees of stretch the resulting increase in length will be only slight. Therefore, more and more points of entanglement will have to be broken to produce a given deformation with increasing load, corresponding to an increase in viscosity. This effect will be further enhanced if the number of points of entanglement increases with increasing elongation.

Granted that curled elements may qualitatively account for the length-tension relation, nevertheless the stiffness-tension relation, the variation of the viscous resistance, and the orientation present in the muscle fibre already at equilibrium length imply that the theories developed for other highly elastic substances cannot be accepted as a basis of the description of the mechanical reaction of the muscle fibre. The simple kinetic theory as well as EYRING and TOBOLSKY's transition theory refer deformations almost exclusively to the textural pattern of the substance. In view of the fact that the orientation in the muscle fibre is altered only insignificantly by stretch it seems reasonable *that the changes in length accompanying stretch and contraction are attributed to alterations in the length of the chain molecules and not to the degree of orientation.* Therefore, transitions between different modifications will have to occur within the polymerized molecule itself. In previous investigations the dependence of dynamic stiffness on frequency, temperature, and load in experiments per-

formed at constant mean length of the muscle fibre led to the assumption that the tension causes altered chemical states of linkage *within* the minute structural element (Buchthal *et al.* 1944a). The present experimental material has supported this assump-

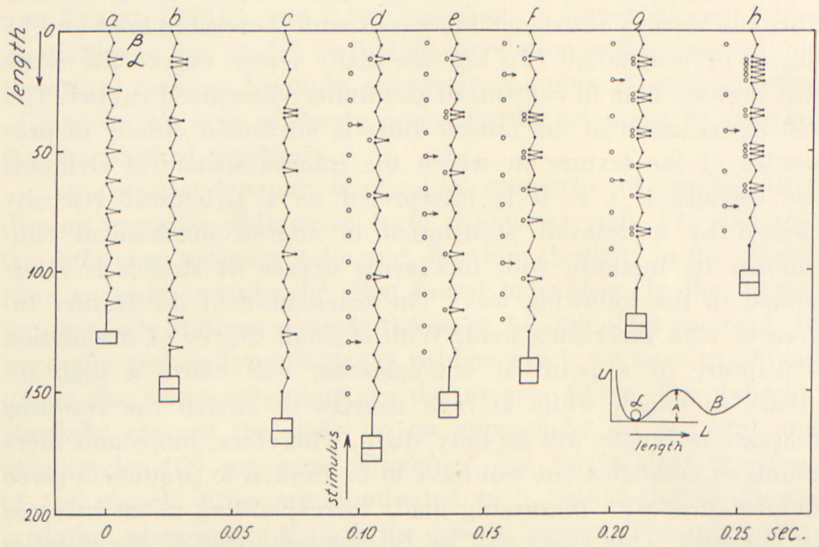

Fig. 91. Schematic representation of the transmutation theory.
a. Transmutation chain at a low load. The number of α- and β-links are approximately equal.
b. Transmutation chain during the adjustment to a higher load. The number of β-links has increased.
c. and *d.* Further developing of the adjustment.
d.—*h.* Contraction of a transmutation chain.
d. The chain just after stimulation. The fixating agent has appeared and has fixated α-links.
e. The fixation brings about an increased number of $\beta \rightarrow \alpha$ transmutations, i. e. shortening. Fixation proceeds.
f.—*h.* Further development of shortening and fixation.
abscissa: time in sec.
ordinate: length in per cent of L_0.
Inset on the right: potential barrier with two equilibrium positions α and β.
ordinate: potential energy U.
abscissa: length L.

tion and enabled us to extend the conception of chains with transmuting links as a basic element of the structure for an explanation of both visco-elastic properties and contractility. Recently reversible changes in the chemical composition induced by alterations of the load have been demonstrated chemically. Thus, Mochulsky and Tobolsky (1948) have produced evidence that

the "cold flow" of polysulfide rubbers is chemical rather than physical in nature. The chemical reaction is considered an intermolecular exchange reaction between a terminal mercaptan group of one chain and a disulfide linkage of an adjacent chain.

It seems to us therefore well motivated to study the quantitative properties of a molecular chain within which a transmutation occurs between states of different length, in such a way that the resulting length of the chain is determined by the ratio between the probabilities of the occurrence of short and long modifications. By this analysis an attempt is made to investigate to what extent a relatively simple model conception can account for complex mechanical reactions which cannot be attributed to the phenomena of adjustment in the texture. Moreover, it turns out that a possibility arises to consider in a new light the minute structural changes concomitant with contraction thereby accounting for the degree of shortening, the shortening velocity, and the relaxation. H. H. WEBER (1934a) described delayed elasticity in myosin threads qualitatively by assuming a transformation between linkages of different lengths within the molecule. In analogy to results obtained from the X-ray diffraction analysis of keratin and myosin ASTBURY (1936, 1947) suggested also in the case of muscle the existence of two different linkages, a long one and a short one, the former arising at a high degree of stretch (cf. p. 223). On the basis of ASTBURY and BELL's (1941) findings in keratin SPEAKMAN and PETERS (1948) calculated the static length-tension diagram of wool fibres. Similar considerations provided the starting point for the quantitative treatment given in the following, although no other structural assumptions are implied than two different modifications within the protein molecule[1].

The single transmutation chain.

The contractile molecular chains are assumed to consist of a large number of links occurring in two stable modifications,

[1] BURTE and HALSEY (1947) have derived both static and dynamic properties for this two-position model. They find the model well suited for dealing with substances of the nylon-rubber-wool type. Their paper contains some of the results which we have obtained independently. In this connection we should like to emphasize the importance which we ascribe to cross-linkages between the minute structural elements e. g. for the understanding of thixotropy. BURTE and HALSEY explain thixotropy by means of a three-position model.

a short one (α) and a long one (β). The difference in length is supposed to arise either from the size of the angle formed by adjacent parts of the molecule or from the change in orientation of cyclic rings building up the links (BAILEY). The rings can alternate in their orientation either longitudinally (β) in the direction of the axis of the chain molecule or transversely to it (α) (fig. 1, cyclic units). Transmutation from the one linkage to the other can be described by the transition over a potential barrier in passing from one potential minimum to another.

The single links of a molecular chain are exposed to thermal bombardments displaying a frequency of approximately 10^{13} per sec. This figure is based on the assumption that the majority of thermal encounterings is caused by water molecules which form the main component of the muscle tissue. As shown by HILL and KUPALOV (1930), water occurs only to a minor degree in a bound state. The frequency of thermal collisions (ν) is determined from the following formula:

$$\nu = \frac{c}{1000} \cdot N \cdot 2\pi r \cdot l \cdot \sqrt{\frac{kT}{2\pi m_{H_2O}}} \qquad (64)$$

where c denotes the concentration of bombarding molecules, $N = 6 \cdot 10^{23}$ Avagadro's number, r and l the radius and length of the transmuting element in the chain molecule, $\sqrt{\frac{kT}{2\pi m_{H_2O}}}$ the mean velocity of water molecules at temperature T, and m_{H_2O} the mass of the water molecule. The length and the radius of the elements are assumed to be 20 and 3 Å respectively.

A small part of the collisions are assumed to have sufficient energy ($\geq$ the activation energy for the transmutation) to release a transmution from one modification to another ($\alpha \rightarrow \beta$ or $\beta \rightarrow \alpha$). The fact that not all thermal encounterings cause a transmutation is due partly to the distribution with regard to the direction of bombardment, partly to the energy distribution of the colliding particles, i. e. the Maxwell distribution corresponding to the temperature in question. The larger the energy necessary for transmutation, the less probable it will be. The probability that a thermal collision has an energy exceeding the temperature energy, kT, according to the Maxwell distribution is

57 per cent. The probability of an energy $> 4\,kT$ is 4.6 per cent and the probability of an energy $> 9\,kT$ is 0.044 per cent. The activation energy in the usual chemical reactions is of the order of magnitude of one electron volt. The temperature dependence of the mechanical reaction of the muscle fibre found from the displacement of the boundaries of the spectrum of retardation times (fig. 26) gives an equivalent activation energy of 0.6 eV. In this estimation we have considered mainly the shortest retardation times which can be expected to be an expression of processes within the molecular chains. The probability that the energy of the colliding particle will exceed 0.6 eV ($> 25\,kT$) at 0° C. is 8×10^{-11}.

The transmutations will cause a continuous alternation between the two modifications of the links in the molecule. However, apart from the energy of activation derived from thermal movements, an additional prerequisite for a transmutation to occur is that there are suitable possibilities for it in space.

According to EYRING's viscosity theory (cf. EYRING and POWELL 1944) the probability of transmutation is relatively small when the molecular packing is tight. Thereby the transmutation frequencies for both $\alpha \rightarrow \beta$ and $\beta \rightarrow \alpha$ is reduced and there will be a spectrum of activation energies instead of a single one.

The energy necessary to cause transmutation apart from thermal agitation is derived from the external load which acts on the molecular chain. In order to keep equilibrium between the stress in the transmuting element and the external load, the length of the individual α and β linkages changes slightly with load.

Let us consider the potential barrier for the unloaded transmuting link as being only one-dimensional and determine the influence of the load on the activation energies of the system. The potential energy (U) is given by

$$U = U(L), \tag{65}$$

where L denotes the length of the link. As postulated above, U has two minima corresponding to the α and β modification and a maximum corresponding to the peak of the barrier. The barrier is not necessarily symmetrical. The activation energy for transmutation $\alpha \rightarrow \beta$ is

$$A_{\alpha \rightarrow \beta} = U(L_1) - U(L_\alpha) \tag{66}$$

and for transmutation $\beta \rightarrow \alpha$

$$A_{\beta \rightarrow \alpha} = U(L_1) - U(L_\beta), \tag{67}$$

where L_1 denotes the length corresponding to the peak of the potential barrier.

A load P is considered to cause a modification of the potential to

$$U_P(L) = U(L) - P \times L. \tag{68}$$

The maximum and minimum for this potential are determined by

$$\frac{dU_P}{dL} = 0, \text{ i. e. } \frac{dU}{dL} = P. \tag{69}$$

Therefore, at load P the length of the α and β modifications $L_\alpha(P)$ and $L_\beta(P)$ are determined by

$$\frac{dU}{dL} = P \quad \text{for} \quad L = L_\alpha(P) \quad \text{and} \quad L = L_\beta(P). \tag{70}$$

Also the maximum is displaced to a position $L_1(P)$ determined by

$$\frac{dU}{dL} = P \quad \text{for} \quad L = L_1(P).$$

If the load P exceeds the maximum gradient of $U(L)$ in the interval $(L_\alpha < L < L_1)$ only one modification can exist, viz. the long one.

According to the potential barrier indicated in fig. 91 (inset) we have

$$L_\alpha < L_\alpha(P) \leqq L_1(P) < L_1 \quad \text{and} \quad L_\beta(P) > L_\beta. \tag{71}$$

Therefore, the activation energies in the loaded state are:

$$A_{\alpha \rightarrow \beta}(P) = U(L_1(P)) - U(L_\alpha(P)) - P \times (L_1(P) - L_\alpha(P)) \tag{72}$$

and

$$A_{\beta \rightarrow \alpha}(P) = U(L_1(P)) - U(L_\beta(P)) + P \times (L_\beta(P) - L_1(P)). \tag{73}$$

By its displacements of the equilibrium positions in both cases the load P causes a decrease in the thermal energy necessary to cause a transmutation (activation energy). In addition, for the transmutation $\alpha \rightarrow \beta$ we have a decrease in activation energy corresponding to the work performed by the tension in surmounting the potential barrier. Conversely for the transmutation $\beta \rightarrow \alpha$ we have an increase in activation energy corresponding to the work to be performed against the load in surmounting the potential barrier.

The frequency of transmutation, $W_{\alpha \rightarrow \beta}(P)$ and $W_{\beta \rightarrow \alpha}(P)$, i. e. the probability per time unit of the transition from one modification to another is assumed to depend on the activation energy (A) in the same way as the reaction velocity of a monomolecular chemical reaction depends on the activation energy, i. e. through the van t'Hoff factor $e^{-\frac{A}{kT}}$ (GIBBS, ARRHENIUS). Here T represents the absolute temperature and k Boltzmann's constant. Hence, the frequencies with which the transmutation occurs, are:

$$\left.\begin{aligned} W_{\alpha \rightarrow \beta}(P) &= \nu_{\alpha \rightarrow \beta}(T, P) \cdot e^{-\frac{A_{\alpha \rightarrow \beta}(P)}{kT}} \\ W_{\beta \rightarrow \alpha}(P) &= \nu_{\beta \rightarrow \alpha}(T, P)\, e^{-\frac{A_{\beta \rightarrow \alpha}(P)}{kT}}. \end{aligned}\right\} \qquad (74)$$

The factor $\nu\,(T, P)$ depends on the frequency of collisions, their spatial distribution, and the spatial possibilities for a transmutation to occur. It follows from the general formula for the dependence of activation energy on the load applied (72, 73) that a load P *increases* the transmutation frequency $\alpha \rightarrow \beta$ partly because the load by its work facilitates the transmutation, partly because the displacement of the equilibrium positions by the load causes a decrease in activation energy. Conversely for the transmutation $\beta \rightarrow \alpha$ the load causes partly a decrease in the frequency of transmutation on account of the extra work necessary when a transmutation occurs against the load, partly an increase which again is due to the displacement of the equilibrium positions. In advance it is impossible to estimate the relative importance of the different factors for the transmutation frequency. Therefore, in order to be able to perform quantitative estimations,

certain assumptions are necessary which, however, appear to be reasonable approximations. The potential $U(L)$ is assumed to have such a shape that the changes in length of the individual α and β link caused by the load and the decrease in activation energy, which arises from these changes, are of secondary importance.

Hence $U(L)$ must increase steeply from the α minimum to the peak of the potential and from the β minimum outwards so that the slope soon equals the load. This will certainly be fulfilled for loads P for which $P \times (L_\beta - L_\alpha)$ is small as compared with the activation energies. As will be shown below (p. 243), this inequality actually exists in the case of the transmutation chains of the muscle fibre. Here, at 0° C., an activation energy (A) of 0.6 eV (14 kcal per mole) corresponds to approximately 25 kT, i. e. 5—8 times the estimated maximum value of $P \times (L_\beta - L_\alpha)$.

With this assumption the activation energies (72, 73) will be:

$$\left.\begin{aligned} A_{\alpha\to\beta}(P) &= A_{\alpha\to\beta} - P\times\lambda_\alpha \\ A_{\beta\to\alpha}(P) &= A_{\beta\to\alpha} + P\times\lambda_\beta \end{aligned}\right\} \qquad (75)$$

where

and

$$\left.\begin{aligned} \lambda_\alpha &= L_1 - L_\alpha \\ \lambda_\beta &= L_\beta - L_1. \end{aligned}\right\} \qquad (76)$$

Moreover, we assume that the proportionality factors $\nu_{\beta\to\alpha}$ and $\nu_{\alpha\to\beta}$ are identical and we disregard their possible dependence on the load.

Hence we get from (74) the following expressions for the frequency of transmutations:

$$\left.\begin{aligned} W_{\alpha\to\beta}(P) &= \nu(T)\, e^{-\frac{A_{\alpha\to\beta} - P\lambda_\alpha}{kT}} \\ W_{\beta\to\alpha}(P) &= \nu(T)\, e^{-\frac{A_{\beta\to\alpha} + P\lambda_\beta}{kT}}. \end{aligned}\right\} \qquad (77)$$

The small temperature dependence of the length of the muscle fibre makes it reasonable to assume that the activation energies $A_{\alpha\to\beta}$ and $A_{\beta\to\alpha}$ are equal. In the following they are denoted by A. Moreover we assume that the potential $U(L)$ is symmetrical,

i. e. $\lambda_\beta = \lambda_\alpha = \lambda$. In the approximation applied in the following calculations a possible asymmetry will be without importance. Thus:

$$\left.\begin{aligned} W_{\alpha\to\beta}(P) &= \nu(T)\, e^{-\frac{A}{kT}}\, e^{\frac{P\lambda}{kT}} \\ W_{\beta\to\alpha}(P) &= \nu(T)\, e^{-\frac{A}{kT}}\, e^{-\frac{P\lambda}{kT}} \end{aligned}\right\} \tag{78}$$

or by introducing

$$W = \nu(T)\, e^{-\frac{A}{kT}} \quad \text{and} \quad p = \frac{P\lambda}{kT}, \tag{79}$$

where p represents a quantity which is proportional to the load:

$$\left.\begin{aligned} W_{\alpha\to\beta}(P) &= We^{p} \\ W_{\beta\to\alpha}(P) &= We^{-p}. \end{aligned}\right\} \tag{80}$$

Based on these assumptions, calculations can be performed regarding the mechanical behaviour of a chain with transmuting links of the type indicated above. Static and dynamic properties will be considered separately and at the end of every section a comparison will be given between theoretical results and experimental findings.

The static length-tension diagram for a transmutation chain.

The basis of the calculations simply is, that if a chain of transmuting elements is in equilibrium with a given load, the number of $\alpha \to \beta$ transmutations per second must be equal to the number of $\beta \to \alpha$ transmutations per second.

Therefore, denoting the number of α-elements in the chain by N_α and the number of β-elements in the chain by N_β we get

$$N_\alpha\, W_{\alpha\to\beta}(p) = N_\beta\, W_{\beta\to\alpha}(p); \tag{81}$$

introducing

$$\alpha = \frac{N_\alpha}{N_\alpha + N_\beta} \quad \text{and} \quad \beta = \frac{N_\beta}{N_\alpha + N_\beta} \tag{82}$$

and (80) we get

$$\frac{\beta}{\alpha} = e^{2p}. \tag{83}$$

Furthermore we have

$$\alpha + \beta = 1. \tag{84}$$

From (83) and (84) we get

$$\beta = \frac{1}{1 + e^{-2p}} \tag{85}$$

and

$$\alpha = \frac{e^{-2p}}{1 + e^{-2p}}. \tag{86}$$

The length $L_N(P)$[1] of the chain is

$$L_N(P) = L_\alpha N_\alpha + L_\beta N_\beta. \tag{87}$$

The length per link $L(P)$, i. e. the mean length of one link in time, therefore is:

$$L(P) = \alpha L_\alpha + \beta L_\beta. \tag{88}$$

By means of (83) this is transformed to

$$L(P) = L_\alpha \left(1 + \beta \frac{L_\beta - L_\alpha}{L_\alpha}\right)$$

and, furthermore, according to (85) we get the following expression for the length per element:

$$L(P) = L_\alpha \left(1 + \frac{L_\beta - L_\alpha}{L_\alpha} \cdot \frac{1}{1 + e^{-2p}}\right). \tag{89}$$

The ratio $\frac{L_\beta}{L_\alpha}$ in the following is put equal to 4. This value is assumed on the basis of the difference between the minimal length of a shortened fibre at a low load and the length of the resting fibre at high degrees of stretch. Finally, using L_α as length

[1] $N = N_\alpha + N_\beta$, the number of links in the chain.

unit the final expression for the length-tension diagram of the transmutation chain is:

$$L(p) = 1 + \frac{3}{1 + e^{-2p}}. \qquad (90)$$

This diagram is given in fig. 92b. For small loads the length-tension relation is linear, i. e. in this range the chain behaves approximately as a body with Hookean elasticity. With larger loads the length approaches asymptotically its limiting value, which referred to L_a as length unit is 4.

The equilibrium length L_0 of the chain, i. e. the length at load $P = 0$ is 2.5 according to (90). Hence, with the present assumptions the chain can be extended by only 60 per cent.

The length-tension diagram for the transmutation chain is similar to the static diagram of the resting muscle fibre (fig. 92a).

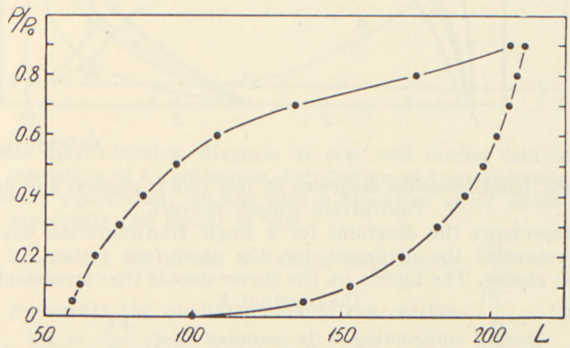

Fig. 92a. Static length-tension diagram at rest and the curve for the isotonic maxima for the muscle fibre (0° C.).
abscissa: length in per cent of L_0.
ordinate: load in units of P_0.

However, in two respects these two diagrams deviate from each other:

1) The transmutation chain can only be extended by 60 per cent, while the fibre can be stretched by more than 100 per cent, and 2) the muscle fibre at low loads displays only a small increase in tension with increasing length. Therefore, the equilibrium length of the transmutation chain is apparently too high. However, as discussed below, the difference can be understood, when a model

is used containing more than one transmutation chain, the different chains being connected by cross-linkages and forming a network.

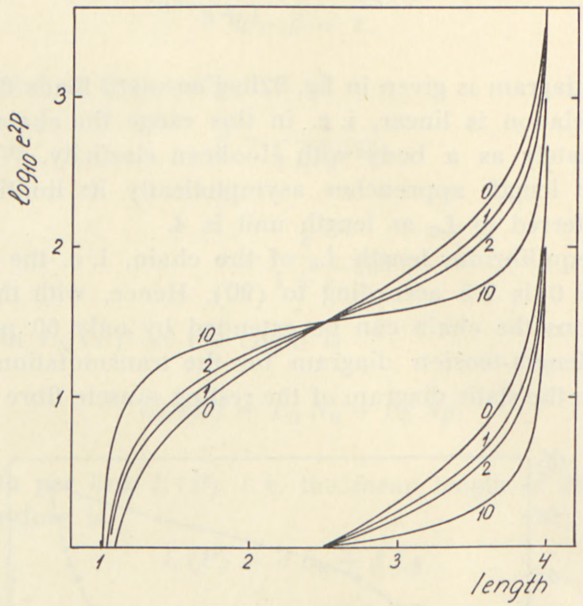

Fig. 92b. Static length-tension diagrams at rest (lower curves) and during tetanic contraction (upper curves).
0 represents the diagrams for a single transmutation chain.
1, 2 and 10 represent the diagrams for the slack-free system of cross-linked transmutation chains. The figures on the curves denote the corresponding values of the constant K.

During contraction it is assumed that: $\frac{FC}{D} = 30$.

abscissa: length per link in units of L_α.

ordinate: tension expressed as $\log_{10} e^{2P}$.

The length of the resting muscle fibre does not go to an asymptotic value when the load is large, as does the transmutation chain according to the present assumptions. This difference will disappear when the deformation is considered which is produced by an elasticity placed in series with the transmutation chain.

This element with Hookean elasticity will not be significantly deformed until the possibilities for changes in length by the $\alpha \rightarrow \beta$ transmutations are practically exhausted. It must be sought

mainly in the deformations of the α- and β-links themselves caused by the load (cf. p. 236).

When a single transmutation chain is used as an essential element in the structural interpretation of the static length-

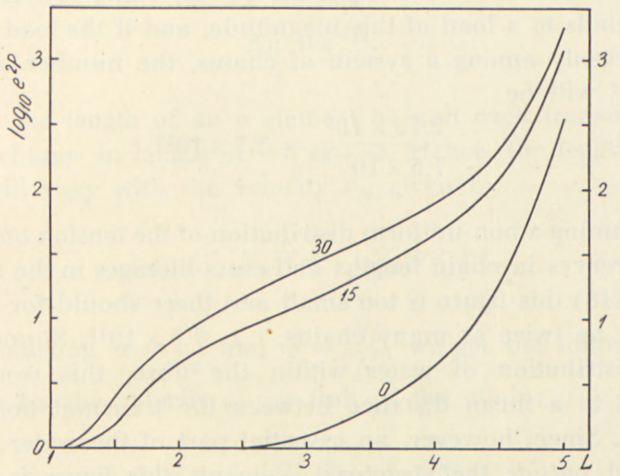

Fig. 92c. Static length-tension diagram at rest and during tetanic contraction for a system consisting of a continuous distribution of transmutation chains with different equilibrium lengths plus a Hookean series elasticity.

0 represents the model at rest.

15 represents the model in tetanic contraction: $\frac{FC}{D} = 15$.

30 represents the model in tetanic contraction: $\frac{FC}{D} = 30$.

The elongation caused by the series elasticity is assumed to be $0.20 \log_{10} e^{2p}$.

abscissa: length per link of the chain with the smallest L_0 in units of L_α.

ordinate: tension expressed as $\log_{10} e^{2p}$.

tension diagram of the muscle fibre, it is a prerequisite that the loads which normally act on the fibre correspond to loads on the transmutation chains which can actually produce an essential part of the possible deformations. Therefore, according to the theoretical length-tension diagram (fig. 92b) $2p$ must assume values of, e. g., 3.0 which corresponds to an elongation of 54.3 per cent in proportion to the 60 per cent which is obtainable. The following estimation shows that it is actually possible to arrive at such values of p. At 0° C. the temperature energy kT

is 3.74×10^{-14} erg. Therefore, at 0° C. $2\,p = 3$ corresponds to an external work of $2P\lambda = 1.12 \times 10^{-13}$ erg. Assuming that $L_\alpha = 5$ Å and $L_\beta = 20$ Å, i. e. that $2\,\lambda = L_\beta - L_\alpha = 15$ Å, $2\,p = 3$ corresponds to a value of P of 7.5×10^{-7} dynes. The maximum force (P_0) which the muscle fibre can develop in an isometric tetanic contraction is 2.75×10^6 dynes per cm² (0° C., Table 10). If $2\,p = 3$ corresponds to a load of this magnitude, and if the load is distributed evenly among a system of chains, the number of chains per cm² will be

$$\frac{2.75 \times 10^6}{7.5 \times 10^{-7}} = 3.7 \times 10^{12}.$$

Assuming a non-uniform distribution of the tension on account of differences in chain lengths and cross-linkages in the structure (cf. p. 248) this figure is too small and there should for example actually be twice as many chains, i. e. 7.5×10^{12}. Supposing an even distribution of water within the fibre, this would correspond to a mean distance between the transmutation chains of 36 Å. Since, however, an essential part of the water must be localized *outside* the structural elements this figure is reduced correspondingly, e. g. by a factor 1.5—2.5, and we arrive at values which appear reasonable in comparison with distances found from X-ray analysis of proteins of the *k-f-m* group (Astbury 1947).

Theory for isotonic transients applied to a transmutation chain.

The length-tension diagram derived for the single transmutation chain represented a static problem. The assumptions made enable us to deal with non-static problems as well. The basis of this treatment is the fact that the velocity of elongation is always proportional to the difference between the number of $\alpha \rightarrow \beta$ and $\beta \rightarrow \alpha$ transmutations per second. Each increase in length must arise from a relative increase in transmutations $\alpha \rightarrow \beta$ as compared with $\beta \rightarrow \alpha$.

Let us consider a chain without equilibrium in the $\alpha \rightleftarrows \beta$ transmutations. The chain is assumed to consist of a large number of elements N, N_α of which are in the α and N_β of which are in the β modification. When the chain is loaded by the load P_1, the

number of transmutations $\alpha \rightarrow \beta$ per second according to (80) will be

$$N_\alpha \cdot We^{p_1}$$

and the number of transmutations $\beta \rightarrow \alpha$ will be

$$N_\beta \cdot We^{-p_1}.$$

With the length of an α element as unit each transmutation gives a change in length of $+3$ or -3. Hence, the length of the chain will vary with the velocity v_N given by:

$$v_N = 3\,[N_\alpha We^{p_1} - N_\beta We^{-p_1}]. \tag{91}$$

By introducing $\alpha = \frac{N_\alpha}{N}$ and $\beta = \frac{N_\beta}{N}$, we get the following expression for the velocity v per link of the chain:

$$v = 3\,W\,[\alpha e^{p_1} - \beta e^{-p_1}]. \tag{92}$$

According to (88) the length of the chain per link is:

$$L = \alpha + 4\,\beta = 1 + 3\,\beta. \tag{93}$$

Hence, the velocity per element is:

$$v = 3\,\frac{d\beta}{dt}. \tag{94}$$

(92), (93), and (94) give the following differential equation relating the variation of L and P in time:

$$\frac{dL}{dt} = 3\,We^{p_1} - W\,(L-1)\,(e^{p_1} + e^{-p_1}),$$

i. e.

$$\frac{dL}{dt} = -\,W\,(e^{p_1} + e^{-p_1})\,L + W\,[4\,e^{p_1} + e^{-p_1}]. \tag{95}$$

Hence, if we know the variation of P_1 with time, we can determine the length L as a function of time from (95).

In applying these results to an isotonic transient, a transmutation chain originally in equilibrium with the load P at time zero is suddenly subjected to a change in load ΔP. Thereby the frequency of transmutations in the two directions, which originally is identical, will suddenly be changed and the transmutation frequency $\alpha \rightarrow \beta$ will be different from that for $\beta \rightarrow \alpha$. Thus, the chain will acquire a velocity of change in length aiming at bringing the chain to the length which corresponds to the static load $P + \Delta P$. The variation of length with time can be determined from (95) by putting $P_1 = P + \Delta P$ and introducing the initial condition

$$L = L(p) \quad \text{at time} \quad t = 0.$$

Thereby we get:

$$L(t) = L(p + \Delta p) - (L(p + \Delta p) - L(p))\, e^{-\frac{t}{\tau}}, \tag{96}$$

where

$$\frac{1}{\tau} = W(e^{p+\Delta p} + e^{-p-\Delta p}), \tag{97}$$

and where $L(p)$ and $L(p + \Delta p)$ represent the static length corresponding to load P and $P + \Delta P$. Thus, the transmutation chain goes exponentially from the initial length to the new final length, with a decay-time τ given by (97). This finding is of particular interest in relation to the Voigt-model applied to describe the reaction of the muscle fibre to an isotonic transient (Part II). It shows that the single transmutation chain reacts to an isotonic transient as a Voigt-element with the elastic stiffness:

$$G_{\text{elast}} = \frac{\Delta P}{L(p+\Delta p) - L(p)} \tag{98}$$

and a retardation time τ given by (97). Hence, the distribution of retardation times characterizing the Voigt-model for the muscle fibre, can be partly understood by using as a model for the muscle fibre a system of cross-linked transmutation chains, in which there is a non-uniform distribution of tension. However, the prolonged creep in the muscle fibre must be considered,

as we have discussed in Part II of this paper, to be due chiefly to the disrupture and reformation of points of entanglement. The dynamic stiffness of the muscle fibre which is determined by the short retardation times (p. 105) arises therefore chiefly from transmutations within the molecule and only to a minor degree from transitions in the texture.

The initial velocity v_0 in the isotonic transient is obtained from (92), when P_1 is put equal to $P + \Delta P$ and α and β are given by (85) and (86).

Hence v_0 is

$$v_0 = 3\,W\left[e^{p+\Delta p}\cdot\frac{1}{1+e^{2p}} - e^{-p-\Delta p}\cdot\frac{1}{1+e^{-2p}}\right] \qquad (99)$$

or

$$v_0 = 3\,W\frac{e^{\Delta p}-e^{-\Delta p}}{e^{p}+e^{-p}}. \qquad (100)$$

By means of this expression and the experimentally found initial velocities in isotonic transients a rough estimation can be attempted of the frequency of transmutation W. With an initial velocity of 10—30 L_0 per sec. = 10—30·2.5 L_α units per sec. (see isotonic transients Table 2) and assuming $2\,p_0 = 3$, we get with $\Delta P = 3\,P$ for small loads values for W of 20—60 $\sec^{-1}$.

However, evidence has been presented in the preceding parts of this paper, that in the transient experiments with large deformations cross-linkages will play a rôle even within the short time interval used for the determination of the initial velocity (5—20 msec.). Hence, the actual values of W must exceed considerably the estimate given here.

Static length-tension diagram for a system of cross-linked transmutation chains.

As emphasized above, a single transmutation chain does not describe satisfactorily the length-tension relationship of the resting fibre. The initial slope calculated for the transmutation chain deviates from that of the fibre.

A more adequate picture of the minute structure comprises a system of transmutation chains which are more or less randomly cross-linked and rather well orientated along the fibre

axis, but which are not necessarily of the same length (i. e. they do not consist of the same number of links). This model is analysed for two simplified cases:

1) a system consisting of parallel chains with different equilibrium length (influence of slack).

2) a cross-linked system of chains without slack (influence of cross-linkages).

1. The length-tension diagram of a system of parallel chains with different numbers of links shows good agreement with the length-tension diagram of the resting muscle fibre. Let us consider a system of chains with the number of links ranging between N_1 and N_2 (both $\gg 1$) and for the sake of simplicity we assume that the different numbers of links are equally probable. The chains are supposed to be coupled at the ends. Therefore, the equilibrium length of the system, i. e. its length at load zero is:

$$L_0 = 2.5 \cdot N_1. \tag{101}$$

The maximum elongation which is possible remains 60 per cent. This implies that chains with a number of links $N > 1.6\, N_1$ never will participate in the load. If the system has a length L, the chains whose equilibrium length is $< L$ will be loaded, the condition being:

$$L > 2.5 \cdot N$$

or

$$N < 0.4\, L. \tag{102}$$

A chain with a number of links which fulfils this condition will be under load $p\,(N)$ determined by

$$L = N \cdot \left[1 + \frac{3}{1 + e^{-2\,p\,(N)}}\right],$$

i. e.

$$2\,p\,(N) = \log \frac{L - N}{4\,N - L}. \tag{103}$$

According to the assumption concerning the distribution of the number of links in the chains the mean tension p is:

$$p = \frac{1}{N_2 - N_1} \sum_{N=N_1}^{N_{max}} p(N), \tag{104}$$

where N_{max} denotes the lowest value of N_2 and $0.4\,L$. By introducing $n = \frac{N}{N_1}$ and by replacing the summation (104) with an integration we get from (103)

$$2\,p = \frac{1}{n_2 - 1} \int_1^{n_{max}} \log \frac{L/N_1 - n}{4\,n - L/N_1}\, dn$$

or

$$2\,p = \frac{1}{n_2 - 1} \Big[(L/N_1 - 1) \log (L/N_1 - 1) - (L/N_1 - n_{max}) \log (L/N_1 - n_{max}) + \frac{1}{4} (4 - L/N_1) \log (4 - L/N_1) - \frac{1}{4} (4\,n_{max} - L/N_1) \cdot \log (4\,n_{max} - L/N_1) \Big]. \tag{105}$$

By assuming a variation in the equilibrium length of the chains of e. g. 30 per cent, i. e. with $N_2 = 1.3\,N_1$, and putting an elasticity in series with the system, we get the length-tension diagram shown in fig. 92 c. With regard to the series elasticity, which must be considered to have both a crystalline and a kinetic component, we have assumed it to increase in length by 0.2 L_a units per unit of load expressed as $\log_{10} e^{2p}$.

It is seen that the initial course of the length-tension diagram which we have obtained, corresponds to that experimentally found in the muscle fibre (fig. 92 a).

These calculations show the effect on the length-tension diagram of slack in the fibre structure, since the parallel chains of different "length" can be considered to correspond to the chains situated between cross-linkages in the structure.

2. Correspondingly we can deal with the isolated effect of cross-linkages. For this purpose we disregard slack and possible different numbers of links in the chains.

Hence, a system will be considered consisting of parallel cross-linked transmutation chains with the same number of links and acted upon by the load p. We assume continuous disrupture and reformation of cross-linkages in the structure. The cross-linkage is

assumed to consist of a coupling of links of the same type. These aggregates can include links from more than two chains, since it is assumed that each link is able to form two cross-linkages.

The probability per second of the formation of a cross-linkage is postulated to be proportional to the possibility for the presence of cross-linkages in the adjacent chains. The proportionality factor is denoted by C_1. The probability per second of disrupture of a cross-linkage is assumed to be constant independent of the load and the size of the aggregate. It is denoted by C_2. The links are grouped according to what type of aggregate they belong to, i. e. aggregates with 2, 3, 4, $\cdots$ links, respectively.

Let us consider a system of chains in which the total number of links is N, N_α of which are α-links and N_β of which are β-links. The system is assumed to contain M aggregates, M_α of which are α-aggregates and M_β of which are β-aggregates. α_2, α_3, α_4 denote the number of aggregates with 2, 3 and 4 links and α_1 the number of free α-links. A corresponding notation is used for the β-links. Then there exist the following relationships between the number of aggregates and the number of α- and β-links:

$$M_\alpha = \alpha_1 + \alpha_2 + \alpha_3 + \cdots \tag{106}$$

$$M_\beta = \beta_1 + \beta_2 + \beta_3 + \cdots \tag{107}$$

and

$$N_\alpha = \alpha_1 + 2\,\alpha_2 + 3\,\alpha_3 + \cdots \tag{108}$$

$$N_\beta = \beta_1 + 2\,\beta_2 + 3\,\beta_3 + \cdots \tag{109}$$

and

$$M = M_\alpha + M_\beta \tag{110}$$

$$N = N_\alpha + N_\beta. \tag{111}$$

As previously we use

$$\alpha = \frac{N_\alpha}{N} \quad \text{and} \quad \beta = \frac{N_\beta}{N}. \tag{112}$$

The length per link in a chain measured in units of L_α is determined by (93)

$$L = 1 + 3\,\beta. \tag{113}$$

In determining the static length-tension diagram simple equilibrium considerations are again applied. It is assumed that only

free elements participate in the transmutations $\alpha \rightleftarrows \beta$. This is justified since the activation energy for a transmutation of an aggregate must be considerably larger than for a single link.

In the stationary state, where we have constant length, the frequency of transmutation $\alpha \rightarrow \beta$ is equal to that of $\beta \rightarrow \alpha$, i. e.

$$a_1 We^{P} = \beta_1 We^{-P}, \tag{114}$$

i. e.

$$\frac{\beta_1}{a_1} = e^{2p}. \tag{115}$$

Moreover, the same number of α-links must enter and leave the aggregates per second, i. e.

$$2 C_2 (a_2 + a_3 + \cdots) = C_1 a_1 \cdot \frac{a_1 + a_2 + a_3 + \cdots}{N}. \tag{116}$$

In this formula, according to the assumptions above, the expression to the left gives the number of free α-links formed per second and the expression to the right gives the number of free α-links, which are taken up in aggregates.

Introducing the constant K:

$$K = \frac{C_1}{C_2}, \tag{117}$$

we get from (116) and (106)

$$2 (M_\alpha - a_1) = K \frac{a_1}{N} \cdot M_\alpha,$$

i. e.

$$a_1 = \frac{2 M_\alpha}{2 + K \cdot \frac{M_\alpha}{N}}. \tag{118}$$

The number of α-aggregates containing n elements is constant as well; expressed mathematically this gives:

$$\left.\begin{aligned}\sum_{r=1}^{\frac{n''}{2}} C_1 \alpha_r \cdot \frac{\alpha_{n-r}}{N} \cdot \frac{1}{1+\delta_{r,n-r}} + 2\,C_2\,(\alpha_{n+1}+\alpha_{n+2}+\cdots\cdot) \\ = C_2 \cdot (n-1)\,\alpha_n + C_1\,\alpha_n \cdot \frac{\alpha_1+\alpha_2+\cdots\cdot}{N}\end{aligned}\right\} \quad (119)$$

where

$$\delta_{r,n-r} = \begin{cases} 0 & \text{for} \quad r \neq \frac{n}{2} \\ 1 & \text{for} \quad r = \frac{n}{2}, \end{cases} \quad (120)$$

and where $\frac{n''}{2}$ indicates a summation to $r \leqq \frac{n}{2}$.

(119) is transformed to

$$K \cdot \sum_{r=1}^{\frac{n''}{2}} \alpha_r \frac{\alpha_{n-r}}{N} \cdot \frac{1}{1+\delta_{r,n-r}} + 2\,(M_\alpha - \alpha_1 - \alpha_2 - \cdots - \alpha_n) = (n-1)\,\alpha_n + K\alpha_n \cdot \frac{M_\alpha}{N}.$$

Hence,

$$\alpha_n = \frac{2\,(M_\alpha - \alpha_1 - \alpha_2 \cdots - \alpha_{n-1}) + K \sum_{r=1}^{\frac{n''}{2}} \alpha_r \frac{\alpha_{n-r}}{N} \cdot \frac{1}{1+\delta_{r,n-r}}}{n+1+K \cdot \frac{M_\alpha}{N}}. \quad (121)$$

Corresponding expressions can be derived for the β-links and for the sake of simplicity let us apply the same value for the constant K.

Expressions (118) and (121) and the corresponding expressions for the β-links make it possible to compute the aggregate distribution as a function of $\frac{M_\alpha}{N}$ and $\frac{M_\beta}{N}$. This is shown in fig. 93 a, b, c for α_1, α_2, $\cdots\cdot$ with the values 1, 2, and 10 for K.

In order to derive a length-tension diagram, in the first place we need to determine α and β or N_α and N_β as a function of $\frac{M_\alpha}{N}$ and $\frac{M_\beta}{N}$. This is done by means of expressions (108), (109),

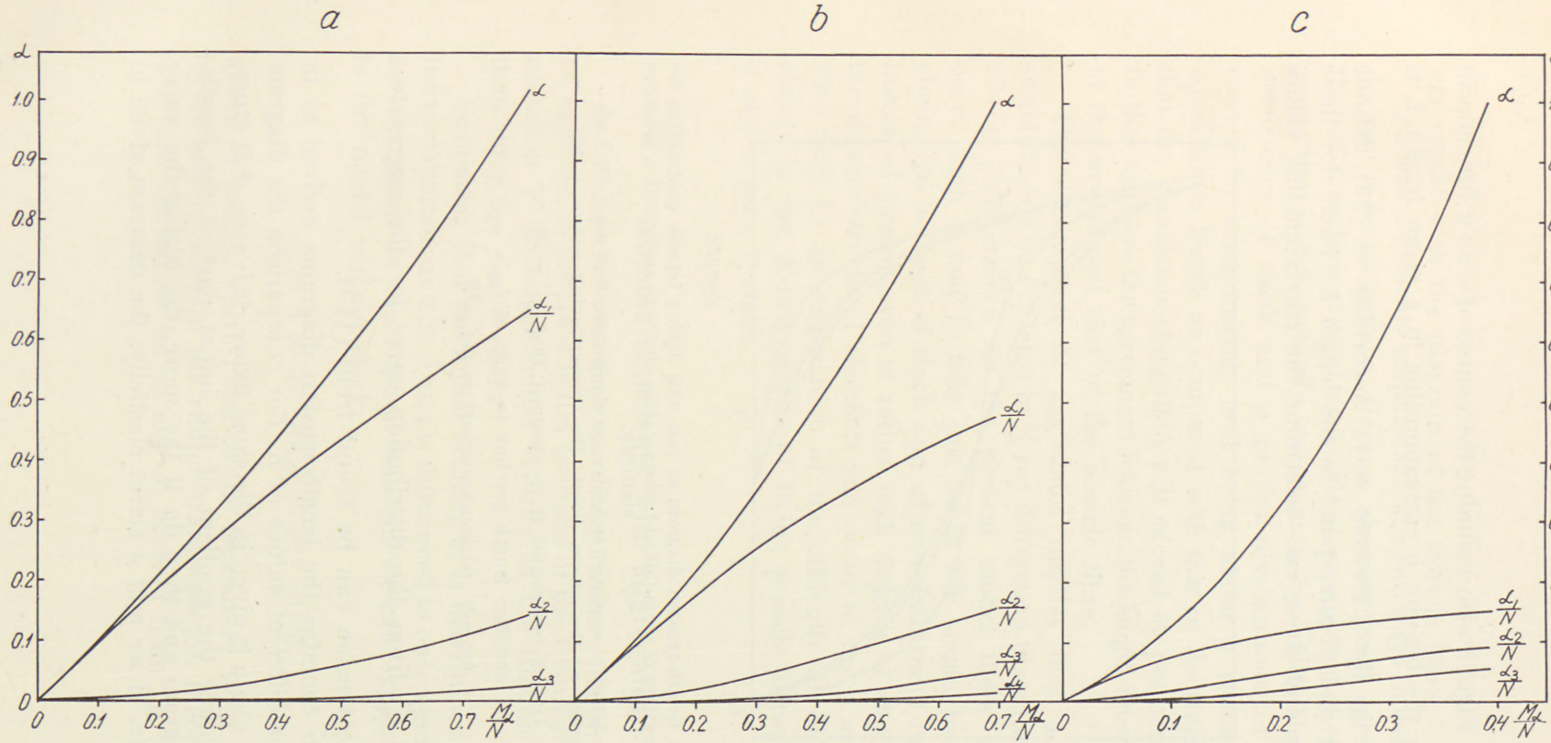

Fig. 93. The aggregate distribution for the slack-free system of cross-linked transmutation chains.

a. $K = 1$ *b*. $K = 2$ *c*. $K = 10$ (see text).

abscissa: $\frac{M_\alpha}{N}$, i. e. the number of α-aggregates per link.

ordinate: $\frac{a_n}{N}$, i. e. the number of α-aggregates consisting of n links per link of the system.

and (112). Fig. 93 also contains the course of α as a function of $\frac{M_\alpha}{N}$. Finally the tension p corresponding to a given length L is determined in the following way: According to (93) definite values of α and β correspond to the length L. Then, for these values of α and β we can determine the corresponding values

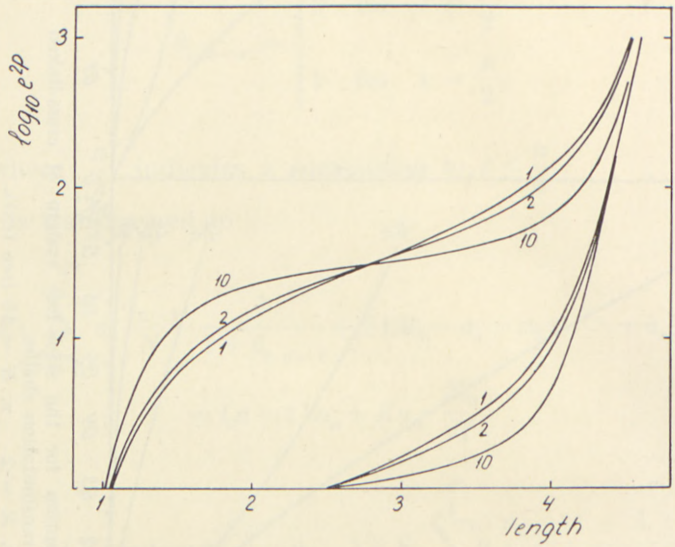

Fig. 94. Static length-tension diagram at rest and during tetanic contraction for the slack-free system of cross-linked transmutation chains in series with a Hookean elasticity.

The latter is assumed to cause an elongation: $0.20 \log_{10} e^{2p}$.

The figures on the curves denote the corresponding values of K.

During contraction it is assumed that $\frac{FC}{D} = 30$.

abscissa: length per link in units of L_α.

ordinate: tension expressed as $\log_{10} e^{2p}$.

for $\frac{\alpha_1}{N}$ and $\frac{\beta_1}{N}$ from the distribution curve for the aggregates. Finally, the tension can be found from (115).

Fig. 92b contains the length-tension diagrams arrived at in this way for different values of K. For comparison the diagram for a single chain is given in the same figure. It is seen that cross-linkages reduce the gradient of the initial part of the length-tension diagram and they do it the more, the higher the value of K we use. If we add a series elasticity, the diagram given in

fig. 94 is obtained. For a value of $K = 2$ we get a satisfactory agreement with the diagram of the muscle fibre.

As was previously emphasized, the two ways in which we have derived a length-tension diagram showing good agreement with that of muscle represent an artificial separation of two essential properties which actually occur side by side. Moreover, the occurrence of slack and a partial disalignment of the chains caused by cross-linking, will bring about a reduction in the equilibrium length as compared with that of the single chains so that the maximum elongation will exceed 60 per cent. This will further improve the agreement between the length-tension diagram of the model and that of the muscle fibre.

The assumption of aggregates implies that a crystalline structure can be expected in X-ray diffraction diagrams (ASTBURY 1947). Furthermore, in the present model there will always occur both α and β links just as in the single transmutation chain. On account of slack and of non-uniformity in the distribution of tension even at rather high degrees of stretch, part of the minute structural elements will occur in the α modification. This may be an explanation of the difficulty of differentiating clearly in the X-ray pattern of living muscle between a pure α and a pure β state.

Isotonic transients with aggregates.

As indicated above, the cross-linked transmutation model can be expected to permit a better estimate of the frequency of transmutation W from the initial velocity in the isotonic transients than does the single chain.

Supposing that the initial velocity v_0 is determined chiefly by the transmutations $\alpha \rightleftarrows \beta$ and is influenced to only a minor degree by alterations in the textural pattern, we can expect according to the model without slack:

$$v_0 = 3\, W\, [e^{p+\Delta p}\, \alpha_1 - e^{-p-\Delta p}\, \beta_1], \qquad (122)$$

where α_1 and β_1 correspond to the tension P. With the values for p_0 and v_0 used in the simple transmutation theory (p. 247) and with the values for α_1 and β_1 derived from fig. 93 we find

that $K = 2$ gives an increase in W of 50 per cent as compared with the single chain (20—60 sec.$^{-1}$) while $K = 10$ gives an increase of 400 per cent.

Theory for contraction of the transmutation chain.

As indicated in Parts II and III of this paper the minute structure of the contracted fibre is assumed not to differ in principle from that of the resting fibre. Therefore, the contracted fibre is considered to consist of a system of more or less randomly cross-linked, rather well aligned transmutation chains. The decrease in length in contraction is taken as an expression of a relative increase in the number of links in the α modification. The increase is assumed to arise from a reduction in the probability of transmutation from the short to the long modifications, i. e. a number of α links are assumed to be excluded from a transmutation. This is supposed to be realized by a *fixation* of links in the α-form in such a way that they are prevented from participating in the $\alpha \rightleftarrows \beta$ transmutations (fig. 91). The fixation is assumed directly or indirectly to be brought about by the stimulus. For the time being the physico-chemical correlate of this fixation can only be a matter for speculation. Thus, it remains an open question whether the fixation consists in the removal or the addition of a "chemical unit" from or to the link. Speculations as to the nature of this unit whether an atomic particle or a more complex molecule, and with respect to its relation to the actin-myosin model and to the interaction between adenosine triphosphate and acto-myosin, seem to us to be premature.

In the active phase we assume a continuous fixation and defixation (i. e. disappearance of fixation) of α links. The frequency of fixation is assumed to be proportional to the concentration C of a fixation agent (factor) and to the number of possibilities for fixation, i. e. proportional to the number of non-fixated α links. The frequency of defixation on the other hand is supposed to be proportional to the number of α links in the fixated state.

Let us first apply these considerations to a single transmutation chain and investigate how far mechanical properties characterizing contraction can be described in terms of this

simple conception. Referred to a given load the activated chain contains a certain fraction β of links in the β state, another fraction α_1 in the transmutable α state and finally a fraction α_f in the fixated α state. Thus we have:

$$\alpha_1 + \alpha_f + \beta = 1. \tag{123}$$

In an equilibrium state, i. e. when the frequency of transmutation $\alpha \rightarrow \beta$ is equal to the frequency of transmutation $\beta \rightarrow \alpha$, we have in analogy to the resting chain:

$$\alpha_1 We^{p} = \beta We^{-p},$$

i. e.

$$\frac{\beta}{\alpha_1} = e^{2p}. \tag{124}$$

The static length-tension diagram of the "tetanically contracted" transmutation chain.

As mentioned above, the activated state is characterized by the concentration C of a fixating element. C is considered constant on the tetanic level of a contraction. According to our general assumptions the number of fixations and defixations per link of the chain per time unit is

$$FC\alpha_1 \text{ (fixation) and}$$

$$D\alpha_f \text{ (defixation),}$$

where F and D are proportionality factors. In the stationary state corresponding to static length and tension these two frequencies are equal and the condition for equilibrium $\alpha_f \rightleftarrows \alpha_1$ therefore is:

$$FC\alpha_1 = D\alpha_f. \tag{125}$$

For α_1, α_f and β we have (123), (124), and (125), which give

$$\beta = \frac{1}{1 + \left(1 + \frac{FC}{D}\right) e^{-2p}}. \tag{126}$$

By introducing this value for β in the expression (93) for the length L per element expressed in units of L_a we get the length-tension diagram in contraction:

$$L_{\text{contr}}(p) = 1 + \frac{3}{1 + \left(1 + \frac{FC}{D}\right) e^{-2p}}. \tag{127}$$

It is seen that the parameters F, C, and D only enter as $\frac{FC}{D}$. With $\frac{FC}{D} = 0$ the expression (127) corresponds to the length-tension diagram of the "resting" chain.

Putting

$$1 + \frac{FC}{D} = e^{2p_{\text{extra}}}, \tag{128}$$

i. e. introducing

$$2p_{\text{extra}} = \log\left(1 + \frac{FC}{D}\right), \tag{129}$$

(127) assumes the simple form:

$$L_{\text{contr}}(p) = 1 + \frac{3}{1 + e^{-2(p - p_{\text{extra}})}}. \tag{130}$$

Comparing this expression (130) for the length-tension diagram in tetanic contraction with that derived for the resting chain (90) we see that at a given length $>$ the equilibrium length the static tension in contraction exceeds the static tension of the resting chain by the constant amount p_{extra}. Hence, the simple transmutation chain is characterized by a constant extra tension in an isometric tetanic contraction. Moreover, it is seen from (130) that the part of the length-tension diagram which corresponds to lengths < 2.5 can be derived as the mirror image through the point $(2.5, p_{\text{extra}})$ of that part which exceeds the length 2.5.

The curves in fig. 95 show the length-tension diagram of the contracted transmutation chain given by (130) for different values of $\frac{FC}{D}$. When $\frac{FC}{D}$ exceeds 5, the diagram acquires a pronounced S-shaped course. There is good agreement with the experimental findings on the muscle fibre, both for the curve of the isometric and of the isotonic maxima. It should be noted that for the transmutation chain the isotonic and the isometric maxima coincide.

The experimental fact that isotonic and isometric maxima for the muscle fibre do not coincide and that the extra tension decreases at high degrees of stretch can be understood from the more complicated model with cross-linked chains (cp. Part III).

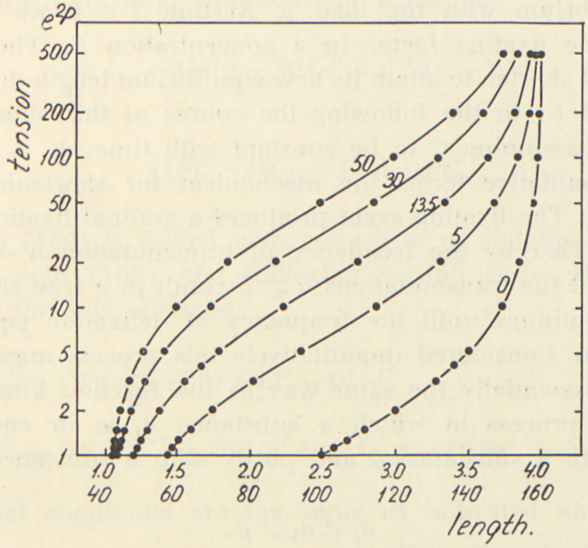

Fig. 95. Static length-tension diagram at rest and during tetanic contraction for the transmutation chain.

0. Rest.

5, 13.5, 30 and 50. Tetanic contraction. The figures on the curves denote the corresponding values of $\frac{FC}{D}$.

abscissa: length per link in units of L_a and in per cent of the equilibrium length ($L_0 = 100$).

ordinate: tension (e^{2p} in logarithmic scale).

The theoretical curves obtained for low values of $\frac{FC}{D}$ should correspond to the diagram of the muscle fibre at low degrees of contraction.

The *dynamic stiffness* of the muscle fibre which is considered to arise mainly from the transmutations within the contractile chains will increase when the transmutation (deformation) of certain elements is impeded. Thus, the fixation of links can account for part of the increase in stiffness which characterizes contraction. This contribution is approximately inversely proportional to $1 - a_f$. As to the other factors involved in the increase in stiffness see changes in texture p. 105.

Shortening- and relaxation velocity in the single transmutation chain.

We shall consider a transmutation chain at rest which is in equilibrium with the load p. At time $t = 0$ we suddenly release the fixating factor in a concentration C. Thereby the chain will shorten to attain its new equilibrium length determined by p and C. In the following the course of this shortening is analysed assuming C to be constant with time.

In qualitative terms the mechanism for shortening is the following: The fixating agent produces a gradual fixation of free α links. Thereby the frequency of transmutation $\alpha \rightarrow \beta$ is reduced and the transmutations $\alpha \rightleftarrows \beta$ result in a true shortening, which continues until the frequency of defixation equals that of fixation. Considered quantitatively this process may be dealt with in esssentially the same way as the reaction kinetics of a chemical process in which a substance a_1 is in equilibrium partly with a substance β and partly with a substance a_f

$$a_f \rightleftarrows a_1 \rightleftarrows \beta. \tag{131}$$

The fixating elements can be compared with a catalyser which makes possible the formation of a_f. In the following mathematical treatment a_1, a_f, and β are studied as functions of time.

With the former assumptions we get the following equations of motion for the course of shortening:

$$\frac{d\beta}{dt} = W\left[a_1 e^{p} - \beta e^{-p}\right] \tag{132}$$

$$\frac{da_1}{dt} = W\left[\beta e^{-p} - a_1 e^{p}\right] + D a_f - FC a_1 \tag{133}$$

$$\frac{da_f}{dt} = FC a_1 - D a_f \tag{134}$$

with the initial conditions at time zero:

$$\beta = \frac{1}{1+e^{-2p}}, \quad a_1 = \frac{1}{1+e^{2p}} \quad \text{and} \quad a_f = 0.$$

According to (123)

$$\alpha_1 = 1 - \alpha_f - \beta. \tag{135}$$

When this is introduced in (132) and (134) we get the following two differential equations for β and α_f:

$$\frac{d\beta}{dt} = -We^p \alpha_f - W(e^p + e^{-p})\beta + We^p, \tag{136}$$

$$\frac{d\alpha_f}{dt} = -(FC + D)\alpha_f - FC\beta + FC. \tag{137}$$

When (136) is solved with respect to α_f and the result introduced into (137), the following second order differential equation for β is obtained:

$$\left.\begin{aligned} &\frac{d^2\beta}{dt^2} + [W(e^p + e^{-p}) + FC + D]\frac{d\beta}{dt} \\ &\quad + [FCWe^{-p} + DW(e^p + e^{-p})]\beta - DWe^p = 0. \end{aligned}\right\} \tag{138}$$

The initial conditions are the same as indicated above, viz.: at $t = 0$

$$\beta = \frac{1}{1 + e^{-2p}} \quad \text{and} \quad \frac{d\beta}{dt} = 0.$$

The general solution of (138) is of the form:

$$\beta(t) = c_1 e^{-\lambda_1 t} + c_2 e^{-\lambda_2 t} + \beta_{\text{contr}}, \tag{139}$$

where the constants λ_1 and λ_2 are given by:

$$\left.\begin{aligned} \lambda_1 + \lambda_2 &= W(e^p + e^{-p}) + FC + D \\ \lambda_1 \cdot \lambda_2 &= W[FCe^{-p} + D(e^p + e^{-p})]. \end{aligned}\right\} \tag{140}$$

β_{contr} according to (138) is:

$$\left.\begin{aligned} \beta_{\text{contr}} &= \frac{DWe^p}{FCWe^{-p} + DW(e^p + e^{-p})} \\ &= \frac{1}{1 + \left(1 + \frac{FC}{D}\right)e^{-2p}}. \end{aligned}\right\} \tag{141}$$

The integration constants c_1 and c_2 are given by the initial conditions:

$$\frac{1}{1+e^{-2p}} = c_1 + c_2 + \frac{1}{1+\left(1+\frac{FC}{D}\right)e^{-2p}} \tag{142}$$

and

$$0 = c_1\lambda_1 + c_2\lambda_2.$$

The solution introduced in (139) gives

$$\left.\begin{aligned}\beta(t) = &\left(\frac{1}{1+e^{-2p}} - \frac{1}{1+\left(1+\frac{FC}{D}\right)e^{-2p}}\right)\cdot \\ &\left[\frac{\lambda_2}{\lambda_2-\lambda_1}e^{-\lambda_1 t} - \frac{\lambda_1}{\lambda_2-\lambda_1}e^{-\lambda_2 t}\right] + \beta_{\text{contr}}.\end{aligned}\right\} \tag{143}$$

Hence, the length $L(t) = 1 + 3\beta(t)$ changes as a function of time according to:

$$L(t) = L_{\text{contr}} + \Delta L\left[\frac{\lambda_2}{\lambda_2-\lambda_1}e^{-\lambda_1 t} - \frac{\lambda_1}{\lambda_2-\lambda_1}e^{-\lambda_2 t}\right], \tag{144}$$

where the final shortening ΔL is

$$\Delta L = L_{\text{rest}} - L_{\text{contr}} = 3\left[\frac{1}{1+e^{-2p}} - \frac{1}{1+\left(1+\frac{FC}{D}\right)e^{-2p}}\right]. \tag{145}$$

The *shortening velocity* $V(t)$ expressed in units of L_a per second is per link of the chain according to (144):

$$V(t) = -\frac{dL}{dt} = \frac{\lambda_1\lambda_2}{\lambda_2-\lambda_1}\Delta L\,[e^{-\lambda_1 t} - e^{-\lambda_2 t}]. \tag{146}$$

In accordance with the assumptions made about the initial state it is seen from this expression that the shortening as a function of time begins with the velocity zero. By differentiation of (146) we find that the velocity is at its maximum at time t_0 determined by:

$$\lambda_1 e^{-\lambda_1 t_0} = \lambda_2 e^{-\lambda_2 t_0},$$

i. e.

$$t_0 = \frac{1}{\lambda_2-\lambda_1}\log\frac{\lambda_2}{\lambda_1}. \tag{147}$$

The shortening $\Delta L(t_0)$ in this state according to (144) is

$$\Delta L(t_0) = L_{\text{rest}} - L(t_0) = \Delta L\left[1 - \left(\frac{\lambda_2}{\lambda_2 - \lambda_1} e^{-\lambda_1 t_0} - \frac{\lambda_1}{\lambda_2 - \lambda_1} e^{-\lambda_2 t_0}\right)\right]$$

or according to (147):

$$\Delta L(t_0) = \Delta L\left[1 - \frac{\lambda_2}{\lambda_2 - \lambda_1}\left(\frac{\lambda_2}{\lambda_1}\right)^{-\frac{\lambda_1}{\lambda_2 - \lambda_1}} + \frac{\lambda_1}{\lambda_2 - \lambda_1} \cdot \left(\frac{\lambda_2}{\lambda_1}\right)^{-\frac{\lambda_2}{\lambda_2 - \lambda_1}}\right]. \quad (148)$$

The course of shortening in the muscle fibre starts with a maximal velocity after a latent period of about 25 msec. (0° C.). Therefore, the parameters of the transmutation chain λ_1 and λ_2 are adjusted in such a way that the maximal shortening velocity is reached when only a minor part of the shortening has been attained. According to (148) this will be the case when

$$\lambda_2 \gg \lambda_1. \quad (149)$$

For example $\frac{\lambda_2}{\lambda_1} = 20$ gives

$$\frac{\Delta L(t_0)}{\Delta L} = 0.10 \quad \text{and} \quad \lambda_1 t_0 = 0.16$$

and $\frac{\lambda_2}{\lambda_1} = 100$ gives $\frac{\Delta L(t_0)}{\Delta L} = 0.036$ and $\lambda_1 t_0 = 0.046$.

According to the equations (140) defining λ_1 and λ_2, the condition (149) is fulfilled when

$$\left.\begin{aligned} FC &\ll W, \\ \text{and thus also} \quad D &\ll W. \end{aligned}\right\} \quad (150)$$

These assumptions imply that fixation and defixation are considered to be slow processes as compared with the transmutations $\alpha \rightleftarrows \beta$. That this is justified can be seen from the curves in fig. 86 showing the course of relaxation, i. e. the course of elongation after the cessation of tetanic stimulation, and the course of the change in length after a quick unloading. The latter, which

must be determined chiefly by the $\alpha \rightleftarrows \beta$ transmutations, proceeds with much higher velocity than the process of relaxation (desactivation), the course of which is determined by FC and D as well (see below).

With the assumption given in (149), the course of shortening as a function of time (144) is practically exponential with the time constant λ_1, since the term of the expression containing $e^{-\lambda_2 t}$ will soon attain values which are extremely small as compared with $e^{-\lambda_1 t}$. This course of shortening as a function of time is seen in fig. 98 a for different values of e^{2p}, with $FC = 9$ sec.$^{-1}$ and $\frac{FC}{D} = 30$. A comparison shows good agreement between these curves and the experimentally found time course of shortening in isotonic tetanic contraction (fig. 98 b).

Thus, the theory for the contraction of the transmutation chain can account for the decrease in shortening velocity with time in the muscle fibre. In qualitative terms this can be understood in the following way: at the moment of stimulation, when most α links are available for fixation, the velocity of fixation is maximal and with a certain delay (t_0, cf. p. 262) gives rise to a maximal shortening velocity. Then, the velocity decreases owing to the gradual decrease in the possibilities of fixation. This decrease is counteracted only partially and little by little through the formation of new α links by thermal agitation.

The maximal shortening velocity V_0 according to (146), (147) and (149) is

$$V_0 \approx \lambda_1 \Delta L. \tag{151}$$

Thus, $\frac{\lambda_2}{\lambda_1} = 20$ gives: $V_0 = 0.85\ \lambda_1 \cdot \Delta L$ and $\frac{\lambda_2}{\lambda_1} = 100$ gives: $V_0 = 0.955\ \lambda_1 \cdot \Delta L$.

λ_1 can be determined from the ratio $\frac{\lambda_1 \lambda_2}{\lambda_2 - \lambda_1}$ in equation (140). Thus, assuming (149) we get

$$\lambda_1 \approx \frac{W\left[FCe^{-p} + D\left(e^{p} + e^{-p}\right)\right]}{W\left(e^{p} + e^{-p}\right) + FC + D} \approx \frac{FC}{1 + e^{2p}} + D. \tag{152}$$

Introducing (152) and (145) in (151) we get the following ap-

proximate expression for the maximum shortening velocity of a transmutation chain:

$$V_0 \approx \frac{3\,FC}{(e^p + e^{-p})^2}. \tag{153}$$

This expression can also be derived from the following simple arguments, which are applicable in the analysis of other properties of the transmutation chain as well.

Assuming that the transmutations represent quick processes as compared with both fixation and defixation, it is justified to suppose that the following relation is valid during the whole course of shortening:

$$\frac{\beta}{a_1} \approx e^{2p}. \tag{154}$$

Introducing this in (123) we get

$$\beta \approx \frac{1 - a_f}{1 + e^{-2p}}. \tag{155}$$

Hence:

$$\frac{d\beta}{dt} \approx -\frac{1}{1 + e^{-2p}} \cdot \frac{da_f}{dt}. \tag{156}$$

The initial velocity with which the a elements are fixated according to (134) is:

$$-\left(\frac{da_f}{dt}\right)_{\text{init}} = \frac{FC}{1 + e^{2p}}. \tag{157}$$

Introducing (157) in (156) one obtains

$$-\left(\frac{d\beta}{dt}\right)_{\text{init}} \approx \frac{FC}{(1 + e^{2p})\,(1 + e^{-2p})}. \tag{158}$$

This corresponds to the expression (153) for the maximal shortening velocity V_0.

The *force-velocity relation* expressed by (153) is given in fig. 96. With $FC = 9$ sec.$^{-1}$ and $e^{2p_0} = 100$, the theoretical curve shows relatively good agreement with the experimental

one obtained from the muscle fibre. This must be considered an expression of an actual agreement between theory and experiment in the range of loads examined. However, it must be kept in mind that the experimental shortening velocity is the external velocity and not the velocity with which the contractile

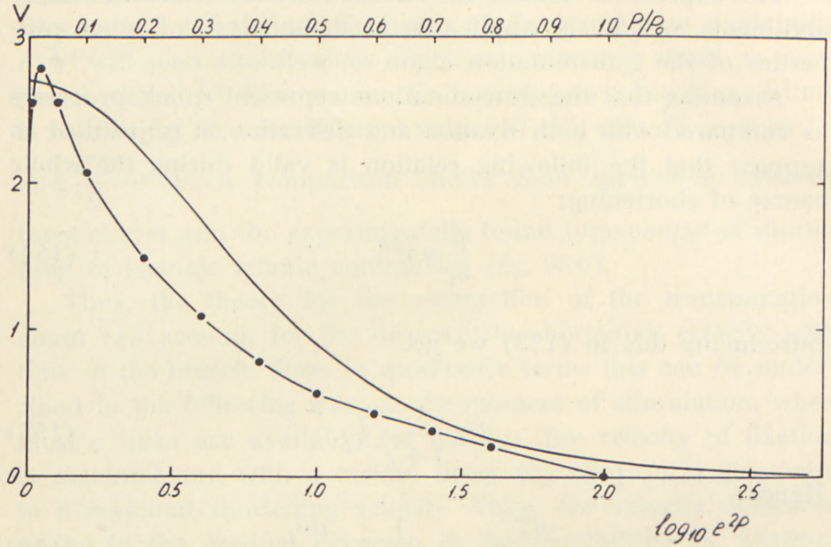

Fig. 96. Maximum shortening velocity as a function of the load for the transmutation chain and for the muscle fibre.
Upper curve: transmutation chain.
Lower curve: muscle fibre (0° C.).
abscissa: above: load on the fibre in units of P_0;
below: tension in the chain expressed as $\log_{10} e^{2P}$.
ordinate: shortening velocity in L_0 per sec.

substance itself shortens. Thereby the difference between the experimental and the computed curves can be accounted for in the following way: the initial maximum which is found in the experimental curve has been interpreted as being caused by the take-up of the slack, which must be most pronounced at small lengths. The fact that the experimental curve has a steeper slope at moderate loads in a range in which the theoretical curve is slightly concave towards the abscissa is explained by the changes of the flow velocity with the load which occur in the visco-elastic series element of the muscle fibre. At low loads the flow velocity must increase with increasing load on account of an increasing pro-

bability of disrupture of points of entanglement. At high loads the possibilities of a flow are restricted owing to the better alignment of the structure (cf. p. 205, Part III).

The variation in time of the degree of fixation α_f can be found by inserting $\beta(t)$ given from (143) in (136). This gives:

$$\left.\begin{aligned} \alpha_f(t) = & \frac{\frac{FC}{D} e^{-2p}}{1+\left(1+\frac{FC}{D}\right)e^{-2p}} \left[1-\left(\frac{\lambda_2}{\lambda_2-\lambda_1} e^{-\lambda_1 t} - \frac{\lambda_1}{\lambda_2-\lambda_1} e^{-\lambda_2 t}\right)\right] \\ & + \frac{FC}{\lambda_2-\lambda_1} \cdot \frac{1}{1+e^{2p}} \left[e^{-\lambda_1 t} - e^{-\lambda_2 t}\right]. \end{aligned}\right\} \quad (159)$$

Introducing the assumptions (149) and (150) into (159) we get the following approximate expression:

$$\alpha_f(t) \approx \frac{\frac{FC}{D} e^{-2p}}{1+\left(1+\frac{FC}{D}\right)e^{-2p}} \left[1-e^{-\lambda_1 t}\right], \quad (160)$$

where λ_1 is determined from (152).

Comparing the expressions (144) and (159) for $\Delta L(t)$ and $\alpha_f(t)$ the following relation is obtained:

$$\Delta L(t) \approx \frac{3}{1+e^{-2p}} \alpha_f(t). \quad (161)$$

Thus, the shortening is approximately proportional to the degree of fixation. This is of interest for the understanding of heat production during contraction (cf. p. 284).

It is now possible to relate the time-interval t_0 (147) required for the transmutation chain to obtain maximal shortening velocity to the latent period of the muscle fibre. According to (152), (140), and (147) the assumptions (150) give the following approximate expression for t_0:

$$t_0 \approx \frac{1}{W(e^p+e^{-p})} \log \frac{W(e^p+e^{-p})}{\frac{FC}{1+e^{2p}}+D}. \quad (147\,a)$$

Table 13 contains values for t_0 in msec. calculated from (147 a) for different loads (i. e. different values of e^{2p}) and with $FC = 9$ sec.$^{-1}$, $\frac{FC}{D} = 30$ and $W = 50$, 100, and 200 sec.$^{-1}$.

TABLE 13.
"Latent" period t_0.

$e^{2p} =$	1	4	9	36	100
$W = 50$ sec.$^{-1}$	30.3	32.7	29.6	20.5	14.2
$W = 100$ sec.$^{-1}$	18.6	19.1	16.9	11.4	7.8
$W = 200$ sec.$^{-1}$	11.1	10.9	9.5	6.3	4.2

It is seen from the table that the times t_0 are of the same order of magnitude as the experimentally determined latent periods for the muscle fibre. Moreover, for loads $< 0.5\, P_0$ ($e^{2p_0} = 100$) t_0 varies only slightly with the load in accordance with the approximately constant latent period found in the muscle fibre.

Relaxation.

Let us consider a transmutation chain which under the load p is contracted tetanically at the concentration C of the fixating factor. When stimulation is interrupted, the concentration C of the fixating factor will decrease, since it will gradually be consumed. In the following analysis it is assumed that the concentration C is zero immediately after the cessation of the stimulation. Obviously this is a simplification as compared with the actual process in the beginning of the relaxation of a muscle fibre. The removal of the fixating factor causes an elongation of the chain, a relaxation. Its mechanism is a spontaneous defixation of fixated elements. Thereby the frequency of transmutations $\alpha \rightarrow \beta$ is increased and the result is a true elongation of the chain.

The equations of motion for the course of relaxation can be derived from the equations (132)—(134) for the course of shortening by putting $C = 0$. Thereby we get:

$$\frac{d\beta}{dt} = W[\alpha_1 e^{p} - \beta e^{-p}], \qquad (162)$$

$$\frac{da_1}{dt} = W\left[\beta e^{-p} - a_1 e^{p}\right] + D a_f, \tag{163}$$

$$\frac{da_f}{dt} = -D a_f. \tag{164}$$

The initial conditions are:

$$\beta = \frac{1}{1 + \left(1 + \frac{FC}{D}\right) e^{-2p}}, \quad a_1 = \beta e^{-2p} \quad \text{and} \quad a_f = \frac{FC}{D} a_1$$

at $t = 0$.

Solution of these equations performed in the same way as was done for the equations for the course of shortening gives

$$L(t) = L_{\text{rest}} - \Delta L \left[\frac{\mu_2}{\mu_2 - \mu_1} e^{-\mu_1 t} - \frac{\mu_1}{\mu_2 - \mu_1} e^{-\mu_2 t}\right], \tag{165}$$

where μ_1 and μ_2 are determined by the equations which correspond to (140)

$$\left.\begin{aligned} \mu_1 + \mu_2 &= W(e^{p} + e^{-p}) + D \\ \mu_1 \mu_2 &= DW(e^{p} + e^{-p}), \end{aligned}\right\} \tag{166}$$

i. e.

$$\left.\begin{aligned} \mu_1 &= D \\ \mu_2 &= W(e^{p} + e^{-p}). \end{aligned}\right\} \tag{167}$$

The *relaxation velocity* $V_d(t)$ expressed in units of L_a per second is per link according to (165):

$$V_d(t) = \frac{\mu_1 \mu_2}{\mu_2 - \mu_1} \Delta L \left[e^{-\mu_1 t} - e^{-\mu_2 t}\right]. \tag{168}$$

It is seen from this expression that the relaxation begins with a velocity zero, in accordance with what could be expected from the initial conditions. With the former assumptions for W and D we get the following expression for the maximum relaxation velocity V_d^0 according to (168) and (167)

$$V_d^0 \approx D \Delta L. \tag{169}$$

Introducing (145) we get:

$$V_d^0 \approx \frac{3\,FC}{(1+e^{2p})\left(1+\left(1+\frac{FC}{D}\right)e^{-2p}\right)}. \qquad (170)$$

The same expression can be obtained from the simple considerations accounted for on p. 265 in connection with the determina-

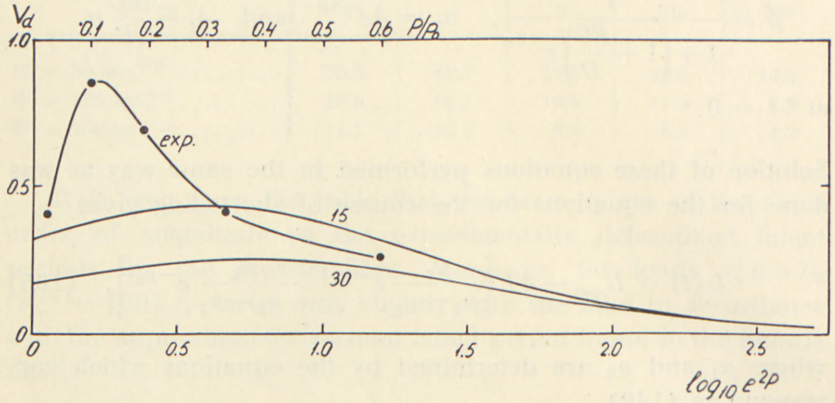

Fig. 97. Maximum relaxation velocity as a function of the load for the transmutation chain and for the muscle fibre.
exp.: muscle fibre (0° C.).
15 and 30: transmutation chain.
The figures on the curves denote the corresponding values of $\frac{FC}{D}$.
abscissa: above: load on the fibre in units of P_0;
below: tension in the chain expressed as $\log_{10} e^{2p}$.
ordinate: relaxation velocity in L_0 per sec.

tion of the maximal shortening velocity. The maximal relaxation velocity in the muscle fibre is reached later than in the single transmutation chain. However, this deviation between theory and experiment could be expected considering that in reality the concentration of the fixating factor will disappear slowly and not suddenly, as assumed in our calculations. In spite of this difference it is of interest to compare the velocity of relaxation as a function of load in the transmutation chain and in the muscle fibre.

In fig. 97 the maximum relaxation velocity for the transmutation chain corresponding to $\frac{FC}{D} = 15$ and 30 and $FC = 9$ sec.$^{-1}$

is shown as a function of the load. The theoretical curves are of the same type as the experimental ones. Both have a maximum and the theoretical velocities have a similar order of magnitude.

The development of tension in the isometric tetanic contraction of a transmutation chain.

We shall consider a transmutation chain which originally is in equilibrium at rest at load P_1. At time $t = 0$ the fixating factor is suddenly released in a concentration C. If we keep the length of the chain constant corresponding to a constant number of β links, the gradual fixation of α links will cause a rise in the ratio between β links and free α links. Thereby a gradual rise is obtained in the tension of the chain. This corresponds to an isometric contraction of a muscle fibre.

The development of tension is determined on the basis of the general equations of "motion" (132)—(134) considering $p = p(t)$ as variable. Since the length remains constant, we have:

$$\beta(t) = \beta_{\text{rest}}(p_1) \tag{171}$$

and hence

$$\frac{d\beta}{dt} = 0. \tag{172}$$

Introducing (171) and (172) in (132) we get

$$\alpha_1(t) = \beta_{\text{rest}} e^{-2p(t)}. \tag{173}$$

Using (123), (171), and (172) the equation of motion for α_1 is

$$\frac{d\alpha_1}{dt} = D(1 - \beta(p_1) - \alpha_1) - FC\alpha_1,$$

i. e.

$$\frac{d\alpha_1}{dt} = D\alpha_{\text{rest}}(p_1) - (FC + D)\alpha_1. \tag{174}$$

Solution of (174) gives

$$\alpha_1(t) = \frac{\alpha_{\text{rest}}}{1 + \frac{FC}{D}} \left[1 + \frac{FC}{D} e^{-(FC+D)t}\right]. \tag{175}$$

Introduced in (173) this gives

$$e^{2(p(t)-p_1)} = \frac{1+\frac{FC}{D}}{1+\frac{FC}{D}\,e^{-(FC+D)t}}. \qquad (176)$$

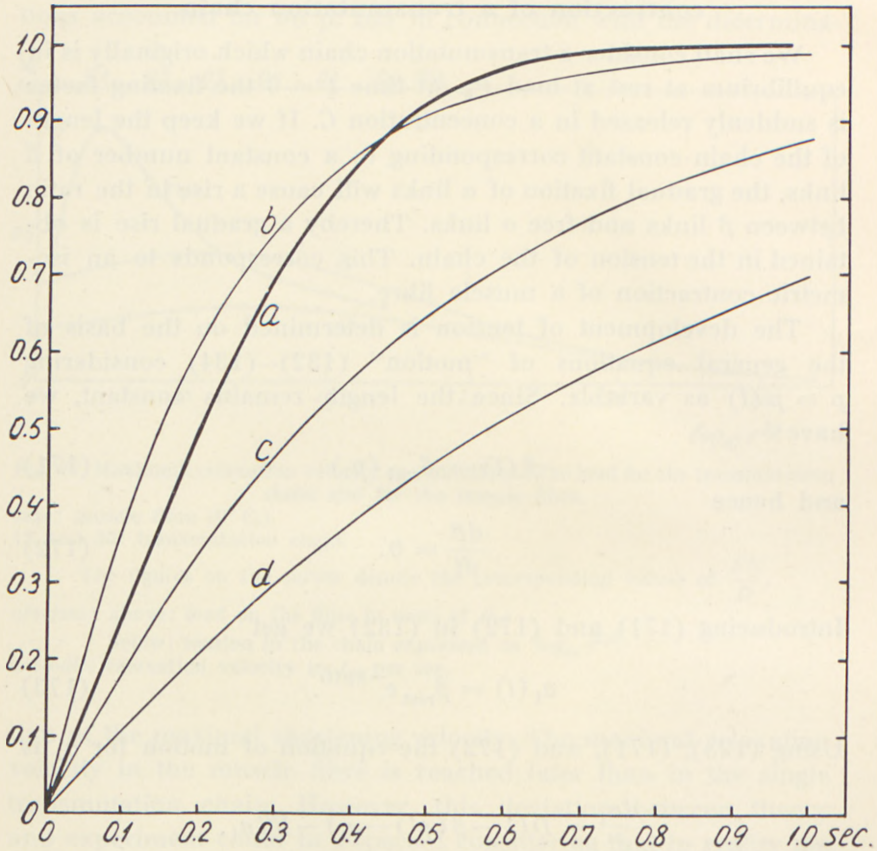

Fig. 98a. Development of tension and the course of shortening in isometric and isotonic tetanic contraction of the transmutation chain.

a. tension
b, *c*, and *d* shortening,
b. $e^{2p} = 1$,
c. $e^{2p} = 4$,
d. $e^{2p} = 9$.

It is furthermore assumed that $\frac{FC}{D} = 30$ and $FC = 9\ \text{sec.}^{-1}$.

abscissa: time in sec.
ordinate: increase in tension and shortening divided by their final values.

Hence the *increase in tension*

$$\Delta p = \Delta p\,(t) = p - p_1$$

is:

$$\Delta p\,(t) = \tfrac{1}{2} \log \frac{1 + \dfrac{FC}{D}}{1 + \dfrac{FC}{D}\, e^{-(FC+D)t}}. \qquad (177)$$

It is seen from this expression that the increase in tension is independent of the initial load and only determined by FC and D.

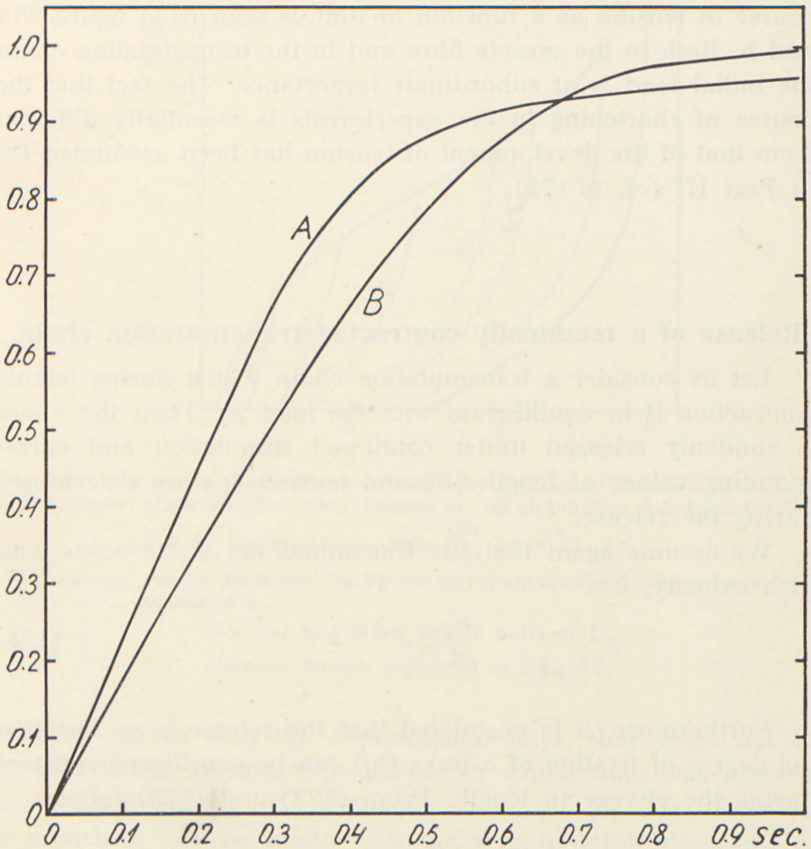

Fig. 98b. Development of tension and the course of shortening in isometric and isotonic tetanic contraction of the muscle fibre (0° C.).
A. extra tension (length 140).
B. shortening (load 0.2 P_0 corresponding to $e^{2p} \simeq 2.5$ cf. fig. 96).
abscissa: time in sec.
ordinate: increase in tension and shortening divided by their final values.

The development of tension computed for $\frac{FC}{D} = 30$ and $FC = 9$ sec.$^{-1}$ is given in fig. 98a. In the same figure examples are given for the theoretical course of shortening (cf. p. 264). With $e^{2p} = 1$, tension and shortening in the single transmutation chain develop with approximately the same velocity. With $e^{2p} = 4$, the development of shortening is delayed as compared with the tension. This difference will increase with increasing values of e^{2p} (cf. the expression for λ_1 (152)).

The agreement between the experimental and the computed course of tension as a function of time is seen from figure 98a and b. Both in the muscle fibre and in the transmutation chain the initial load is of subordinate importance. The fact that the course of shortening in the experiments is essentially different from that of the development of tension has been accounted for in Part III (cf. p. 172).

Release of a tetanically contracted transmutation chain.

Let us consider a transmutation chain which during tetanic contraction is in equilibrium with the load p_1. Then the chain is suddenly released under continued stimulation and corresponding values of length (L) and tension (p) are determined during the release.

We assume again that the transmutations $\alpha \rightleftarrows \beta$ occur with high velocity, i. e.

$$\frac{a_1}{\beta} \simeq e^{-2p}. \tag{178}$$

Furthermore, it is postulated that the release is so fast that the degree of fixation of α links (a_f) can be considered constant during the change in length. From (123) and (178) follows

$$\beta = 1 - a_f^{\text{contr}}(p_1) - \beta e^{-2p},$$

i. e.

$$\beta = \frac{1 - a_f^{\text{contr}}(p_1)}{1 + e^{-2p}},$$

and hence:

$$L_{\text{release}}(p) = 1 + 3\frac{1 - a_f^{\text{contr}}(p_1)}{1 + e^{-2p}}. \qquad (179)$$

The calculated release diagrams for $\frac{FC}{D} = 30$ are shown in fig. 99 for different degrees of fixation. In comparing these cal-

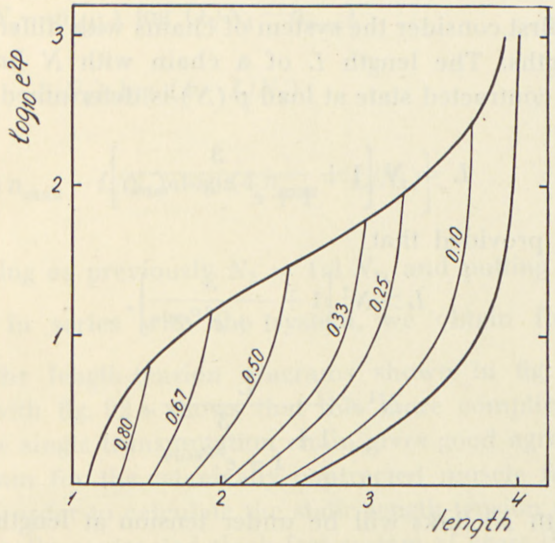

Fig. 99. Quick release diagrams for a tetanically contracted transmutation chain. *Thick curves*: static length-tension diagram at rest and during tetanic contraction for the transmutation chain $\left(\frac{FC}{D} = 30\right)$.

Thin curves: release diagrams. The figures on the curves denote the corresponding values of a_f.

abscissa: length per link in units of L_a.

ordinate: tension expressed as $\log_{10} e^{2p}$.

culated curves with the experimental ones, they must not be related to the release experiments in which time was allowed for the adjustment of a stationary value (cf. fig. 50). However, comparison can be made with the semi-dynamic diagrams as represented in fig. 19 in a previous communication (BUCHTHAL 1942). As to the relation between shortening heat and fig. 99 see p. 284.

The static length-tension diagram for a tetanically contracted system of cross-linked transmutation chains.

Let us determine the static length-tension diagram during tetanic contraction for the two systems previously considered, viz. the system consisting of transmutation chains with different equilibrium lengths and the slack-free system of cross-linked chains.

1). We first consider the system of chains with different equilibrium lengths. The length L of a chain with N links in the tetanically contracted state at load $p(N)$ is determined by (130):

$$L = N\left[1+\frac{3}{1+e^{-2(p-p_{\text{extra}})}}\right]. \tag{180}$$

Therefore, provided that

$$L > N^1\left[1+\frac{3}{1+e^{2p_{\text{extra}}}}\right],$$

i. e.

$$N^1 < \frac{L}{1+\frac{3}{1+e^{2p_{\text{extra}}}}}, \tag{181}$$

a chain with N^1 links will be under tension at length L of the system. The tension $p(N)$ in a chain satisfying this condition is according to (180) determined by:

$$2(p(N)-p_{\text{extra}}) = \log\left(\frac{L-N}{4N-L}\right). \tag{182}$$

The mean tension p at length L for the system of chains is (104):

$$p = \frac{1}{N_2-N_1}\sum_{N=N_1}^{N_{\max}} p(N), \tag{183}$$

where now $N_{\max}$ is the lowest of the figures N_2 and $\dfrac{L}{1+\dfrac{3}{1+e^{2p_{\text{extra}}}}}$.

Introducing $n = \dfrac{N}{N_1}$ and replacing the summation with an integration, (182) and (183) will give:

$$2p = 2p_{\text{extra}} \cdot \frac{n_{\max} - 1}{n_2 - 1} + \frac{1}{n_2 - 1} \int_1^{n_{\max}} \log \frac{L/N_1 - n}{4n - L/N_1} \, dn. \qquad (184)$$

From this we obtain:

$$\left.\begin{aligned} 2p = 2p_{\text{extra}} \cdot \frac{n_{\max} - 1}{n_2 - 1} + \frac{1}{n_2 - 1} \Big[& (L/N_1 - 1) \log (L/N_1 - 1) \\ & - (L/N_1 - n_{\max}) \log (L/N_1 - n_{\max}) \\ & + \frac{1}{4} (4 - L/N_1) \log (4 - L/N_1) \\ & - \frac{1}{4} (4 n_{\max} - L/N_1) \log (4 n_{\max} - L/N_1) \Big]. \end{aligned}\right\} \qquad (185)$$

Choosing as previously $N_2 = 1.3 N_1$, and putting a Hookean elasticity in series with the system, we obtain for $\frac{FC}{D} = 15$ and 30 the length-tension diagrams shown in fig. 92c. Comparison with fig. 92a shows that this more complicated model just as the single transmutation chain gives good agreement with the diagram for the tetanically contracted muscle fibre.

2). In order to calculate the static length-tension diagram for the tetanically contracted slack-free system of cross-linked transmutation chains, we will assume that the fixating agent can act both on free α-links and on α-links in aggregates. Furthermore, we assume that fixation does not alter the ability of the links to form cross-linkages. The equilibrium conditions corresponding to (124) and (125) show that with these assumptions the length-tension diagram in contraction can be obtained from the diagram at rest in the same simple way, as the contraction diagram for a transmutation chain can be derived from its diagram at rest.

Fig. 92b shows the contraction diagrams obtained in this way from the rest diagrams shown in the same figure. The difference between these contraction diagrams and that of a single transmutation chain is only of minor importance. The similarity with the diagrams of the muscle fibre is striking. It is further increased when a Hookean elasticity is put in series with the cross-linked system of transmutation chains (fig. 94).

Shortening velocity and relaxation velocity in a system of cross-linked transmutation chains.

As shown in the preceding section, there was a remarkable similarity between the force-velocity relations both with regard to shortening and relaxation in the single transmutation chain

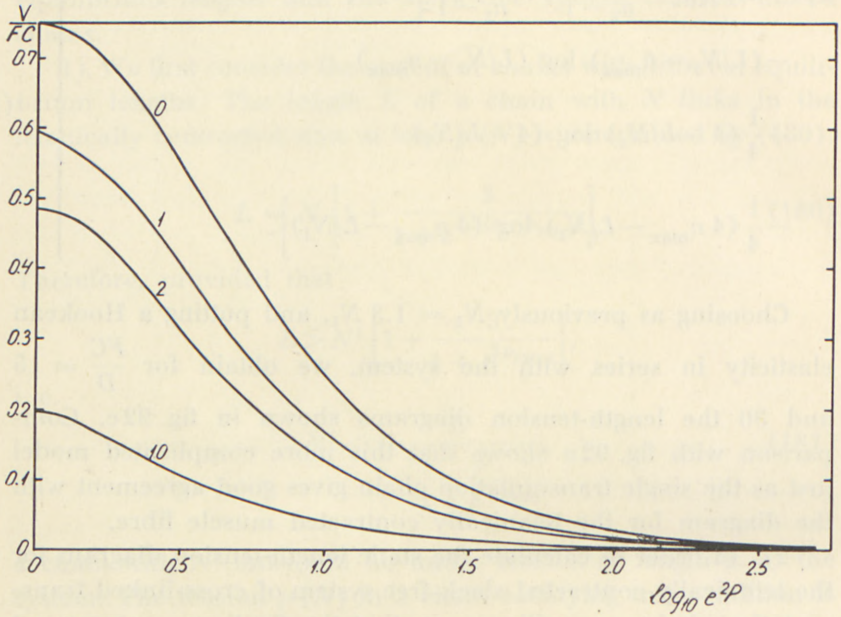

Fig. 100. Maximum shortening velocity as a function of the load for the slack-free system of cross-linked transmutation chains.
The figures on the curves denote the corresponding value of K, defined by (117). The curve denoted by 0 is that for a single transmutation chain.
abscissa: tension expressed as $\log_{10} e^{2p}$.
ordinate: shortening velocity in L_0 per sec. divided by FC.

and in the muscle fibre. This makes it worth while to analyse the force-velocity relations in a system of cross-linked chains, the mechanical reactions of which in several respects are more closely related to those of the muscle fibre. Let us for this purpose consider the slightly simplified model with cross-linkages but without slack (p. 249). By using the formerly applied arguments based on the assumption given in (150) we get the following expressions for the maximum velocities of shortening and relaxation:

$$V_0 \approx \frac{3\,FC}{1+e^{-2p}} \cdot \left(\frac{\alpha_1}{N}\right)_{\text{rest}} \tag{186}$$

and

$$V_d^0 \approx \frac{3\,D}{1+e^{-2p}} \cdot \left(\frac{\alpha_{1f}}{N}\right)_{\text{contr}}, \tag{187}$$

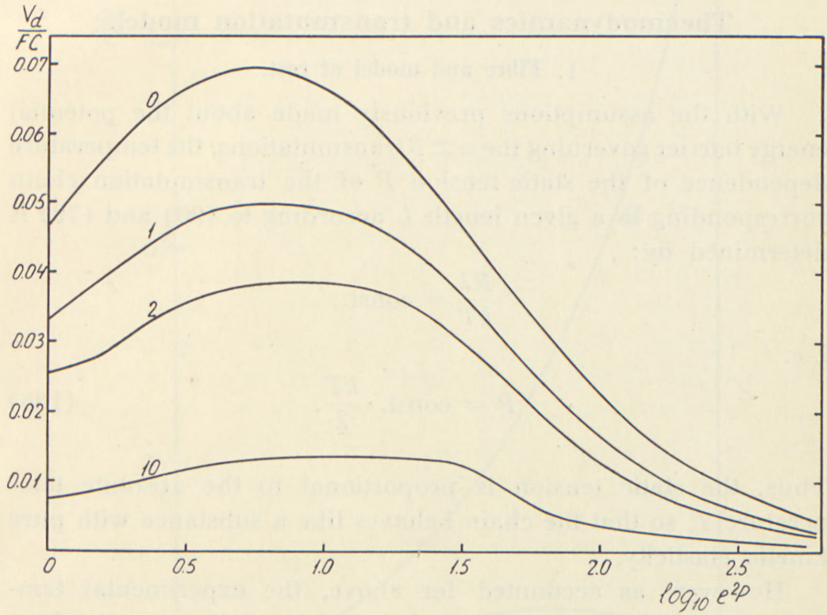

Fig. 101. Maximum relaxation velocity as a function of the load for the slack-free system of cross-linked transmutation chains.
The figures on the curves denote the corresponding values of K, defined by (117). The curve denoted by 0 is that for a single transmutation chain.

$$\frac{FC}{D} = 30.$$

abscissa: tension expressed as $\log_{10} e^{2p}$.
ordinate: relaxation velocity in L_0 per sec. divided by FC.

where $\left(\frac{\alpha_{1f}}{N}\right)$ denotes the fraction of links which are fixated but not cross-linked. By introducing the values for $\left(\frac{\alpha_1}{N}\right)_{\text{rest}}$ and $\left(\frac{\alpha_{1f}}{N}\right)_{\text{contr}}$ we can calculate the force-velocity relations given in figs. 100 and 101. A comparison of these curves with the relation found for the single chain shows that the application of the cross-linked system mainly changes the level but not the shape of the curves. Thus, the cross-linked system will be suited to

describe force-velocity relations as well, when the values chosen for FC are correspondingly increased as compared with those applied in the single chain.

Thermodynamics and transmutation model.

1. Fibre and model at rest.

With the assumptions previously made about the potential energy barrier governing the $\alpha \rightleftarrows \beta$ transmutations, the temperature dependence of the static tension P of the transmutation chain corresponding to a given length L according to (90) and (79) is determined by:

$$\frac{P\lambda}{kT} = \text{const.},$$

i. e.

$$P = \text{const.} \cdot \frac{kT}{\lambda}. \tag{188}$$

Thus, the static tension is proportional to the absolute temperature T, so that the chain behaves like a substance with pure kinetic elasticity.

However, as accounted for above, the experimental temperature coefficient of the static tension of the muscle fibre is at most only one third of that corresponding to kinetic elasticity .This implies that the simple kinetic theory of elasticity is not suited for the description of the elasticity of the muscle fibre. A calculation of that part of the tension $\left(T\frac{dP}{dT}\right)$ which might arise from changes in entropy, based on the experimentally determined temperature dependence of the static tension of the muscle fibre (Buchthal *et al.* 1944 a), clearly demonstrates this fact.

From the curves of fig. 102 it is seen that entropy at small degrees of stretch may account for at most approximately 40 per cent of the total tension in the fibre. With increasing elongation the possible part played by entropy decreases considerably and at length 180 it is reduced to only 10 per cent. Corresponding results were obtained by Woods (1946) in an investigation of

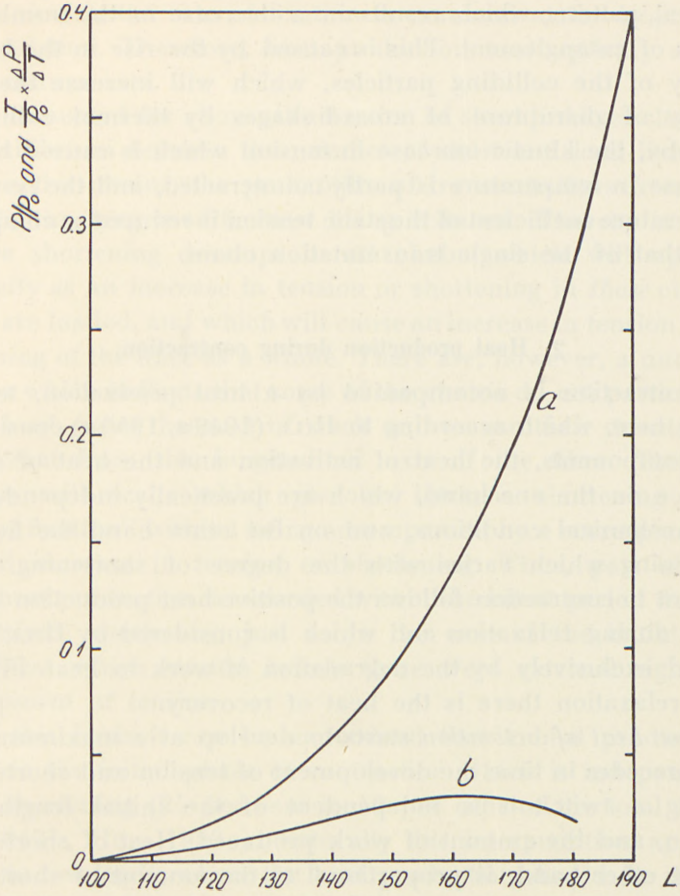

Fig. 102. The component of the tension in the resting fibre arising from entropy.
a) length-tension diagram, 0° C.
b) $T \frac{\Delta P}{\Delta T}$.
ordinate: tension and possible entropy contribution in units of P_0.
abscissa: length in per cent of L_0.

the temperature dependence of the static tension in wool fibres and myosin films.

While the single chain cannot adequately account for the experimental findings, the system of cross-linked transmutation chains can help to understand the reduction in the temperature coefficient which characterizes the muscle as compared with the single chain. A rise in temperature will cause a change in the

textural pattern, which results in a decrease in the number of points of entanglement. This is caused by the rise in the kinetic energy of the colliding particles, which will increase the possibility of disrupture of cross-linkages by thermal collisions. Thereby, the kinetic increase in tension which is caused by the increase in temperature is partly counteracted, and the resulting temperature coefficient of the static tension is reduced as compared with that of the single transmutation chain.

2. Heat production during contraction.

Contraction is accompanied by a heat production, termed initial heat, which according to HILL (1949a, 1950a) consists of two components, the heat of activation and the heat of maintenance on the one hand, which are practically independent of the mechanical conditions, and on the other hand the heat of shortening which varies with the degree of shortening. Subsequent to contraction follows the positive heat production which arises during relaxation and which is considered by HILL to be caused exclusively by the degradation of work to heat. Finally, after relaxation there is the heat of recovery.

The *heat of activation* starts to develop at a maximum rate and precedes in time the development of tension and shortening. During a twitch it is independent of the initial length, the tension, and the amount of work produced. Heat of shortening, on the other hand, is proportional to the amount of shortening but independent of the work produced.

Obviously it is imperative for any theory of contraction that an attempt be made to account for these different phases of heat production, for their rate of development, and their dependence or independence of the mechanical conditions.

The present theory assumes a fixation of short linkages as an essential prerequisite for the process of contraction. Let us assume that this fixation is accompanied by a positive heat production arising from the reaction heat produced by the interaction of groups in the α link with the fixating factor and from the decrease in internal energy due to the exclusion of the short modification from a transmutation. Since at the start of stimulation the fixating factor can attack the relatively largest number of

short linkages, the rate of fixation is maximal at the beginning of stimulation. Therefore, heat production must quickly attain its maximum rate.

As accounted for above, the fixation of short linkages changes the equilibrium between the number of short and long linkages in the active chains, the probability of transmutations from the short to the long modification being reduced. Thereby a progressive shortening develops in all chains which will appear externally as an increase in tension or shortening in *those* chains which are loaded, and which will cause an increase in tension or in shortening of the fibre as a whole. There are, however, a number of signs which indicate that some of the chains do not participate in the load, either because of slack or because their orientation is different from the longitudinal axis of the fibre. Thereby fixations will occur which give an intrinsic shortening with "heat of fixation" without being accompanied by a corresponding external increase in tension or shortening. Thus, part of the initial heat production is recorded within the latent period during the intrinsic shortening, just as in the case of the initial rise in stiffness which started before there were external signs of development of tension.

On this basis it can be understood that a heat production occurs in the initial phase of contraction which is independent of the shortening (25 per cent to 50 per cent of the total heat, HILL 1949b, HILL 1950c). Naturally this interpretation applies chiefly to low loads, where the heat production should be determined exclusively by the slack in the minute structure. Assuming that heat of activation arises from internal shortening which causes the disappearance of slack, one should expect that the amount of heat would be reduced when contraction is initiated at high initial length, since slack is diminished. The protracted production of heat which actually occurs at high elongations could partly be interpreted by this reduction in slack (HILL 1950c). However, the finding that the amount of heat of activation is of the same order of magnitude at low and high degrees of stretch needs an additional explanation. One might assume that heat of activation at high stretch is due chiefly to the extension of the previously mentioned visco-elastic series element (cf. p. 170). The elongation of this element is compensated for by the internal

shortening which in turn gives rise to heat of activation in the active part and heat arising from degraded work in the passive part of the structure.

If the transmutation chain is allowed to shorten, the number of fixations will increase approximately linearly with the isotonic shortening (cf. p. 267). The amount of heat produced will only depend on the number of fixations and not on the velocity with

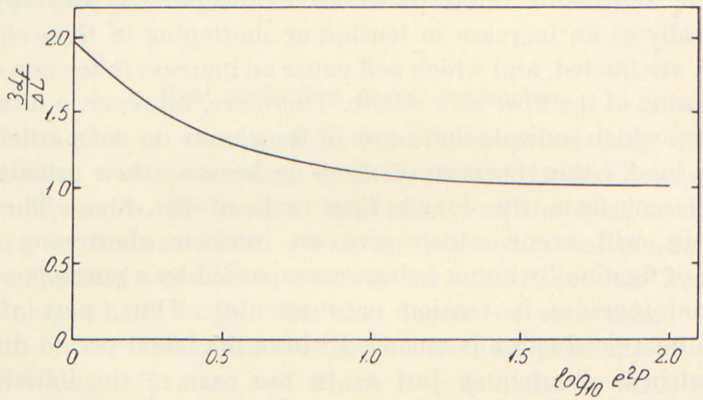

Fig. 103. The ratio between degree of fixation and shortening as a function of the tension in the transmutation chain.

abscissa: tension expressed as $\log_{10} e^{2p}$.

ordinate: $\frac{3\alpha_f}{\Delta L}$, where α_f is the degree of fixation and ΔL is the shortening; approximated by $1 + e^{-2p}$.

which the fixations occur, i. e. it will be independent of the shortening velocity. Thus, that part of the shortening in the chains which is not manifested externally, accounts for the heat of activation; while the part responsible for the external shortening accounts for the *heat of shortening* which at a given load is proportional to the amount of shortening. This is in agreement with the experimentally found proportionality between heat of shortening and shortening (HILL 1938, 1949a). In the transmutation chain the proportionality factor for this relation will vary with the load. Fig. 99 gives the length-tension relation for a transmutation chain with different degrees of fixation (different values of α_f). Under isotonic conditions a given variation in α_f causes a larger variation in length at high loads than at low loads. By definition a given variation in α_f corresponds to a given amount of shortening.

Therefore, the shortening heat per unit of shortening decreases with increasing load. The proportionality factor for this decrease $\approx 1 + e^{-2p}$ is given in fig. 103. A corresponding tendency to a change in the proportionality factor between heat of shortening and shortening (a) can also be observed in whole muscle (cf. e. g. the experiment given in fig. 7, HILL 1949b). The theoretically found decrease in shortening heat with increasing load may, however, be concealed in the muscle. Considering that especially at high load the work of the transmutation chains is impeded by shunt and series elastic elements, a given external shortening velocity will correspond to a somewhat higher internal shortening, which in turn is associated with a mechanical loss and an increased heat production.

The fact that tensionless relaxation occurs without a measurable heat production according to HILL (1949b) is due either to a relaxation which actually has no heat production or to the compensation of a negative heat by a corresponding positive heat production. In an earlier part of this paper we have dealt with the strong internal forces which must be assumed to arise during contraction and which impede shortening of the muscle fibre even when it does not shorten against an external load (elastic locking). This internal resistance represents a certain amount of potential energy which is degraded to heat in the relaxation phase. Hence, if there is no external positive heat production, one must expect a negative heat associated with the process of relaxation which neutralizes the previously mentioned "frictional" heat.

It is in agreement with this assumption, that a slow stretch during isometric contraction is associated with a negative heat production (HILL 1938, FENN 1924, AUBERT 1948); this effect is interpreted as being due to an enforced relaxation in the structure arising from the elongation.

Maintenance of contraction in a tetanus is associated with *heat of maintenance*. According to HILL (1949a) this is considered the summed effect of the heat of activation released by each stimulus, implying that the heat production during relaxation is zero. At the level of tetanic contraction, activation and relaxation balance each other and it is the intensity of relaxation which determines the intensity with which a reactivation will take place. As mentioned, there are certain indications that

relaxation is accompanied by a negative heat which counteracts the positive heat produced by the intrinsic work of deformation. According to this conception heat of maintenance would be interpreted as the difference between heat of activation (i. e. the positive heat accompanying fixation) and the negative heat concomitant with relaxation. It may be emphasized that the occurrence of a heat of maintenance is incompatible with the assumption of reversibility between fixation and defixation since this would imply that heat of maintenance was zero. Hence, the negative heat supposed to be associated with relaxation must be somewhat less than the positive heat which accompanies fixation and the mobilization of the fixating factor.

According to ABBOTT (1951) the heat of maintenance decreases asymptotically within the first 5 seconds of tetanic contraction. This course of heat production may indicate that the asymptotic value corresponds to the *actual* heat of maintenance, while the excess heat is the result of the internal adjustment in the texture (internal shortening in slack chains and degraded work arising from the elongation of the visco-elastic series element). This interpretation is supported by the finding that the maximum relaxation velocity within the same time interval of 5 seconds (0° C.) is reduced in the same way as heat of maintenance (p. 183). Moreover, the time course of adjustment after an isotonic transient during contraction extends over several seconds as well.

Summary of transmutation theory (Part IV).

In the first section of this Part a review is given of direct investigations of the minute structure of muscle. This includes investigations with the ordinary microscope, measurements of birefringence, transparency and diffraction with visible light, electron microscopy, and X-ray analysis. The muscle fibre in its minute structure has a relatively good, but not complete longitudinal orientation. This orientation is somewhat increased by both stretch and contraction. However, the increase in orientation by stretch is essentially less than in a substance with pure kinetic elasticity. There exists a considerable degree of orientation in the muscle fibre already at equilibrium length and the deformation

caused by stretch and contraction must be attributed mainly to alterations in the length of the chain molecule.

The basic minute structural element is assumed to consist of a molecular chain characterized by two states of equilibrium with different lengths. A transmutation from one state to the other is described as a transition over a potential energy barrier, from one potential minimum to another. The energy for transmutations is derived from thermal collisions and from the external load acting on the chain. The transmutations will cause a continuously repeated alternation between the two modifications within the molecule. A chain of this type will display both long-range elasticity and delayed adjustment, i. e. visco-elasticity.

The static and dynamic mechanical properties of a transmutation chain were analysed quantitatively and compared with the experimental findings on isolated fibres at rest. Furthermore, chains with transmuting links as structural elements give a possibility to consider in a new light the mechanical reactions and the minute structural changes which accompany contraction, thereby giving a possibility to develop a theory of contraction in quantitative terms.

The *static properties* of the single transmutation chain were derived from a calculation of the probability per time unit ($W_{\alpha \to \beta}$) of the occurrence of a transmutation from the short (α) to the long (β) modification and vice versa ($W_{\beta \to \alpha}$). The probability per second of an $\alpha \to \beta$ transmutation is given by the expression

$$W_{\alpha \to \beta} \approx \nu e^{-\frac{A - P\lambda}{kT}},$$

where A represents the energy of activation, P the load acting on the chain, λ the distance between the equilibrium position (potential minimum) and the peak of the potential barrier, kT the temperature energy, and ν a factor giving the frequency of thermal collisions with due consideration to the spatial possibilities of a transmutation.

Conversely, the probability per sec. ($W_{\beta \to \alpha}$) of a transmutation from the long to the short modification is given by:

$$W_{\beta \to \alpha} \approx \nu e^{-\frac{A + P\lambda}{kT}}.$$

The *static length-tension diagram* of the transmutation chain is similar to that of the resting fibre (cf. fig. 92a and b). The minor deviations can be accounted for by assuming a Hookean elasticity in series with a system of cross-linked transmutation chains. Owing to the non-uniform distribution of tension and the slack which will occur in this network, even at high degrees of stretch part of the links will be in the α modification. This may explain the difficulty of clearly differentiating in the X-ray diffraction pattern between a pure α and a pure β state.

Dynamic properties of a single transmutation chain as computed from the adjustment after a sudden increase or decrease in load (isotonic transient) can be expressed in terms of a single Voigt-*element*. A cross-linked system of chains, on the other hand, can be described by a spectrum of retardation times for a Voigt-*model* of a similar type as that used to describe the dynamic properties of the muscle fibre. The long retardation times, characterizing the course of creep and stress-relaxation in the muscle fibre, are mainly caused by disrupture and reformation of points of entanglement in the texture in which the transmutation chains are organized. The short retardation times correspond to adjustment in the chains themselves as well.

The configuration of the minute structure during *contraction* is assumed not to differ in principle from that of the resting fibre. In the model of transmutation chains, developed to describe the mechanical properties of the resting fibre, the length of the molecular chain is determined by the ratio of short and long links. At rest this ratio is influenced by the load via its influence on the probability of transmutations. If we assume the probability of a long $\rightarrow$ short transmutation to be increased or the short $\rightarrow$ long transmutation in some way to be reduced, an active shortening can be obtained at constant load. The decrease in length in contraction is taken as an expression of a relative increase in the number of links in the α modification. This increase is assumed to arise from a fixation of a number of links in the α-state in such a way that they are prevented from participating in the $\alpha \rightleftarrows \beta$ transmutations. The fixation is thought to be brought about directly or indirectly by the stimulus, e. g. by a "factor" which reacts with the α links of the protein chains, which thereby are locked and excluded from transmutation.

For the time being the physico-chemical correlate of this fixation can only be a matter for speculation, and it remains an open question whether it consists in the removal or in the addition of some compound to the α link. In the active phase we assume a continuous fixation and defixation (i. e. disappearance of fixations) of α links. The frequency of fixations is assumed to be proportional to the concentration C of a fixating agent and to the number of possibilities of fixation, i. e. proportional to the number of non-fixated α links. The frequency of defixation on the other hand is supposed to be proportional to the number of α links in the fixated state. On this basis we have calculated both the static and dynamic behaviour of the chain with fixated links. The S-shaped length-tension diagram of the tetanically contracted transmutation chain is in good agreement with the experimental findings (fig. 92 a and b). In the transmutation chain the curves for isotonic and isometric contraction coincide. The difference found in the experiments can be accounted for by the internal forces arising in the more complicated model with cross-linked chains The increased stiffness which characterizes contraction can be understood from the reduced number of links which can participate in the transmutations. Thus, if half of the links are fixated, the stiffness will be doubled. The theory can account not only for stationary or quasi-stationary properties in contraction. There is good agreement between the calculated increase in tension in a chain and the development of tension as a function of time found in the experiments (fig. 98 a and b). Both in the muscle fibre and in the transmutation model the initial load is of minor importance for the development of tension. The theory can also explain that a shortening develops more slowly as a function of time than a change in length when a transient is applied to the resting fibre. Since the largest number of α links is available for fixation at the beginning of contraction, shortening with a certain delay will attain a maximum velocity. Then it will continue more slowly as possibilities arise for fixation when new links are formed by thermal collisions. The shortening is approximately proportional to the degree of fixation. This is of interest for the understanding of heat production when shortening heat is assumed to arise from the processes associated with the fixation. The relation between *shortening velocity and load* as calculated

for the transmutation chain compares well with the experimental force-velocity relation (fig. 96).

Relaxation is considered to be brought about by the removal of the fixating factor, thereby giving rise to an increased possibility of $\alpha \rightarrow \beta$ transmutations which in turn cause an elongation of the chain. As a function of load the computed curves are of the same type as the experimental ones (fig. 97). Both have a maximum at a moderate load and the calculated velocities are of a similar order of magnitude. The investigation of a cross-linked model of transmutation chains with fixated elements shows in principle the same properties as the single transmutation chain with respect to the length-tension diagram, the force-velocity relation, and the relation between relaxation velocity and load.

Thermodynamics: The temperature dependence of tension at constant length in the single transmutation chain at rest corresponds to a proportionality between tension and absolute temperature, just as in a pure kinetic elasticity. However, with increasing temperature the textural pattern arising from the cross-linked network of transmutation chains will become more flexible, the number of points of entanglement being reduced. Thus, the interaction between the chains will reduce the temperature coefficient. In the experiments on the isolated resting fibre the temperature dependence maximally amounted to one third of that which corresponds to a proportionality with absolute temperature and, therefore, entropy would account for at most one third of the static tension. This finding is considered an indication that the simple kinetic theory of rubber-like substances does not apply to the muscle fibre.

Finally an attempt was made to interpret the different phases of heat production during contraction in terms of the transmutation model. Assuming that fixation is accompanied by a positive heat production, the latter will quickly attain its maximum value, since the velocity of fixation is maximal in the initial phase of contraction. Moreover, the proportionality which in the experiments on whole muscle was found to exist between shortening and shortening heat (Hill 1938) corresponds to the approximate proportionality between fixation and shortening in the activated transmutation chain. The fact that part of the heat produced (heat of activation) is recorded early after the stimulus and is

independent of the external mechanical conditions, such as load and shortening, is explained by the presence of slack elements the activation of which will cause heat without manifesting itself as external shortening.

It is by no means suggested that the scheme of minute structural organization and function outlined here is final, but it appears to us that it comprises a framework with a simple theoretical basis into which most of the data for a large number of different experimental conditions can be quantitatively fitted with an error not exceeding the variation which is unavoidable in biological material.

APPENDIX I

The non-linear length-tension diagram and the amplitude dependence of the stiffness.

A non-linear length-tension diagram can be expected to cause a variation of the vibrational stiffness with changes in the amplitude of the vibrations. In the following we shall investigate whether the approximately exponential length-tension relation for the muscle fibre which is found statically and dynamically:

$$P(L) \approx P_{st} \cdot [e^{\varkappa (L-L_0)} - 1] \tag{1}$$

can explain the direction and magnitude of the experimentally found variations of stiffness with amplitude.

The change in tension ΔP accompanying a small change in length γ from an initial length L can be written as a Taylor's expansion:

$$\Delta P(\gamma) = G \cdot \gamma + k_1 \gamma^2 + k_2 \gamma^3 + \cdots, \tag{2}$$

where G, $k_1, k_2 \cdots$ are constants depending on L, characterizing the length-tension relation. From (2) it is seen that

$$G = \frac{dP}{d\gamma} \quad \text{for} \quad \gamma = 0, \tag{3}$$

i. e. G is the stiffness at length L. If $k_1 = k_2 = \cdots = 0$, we have a material which at least for small values of γ, obeys Hooke's law.

The higher order terms in (2) represent for the amplitudes applied to the muscle fibre only small corrections of the first order term $G\gamma$. From (1) we obtain the following expression for $\Delta P(\gamma)$:

$$\Delta P(\gamma) = P_{st} e^{\varkappa (L-L_0)} \left[\varkappa \gamma + \frac{1}{2} \varkappa^2 \gamma^2 + \frac{1}{6} \varkappa^3 \gamma^3 + \cdots \right]. \tag{4}$$

Comparison with (2) gives:

$$G(L) = \varkappa (P(L) + P_{st}). \tag{5}$$

This shows that $\varkappa$ is the relative stiffness.

We now impose upon the fibre the external alternating force: $\sigma(t) = \sigma_0 \sin \omega t$. Here σ_0 denotes the amplitude of the force and ω its cyclic frequency. The total system: muscle fibre plus equivalent mass m of the recording system moves according to the equation of motion:

$$m\frac{d^2\gamma}{dt^2} + \eta\frac{d\gamma}{dt} + \Delta P(\gamma) = \sigma_0 \sin \omega t, \tag{6}$$

where $\eta\dfrac{d\gamma}{dt}$ denotes the damping force. The resulting periodic motion can formally be written:

$$\gamma(t) = a_0 + a_1 \cos \omega t + b_1 \sin \omega t + a_2 \cos 2\,\omega t + b_2 \sin 2\,\omega t + \cdots, \tag{7}$$

where the constants $a_0\, a_1\, b_1\, a_2\, b_2 \cdots$ depend on ω and σ_0. The main terms in this expression in our case, where the higher order terms in (2) are small, will be $a_1 \cos \omega t$ and $b_1 \sin \omega t$. The other terms only represent minor corrections.

We can define the *resonance frequency* ω_0 as the frequency at which $b_1 = 0$, i. e. the main term of (7) is displaced 90° in relation to the alternating force. The resonance frequency ω_0 and the corresponding values of the constants in (7) can be determined from the infinite number of equations obtained when (7) and (2) are inserted in (6).

Neglecting the higher order terms in (2) one gets the well-known expressions:

$$\omega_0 = \sqrt{\frac{G}{m}} \tag{8}$$

and

$$\gamma(t) = \gamma_0 \cos \omega_0 t, \quad \text{where} \quad \gamma_0 = \frac{\sigma_0}{\eta\omega_0}.$$

The resonance frequency is independent of the amplitude σ_0 and, therefore, of γ_0 as well, i. e. we have no amplitude dependence in the first order approximation.

Next we will take into account the second term: $k_1\gamma^2$ in (2). As mentioned, this term in our case is considerably smaller than $G\gamma$. According to (4) the ratio between the two terms is $\frac{1}{2}\varkappa\gamma$. From the experimental values of $\varkappa$ the ratio is estimated maximally to be of the order of magnitude of 0.10.

The relative change of the resonance frequency with amplitude which is half the relative change in $m\omega_0^2$ (elastic stiffness) in the second order approximation is found to be approximately: $-\dfrac{1}{2}\left(\dfrac{k_1 a_1}{G}\right)^2$, i. e. proportional to the square of the ratio mentioned above. One might have expected that the change would be proportional to $\dfrac{k_1 a_1^2}{G a_1}$. How-

ever, the change is reduced to the amount stated since the term $k_1\gamma^2$ in the half-period where $\gamma > 0$ causes an *in*crease in stiffness, while in the half-period where $\gamma < 0$ it produces a corresponding *de*crease.

The extra contribution to the relative change in resonance frequency arising from the third order term $k_2\gamma^3$ is approximately: $\frac{3}{8}\frac{k_2 a_1^2}{G}$ (ignoring the influence of the damping which is of minor importance). The third order term thus gives either a positive or a negative contribution according as $k_2 > 0$ or < 0. Comparison with (4) shows that this contribution in the case of the muscle fibre is positive and equal to one half of that arising from the second order term.

Expressed as the decrease in $m\omega_0^2$ with amplitude, the amplitude dependence resulting from the second and the third order terms in (2) can therefore be written:

$$C a_1^2, \tag{9}$$

where C depends on G, k_1, and k_2, and to a smaller degree on η. Disregarding the dependence on η, one obtains:

$$C = \frac{1}{8}\varkappa^2 G. \tag{10}$$

If G' and G'' denote the stiffnesses (i. e. $m\omega_0^2$) corresponding to the amplitudes a_1' and a_1'', we have according to (9):

$$C = \frac{G' - G''}{(a_1'')^2 - (a_1')^2}. \tag{11}$$

In the following table we show values of C calculated from (10) giving a measure of the amplitude dependence which can arise from the non-linearity of the length-tension diagram of the muscle fibre. For $\varkappa$ the expression (5) is applied and for G we use the limiting value of $m\omega_0^2$ corresponding to very small amplitudes. Furthermore, Table 14 contains values of C calculated from (11) giving the actually determined amplitude dependence. The data are based on a series of experiments with different fibre lengths. The equilibrium length on an

TABLE 14.
Amplitude dependence and length-tension diagram.

length in per cent of L_0	load P in dynes	G' dynes $\times$ cm^{-1}	G'' dynes $\times$ cm^{-1}	C (10)	C (11)
		$\times 10^3$	$\times 10^3$	$\times 10^7$	$\times 10^7$
130	140	10.0	9.0	0.42	145
155	315	16.4	15.7	0.37	102
169	670	31.3	28.8	0.56	362
201	1310	58.5	52.6	1.16	855

average amounted to 0.48 cm.; the equivalent mass m was 0.045 g, a'_1 was 0.1 per cent, and a''_1 0.2 per cent of the equilibrium length.

It is seen from Table 14 that the amplitude dependence of $m\omega_0^2$ which can be expected solely from the non-linear length-tension relation of the muscle fibre found dynamically and statically, is 300—700 times less than that found experimentally.

(For mathematical details compare e. g. N. W. McLachlan 1950, chapter IV).

APPENDIX II

Amplitude dependence of vibrational stiffness.

The experimental variation of vibrational stiffness with amplitude could not be derived from the non-linearity of the length-tension diagram of the muscle fibre (cf. Appendix I). We had hoped that the transmutation chains introduced in Part IV would give an adequate explanation. In these chains tension is no longer an unambiguous function of the length, since the velocity influences the length-tension diagram as well. However, a calculation of the behaviour of transmutation chains showed that changes in resonance frequency will only appear in the second approximation and, therefore, to a much lower degree than found experimentally. This agrees with the finding that the mechanical reaction of the single transmutation chain to an isotonic transient can be described in terms of a Voigt-element (a linear system) (cf. p. 246).

A system of parallel chains with different equilibrium lengths which can account for the initial slope of the length-tension diagram of the muscle fibre, cannot as such give a significant variation of stiffness with vibrational amplitude.

However, the presence of a large stiffness in series with the transmutation chains can give rise to a significant amplitude dependence of the stiffness. In the calculations it is permissible to consider formally the transmutation chains as Voigt-elements. The viscosity of a Voigt-element in a certain phase of the vibration period may prevent it from following the decreasing external force. This causes the element (i. e. the chain) to become without tension (slack). With increasing amplitude the probability of slack increases. Hence, one gets a decrease in stiffness with increasing amplitude. For suitably high amplitudes all the chains will be without tension during part of the oscillation period. This will occur when the inertial force plus the external alternating force exceeds the constant force acting on the fibre.

As previously mentioned, X-ray diffraction patterns strongly indicate the presence of a crystalline elasticity (G_c) in the muscle fibre. The elasticity of the contractile minute structural elements can be accounted for by transmutations between modifications of different lengths within the protein molecule (cf. Part IV). The essentially stiffer

crystalline elasticity is assumed to follow Hooke's law and to have a stiffness exceeding that of the system of chains at the mean tension considered by e. g. 200 times.

In the quantitative treatment we consider a system consisting of a single transmutation chain in series with a Hookean elasticity G_c. Furthermore, the transmutation chain is treated as a Voigt-element with an elasticity G_l and a viscosity η.

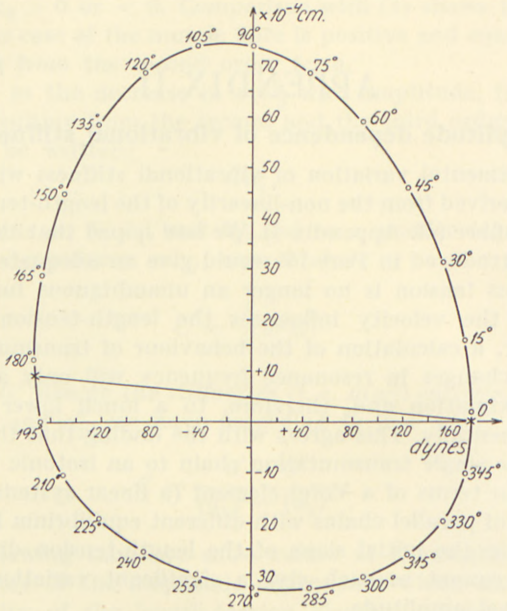

Fig. 104. Lissajous-figure relating the external alternating force and the resulting periodic motion of the system consisting of a Voigt-element in series with a Hookean elasticity plus an inertia.
Constant load = 1000 dynes.
Amplitude of the external alternating force = 170 dynes.
The figures on the curve represent the time, 360° = 1 oscillation period, frequency 400 c.p.s.
abscissa: alternating force in dynes.
ordinate: change in length in μ.

For the measuring of stiffness the recording system plus the analogue of the muscle fibre are acted upon by a periodically alternating force. In a phase in which the imposed force decreases, the large stiffness G_c adjusts itself instantaneously to the varying tension while the damped elasticity (the Voigt-element) cannot follow, i. e. hardly shortens at all. Since the change in length in the crystalline element G_c is insignificant, the inertia of the total system will quickly reduce the tension in the chain to zero and cause it to become slack. As mentioned, this behaviour

will give rise to an essential decrease in stiffness with increasing vibrational amplitude.

In order to evaluate the order of magnitude of this amplitude dependence we have solved the equations of motion for the oscillating system in its "free" phase, i. e. the phase in which there is slack, and in the coupled phase, i. e. the phase during which the chain is able to follow the changes in load. The solutions are adjusted so that the resulting motion is periodic with the frequency of the external alternating force. The result, which varies with the amplitude and the frequency of the alternating force, is given as a vector diagram in which the abscissa gives the alternating force, and the ordinate the change in length. The closed curve obtained corresponds to the experimentally found Lissajous figures. The figures given on the periphery of the calculated curve (fig. 104) indicate the time, 360° denoting one oscillation period.

With fixed values of the constant tension and the amplitude of the alternating force, varying frequency gives a number of these Lissajous figures. Among them we select the one which is nearest to resonance, i. e. when the length axis of the egg-shaped curve coincides with the ordinate. When this procedure is used for different force amplitudes, we find that the resonance frequency decreases strongly with increasing force amplitude. As in the experiments the calculated Lissajous figures (fig. 104) are not entirely symmetrical along their length axis.

In the calculations represented in fig. 104 we have used the following values for the parameters of the system:

$$\begin{aligned} G_c &= 5 \cdot 10^5 \text{ dynes} \times \text{cm}^{-1} \\ G_t &= 2.5 \cdot 10^3 \text{ dynes} \times \text{cm}^{-1} \\ \eta &= 4.45 \cdot 10^2 \text{ dynes} \times \text{cm}^{-1} \times \text{sec.} \\ \text{and } m &= 0.05 \text{ g,} \end{aligned}$$

where m is the equivalent mass of the total system. We have calculated partly the resonance frequency corresponding to very small amplitudes and partly the resonance frequency corresponding to a force amplitude of 17 per cent of the constant load, P, which is assumed to be 1000 dynes.

In the experiments we have found for the same load and the same force amplitude a reduction in the resonance frequency of 10 per cent. The calculations give a reduction amounting to 20 per cent. The experimental and theoretical results are compiled in Table 15.

It appears from the table that the constants used in the present example are not completely suited for a description of the dynamic properties of the muscle fibre. However, the main object of the calculations was to show that the model used really displays an amplitude dependence of a direction and magnitude similar to that found experimentally.

The different amplitude dependence found in the resting muscle fibre and in the tetanically contracted fibre, and the difference between

TABLE 15.
Amplitude dependence.

	force ampl. in per cent of P	length ampl. in per cent of L_0	elastic stiffness	viscous stiffness	stiffness ratio	frequency c. p. s.
			$\times 10^3$	$\times 10^3$		
exp.	$\sim$ 0	$\sim$ 0	55	85	1.54	169
	17	0.5	46	81	1.76	153
calc.	$\sim$ 0	$\sim$ 0	500	58	0.116	500
	17	1.1	312	32	0.100	400

amplitude dependence in rubber and in muscle must be ascribed to the difference in slack and creep properties in the different cases.

APPENDIX III

Shortening velocity as a function of load in the isolated fibre and in whole muscle.

Let us consider a "muscle" consisting of two fibres, fibre 1 and fibre 2, where the equilibrium length of fibre 2 is 20 per cent higher than that of fibre 1, and where the ends of the fibres are supposed to be coupled. We shall determine the relation between shortening velocity and load for this idealized muscle.

On account of the difference in equilibrium length a load P will be unevenly distributed between the fibres and the ratio in which it is divided will vary with the load. From the static length-tension diagram of the muscle fibre (fig. 11) one finds the ratio to vary between 2.4 and 4 when P varies between 0.1 P_0 and 2 P_0 (P_0 referring to a single fibre). In the following calculations we assume a value of 3 for the ratio independent of the load.

The fibres are considered to be composed of a contractile component obeying the force-velocity relation and an exponential series elasticity. Thus, we have for the elasticities:

$$\frac{dP_1}{dL} = \varkappa^1 (P_1 + P_{st}^1) \tag{1}$$

and

$$\frac{dP_2}{dL} = \frac{\varkappa^1}{1.2} (P_2 + P_{st}^1), \tag{2}$$

where P_1 and P_2 denote the load on fibre 1 and 2, respectively, i. e.

$$P_1 + P_2 = P, \tag{3}$$

and where L is the length while $\varkappa^1$ and P^1_{st} are constants to which in accordance with the experiments (cf. Part III) we ascribe the values:

$$P^1_{st} = 0.05\, P_0 \tag{4}$$

and

$$\varkappa^1 = 33\ \mathrm{cm}^{-1}. \tag{5}$$

For loads below P_0 we determine the shortening velocity of the contractile components of the fibres from HILL's equation, i. e.:

$$(P_1 + a)\,(V_1 + b) = (P_0 + a) \cdot b \tag{6}$$

and

$$(P_2 + a)\,(V_2 + 1.2\,b) = (P_0 + a) \cdot 1.2b. \tag{7}$$

For loads exceeding P_0 we modify these relations to

$$(P_1 + a)\,(4\,V_1 + b) = (P_0 + a) \cdot b \tag{8}$$

$$(P_2 + a)\,(4\,V_2 + 1.2b) = (P_0 + a) \cdot 1.2b. \tag{9}$$

This seems justified from KATZ's force-velocity curves (KATZ 1939).

From (6) and (7) one obtains:

$$V_1 = b \cdot \frac{P_0 - P_1}{P_1 + a} \quad \text{for} \quad P_1 < P_0 \tag{10}$$

and

$$V_2 = 1.2\,b \cdot \frac{P_0 - P_2}{P_2 + a} \quad \text{for} \quad P_2 < P_0. \tag{11}$$

Furthermore:

$$V_1 = \frac{1}{4}\, b \cdot \frac{P_0 - P_1}{P_1 + a} \quad \text{for} \quad P_1 > P_0 \tag{12}$$

and

$$V_2 = \frac{1}{4} \cdot 1.2\,b \cdot \frac{P_0 - P_2}{P_2 + a} \quad \text{for} \quad P_2 > P_0. \tag{13}$$

The coupling of the fibres will force them to shorten externally with a velocity V lying between V_1 and V_2. Consequently, the series elasticity of fibre 1 is stretched with the velocity $V_1 - V$, while that of fibre 2 shortens with the velocity $V - V_2$. According to (1) and (2) these processes will bring about variations in the loads P_1 and P_2, governed by:

$$\frac{dP_1}{dt} = \frac{dP_1}{dL} \cdot \frac{dL}{dt} = \varkappa^1 (P_1 + P_{st}^1)(V_1 - V) \tag{14}$$

and

$$\frac{dP_2}{dt} = \frac{dP_2}{dL} \cdot \frac{dL}{dt} = \frac{\varkappa^1}{1.2} (P_2 + P_{st}^1)(V_2 - V). \tag{15}$$

We are considering isotonic conditions, i. e. the load P is constant. This implies according to (3) that:

$$\frac{dP_1}{dt} + \frac{dP_2}{dt} = 0. \tag{16}$$

(14), (15), and (16) give:

$$V = \frac{(P_1 + P_{st}^1) V_1 + \frac{1}{1.2}(P_2 + P_{st}^1) V_2}{P_1 + P_{st}^1 + \frac{1}{1.2}(P_2 + P_{st}^1)}. \tag{17}$$

We now introduce the above mentioned assumption:

$$P_1 = 3 P_2, \tag{18}$$

i. e.

$$P_1 = 0.75 P \quad \text{and} \quad P_2 = 0.25 P. \tag{19}$$

Thus, $P_1 < P_0$ is equivalent to $P < 1.33 P_0$, while $P_2 < P_0$ is equivalent to $P < 4 P_0$.

Inserting the expressions (10)—(13) for V_1 and V_2 and the assumptions (18) and (19) in (17), we obtain the following relation between shortening velocity and load for our "muscle":

$$\left.\begin{aligned} V = b \cdot \frac{(0.75 P + 0.05 P_0) \cdot \frac{P_0 - 0.75 P}{0.75 P + a} + (0.25 P + 0.05 P_0) \frac{P_0 - 0.25 P}{0.25 P + a}}{0.75 P + 0.05 P_0 + \frac{1}{1.2}(0.25 P + 0.05 P_0)} \\ \text{for} \quad P < 1.33 P_0 \end{aligned}\right\} \tag{20}$$

$$\left.\begin{aligned} V = b \cdot \frac{(0.75 P + 0.05 P_0) \frac{1}{4} \frac{P_0 - 0.75 P}{0.75 P + a} + (0.25 P + 0.05 P_0) \frac{P_0 - 0.25 P}{0.25 P + a}}{0.75 P + 0.05 P_0 + \frac{1}{1.2}(0.25 P + 0.05 P_0)} \\ \text{for} \quad 1.33 P_0 < P < 4 P_0. \end{aligned}\right\} \tag{21}$$

Putting $a = 0.30\ P_0$ and $b = 0.92\ L_0$/sec. we get from (20) and (21) the force-velocity relation shown in fig. 105, where the load on the "muscle" is measured in units of P_{0M}, the load at which $V = 0$. According to (21) $P_{0M} = 2.75\ P_0$. Fig. 105 also contains the force-velocity

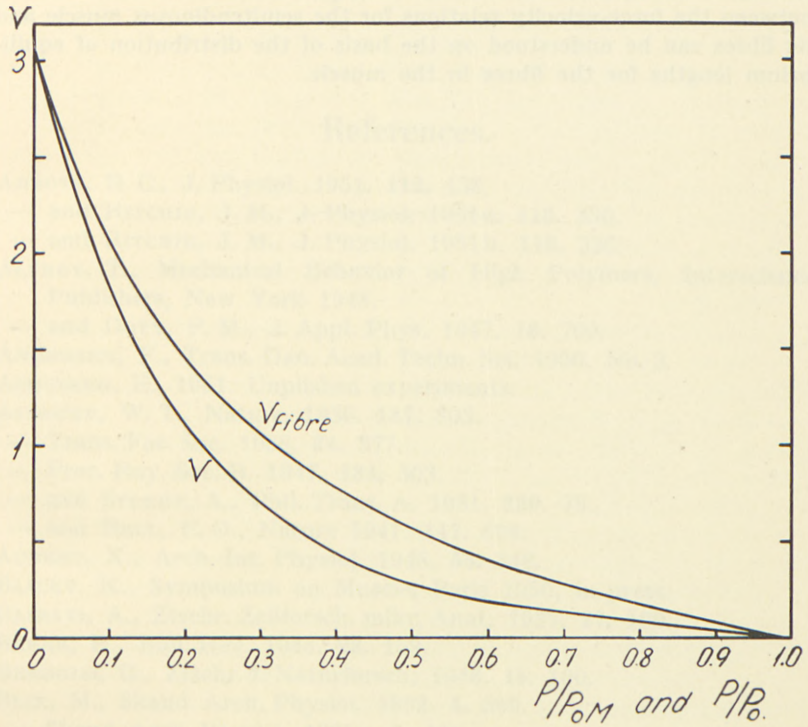

Fig. 105. Maximum shortening velocity as a function of the load for a single fibre and for a "muscle" consisting of two fibres with a difference in equilibrium length of 20 per cent.

V_{fibre}: single fibre.
V : "muscle".
abscissa: load on the fibre in units of P_0 and load on the "muscle" in units of P_{0M}.
ordinate: shortening velocity in units of L_0 per sec.

curve for fibre 1 given by (10). Comparison with the experimental curves for fibre and muscle shows that the theoretical difference between fibre and "muscle" is of the right order of magnitude (fig. 63).

If the "muscle" curve in fig. 105 is approximated by curves determined by HILL's equation:

$$(P + a_M)(V + b_M) = (P_{0M} + a_M)\, b_M, \qquad (22)$$

one finds values of a_M between $0.145\ P_{0M}$ and $0.12\ P_{0M}$. The corresponding values for b_M are $0.445\ L_0$/sec. and $0.36\ L_0$/sec. The experimentally

determined constants for the semitendinosus muscle are: $a_M = 0.125\ P_{0M}$ and $b_M = 0.38\ L_0$/sec.

As described in Part III (fig. 80) the fibres of a muscle have actually differences in equilibrium length of the order of magnitude assumed in the above calculations. Therefore, we may conclude that the difference between the force-velocity relations for the semitendinosus muscle and its fibres can be understood on the basis of the distribution of equilibrium lengths for the fibres in the muscle.

References.

Abbott, B. C., J. Physiol. 1951. **112.** 438.
— and Ritchie, J. M., J. Physiol. 1951a. **113.** 330.
— and Ritchie, J. M., J. Physiol. 1951b. **113.** 336.
Alfrey, T., Mechanical Behavior of High Polymers, Interscience Publishers, New York 1948.
— and Doty, P. M., J. Appl. Phys. 1947. **16.** 700.
Andersen, F., Trans. Dan. Acad. Techn. Sci. 1950. No. 3.
Asmussen, E., 1951. Unplished experiments.
Astbury, W. T., Nature, 1936. **137.** 803.
— Trans. Far. Soc. 1938. **34.** 377.
— Proc. Roy. Soc. B. 1947. **134.** 303.
— and Street, A., Phil. Trans. A. 1931. **230.** 75.
— and Bell, F. O., Nature 1941. **147.** 696.
Aubert, X., Arch. Int. Physiol. 1948. **55.** 348.
Bailey, K., Symposium on Muscle, Paris 1950, in press.
Bairati, A., Ztschr. Zellforsch. mikr. Anat. 1937. **27.** 100.
Barer, R., Biol. Rev. 1948. **23.** 159.
Bergold, G., Ztschr. f. Naturforsch, 1946. **1b.** 100.
Blix, M., Skand. Arch. Physiol. 1892. **4.** 399.
— Skand. Arch. Physiol. 1895a. **5.** 150.
— Skand. Arch. Physiol. 1895b. **5.** 173.
Böhm, G., Ztschr. Biol. 1931. **91.** 204.
— and Weber, H. H., Kolloidztschr. 1932. **61.** 269.
Boyle, P. J. and Conway E. J., J. Physiol. 1941. **100.** 1.
Bozler, E. and Cottrell, C. L., J. Cell. Comp. Physiol. 1937. **10.** 165.
Bragg, L., Science, 1948. **108.** 455.
Brenschede, W., Kolloidztschr. 1943. **104.** 1.
Buchthal, F., Dan. Biol. Medd. 1942. **17.** no. 2.
— and Lindhard, J., Skand. Arch. Physiol. 1936. **74.** 223.
— and Knappeis, G. G., Skand. Arch. Physiol. 1938. **78.** 97.
— and Lindhard, J., Dan. Biol. Medd. 1939. **14.** no. 6.
— and Knappeis, G. G., Skand. Arch. Physiol. 1940. **83.** 19.
— and Knappeis, G. G., Acta Physiol. Scand. 1943. **6.** 123.
— and Kaiser, E., Acta Physiol. Scand. 1944. **8.** 38.
— Knappeis, G. G., and Lindhard, J., Skand. Arch. Physiol. 1936. **73.** 163.

Buchthal, F., Knappeis, G. G., and Sjöstrand, T., Skand. Arch. Physiol. 1939. **82.** 225.
— Kaiser, E., and Knappeis, G. G., Acta Physiol. Scand. 1944a. **8.** 16.
— Deutsch, A., and Knappeis, G. G., Acta Physiol. Scand. 1944b. **8.** 271.
— Deutsch, A., Knappeis, G. G., and Munch-Petersen, A., Acta Physiol. Scand. 1949. **16.** 326.
Bull, H. B., J. Am. Chem. Soc. 1945. **67.** 2047.
Burte, H. and Halsey, G., Text. Res. J. 1947. **17.** 465.
Busse, W. F., J. Phys. Chem. 1932. **36.** 2862.
Casella, C., Acta Physiol. Scand. 1951. **21.** 380.
Caspersson, T. and Thorell, B., Acta Physiol. Scand. 1942. **4.** 97.
Cronkite, A., Anat. Rec. 1936. **64.** 173.
Demsey, E. W., Wislocki, G. B., and Singer, M., Anat. Rec. 1946. **96.** 221.
Draper, M. H. and Hodge, A. J., The Austral. J. Exper. Biol. Med. Science. 1949. **27.** 465.
Dubuisson, M., Biol. Rev. 1950a. **25.** 46.
— Biochem. et Biophys. Acta 1950b. **4.** 25.
Evans, L. C., Principles of Human Physiology. London 1947. p. 116.
Eyring, H. and Powell, R. E., Rheological Properties of Simple and Colloidal Systems, in Colloid Chemistry, Theoretical and Applied, ed. by J. Alexander. Vol. V 1944, p. 236 ff.
Fenn, W. O., J. Physiol. 1923. **58.** 175.
— J. Physiol. 1924. **58.** 373.
— Cold Spring Harbor Symp. Quant. Biol. 1936. **4.** 233.
— Contractility, in Physical Chemistry of Cells and Tissues, by R. Höber, Section 7. p. 445, Philadelphia, Blakiston Co., 1945.
Fick, A., Pflügers Arch. Physiol. 1871. **4.** 301.
— Mechanische Arbeit und Wärmeentwicklung bei der Muskeltätigkeit, Leipzig 1882.
Fischer, E., Cold Spring Harbor Symp. Quant. Biol. 1936. **4.** 214.
— J. Cell. Comp. Physiol. 1944. **23.** 113.
— Ann. New York Acad. Sc. 1947. **47.** 783.
Gasser, H. S. and Hill, A. V., Proc. Roy. Soc. B. 1924. **96.** 398.
Gross, B., J. Appl. Phys. 1947. **18.** 212.
— J. Appl. Phys. 1948. **19.** 257.
Hall, C. E., Jakus, M. A., and Schmitt, F. O., Biol. Bull. 1946. **90.** 32.
Halsey, G. and Eyring, H., Text. Res. J. 1945. **15.** 451.
— and Eyring, H., Text. Res. J. 1946a. **16.** 124.
— and Eyring, H., Text. Res. J. 1946b. **16.** 329.
— White, H. S., and Eyring, H., Text. Res. J. 1945. **15.** 295.
Hartree, W. and Hill, A. V., J. Physiol. 1921. **55.** 389.
Hill, A. V., Adventures in Biophysics, Oxford Univ. Press 1931, p. 120.
— Proc. Roy. Soc. B. 1937. **124.** 114.

Hill, A. V., Proc. Roy. Soc. B. 1938. **126.** 136.
— Proc. Roy. Soc. B. 1939. **127.** 849.
— Proc. Roy. Soc. B. 1940. **128.** 263.
— Proc. Roy. Soc. B. 1949a. **136.** 195.
— Proc. Roy. Soc. B. 1949b. **136.** 211.
— Proc. Roy. Soc. B. 1949c. **136.** 242.
— Proc. Roy. Soc. B. 1949d. **136.** 399.
— Proc. Roy. Soc. B. 1949e. **136.** 420.
— Proc. Roy. Soc. B. 1950a. **137.** 268.
— Proc. Roy. Soc. B. 1950b. **137.** 273.
— Proc. Roy. Soc. B. 1950c. **137.** 330.
— and Kupalov, P. S., Proc. Roy. Soc. B. 1930. **106.** 445.
Hill, D. K., J. Physiol. 1949. **108.** 292.
Höncke, P., Acta Physiol. Scand. 1947. **15.** Suppl. 48.
Holland, H. D., Halsey, G., and Eyring, H., Text. Res. J. 1946. **16.** 201.
Huxley, H. E. and Perutz, M. F., Nature 1951. **167.** 1054.
Jones, W. M. and Barer, R., Nature 1948. **161.** 1012.
Jordan, H. J., First Report on Viscosity and Plasticity, Kon. Ned. Akd. Wet. Verhand. 1939, Part 15, Chapter 4. p. 214.
Josenhans, W., Ztschr. Biol. 1949. **103.** 61.
Kaiser, K., Ztschr. Biol. 1896. **33.** 157.
— Zbl. Physiol. 1900. **14.** 195.
Katz, B., J. Physiol. 1939. **96.** 45.
— Proc. Roy. Soc. B. 1948. **135.** 507.
Lord Kelvin, Elasticity, Encyclopaedia Britannica, 9. ed. 1875.
Knappeis, G. G., Acta Physiol. Scand. 1948. **16.** Suppl. 53. p. 40.
v. Kries, J., Arch. Anat. Physiol., Physiol. Abt. 1880. p. 348.
Kühne, W., Arch. Anat. Physiol. 1859. p. 815.
Kuhn, W., Künzle, O., and Preissmann, A., Helv. Chim. Acta 1947a. **30.** 307.
— Künzle, O., and Preissmann, A., Helv. Chim. Acta 1947b. **30.** 464.
Levin, A. and Wyman, J., Proc. Roy. Soc. B. 1924. **96.** 398.
Lindhard, J., Ergebn. Physiol. 1931. **33.** 337.
Long, M. E., Am. J. Anat. 1947. **81.** 159.
Maltoltsi, A. G. and Gerendás, M., Nature 1947. **159.** 502.
Mauro, A., Acta Physiol. Scand. 1951. **25.** Suppl. 89. p. 59.
Maxwell, J. C., Phil. Mag. 1868 (IV) **35.** 134.
McLachlan, N. W., Ordinary non-linear differential equations in engineering and physical sciences, Oxford 1950, Chapter IV.
Meyer, K. H. and Ferri, C., Pflügers Arch. Physiol. 1936. **238.** 78.
— and Picken, L. E. R., Proc. Roy. Soc. B. 1937. **124.** 29.
— v. Susich, S., and Valkó, E., Kolloidztschr. 1932. **59.** 208.
Mochulsky, M. and Tobolsky, A. V., Indust. Eng. Chem. 1948. **40.** 2155.
v. Muralt, A., Pflügers Arch. Physiol. 1932. **230.** 299.
— Pflügers Arch. Physiol. 1934. **234.** 653.

Noll, K. and Weber, H. H., Pflügers Arch. Physiol. 1934. **235.** 234.
Ostwald, W., Kolloidztschr. 1926. **40.** 58.
Pauling, L., Corey, R. B., and Branson, H. R., Proc. U. S. Nat. Acad. Sci. 1951. **37.** 205.
— and Corey, R. B., Proc. U. S. Nat. Acad. Sci 1951. **37.** 235, 241, 251, 256, 261, 272, 282.
— and Corey, R. B., Proc. U. S. Nat. Acad. Sci 1951a. **37.** 261.
Perutz, M. F., Nature 1951. **167.** 1053.
Ralston, H. J., Inman, V. T., Strait, L. A., and Shaffrath, M. D., Am. J. Physiol. 1947. **151.** 614.
— Polissar, M. J., Inman, V. T., Close, J. R., and Feinstein, B., J. Appl. Physiol. 1949. **1.** 526.
Ramsey, R. W., Ann. New York Acad. Science 1947. **47.** 675.
— R. W. cit. from W. O. Fenn in Physical Chemistry of Cells and Tissues, by R. Höber, Philadelphia, Blakiston Co. 1945. p. 509.
— and Street, S. F., J. Cell. Comp. Physiol. 1940. **15.** 11.
— and Street, S. F., Biol. Symp. 1941. **3.** 9.
Ranvier, L., Arch. Physiol. Norm. Path. 1874. ser. 2. part I. p. 774.
Reichardt, C. H. and Eyring, H., Text. Res. J. 1946. **16.** 635.
Reichel, H., Ztschr. Biol. 1936. **97.** 429.
— Ztschr. Biol. 1938. **98.** 510.
Reiner, M., Twelve Lectures on Theoretical Rheology, Amsterdam 1949.
— Deformation and Flow, London, 1949b. Lewis.
Rieser, P., Protoplasma 1949. **39.** 95.
Romeis, B., Taschenbuch d. mikroskop. Technik, München 1928. p. 418.
Rozsa, G., Szent-Györgyi, A., and Wyckoff, R. W. G., Exp. Cell Res. 1950. **1.** 194.
Sandow, A., J. Cell. and Comp. Physiol. 1936a. **9.** 37.
— J. Cell. and Comp. Physiol. 1936b. **9.** 55.
— J. Cell. and Comp. Physiol. 1944. **24.** 221.
— Ann. New York Acad. Science 1947. **47.** 895.
Schenck, F., Pflügers Arch. Physiol. 1895. **61.** 77.
Sitaramayya, C., J. Physiol. 1951. **114.** 27 P.
Speakman, J. B. and Peters, L., J. Text. Inst. 1948. **39.** 253.
Stein, R., Halsey, G., and Eyring, H., Text. Res. J. 1946. **16.** 53.
Sten-Knudsen, O., Acta Physiol. Scand. 1948. **16.** Suppl. 153. p. 58.
— Internat. colloquium on rheolog. problems in biology, Lund 1950 in press.
Stübel, H., Pflügers Arch. Physiol. 1923. **201.** 629.
Sulzer, R., Ztschr. Biol. 1930. **90.** 13.
Szent-Györgyi, A., Biol. Bull. 1949. **96.** 140.
Tobolsky, A. and Eyring, H., J. Chem. Phys. 1943. **11.** 125.
— Powell, R. E., and Eyring, H., Elastic-viscous Properties of Matter in "The Chemistry of Large Molecules", Interscience Publ. New York 1943.

Treloar, L. R. G., Trans. Far. Soc. 1943. **39.** 241.
— The Physics of Rubber Elasticity, Oxford 1949 (Clarendon Press).
— Nature 1951. **167.** 425.
Varga, L., Enzymologia 1950. **14.** 196.
Voigt, W., Abh. Königl. Gesell. Wiss. Göttingen 1890. **36.** Mathem. Kl. Nr. 1.
Wall, F. T., J. Chem. Phys. 1942. **10.** 485.
Walter, W G., Arch. Néerland. Physiol. 1944—1947. **28.** 655.
Weber, H. H., Pflügers Arch. Physiol. 1934a. **235.** 205.
— Ergeb. Physiol. 1934b. **36.** 109.
Wöhlisch, E., Kolloidztschr. 1939. **89.** 239.
— and Grüning, W., Pflügers Arch. Physiol. 1943. **246.** 469.
— Mesnil de Rochemont, R., and Gerschler, H., Z. Biol. 1927. **85.** 325.
Woods, H. J., J. Colloid Sci. 1946. **1.** 407.

List of symbols.

		Definition on page
A, $A_{\alpha \to \beta}$, $A_{\beta \to \alpha}$	activation energy	235
a	constant in Hill's equation (expressed in units of P_0)	177
$\alpha -$	short modification of keratin, fibrinogen, and myosin	223
α	fraction of links in the α-modification	239
α_2, $\alpha_3 - - -$	number of α-aggregates with 2, 3 $- - -$ links respectively	250
α_f	fraction of links in the fixated α-state	257
α_1	fraction of links in the non-fixated α-state	257
b	constant in Hill's equation (expressed in units of L_0 per sec.)	177
$\beta -$	long modification of keratin, fibrinogen, and myosin	223
β	fraction of links in the β-modification	239
β_2, $\beta_3 - - -$	number of β-aggregates with 2, 3 $- - -$ links respectively	250
C	concentration of fixating factor	256
c	constant in the distribution function of retardation times	71
C_l	experimental constant from creep experiments	55
C_p	experimental constant from isometric transients (stress-relaxation)	63
C_1 and C_2	proportionality factors in aggregate formation and break-down	250
D	defixation factor in the contraction theory	257
ΔL	change in length	56
ΔP	change in load	45
Δp	increase in tension in the transmutation chain	246
η	damping, viscosity, friction	17
FC	fixation factor in the contraction theory	257

		Definition on page
G	stiffness, elasticity	39, 49, 60
G_{elast}	elastic stiffness	17
G_{visc}	viscous stiffness	18
G_{tot}	total stiffness $= \sqrt{G_{elast}^2 + G_{visc}^2}$	19
$G(\tau)$	distribution function of relaxation times	69
γ	deformation	17
γ_0	deformation amplitude	17
I	moment of inertia	22
J	reciprocal elastic stiffness (compliance)	66
$J(\tau)$	distribution function of retardation times	67
$j(\tau)$	normalized distribution function	72
K	constant in the aggregate theory $= \frac{C_1}{C_2}$	251
$K(\log \tau)$	distribution function of relaxation times in logarithmic time scale $= \tau \cdot g(\tau)$	75
$\varkappa$	constant in the length-tension relation of the muscle fibre = relative stiffness	59, 292
L	fibre length	38
L_0	equilibrium length of the muscle fibre	35
$L(\log \tau)$	distribution function of retardation times in logarithmic time scale $= \tau \cdot j(\tau)$	72
L_α and L_β	length of the α- and β-modifications respectively	235
λ_α	distance from the α-minimum to the peak of the potential energy barrier	238
λ_β	distance from the β-minimum to the peak of the potential energy barrier	238
2λ	distance from the α-minimum to the β-minimum	239
λ_1 and λ_2	decay constants in the theoretical course of shortening	261
M	number of aggregates	250
M_α and M_β	number of α- and β-aggregates respectively	250
m	mass, equivalent mass	17
μ_1 and μ_2	decay constants in the theoretical course of relaxation	269
N	number of links	240
N_α and N_β	number of links in the α- and β-modifications respectively	239
n	relative number of links in a chain	249
ν_0	resonance frequency (c. p. s.)	20
ν	collision frequency	234

		Definition on page
ω	cyclic frequency	17
ω_0	resonance frequency (cyclic)	18
P	load on the fibre	38
P_0	reference load = the load at which the shortening velocity is zero	38
P_m	mean load	60
P_i	internal tension in the contractile elements	173
P_{st}	stiffness-tension	84
p	measure of the load on a transmutation chain $= \frac{P \cdot \lambda}{k \cdot T}$	239
p_{extra}	extra tension	258
ψ	phase displacement	17
r	proportionality factor in the Tobolsky-Eyring sinh-equation	229
σ	force	17
σ_0	force amplitude	17
σ_f	force acting on the fibre	80
σ_i	inertial force	80
sr	stiffness ratio $= \frac{G_{visc}}{G_{elast}}$	19
t_0	"latent period" = time required for a transmutation chain to obtain maximal shortening velocity	262
τ	relaxation and retardation time	66, 68
τ_1 and τ_2	boundaries in the spectrum of retardation times	71
$U(L)$	potential energy barrier governing the $\alpha \rightleftarrows \beta$ transmutations	235
V	shortening velocity	147
V_0	maximal shortening velocity in the transmutation theory	264
V_d	relaxation velocity	181
V_d^0	maximal relaxation velocity in the transmutation theory	269
v	velocity in transients	55
$W_{\alpha \to \beta}$ and $W_{\beta \to \alpha}$	transmutation frequencies per link	237
W	proportionality factor in the transmutation frequency per link	239

Index of subjects.

Indleveret til selskabet den 9. maj 1951.
Færdig fra trykkeriet den 15. december 1951.